

Identification of small RNAs during abiotic stresses in *Arabidopsis thaliana*

Dissertation

zur Erlangung des Grades eines Doktors der
Naturwissenschaften

an der Fakultät für Biologie

der Ludwig-Maximilians-Universität München

vorgelegt von

Bhavika Tiwari

München, 2021



Die vorliegende Doktorarbeit wurde im Zeitraum von
September 2016 bis März 2021
an der Ludwig-Maximilians-Universität München in
Martinsried durchgeführt.

Supervisor und Erstgutachter: Prof. Dr. Wolfgang Frank

Biozentrum der LMU München
Department Biology I

Zweitgutachter: Dr. Jörg Meurer

Datum der Abgabe: 30.11.2020

Datum der Prüfung: 19.03.2021

Eidesstattliche Erklärung

Hiermit versichere ich an Eides statt, dass ich die vorliegende Arbeit selbstständig verfasst habe, keine als die angegebenen Quellen und Hilfsmittel benutzt wurden und alle Zitate kenntlich gemacht sind. Des Weiteren versichere ich, nicht anderweitig ohne Erfolg versucht zu haben, eine Dissertation einzureichen oder mich einer Doktorprüfung zu unterziehen. Die vorliegende Dissertation liegt außerdem keiner anderen Prüfungskommission vor.

I hereby confirm that I have written the accompanying thesis by myself, without contributions from any sources other than those cited in the text. This also applies to all graphics, drawings and images included in this thesis. Moreover, I declare that I have not submitted or defended a dissertation previously without success. This thesis has not been presented to any other examining board.

München, 7 April 2021

Bhavika Tiwari

Table of Contents

ABBREVIATIONS.....	V
LIST OF PUBLICATIONS AND CONTRIBUTIONS OF AUTHORS.....	VI
ZUSAMMENFASSUNG	VII
SUMMARY	VIII
1 INTRODUCTION.....	1
1.1 Cold stress	1
1.1.1 Cold alters cell structure.....	1
1.1.2 Low temperature affects photosynthesis.....	2
1.1.3 Production of ROS in cold stress	3
1.1.4 Cold stress related transcriptional cascades	3
1.1.5 Regulation of cold stress signaling pathway.....	6
1.2 Light stress.....	7
1.2.1 Physiological effects of light stress	7
1.2.2 Photoreceptors in light signaling	8
1.2.3 Light induced signaling	8
1.2.4 High light induced alterations in photosynthetic machinery	9
1.3 Retrograde signaling.....	12
1.3.1 Retrograde signaling in cold stress	14
1.3.2 Excess light induced retrograde signals.....	15
1.4 Non-coding RNAs in abiotic stress	15
1.4.1 Long non-coding RNAs and their mode of action	15
1.4.2 Small RNAs in abiotic stress.....	16
2 RESULTS.....	24

2.1 Publication 1 (Tiwari et al. 2020).....	24
2.2 Publication 2 (Habermann et al. 2020).....	50
2.3 Publication 3 (Tiwari et al. 2021).....	69
3 DISCUSSION.....	101
3.1 Cold stress.....	102
3.2 High light stress.....	104
3.3 Retrograde Signaling.....	106
3.4 Comparison of cold stress, high light stress and retrograde signaling affected non-coding RNAs.....	108
3.5 Outlook.....	112
4 REFERENCES.....	114
5 ACKNOWLEDGEMENTS.....	130
6 CURRICULUM VITAE.....	132

Abbreviations

sRNAs/ siRNAs: small RNAs/ small interfering RNAs

miRNA: microRNA

ncRNA: non-coding RNA

lncRNA: long non-coding RNA

ta-siRNA: trans-acting siRNA

cis/trans-NAT: *cis/trans*-natural antisense transcript

NAT: Natural antisense transcript

DE: differentially expressed

DEG: differentially expressed gene

TE: transposable element

TF: transcription factor

pc: protein coding

nc: non-coding

GO: gene ontology

ABA: abscisic acid

PHY: phytochromes

CRY: cryptochromes

ROS: reactive oxygen species

PAP: 3'-phosphoadenosine 5'-phosphate

DCL1: DICER-LIKE1

ea-siRNA: epigenetically activated siRNA

HY5: ELONGATED HYPOCOTYL 5

P5CDH: delta-pyrroline-5-carboxylate dehydrogenase

SRO5: Similar to Radicle Induced Cell Death One 5

PPR: pentatricopeptide repeat superfamily protein

tRF: tRNA-derived RNA fragments

SPL: Squamosa promoter binding protein-like

RdDM: RNA-directed DNA methylation

TCP: Teosinte Branched 1, Cycloidea, members of the PCF

OST1: OPEN STOMATA 1

ICE1: Inducer of CBF expression

CBF: C-repeat binding factors

DREB: Dehydration responsive element binding factors

CRT/DRE: Cold response sensitive transcription factors/dehydration responsive elements

COR: Cold-responsive

ABFs: ABRE-binding factors

RdDM: RNA-directed DNA methylation

FLC: Flowering locus C

LCR: LEAF CURLING RESPONSIVENESS

DDM1: Decreased DNA methylation 1

TIM: Translocase Inner Membrane Subunit

RAN2: RAS-Related GTP-Binding Nuclear Protein

PPR: Pentatricopeptide repeat superfamily protein

NFY: Nuclear Factor-Y

HSF: Heat shock factors

ACC synthase: Amino-cyclopropane-1-carboxylate synthase

MATE: Multi-antimicrobial extrusion protein

List of publications and contributions of authors

1. Tiwari, B., Habermann, K., Arif, M.A., Weil, H.L., Mühlhaus, T., Frank, W. Identification of small RNAs during cold acclimation in *Arabidopsis thaliana*. BMC Plant Biology 20, 298 (2020). <https://doi.org/10.1186/s12870-020-02511-3>

WF and MAA designed the research; BT performed the research with the help of MAA and KH; BT, MAA, KH and WF analyzed the data; AGM and TK provided the 3 h and 2 d mRNA/lncRNA mRNA sequencing raw data; miRNA-TF network was constructed by HLW and TM; and BT, MAA, HLW and WF wrote the paper.

2. Habermann, K., Tiwari, B., Krantz, K., Adler O, S., Klipp, E., Arif, M.A., Frank, W. Identification of small non-coding RNAs responsive to GUN1 and GUN5 related retrograde signals in *Arabidopsis thaliana*. *The Plant Journal* (2020). <https://doi.org/10.1111/tpj.14912>

WF and MAA designed the research; KH performed the research with help from MAA and BT; KH, MAA, BT and WF analyzed the data; network analysis was performed by SOA, MK and EK; and KH, MAA, MK, SOA and WF wrote the paper.

3. Tiwari, B., Habermann, K., Arif, M.A., Top, O., Frank, W. Identification of small RNAs during high light acclimation in *Arabidopsis thaliana*. (Submitted to *Frontiers in Plant Science*)

WF designed the research; BT performed the research with the help of MAA and KH; BT, MAA, KH, OT and WF analyzed the data; and BT, OT and WF wrote the paper.

Hereby we confirm the stated contributions to the mentioned publications (1, 2 and 3)

Bhavika Tiwari

Prof. Dr. Wolfgang Frank

Zusammenfassung

Abiotische Stressbedingungen wie Kälte und Starklicht haben einen negativen Einfluss auf das Wachstum von Pflanzen und verursachen weltweit große Ertragsverluste. Daher ist es wichtig, die molekularen Anpassungsmechanismen zu verstehen, um Pflanzen mit einer gesteigerten Toleranz gegenüber den vielfältigen Belastungen zu erzeugen. Um sich an diese Umweltveränderungen anpassen zu können, ist eine Veränderung der Genexpression notwendig, wobei kleine, nicht-kodierende RNAs (*small RNAs*: sRNAs) wesentlich zu Veränderungen in der Genexpression beitragen, indem sie in erster Linie posttranskriptionell wirken und zum RNA-Abbau beitragen oder deren Translation inhibieren. Um Veränderungen im Expressionsmuster kleiner, nicht-kodierender zu untersuchen, wurde *Arabidopsis thaliana* 3 Stunden, 6 Stunden und 2 Tage einer Kälte- bzw. einer Starklichtbehandlung unterzogen. Zusätzlich wurde *A. thaliana* Wildtyp zusammen mit zwei retrograden Signalmutanten (*gun1* und *gun5*) mit Norflurazon (NF) behandelt. Die aus den behandelten Pflanzen erhaltene RNA wurden mithilfe von *next generation sequencing* sequenziert und die Rohdaten unter Verwendung der GALAXY- und Shortstack-Software analysiert. Die mRNA-Daten und die sRNA-Sequenzierungsdaten wurden korreliert, um das sRNA-Repertoire in *Arabidopsis* aufzudecken und ihre Beteiligung an der Regulation der mRNA-Genexpression zu identifizieren. Die Studie konzentriert sich insbesondere auf microRNAs (miRNAs), von denen bekannt ist, dass sie zu den Hauptregulatoren der Genexpression zählen. Um den Einfluss differentiell exprimierter miRNAs zu untersuchen, haben wir deren mutmaßlichen proteinkodierenden und nichtkodierenden Zieltranskripte mithilfe des psRNATarget-Tools identifiziert. Um die Auswirkungen anderer sRNA-produzierender Klassen auf abiotischen Stress und auf die retrograde Signalübertragung zu verstehen, haben wir die Identifizierung von sRNAs eingeschlossen, die von *cis*- und *trans*-NATs, long non-coding RNAs, phased interfering sRNAs und *trans*-acting sRNAs abgeleitet sind. Die Ergebnisse zeigen, dass eine große Anzahl von *cis*- und *trans*-nat-siRNAs, gefolgt von miRNAs, an Veränderungen der Genexpression beteiligt sind. Unter Verwendung unserer mRNA- und sRNA-Sequenzierungsdaten in Verbindung mit öffentlich verfügbaren Datensätzen haben wir weiterhin ein mit der Kälteakklimatisierung verbundenes miRNA-Transkriptionsfaktor-Regulationsnetzwerk modelliert. Aus diesem Regulationsnetzwerk können die Beziehungen der beteiligten miRNAs zueinander ausgelesen und zur Untersuchung der neuartigen regulatorischen Beziehungen verwendet werden. Die vorhergesagten Ziele differentiell exprimierter miRNAs zeigten eine Überrepräsentation von Genen, die TFs codieren, und signalbezogenen Proteinen, die für die Regulation der Genexpression notwendig sind. Wir haben neue differentiell exprimierte sRNAs identifiziert, die zu allen verschiedenen sRNA-Klassen gehören. Zusammenfassend bietet diese Studie ein grundlegendes Netzwerk, um unser Wissen zu vertiefen und die Bedeutung von sRNAs bei abiotischem Stress und retrograden Signalmechanismen zu verstehen.

Summary

Abiotic stresses such as cold and high light are unfavorable for the growth and development of plants and cause a great yield loss worldwide. Thus, it is critical to understand underlying molecular mechanisms of stress adaptations and engineer plants to enhance their tolerance to multiple stresses. Due to these inevitable environmental changes, the gene expression alteration is necessary and studies have confirmed the importance of small RNAs in regulating gene expression. We subjected wild type (WT) *Arabidopsis thaliana* plants to cold and high light treatments for three time points (3 h, 6 h and 2 d) and, WT plants along with two additional retrograde signaling mutants *gun1* and *gun5* were treated with Norflurazon (NF). The RNA extracted from the treated aerial tissues was sequenced through Next-generation sequencing platform and the raw data was analyzed using GALAXY and Shortstack. The mRNA and sRNA sequencing data were correlated to uncover the small RNA (sRNA) repertoire in *Arabidopsis* and to identify their involvement in the regulation of mRNA gene expression. This study has a special focus on miRNAs, which are powerful regulators of gene expression. To study the impact of differentially expressed miRNAs, we identified the putative protein-coding and non-coding RNA targets through psRNATarget tool. To understand the implications of other sRNA producing classes in abiotic stresses and retrograde signaling, we identified sRNAs derived from *cis*- and *trans*- natural antisense transcripts (NATs), long non-coding RNAs (lncRNAs), PHAS and trans-acting siRNA producing transcripts (tasiRNAs). The results revealed that a large number of *cis*- and *trans*-nat-siRNAs followed by miRNAs were involved in gene expression alterations. Using our mRNA and sRNA sequencing data along with publicly available datasets, we reconstructed a cold acclimation related miRNA-transcription factor (TF)-target gene regulatory network (GRN). The subnetworks of miRNAs can be extracted from the GRN to study the novel regulatory relationships. We identified novel differentially expressed sRNAs belonging to all different sRNA classes and the predicted targets of differentially expressed miRNAs indicated an overrepresentation of genes encoding TFs and signal-related proteins necessary for the regulation of gene expression. We conclude that this study provides a fundamental database to deepen our knowledge and understanding of the importance of sRNAs in abiotic stresses and retrograde signaling mechanisms.

1 Introduction

Plants are severely affected by dynamic and extreme climatic conditions. Abiotic stresses such as temperature and light globally alter the development of plants, and hinder their spatial distribution impacting the total agricultural productivity (Gornall et al. 2010). Any deviation from the optimal conditions lead to physiological, biochemical and molecular alterations in plants. When the conditions are progressively unfavorable, inhibited cellular processes cause extreme survival pressure on plants. Under extremely adverse conditions, plants experience acute molecular dysfunction which ultimately leads to their death.

1.1 Cold stress

1.1.1 Cold alters cell structure

Plant cells perceive cold stress by detecting reduced cell membrane fluidity that triggers specific signaling cascades (Solanke and Sharma 2008). The cold-adapted plants are able to increase the amounts of unsaturated fatty acids in their cell membranes and thus elevate membrane fluidity at low temperatures. But in non-acclimated plants, freezing leads to severe dehydration which causes membrane damage induced by freezing (Steponkus 1984). Cold stress alters the lipid membranes and leads to accumulation of solutes (Kazuo Shinozaki and Kazuko Yamaguchi-Shinozaki 2000) and reactive oxygen species (ROS). In order to acclimate to the altered ROS levels, the plant produces abundant ROS scavenging enzymes and alters carbohydrate metabolism (Frankow-Lindberg 2001). The change in membrane integrity causes leakage of solutes from essential organelles, thereby disrupting the organelles and affecting crucial metabolic processes such as photosynthesis. On the whole plant level, low temperature reduces the growth of plants by restraining water and nutrient uptake. Due to this, there is a substantial reduction in the consumption of photosynthates and the photochemical processes are adjusted to the reduced requirements of plants. These overall changes eventually determine the yield and distribution of plants (Frankow-Lindberg 2001).

1.1.2 Low temperature affects photosynthesis

Chilling injury in the presence of low light selectively inhibits photosystems and in contrast to PSII (Photosystem II), PSI (Photosystem I) is more susceptible to low temperature stress (Suping Zhang and Scheller 2004). At low temperatures, the energy equilibrium between the photochemistry, electron transport, and metabolism are extremely disturbed. Due to reduced photosynthetic capacities, plants urge to increase photon capture (Ensminger et al. 2006) but as a result, they accumulate higher amounts of chlorophyll b and carotenoid pigments associated with light harvesting complex a/b (LHCa and LHCb). It has been shown that the cold stress slows down the replenishment of D1 proteins, and an equilibrium between degraded and the newly synthesized D1 proteins determines the extent of PSII photoinhibition (Aro et al. 1993, Gombos et al. 1994). Altogether, the plant experiences a drop in photosynthetic efficiencies and photosynthates transport. Under normal conditions, the excitation energy between PSII and PSI is balanced to maintain an optimal photosynthetic rate. However, during low temperature stress in the presence of light, the PSII is exposed to high excitation energy which is compensated by deviating this excess energy to PSI. Under such circumstances, the state transition mechanism redistributes the harnessed energy and reduces the uneven distribution of excitation energy. Prolonged cold stress either reduces the photosynthetic antenna size or produces stress proteins and lipophilic antioxidant molecules (Dalal and Tripathy 2018). Another alternate mechanism is the dissipation of the excess energy absorbed by light-harvesting chlorophyll protein complexes (LHC) in the form of heat, known as non-photochemical quenching (NPQ). Under normal conditions, the light-induced proton gradient across thylakoid lumen helps in ATP production. Due to constant pumping of protons into the lumen, the pH in the stroma becomes alkaline which is necessary to activate the Calvin Benson cycle enzymes (Hohner et al. 2016).

In case of low temperature stress and excess energy, there is a sudden increase in proton pumping across the lumen, causing acidification of the lumen and protonation of LHCII polypeptides (Havaux and Kloppstech 2001). This change in the pH gradient across thylakoid membrane induces the photoprotective xanthophyll cycle and leads to activation of violaxanthin de-epoxidase enzyme. This enzyme converts violaxanthin into antheraxanthin and zeaxanthin (Adams et al. 1989, Savitch et al. 2002). Production of zeaxanthin accompanied by protonation of LHCs are necessary for NPQ and a decrease in singlet-excited chlorophylls leads

to reduction in energy delivered to PSII. It is known that xanthophyll is an abscisic acid precursor and elevated levels of endogenous abscisic acid (ABA) was found in plants experiencing cold stress (Gusta et al. 2005). Another pathway, namely chlororespiration protects PSII from damage during cold stress particularly in the absence of PSI cyclic electron flow (Paredes and Quiles 2015).

1.1.3 Production of ROS in cold stress

One of the prominent biochemical changes in cold stressed plants is the production of ROS in vital processes like photosynthesis and respiration. To cope with the oxidative damage caused to the plant cells, an advanced ROS scavenging system exists comprising of scavenging enzymes such as superoxide dismutase (SOD), catalase, ascorbate peroxidase and guaiacol peroxidase (Erdal et al. 2015), and non-enzymatic antioxidants like proline, glycine betaine, sugars, polyphenols, and glutathione (Zouari et al. 2016). Low temperature stress causes the accumulation of H₂O₂ in cells which serves dual roles by acting as a signaling molecule when present in low concentrations and toxifies the cell when found in abundance (Das and Roychoudhury 2014). The SOD catalyzes the conversion of superoxide radicals (O₂⁻) into molecular oxygen (O₂) or hydrogen peroxide (H₂O₂) (Mizuno et al. 1998). On the other hand, non-enzymatic antioxidants like proline and betaine not only help in maintenance of cell osmolarity, but also promote detoxification of a cytotoxic compound known as methylglyoxal (MG) and protect plants from lipid peroxidation (Yadav 2009). Apart from the well-known antioxidant systems, the mitochondrial AOX pathway also works against oxidative damage (Erdal et al. 2015).

1.1.4 Cold stress related transcriptional cascades

The low temperature stress is perceived by the cell membrane that relays signals downstream through the transducers. This relayed signal leads to altered transcription of stress-related genes. Currently, the best-characterized pathway is the CBF-dependent signaling pathway (Figure 1), in which ABA accumulates under stress conditions and binds to the pyrabactin resistance regulatory component of ABA receptor (PYR/PYL/RCAR) ABA receptors. This ABA signal-receptor complex then interacts and inhibits type 2C protein phosphatase (PP2Cs) to

block its active site (Park et al. 2009). This interaction abolishes phosphatase activity of PP2Cs and allows autophosphorylation and activation of the OPEN STOMATA 1 (OST1)/SnRK2.6/SNF1-related protein kinase 2 (SnRK2E) (Soon et al. 2012). During non-stressed conditions, the PP2Cs keep SNRK2 in an inactive state through physical interaction and dephosphorylation (Vlad et al. 2009). The activated OST1 was demonstrated to phosphorylate and activate the upstream transcriptional activator inducer of CBF expression (ICE1) which encodes for a MYC-like bHLH protein (Ding 2015). The presence of activated OST1 suppressed high expression of osmotically responsive gene 1 (HOS1) which acts as a repressor of ICE1, and causes its ubiquitination and degradation (Dong 2006). On the other hand, SUMO E3 ligase SIZ1 causes sumoylation and represses the polyubiquitination providing increased stability to ICE1 (Miura et al. 2007). ICE1 is also necessary to cause a delay in flowering during cold stress as SUPPRESSOR OF OVEREXPRESSION OF CONSTANS 1 (SOC1) prevents the binding of ICE1 to the CBF promoter causing decreased expression of CBFs. But it is known that CBFs induce the expression of FLOWERING LOCUS C (FLC) which is a negative regulator of SOC1. Thus a feedback loop exists which regulates the cold stress response and flowering time (Seo et al. 2009).

ICE1 further binds to the MYC *cis*-elements in the promoters of genes encoding C-repeat binding factors (CBF) and similarly induces the expression of several CBF/ dehydration responsive element binding factors (DREB) transcription factors. The CBF family contains four homologs in *Arabidopsis* but only three CBF1, CBF2 and CBF3 are functional in cold stress response (Medina et al. 1999). CBFs belong to the APETALA2/ethylene response factor (AP2/ERF) family of transcription factors (Stockinger et al. 1997). CBF factors bind to the cold response sensitive transcription factors/dehydration responsive elements (CRT/DRE) promoter elements generally having a 5 bp core sequence 'CCGAC' and these elements are responsible for salt, dehydration and low temperature induced gene expression regulation (Yamaguchi-Shinozaki and Shinozaki 1994). The low temperature stress induces the expression of CBF downstream genes known as the cold-responsive (*COR*) genes. The *COR* genes protect the plants against the cold stress and encode for cryoprotective proteins, antioxidants, lipids, phenylpropanoids and antifreeze proteins which maintain the stable state of plant cells in low temperature conditions (Chinnusamy et al. 2010, Cuevas-Velazquez et al. 2014). Some of the well-known *COR* genes in *Arabidopsis* are *COR15a*, *COR47*, *COR78* and *COR6.6* (Yamaguchi-Shinozaki and Shinozaki 1993, Uemura et al. 1996). For instance, *COR15a* encodes for a

cryoprotectant plastid-targeted protein that alters the membrane lipid composition and regulates proline levels, thereby stabilizes the cold stress-induced injury (Thalhammer et al. 2014).

ABA is a central stress hormone that is important for tolerance related to cold, salt and drought stress (Sakuma et al. 2002). CBF transcription factors are considered to be the “master switches” that regulate genes associated with an increase in low temperature stress tolerance (Thomashow 1999). But what factors regulate these master switches was unknown until studies found out that ABA treatment can replace the cold stress stimulus (Chen and Gusta 1983). Contrary to these findings, other studies found little or no effect of ABA in low temperature stress tolerance (Hsu et al. 2018). These conflicting results lead to the conclusion that there might be an ABA-dependent and ABA-independent pathways (Gusta et al. 2005).

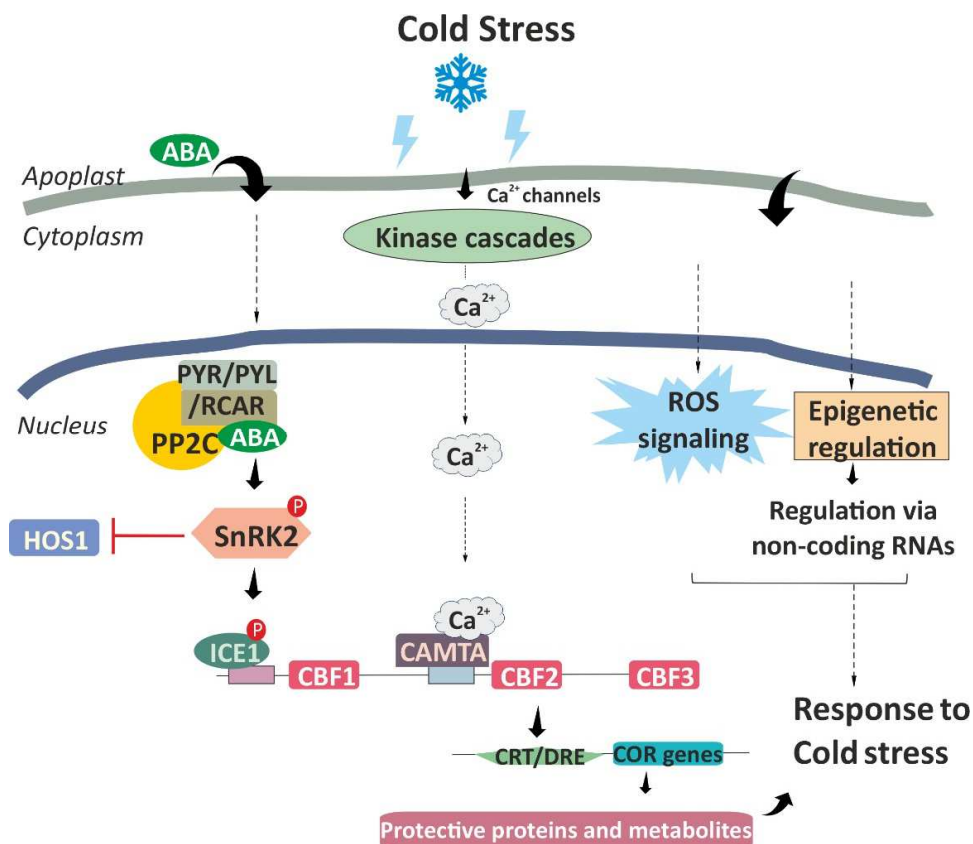


Figure 1. Signal transduction during cold stress acclimation. Cold perception and signaling involves multiple regulatory mechanisms. Transduction could take place in an ABA-dependent manner involving the association of ABA to its receptor and downstream phosphorylation of ICE1 to induce the CBF transcripts. The ABA independent pathway involves calcium ions which drive the intracellular signaling to induce the CBF transcripts. The epigenetic regulation involves regulation of coding RNA transcripts with the help of non-coding RNAs. The major components of CBF dependent signaling are illustrated.

ABA, abscisic acid; PP2C, Protein phosphatase 2C; SnRK2, SNF1-related protein kinase 2; HOS1, High expression of osmotically responsive genes 1; ICE1, Inducer of CBF expression 1; CBF, C-repeat binding factors; CAMTA, CaM-binding transcriptional activator; CRT/DRE, C-repeat (CRT) or dehydration-responsive element (DRE); *COR*, cold-regulated. Source: Figure adapted from Shi et al. (2015)

The ABA-dependent pathway requires the binding of bZIP transcription factors known as ABRE-binding factors (ABFs) to ABA-responsive promoter elements to control the *COR* gene expression (Devert et al. , Wang et al. 2017). Furthermore, studies in *Arabidopsis* have shown that DREB1A/CBF1 and DREB2A/CBF2 can physically interact with ABF2 and, DREB2C/CBF3 interacts with ABF3 and ABF4 to activate downstream ABA-responsive genes (Lee et al. 2010). The CRT/DRE and ABRE domains are present in many cold inducible genes and indicate a tight link between the ABA-dependent pathway and the ICE-CBF-COR pathway (Wang et al. 2017).

1.1.5 Regulation of cold stress signaling pathway

In addition to the transcription factor-mediated control of gene expression, epigenetic modifications affecting the DNA or histones contribute to the control of gene expression in cold stress. Chromatin remodeling refers to the dynamic modification in the architecture of genomic DNA which restricts the access of the transcriptional machinery and alters gene expression. Such modifications determine the accessibility of DNA in chromatin and the efficiency of the transcription machinery (Banerjee et al. 2017, Lamke and Baurle 2017). The H3K27me3 histone modification causes methylation of a lysine residue and this epigenetic modification was observed in *COR15a* and *Galactinol Synthase 3* gene, which de-repressed the expression of cold-responsive genes with a decrease in H3K27me3 (Bowman et al. 2014). Likewise, histone acetylation was observed in *Drought Responsive Element Binding 1* (DREB) in *Zea mays* (Hu et al. 2011) and *Oryza sativa* (Roy et al. 2014).

Besides this, various post-transcriptional and post-translational changes also take place. For example, post-transcriptional regulation in *Arabidopsis* can be achieved by alternative splicing. In *Arabidopsis*, pre-mRNAs encoding the serine/arginine-rich (SR) protein were found to produce different SR isoforms. SR proteins are part of the spliceosome and promote alternative splicing of pre-mRNAs in response to various stresses (Palusa et al. 2007). Another important post-transcriptional control of mRNA stability is mediated through RNA silencing. The RNA silencing mechanism implicates inhibition of gene expression in a sequence-specific manner through non-coding RNAs (ncRNAs). The ncRNAs are classified depending on their length into

long non-coding RNAs (lncRNAs) that contribute to the control of gene expression involving transcriptional and post-transcriptional pathways (Chekanova 2015) and small non-coding RNAs (sRNAs) that bind to reverse complementary target RNAs to confer target RNA cleavage or translational inhibition (Li et al. 2017). Also, sRNAs can interfere with transcription via epigenetic mechanisms such as RNA-directed DNA methylation (RdDM) (Ku et al. 2015).

1.2 Light stress

Light is a variable environmental factor and changes rapidly throughout the day. It not only acts as an energy source for plants but also plays a key role in developmental processes from seed germination to senescence (Jiao et al. 2007). Plants encounter changes in the light intensity and wavelengths for which they have evolved specialized photoreceptor systems. As soon as the plant experiences fluctuations in light, the stress inhibits the plant growth by disrupting the photosynthetic pathway (Greenberg et al. 1989, McKenzie et al. 2007). To counter the damaging effects of light stress, phytohormones play a prime role in activating signaling cascades that ultimately regulates the expression of stress-responsive genes (Effendi et al. 2013).

1.2.1 Physiological effects of light stress

UV-B radiations have shorter wavelengths and are one of the major threats to the plant species. UV-B light can cause chlorophyll degradation and DNA damages due to photoinhibition (Sztatelman et al. 2015). Upon UV-B exposure, lignin content, thickness and surface reflectivity of the leaves increases (Rozema et al. 1997, Nogues et al. 1998, Zhou et al. 2018). In Qinoa, the effect of these physiological changes could lead to stunted growth, inhibited photosynthetic activity and reduced stomatal conductance (Reyes et al. 2018). Bleaching of leaves and damaged cell membranes were observed post-exposure to UV-B light (Stapleton 1992, Hollosy 2002). High light intensity often causes accumulation of flavonoids, phenolics and pigments (Tattini et al. 2004). In the case of wheat seedlings exposed to blue light, heat production was increased as compared to those grown under red light (Alyabyev A. et al. 2002).

1.2.2 Photoreceptors in light signaling

The light is perceived by unique photoreceptors (Pr) that detect different facets of the solar spectrum. The phytochromes (PHY A-E) detect the far-red (FR) light and red (R) light, but PhyA and PhyB are the dominant players (Sharrock and Quail 1989, Smith 2000). Phytochromes exist in two interconvertible states; R light-absorbing inactive Pr form and FR light-absorbing biologically active Pfr form. PhyA accumulates in the dark and in FR light, but is degraded in the R light (Rockwell et al. 2006), whereas PhyB is comparatively stable and plays a major role in R light related photomorphogenic responses. The cryptochromes (CRY1/CRY2/CRY3) and phototropin photoreceptors sense the blue light or UV-A radiation (Lin et al. 1998, Christie 2007). The cryptochromes are flavoprotein photopigments containing the PHR domain which is essential for light absorption by non-covalently binding to chromophore flavin adenine dinucleotide (FAD). Upon absorption of photons, these proteins get photoexcited and lead to flavin photoreduction. The flavin can have an oxidized state (FAD), which is the ground state that can absorb blue light to convert into its signaling state called as semi-reduced semiquinone (FADH[•] or FAD⁻), then in the dark this semi-reduced state can be converted back to the oxidized state to complete the photocycle (Ahmad and Cashmore 1993, Lin et al. 1998, Banerjee et al. 2007, Chaves et al. 2011). Phototropins, on the other hand, are light activated serine/threonine protein kinases. They contain a repeated motif at the N-terminus known as the LOV (Light-oxygen-voltage-sensing) domain which gets photoexcited to cause receptor autophosphorylation and initiate phototropin signaling (Christie 2007). In addition, three new receptors have been identified for blue or UV-A light perception, namely ZEITLUPE (ZTL), FLAVIN-BINDING KELCH REPEAT F-BOX (FKF), and LOV KELCH REPEAT PROTEIN 2 (LKP2) (Suetsugu and Wada 2013). Lastly, the UV Resistance Locus 8 (UV8) is responsible for mediating the UV-B light signaling (Brown et al. 2005, Rizzini et al. 2011).

1.2.3 Light induced signaling

The light signaling pathway regulates the expression of chloroplast genes *psbD* and *psbA* that encode for the reaction center II components D1 and D2 proteins. The light photoreceptors perceive the photons and induce the expression of bZIP transcription factor ELONGATED HYPOCOTYL 5 (HY5) which is known to be a key modulator of signal transduction pathways in developmental processes (Oyama et al. 1997). CONSTITUTIVELY PHOTOMORPHOGENIC 1

(COP1) is an E3 ubiquitination ligase that targets numerous substrates for ubiquitination and proteolysis (Hoecker 2017). Upon receiving light, the CRY and UVR8 compete for binding of COP1 thereby preventing its interaction with the HY5 substrate (Lau et al. 2019, Xu 2019). HY5 directly or indirectly controls about one-third of the gene expression in *Arabidopsis* (Lee et al. 2007, Zhang et al. 2011). The transcription specificity of the plastid encoded polymerase (PEP) is modulated by sigma factors (SIG1 to SIG6) in *Arabidopsis*. The SIG5 sigma factor is induced by various stresses including high light and low temperature (Nagashima et al. 2004). Studies have shown that SIG5 is expressed in a HY5- and COP1-controlled manner where COP1-induced HY5 binds to SIG5 promoter elements and mediates its expression. After translation, the SIG5 protein is targeted to the chloroplast and promotes expression of *psbD* and *psbA* (Mellenthin et al. 2014). Besides, HY5 has been known to promote anthocyanin production, ROS homeostasis and regulate cold inducible genes (Catala et al. 2011).

1.2.4 High light induced alterations in photosynthetic machinery

The photosynthetic machinery comprises of membrane protein complexes, PS I and II situated in the thylakoids of chloroplasts. The two PS complexes are part of the electron transport chain and absorb different spectra of light. The PSII is vulnerable to excess of light and could lead to photodamage of the protein complex (Townsend et al. 2018). The PSII gets damaged when the available light energy exceeds the optimum amounts required to perform carbon fixation (Murata et al. 2007). This exposure to high light causes inhibition of PSII activity and the phenomenon is called photoinhibition (Powles 1984). However, plants have developed efficient repair mechanisms to repair photodamaged PSII that are necessary to overcome lethal effects of excess light (Leitsch et al. 1994, Aro et al. 2005). But the extent of photoinhibition depends on the rates of the PSII damage and its repair.

Photosystem II (PSII) is an oxidoreductase found in the thylakoid membrane and catalyzes oxidation of H_2O to O_2 and reduction of plastoquinone (PQ) to plastoquinol (PQH_2) (Dau et al. 2012). Due to leakage of electrons, the one-electron reduction of molecular oxygen produces superoxide (O_2^-) which acts as a precursor of most of the other ROS (Turrens 2003, Sharma et al. 2012). The two-electron oxidation of H_2O produces H_2O_2 which later forms O_2^- and HO^\bullet (Pospíšil 2016). ROS such as peroxides, superoxide hydroxyl radical, singlet oxygen and alpha-oxygen are formed as a natural byproduct of O_2 reduction processes and mediate cell signaling

and homeostasis (Hayyan et al. 2016, Waszczak et al. 2018). In cases of environmental stress such as high light or heat (Pospíšil 2016), the increase in ROS levels could cause significant damages to DNA, proteins, lipids and even cell death in the plants (Tripathy and Oelmüller 2012).

The photosynthetic organisms evolved adaptive mechanisms to cope with the harsh effects of excess light such as the movement of chloroplasts, reducing antenna size, decelerating the regulatory mechanisms, inducing alternative electron transport mechanisms and triggering the ROS scavenging pathways (Figure 2) (Jarillo et al. 2001, Frigerio et al. 2007, Okegawa et al. 2010). One of the most effective photoprotective mechanisms known is non-photochemical quenching (NPQ). It is triggered rapidly upon exposure to excess solar energy and protects plants against the excess light by converting the absorbed photons into heat (Niyogi et al. 1998). In this process the excitation energy is redistributed (state transitions) between the photosystems and xanthophyll cycle is activated (Bellafiore et al. 2005).

The current model of NPQ state transition mentions that the light-harvesting complex II (LHCII) undergoes a reversible phosphorylation in order to redistribute the imbalanced energy. State 1: When PSI is overexcited, the PQ pool is oxidized and the unphosphorylated LHCII antennae remain bound to PSII; Transient state: PSII excitation begins, the PQ pool gets reduced and STN7 kinase gets activated which leads to phosphorylation of LHCII releasing them from PSII; State 2: The mobile LHCII binds to PSI forming a super complex, which is required to establish the cyclic electron flow between PSI and the PQ pools generating ATP (Bellafiore et al. 2005, Minagawa 2013). Apart from state transition strategy, xanthophylls, a group of oxygenated carotenoids, bound to chlorophyll have been known to be essential for photoprotection. Under excessive light illumination, xanthophylls facilitate the de-excitation of singlet chlorophyll. The de-excitation is measured as NPQ of chlorophyll fluorescence which decreases with the thermal dissipation of heat. Studies in the photosynthetic alga *Chlamydomonas reinhardtii* revealed that α -carotene-derived xanthophylls such as lutein can mediate nonradiative dissipation of excess photons absorbed (Niyogi et al. 1997). As the NPQ is triggered, violaxanthin de-epoxidase converts violaxanthin (V) to zeaxanthin (Z) and antheraxanthin (A) via the xanthophyll cycle. It is known that Z can deactivate the excited singlet chlorophyll in PSII and protect membrane lipids in association with tocopherols (Wrona et al. 2004). Studies on high light grown plants confirmed a larger pool size of the pigments of xanthophyll cycle

(zeaxanthin, antheraxanthin and violaxanthin) compared to the low light grown plants (Demmig et al. 1988, Verhoeven et al. 1997).

The cyclic electron flow (CEF) also termed as cyclic photophosphorylation refers to the cyclic transfer of electrons within the PSI in photosynthetic organisms to synthesize ATP without generating NADPH and O₂. The CEF leads to the development of a pH gradient across the thylakoid membrane and this gradient induces the NPQ mechanism. Studies in tobacco leaves have confirmed that the activity of CEF-PSI increases upon high light stress and it induces the NPQ of chlorophyll fluorescence (Miyake et al. 2004).

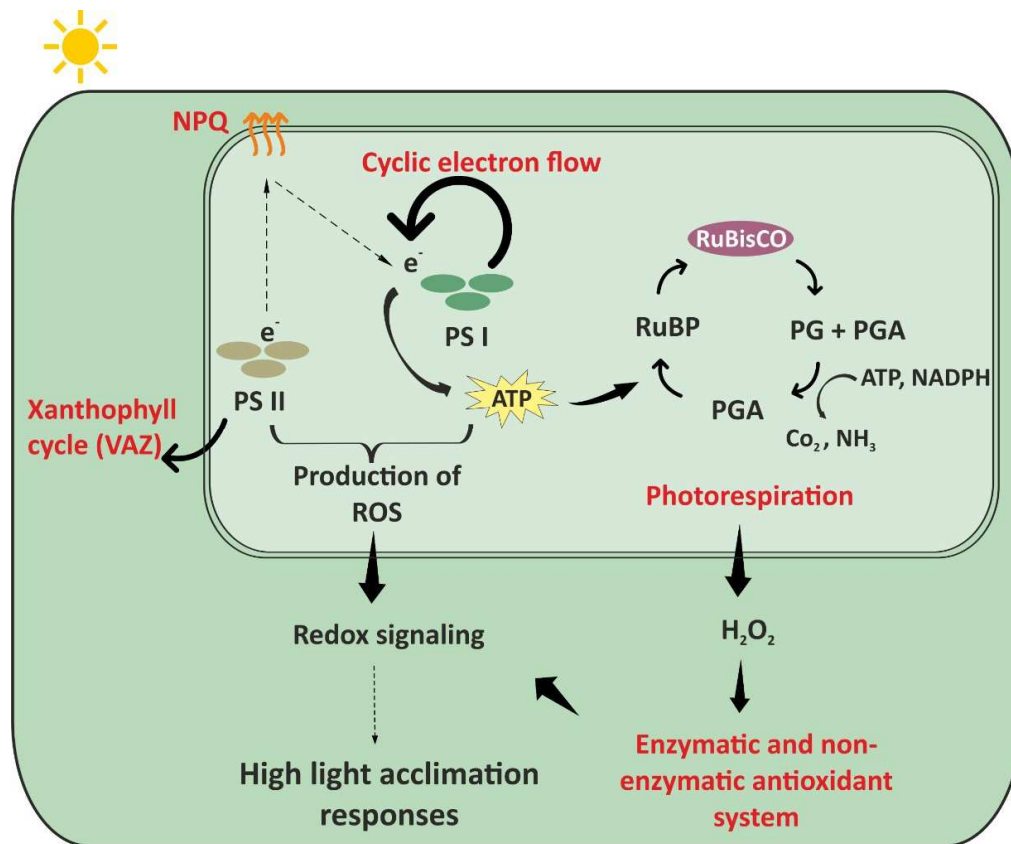


Figure 2. High light induced photoprotective mechanisms. High light induces responses via changes in the photosynthetic electron transport chain which triggers ROS production. The ROS scavenging system takes control of the ROS metabolism and affects the redox homeostasis to regulate short- and long-term high light responses. Alternatively, excess light energy is dissipated in the form of heat (NPQ) and produces ATP through CEF which is used in the process of photorespiration. NPQ, non-photochemical quenching; VAZ cycle, violaxanthin-antheraxanthin-zeaxanthin cycle; PSII and I, photosystem II and I; ATP, adenosine triphosphate; NADPH, reduced form of nicotinamide adenine dinucleotide phosphate; ROS, reactive oxygen species; RuPB, ribulose 1,5-bisphosphate; PG, 2-phosphoglycolate; PGA, 3-phosphoglycerate; Rubisco, ribulose-1,5-bisphosphate carboxylase/oxygenase. Source: Figure adapted from Szymańska et al. (2017).

Studies in tobacco and pea plants observed an increase in the levels of electron transport chain components, Ribulose-1,5-bisphosphate carboxylase/oxygenase (RuBisCO) and Calvin Cycle enzymes when exposed to high light irradiance (Evans 1987, Yamori et al. 2010). It was concluded that leaves exposed to excess light have a higher abundance of electron transport chain and CO₂ assimilation, which could indicate an involvement of photorespiratory pathway in high light acclimation (Yamori et al. 2010, Huang et al. 2014). Photorespiration is a process where RuBisCO enzyme oxygenates D-ribulose-1,5- bisphosphate (RUBP) into glycolate-2-phosphate and glycerate-3-phosphate (Ogren 1984). This process is considered to be wasteful as it does not produce sugars or ATP but rather consumes ATP and NADPH, and loses fixed carbon in the form of CO₂ (Busch et al. 2013). The pathway is known to serve as an energy sink thereby preventing the over reduction of electron transport chain under stress conditions (Wingler et al. 2000). The glycolate-2-phosphate is a potential inhibitor of chloroplast function (Anderson 1971) and can be converted into glycerate-3-phosphate through photorespiration. Since photorespiration occurs in three organelles, namely chloroplast, peroxisomes and mitochondria, the process also produces glycine in mitochondria that acts as a precursor of glutathione and glycine betaine, known to play role in stress protection (Sakamoto and Murata 2002).

1.3 Retrograde signaling

The chloroplast plays a major role in sensing environmental changes and the photosynthetic activities take place in this organelle to provide energy, oxygen and reduced carbon. Plants exposed to stress experience decreased photosynthetic efficiency followed by reduced respiration rate which ultimately causes a lack of cellular energy. Any changes in the developmental or environmental state of the plants can have a profound effect on the transcript profiles of nuclear genes. In order to survive in the stress conditions, plants need to restore their homeostasis by altering the gene expression and metabolism towards acclimation.

The endosymbiotic theory of evolution states that the mitochondria, plastids and other organelles of the eukaryotic cells have descended from the prokaryotic organisms. These were considered to be integrated into the ancestral eukaryotic cells through the process of

endosymbiosis (Goksoyr 1967). The nucleus of the host contained major part of its genome required to control most of the cell functions. But a small part of their genome was retained in each organelle that encodes proteins necessary for the organelle function (Dyall et al. 2004). To coordinate the gene expression, nucleus and organelles communicate with each other and the signals sent from the nucleus to organelles are known as anterograde signals. If the plant experiences any deviations from the optimum conditions which leads to redox imbalance, the chloroplast and mitochondria are able to sense it and transmit signals to the nucleus through retrograde signaling cascades (Surpin and Chory 1997, Surpin et al. 2002). The chloroplast is susceptible to oxidative damage due to its demand to reduce NADP^+ and accumulate excess energy at PSII (Baier and Dietz 2005). Lincomycin causes inhibition of plastid translation which hinders the expression of nuclear encoded photosynthesis associated nuclear genes (*PhANGs*). The studies with this antibiotic indicate that the plastid transmits retrograde signals to the nucleus in order to regulate the nuclear gene expression (Gray et al. 2003). Norflurazon is another important herbicide that is an inhibitor of the phytoene desaturase which produces β -carotenoids. This action of norflurazon inhibits the carotenoid biosynthetic pathway as well as *PhANGs* expression which clearly indicates that plastid can communicate with the nucleus in order to regulate *PhANG* expression (Woodson et al. 2011).

Studies with WT *Arabidopsis* grown in the presence of norflurazon suggest a downregulation of *PhANG* expression as the chloroplast biogenesis is blocked. To study the pathway of retrograde signaling, *genomes uncoupled (gun)* mutants have been studied since these mutants have impaired retrograde communication (Susek et al. 1993). Unlike WT, these mutants de-repressed *PhANGs (LhcbI)* even in the presence of norflurazon and were concluded to affect the plastid to nucleus signaling (Susek et al. 1993, Larkin 2014). The mutated loci in the *gun2*, *gun3*, *gun4* and *gun5* mutants code for heme oxidase, phytochromobilin synthase, Mg-chelatase regulator and H-subunit of Mg-chelatase, respectively (Mochizuki et al. 2001, Larkin et al. 2003, Strand et al. 2003). *GUN1* encodes for a nuclear encoded and plastid localized PPR protein. This protein regulates tetrapyrrole synthesis pathway, plastid gene expression and photosynthetic electron transport related signals (Koussevitzky et al. 2007). Chlorophyll is a tetrapyrrole molecule and it is produced through the tetrapyrrole biosynthetic pathway involving GUN2 to GUN6 factors (Brzezowski et al. 2015). Chlorophyll molecule constitutes a porphyrin ring having four N atoms and a central Mg^{2+} ion which is inserted by the Mg-chelatase/CHLH enzyme i.e. GUN5 (Mochizuki et al. 2001). Mg-protoporphyrin IX (Mg-

Proto IX) is a precursor of chlorophyll and is known to accumulate in the chloroplast during stress conditions and to negatively regulate *PhANG* expression (Strand et al. 2003, Zhang et al. 2011). Apart from controlling the nuclear gene expression, Mg-Proto IX also controls plastid encoded photosynthetic genes by altering the expression of sigma factors that are required for efficient transcription mediated by PEP (Ankele et al. 2007).

1.3.1 Retrograde signaling in cold stress

A recent study claims that the accumulation of Mg-Proto IX induces the cyanide resistant respiration which is known to facilitate cold stress tolerance and Mg-Proto IX also enhanced antioxidant enzyme activities and increased glutathione levels during cold stress (Zhang et al. 2016). Further studies in tobacco lines showed that changes in Mg-Proto IX due to Mg Proto IX methyl transferase correlated with similar changes in levels of *PhANGs* (Brzezowski et al. 2015). Apart from the role of Mg-chelatase in tetrapyrrole biosynthesis and retrograde signaling, it is known that CHLH is associated with the chloroplast envelope which indicates that it could possibly sense the changes in membrane fluidity caused due to low temperature. Studies have shown that two lines with mutant alleles of CHLH namely *gun5-1* and *cch* show impaired cold acclimation abilities. The mutants also showed impaired protein translation in conditions of low temperatures, increased levels of *CBF* transcripts but lower levels of *COR15a*, *COR47* and *COR78* genes which indicates that a functional chloroplast is necessary for cold acclimation process (Kindgren et al. 2015). GUN1 also plays an important role in chloroplast protein homeostasis; it controls the accumulation of chloroplast ribosomal proteins S1 (PRPS1) and interacts with components of tetrapyrrole biosynthesis pathway including CHLH which are known to activate the retrograde signaling. The association of PRPS1 and CHLH with protein complexes through GUN1 indicates its role in retrograde signaling (Tadini et al. 2016). A recent study demonstrated that FUG1, a chloroplast translation initiation factor IF-2 is required for effective cold acclimation since it is a component of the plastid translation machinery. It was also shown that due to reduced levels of FUG1, GUN1 was able to facilitate cold acclimation implying its role in plastid proteostasis during cold stress (Marino et al. 2019)

1.3.2 Excess light induced retrograde signals

Studies with meta-analysis of transcriptomes have confirmed that about 10% to 20% of chloroplast localized proteins could have a role in plant stress responses (Kmieciak et al. 2016). The plastoquinone redox state changes rapidly in response to excess light and causes alterations in the gene expression (Fey et al. 2005). SAL1, a bifunctional protein with nucleotidase/phosphatase activity, is encoded in the nucleus and phosphonucleotide 3'-phosphoadenosine 5'-phosphate (PAP) is regulated by SAL1. PAP is a retrograde signal, produced in plastids and is responsible for inhibiting exoribonucleases XRN2, 3 and 4 that mediate degradation of aberrant RNAs (Gy et al. 2007). SAL1 negatively regulates PAP which is known to accumulate in response to high light and drought conditions (Estavillo et al. 2011). Methylerythritol cyclodiphosphate (MEcPP) is the precursor of carotenoids and is known to elicit expression of nuclear-encoded plastidial proteins related to environmental stress (Xiao et al. 2012). MEcPP is a retrograde-signaling metabolite which is also known to coordinate stress-responsive genes in high light stress (Kleine and Leister 2016). Research reveals that 81% of high light responsive genes required photosynthetic electron transport (PET) for their expression and 68% of these genes were ABA-responsive indicating that both the signals were necessary for the expression of high light responsive genes (Bechtold et al. 2008). Retrograde regulation uses alternate signaling pathways and modifies the signaling patterns in response to excess of light. A time-dependent study suggested that oxylipins, metabolites and redox cues predominantly control the light acclimation process (Alsharafa et al. 2014). *MAP kinase 6* (*MAPK6*) and *APETALA2/ETHYLENE RESPONSE FACTOR* (*AP2/ERF*) transcripts are also known to show induced expression in response to high light treatment indicating the role of retrograde signaling in light stress response (Kleine and Leister 2016).

1.4 Non-coding RNAs in abiotic stress

1.4.1 Long non-coding RNAs and their mode of action

LncRNAs are longer than 200 nt and possess 5' capping and 3' polyadenylation similar to mRNAs (Ransohoff et al. 2018). Often, they are expressed in a tissue-specific or stimulus-dependent manner and their sequences are not conserved across different plant species (Wang et al. 2011). Also, certain non-polyadenylated lncRNAs were shown to be induced by abiotic stress conditions and to be involved in the regulation of gene expression (Di et al. 2014).

LncRNAs exert their function by different modes of action, for instance, lncRNAs restrain the accessibility of regulatory proteins to nucleic acids by serving as decoys (Wang and Chang 2011). Another mechanism is presented by the well-characterized lncRNA *IPS1*, which acts as a non-cleavable competitor for the *PHO2* (*Phosphate 2*) mRNA that is targeted by miR399 for degradation (Franco-Zorrilla et al. 2007). Several other lncRNAs that may act as target mimics of miRNAs have been predicted using bioinformatics tools (Wu et al. 2013). LncRNAs also cause epigenetic alterations such as histone modifications as identified in the vernalization process where prolonged cold stress leads to epigenetic silencing of the *FLC* locus that controls flowering time (Swiezewski et al. 2009, Csorba et al. 2014). Here, the lncRNA cold induced long antisense intragenic RNA (*COOLAIR*) interacts with a polycomb repressive complex (PRC2) and subsequently causes histone methylation and silencing of the *FLC* locus. LncRNAs also assist in *de novo* methylation of DNA cytosine residues and cause transcriptional silencing of genes by RdDM (Matzke and Mosher 2014, Au and Dennis 2017). Another mode of action of lncRNAs is presented by *HIDDEN TREASURE 1* (*HID1*) that positively regulates red light mediated photomorphogenesis by repressing *PHYTOCHROME-INTERACTING FACTOR 3* (*PIF3*) encoding a transcription factor that inhibits red light responses (Wang et al. 2014).

1.4.2 Small RNAs in abiotic stress

Small RNAs are 21-24 nt in size and efficiently regulate mRNA transcript levels, mRNA translation and also mediate epigenetic silencing (Mallory and Vaucheret 2006). The two main classes of small RNA are microRNAs (miRNAs) that are processed from single-stranded precursors forming a partially double-stranded hairpin structure and small interfering RNAs (siRNAs) that are generated from double-stranded RNA precursors.

a) microRNA biogenesis

MicroRNA biogenesis occurs in a multistep fashion starting with the transcription of nuclear encoded *MIR* genes by RNA Polymerase II to produce a 5' capped and poly A-tailed primary miRNA transcript (pri-miRNA) (Vazquez et al. 2008). A dicing complex containing the ribonuclease III-like enzyme DICER-LIKE1 (DCL1) and accessory proteins such as Hyponastic Leaves 1 (HYL1) and Serrate (SE) precisely excise a miRNA duplex from the double-stranded hairpin region. Subsequently, the 3' ends of the duplex are methylated by HEN1 (Hua Enhancer 1) to increase miRNA stability (Bin Yu et al. 2005) and the miRNA duplex is translocated to the

cytoplasm by the exportin HASTY (HST) (Sunkar and Zhu 2007). The mature miRNA is loaded onto an ARGONAUTE (AGO) protein that is a part of the RNA induced silencing complex (Pratt and MacRae 2009) and guides the RISC to pair with target RNA sequences to mediate their cleavage or mediate translational inhibition (Wightman et al. 1993, Carmell 2002, Eulalio et al. 2008).

b) miRNAs in abiotic stress

Studies have shown that plant miRNAs play important roles in a wide range of biological processes including development and stress adaptation (Lima et al. 2012). To uncover the changes in miRNA repertoire in response to stress, small RNA libraries were generated from plants subjected to diverse stress conditions and analyzed by RNA sequencing approaches (Baev et al. 2014, Song et al. 2017). Additional approaches such as *MIR* overexpression (Ma et al. 2015), miRNA target mimicry (Franco-Zorrilla et al. 2007), the generation and expression of miRNA-resistant RNA target RNAs (Li and Millar 2013) were applied to study the impact of stress-related miRNA on stress adaptation.

Previous studies in *Arabidopsis* reported differential upregulation of isoforms of miR171 at low as well as elevated temperature stress (Liu et al. 2008), miR171 was found to target *SCARECROW-LIKE6-III (SCL6-III)* and *SCL6-IV* transcripts coding for GRAS family transcription factors (Mahale et al. 2013, Zhang et al. 2014). MiR408 was recognized to be induced by cold and other abiotic stresses. It regulates transcripts encoding phytoeyanin family proteins (cupredoxin, plantacyanin and uclacyanin) which act as electron transfer shuttles between proteins (Rienzo et al. 2000). It also regulates transcripts of phytophenol oxidases called Laccases (LAC3, LAC12 and LAC13) (Pilon 2008) which are known to oxidize flavonoids during seed development and environmental stress (Pourcel et al. 2007). Laccases are essential to maintain cell wall functions and are important to regulate biological pathways necessary for abiotic stress responses (Liang et al. 2006). Recent investigations validated the involvement of miR394 and one of its targets *LEAF CURLING RESPONSIVENESS (LCR)* in regulation of leaf development (Song et al. 2012, Knauer et al. 2013) and mediating responses to cold, salt and drought stress in an ABA dependent manner (Song et al. 2013, Song et al. 2016). In *Arabidopsis*, miR397 was shown to positively regulate cold tolerance via the CBF-dependent signaling pathway and overexpression of miR397a caused increased *CBF* transcript levels leading to an induction of cold-responsive *COR* genes (Dong and Pei 2014).

c) siRNAs derived from other RNA classes

In contrast to miRNAs, siRNAs are generated from dsRNA molecules and are sub-classified based on their specific biogenesis pathways. A subset of siRNAs are the natural antisense transcript derived short interfering RNAs (nat-siRNAs) which are produced from overlapping regions of antisense transcripts transcribed by RNA polymerase II (Kumar and Carmichael 1998). It has been suggested that about 9% of all *Arabidopsis* genes overlap and have the potential to generate *cis*-natural antisense transcripts (*cis*-NATs) (Werner and Berdal 2005). It is known that siRNA producing transcripts are regulated with the help of siRNA mediated RNA silencing which greatly affects their transcript levels. Studies in *Arabidopsis* found light responsive lncNATs (long non-coding natural antisense transcript) having one lncRNA in a pair of NATs. A large number of lncNAT were differentially expressed after 6 h of continuous white light and the study concluded that the transcription of light regulated NATs change depending on the histone H₃ acetylation (Wang et al. 2014). Recent studies have found involvement of lncRNAs in light regulated processes. lncRNA *HIDDEN TREASURE 1 (HID1)* was found to act through PIF3 which is a key repressor of photomorphogenesis (Wang et al. 2014). Another lncRNA *CDF5 LONG NONCODING RNA (FLORE)* is a NAT of *CYCLING DOF FACTOR 5 (CDF5)*. *FLORE* caused repression of *CDF5* gene and promoted transcription of *FLOWERING LOCUS T (FT)* which is involved in promoting flowering in favorable environmental conditions (Henriques et al. 2017). lncRNAs can be processed to yield siRNAs (Affymetrix and Cold Spring Harbor Laboratory 2009) or they can bind with sRNAs to modulate their activity. In *Arabidopsis*, long ncRNA *IPS1 (INDUCED BY PHOSPHATE STARVATION 1)* binds with miR399 in a non-cleavable manner and sequesters it to inhibit miRNA interaction with its target transcripts. This phenomenon of target mimicry by *IPS1* was observed upon phosphate starvation (Franco-Zorrilla et al. 2007).

NATs also have a capability to generate siRNAs from their overlapping regions and depending on their genomic loci, can be divided into two; *cis*-NATs, that are transcribed from the complementary regions of the same genomic loci and *trans*-NATs that are transcribed from different genomic loci and could have sequence complementarity to more than one transcripts (Lavorgna et al. 2004). The two overlapping transcripts can undergo several regulatory events such as RNA interference (RNAi) where the two transcripts can be cleaved into endo-siRNAs with the help of Dicer like proteins, reducing the transcript levels. A detailed overview of possible mechanisms that produce siRNAs from *cis*-NATs are illustrated in Figure 3. The two

transcripts can undergo transcriptional interference where the transcription machinery associated with one of the transcripts hinders the transcription of the other, thereby affecting transcript levels of one or both the transcript. The antisense transcript can methylate the regions of sense transcript in the genome thereby reducing the transcription of sense transcript (Lavorgna et al. 2004). A high salinity responsive nat-siRNA was first identified in

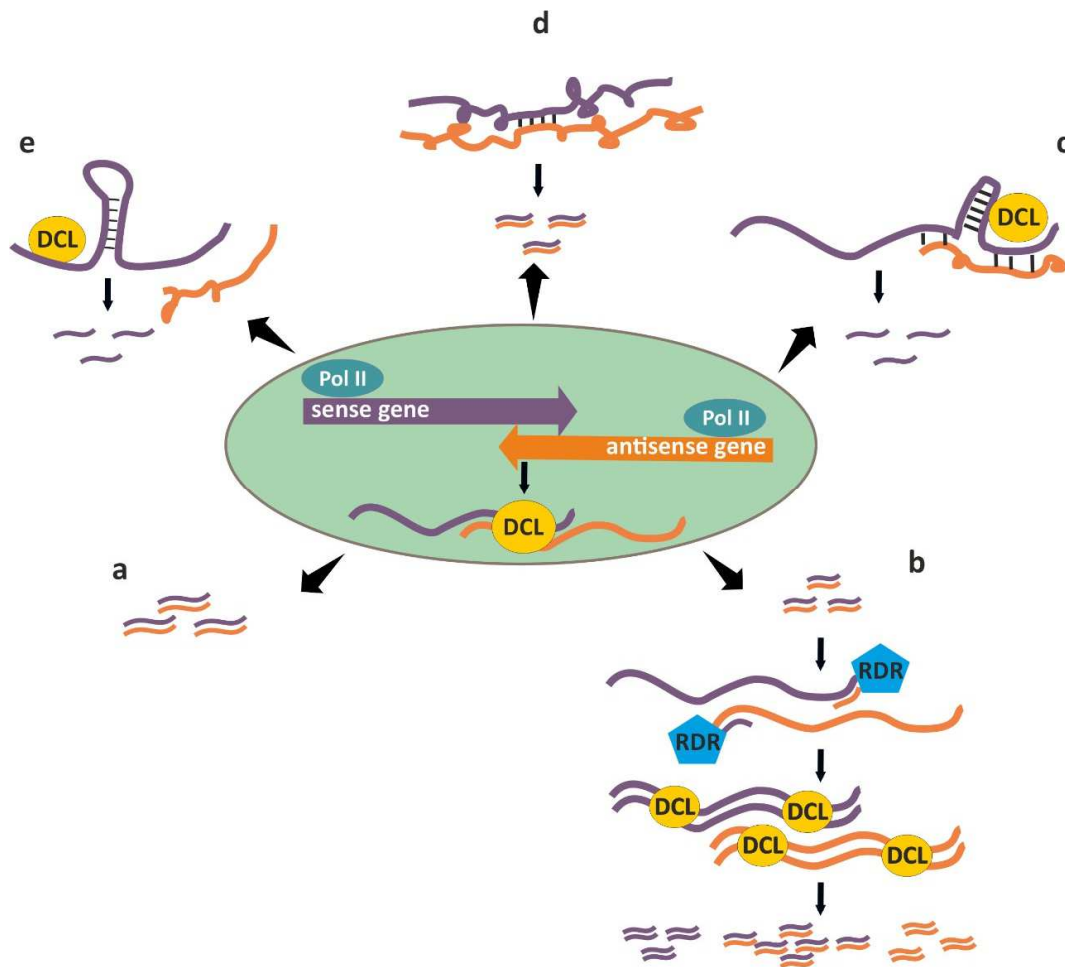


Figure 3. Mechanisms of siRNA production from *cis*-NATs. The sense and antisense transcripts pair up and (a) dsRNAs are recognized by transcriptional machinery to produce nat-siRNAs (b) dsRNA produces nat-siRNAs, the nat-siRNAs further bind to the single-stranded transcript and using these transcripts as templates produce another dsRNA which are processed into secondary nat-siRNAs (c) DCL recognizes a secondary structure in one of the transcripts to produce site-specific nat-siRNAs (d) both transcripts form a complex secondary structure recognized by DCL to produce nat-siRNAs (e) On the other hand, these transcripts do not undergo pairing, rather one of the transcript forms a secondary structure and is recognized by DCL to produce siRNAs. Source: Figure modified from Zhang et al. (2013)

Arabidopsis where the constitutively expressed gene *delta-pyrroline-5-carboxylate dehydrogenase (P5CDH)* and the salt induced gene *Similar to Radicle Induced Cell Death One 5 (SRO5)* are encoded on opposing strands of an overlapping genomic region. The *SRO5* mRNA

is induced by salt stress and forms a dsRNA with the constitutively expressed *P5CDH* transcript and DCL2 processes a distinct 24 nt nat-siRNA from the dsRNA region. The generated nat-siRNA targets the *P5CDH* transcript and mediates its cleavage thereby suppressing proline degradation and inducing salinity tolerance (Borsani et al. 2005). In addition to nat-siRNAs produced from *cis*-NATs, *trans*-NATs can also be generated when antisense-mediated pairing of transcripts occurs that are derived from non-overlapping genes (Wight and Werner 2013). The formation of these dsRNAs takes place in diverse trans-combinations i.e. between long non-coding RNAs, pre-tRNAs, transposable elements, protein coding transcripts and homologous pseudogenes (Wang et al. 2005, Yuan et al. 2015).

The mature tRNAs are 73 to 90 nucleotides (nt) in length and are known to produce 18–40 nt tRNA-derived small RNAs (tsRNAs) in bacteria and eukaryotes. Studies identified ~20 nt small tRNA-derived fragments (tRFs) and ~30 nt tRNA-derived halves (tRHs) which were produced from pre-tRNAs or mature tRNAs using RNA Pol III. Pre-tRNAs can produce 5' leader tRFs and 3' U tRFs (or 3' U trailer tRF) whereas mature tRNAs generate 5' tRFs from the D-loop and 3' tRFs from the T-loop. Initially, it was thought that these tsRNAs are random degradation products of endonucleases but over the last few years studies suggest their role in cell proliferation, tumor formation, stress response, intergenerational epigenetic inheritance, and genome stability maintenance (Zhu et al. 2018, Zhu et al. 2019).

Expression of tRNA derived sRNAs has been found in plants. To identify phosphate deficiency responsive sRNAs in *Arabidopsis*, small RNA profiles of normal and Pi deficient plants were analyzed. They found about 30% sRNAs in roots and about 5% in shoots comprised of 16-27 nt tsRNAs. Especially 5' tRF-Gly^{TCC} represented about 80% of total tsRNAs which indicates biogenesis of tsRNAs in response to Pi deficiency (Hsieh et al. 2009). In barley shoots, in the presence and absence of phosphorous, tsRNAs from Gly^{TCC} –tRNA comprised 58% of total sRNAs whereas in rice, 5' tRF-Ala^{AGC} represented 82% of total tsRNA (Hackenberg et al. 2013). In Chinese cabbage, it was found that tsRNAs were being produced from chloroplast genome (csRNAs) which mostly constituted the 5' parts of the molecules. It was observed that in heat stressed seedlings, the longer csRNAs (29–32 nt) decreased whereas the shorter ones (16–25 nt) increased. Two csRNAs originating from chloroplast tRNA^{Ala} were the most prominent. The researchers concluded that reduction in longer csRNAs in response to heat could mediate maintenance of subcellular structures and photosynthetic capacity of chloroplasts (Wang et al. 2011). These studies revealed that under a certain condition or a developmental stage, one or

two tsRNA species were abundant. They found abundance of 5' tRFs in most of the plant species and the abundance was induced in the presence of stress treatment. The observed tsRNA abundance was unrelated to the copy number of the tRNA gene and plastid encoded tRNA genes produced a large amount of tsRNAs. The stability of the tRNA structures plays an important role in tRFs biogenesis.

In humans, reduced levels of Lupus autoantigen (La) protein which stabilizes RNA pol III caused transport of misfolded tRNAs into the cytoplasm. Later, Dicer was found to cleave these immature tRNA transcript fragments and incorporate them into AGO proteins (Hasler et al. 2016). Such evidence suggests the association of tRF expression with stress. Another possibility is that they are loaded into the AGO complex and could mediate posttranscriptional regulation (Loss-Morais et al. 2013). This could also indicate the hijacking of RNAi pathways and restricting the incorporation of miRNAs and other sRNAs. Due to their abundance, tRFs on one hand, can exhaust the availability of AGO complexes for other small RNAs and on the other hand, could be free in the cytoplasm to interact with the ribosome and interfere with translation (Martinez 2018). A recent study in soybean revealed that tRFs can act as signal molecules in modulating host nodulation and three tRFs were confirmed to regulate host genes associated with nodule initiation by hijacking the AGO proteins (Ren et al. 2019). It has been known that tRFs target numerous protein encoding mRNAs in plants and their abundance correlates with reduced transcripts for some of their predicted targets (Wang et al. 2016).

In Yeast, a wide range of tRNA halves and rRNA fragments were detected when it was subjected to oxidative stress. The results indicated the occurrence of tRNA processing and involvement of ribosomes in case of stress which indicates their potential function in protein biosynthesis (Thompson et al. 2008, Gebetsberger et al. 2012). In animals, tRFs are incorporated into the AGO protein which mediates RNA interference. Similarly, in rice and *Arabidopsis*, sequenced libraries of immunoprecipitated AGO proteins (AGO-IP) proved the interaction between AGOs and tRFs (Loss-Morais et al. 2013, Alves et al. 2017). In plants such as *Physcomitrella*, 19 nt tRFs derived from 5' and 25 nt tRFs derived from 3' arising from m tsRNA-Glu^{TTC} and Asp^{GTC} respectively were most abundant. In case of *Chlamydomonas*, 19, 20 nt tRFs derived from 5' and 23, 24 nt tRFs derived from 3' were found in large amounts. Recent studies revealed that 19 nt tRFs suppressed the expression of transposable elements through AGO specific for miRNAs (Martinez et al. 2017, Zhu et al. 2018).

In addition, similar to *MIR* precursors some transposable element derived transcripts can form a stem-loop structure from which siRNAs can be processed (Piriyapongsa and Jordan 2008). Research in last few years confirmed the occurrence of sRNAs from transposons known as easiRNAs (Creasey et al. 2014) which have the potential to affect non-TE transcripts by sequence complementarity (Cho 2018). Transposable elements also encode lncRNAs and there is a rising evidence that environmental factors lead to altered chromatin organization and the expression of lncRNAs that may have functions in the adaptation to altered environmental conditions that can even be inherited (Wang et al. 2017). This study in *Arabidopsis* reports on a transposable element-derived TE-lincRNA1195 that was shown to be involved in the ABA response and to contribute to abiotic stress adaptation. In *Arabidopsis* pollen grains, the transcriptional activation of TE resulted in their degradation into siRNAs which further regulated other targets (Slotkin et al. 2009).

Trans-acting siRNAs (ta-siRNAs) are endogenous plant-specific small RNAs that are capable of acting in trans and have the potential to repress distinct mRNA transcripts. The production of ta-siRNAs is triggered by the cleavage of primary *TAS* transcripts by specific miRNAs. The cleaved transcripts are converted into dsRNA by RDR6 and processed by DCL4 into 21 nt ta-siRNAs in a phased manner (Peragine et al. 2004, Vazquez et al. 2004). In *Arabidopsis*, several *TAS* families (*TAS1*, *TAS2*, *TAS3*, *TAS4*) have been identified that are mainly classified according to the miRNA mediating their initial cleavage (Allen et al. 2005, Rajagopalan et al. 2006, Howell et al. 2007). Ta-siRNAs have been shown to regulate plant development (Guan et al. 2017) and recent studies also suggest a role of ta-siRNAs in environmental stress adaptation. For example, 14 hypoxia-responsive ta-siRNAs have been identified in *Arabidopsis* that are processed from *TAS1a*, *b*, *c*, *TAS2* and *TAS3a* precursors (Moldovan et al. 2010). The expression of a *TAS1*-derived ta-siRNA and its target transcript encoding heat-induced *TAS1* target (HTT4) were shown to be regulated by temperature shifts (Kohei 2010). Furthermore, the generation of *TAS4*-derived ta-siRNAs was shown to be triggered by miR828 under phosphate deficiency (Hsieh et al. 2009). Pseudogenes are also known to promote the processing of mRNAs into siRNAs in mammalian system (Tam et al. 2008). For example, the class of *trans*-NATs that are produced from pseudogenes can regulate their homologous protein encoding transcript levels (Zhang et al. 2013).

In our study, we have used RNA sequencing to uncover the cold, high light and retrograde signaling-responsive non-coding RNA repertoire in *Arabidopsis* and to study their role in the regulation of various target RNAs. We subjected *Arabidopsis* plants to cold and high light treatments for 3 h, 6 h and 2 d. To identify sRNAs involved in retrograde signaling, we treated WT plants and two additional mutants *gun1* and *gun5* with norflurazon. We sequenced mRNAs and sRNAs libraries from the treated plants and analyzed the raw sequencing data to find the differential expression of mRNA/lncRNAs and sRNAs. The putative correlations between differentially expressed small RNAs and their protein coding targets was performed. We found the involvement of miRNAs, sRNAs derived from *cis*- and *trans*-NAT gene pairs and sRNAs derived from lncRNAs in response to cold, high light and NF treatment. Overall, our study provides the fundamental knowledge related to the role of non-coding RNAs in response to different abiotic stresses.

2 Results

2.1 Publication 1 (Tiwari et al. 2020)

Identification of small RNAs during cold acclimation in *Arabidopsis thaliana*.

Bhavika Tiwari, Kristin Habermann, M. Asif Arif, Heinrich Lukas Weil, Antoni Garcia-Molina, Tatjana Kleine, Timo Mühlhaus & Wolfgang Frank

BMC Plant Biology volume 20, Article number: 298 (2020)

<https://doi.org/10.1186/s12870-020-02511-3>

RESEARCH ARTICLE

Open Access

Identification of small RNAs during cold acclimation in *Arabidopsis thaliana*



Bhavika Tiwari¹, Kristin Habermann¹, M. Asif Arif¹, Heinrich Lukas Weil², Antoni Garcia-Molina³, Tatjana Kleine³, Timo Mühlhaus² and Wolfgang Frank^{1*}

Abstract

Background: Cold stress causes dynamic changes in gene expression that are partially caused by small non-coding RNAs since they regulate protein coding transcripts and act in epigenetic gene silencing pathways. Thus, a detailed analysis of transcriptional changes of small RNAs (sRNAs) belonging to all known sRNA classes such as microRNAs (miRNA) and small interfering RNA (siRNAs) in response to cold contributes to an understanding of cold-related transcriptome changes.

Result: We subjected *A. thaliana* plants to cold acclimation conditions (4 °C) and analyzed the sRNA transcriptomes after 3 h, 6 h and 2 d. We found 93 cold responsive differentially expressed miRNAs and only 14 of these were previously shown to be cold responsive. We performed miRNA target prediction for all differentially expressed miRNAs and a GO analysis revealed the overrepresentation of miRNA-targeted transcripts that code for proteins acting in transcriptional regulation. We also identified a large number of differentially expressed *cis*- and *trans*-nat-siRNAs, as well as sRNAs that are derived from long non-coding RNAs. By combining the results of sRNA and mRNA profiling with miRNA target predictions and publicly available information on transcription factors, we reconstructed a cold-specific, miRNA and transcription factor dependent gene regulatory network. We verified the validity of links in the network by testing its ability to predict target gene expression under cold acclimation.

Conclusion: In *A. thaliana*, miRNAs and sRNAs derived from *cis*- and *trans*-NAT gene pairs and sRNAs derived from lncRNAs play an important role in regulating gene expression in cold acclimation conditions. This study provides a fundamental database to deepen our knowledge and understanding of regulatory networks in cold acclimation.

Keywords: *Arabidopsis thaliana*, Cold acclimation, Small non-coding RNA, Gene regulation, RNA sequencing, miRNA-transcription factor network

Background

Plants are severely affected by dynamic and extreme climatic conditions. Changes in temperature is one of the most critical factors for plants to exhibit flourishing growth and low temperature stress globally influences the development of plants and restricts their spatial distribution affecting the total agricultural productivity [1].

Although most plant species have evolved a certain degree of cold tolerance, deviations from the optimal conditions lead to restructuring at the gene level enabling the plant to cope with the environmental fluctuations [2].

Plant cells perceive cold stress by detecting reduced cell membrane fluidity that triggers specific signaling cascades [3] to induce the expression of cold responsive genes [4]. Currently, the best characterized pathway is the C-repeat binding factor (CBF)-dependent signaling pathway in which OPEN STOMATA 1 (OST1)/SNF1-related protein kinase 2 (SnRK2.6/SnRK2E) is released from type 2C protein phosphatase (PP2Cs) in response

* Correspondence: wolfgang.frank@lmu.de

¹Department of Biology I, Plant Molecular Cell Biology, Ludwig-Maximilians-Universität München, LMU Biocenter, Großhaderner Str. 2-4, 82152 Planegg-Martinsried, Germany

Full list of author information is available at the end of the article



© The Author(s). 2020 Open Access This article is licensed under a Creative Commons Attribution 4.0 International License, which permits use, sharing, adaptation, distribution and reproduction in any medium or format, as long as you give appropriate credit to the original author(s) and the source, provide a link to the Creative Commons licence, and indicate if changes were made. The images or other third party material in this article are included in the article's Creative Commons licence, unless indicated otherwise in a credit line to the material. If material is not included in the article's Creative Commons licence and your intended use is not permitted by statutory regulation or exceeds the permitted use, you will need to obtain permission directly from the copyright holder. To view a copy of this licence, visit <http://creativecommons.org/licenses/by/4.0/>. The Creative Commons Public Domain Dedication waiver (<http://creativecommons.org/publicdomain/zero/1.0/>) applies to the data made available in this article, unless otherwise stated in a credit line to the data.

to elevated abscisic acid (ABA) [5] levels to activate the upstream transcription factor (TF) inducer of CBF expression (ICE1) by phosphorylation [6]. ICE1 further induces the expression of several CBF/ dehydration responsive element binding factors (DREB) TFs that bind to the cold response sensitive TFs/dehydration responsive elements (CRT/DRE) promoter elements of cold-responsive (*COR*) genes, which act in the adaptation to low temperature conditions [7, 8]. Another ABA-dependent pathway that controls *COR* gene expression is mediated through the binding of bZIP TFs known as ABRE-binding factors (ABFs) to ABA-responsive promoter elements [9, 10]. Furthermore, studies have shown that DREB/CBF can physically interact with ABFs to express ABA responsive genes [11]. The CRT/DRE and ABRE regions are present in many cold-inducible genes and indicate a tight link between the ABA-dependent pathway and the ICE-CBF-COR pathway [10].

In addition to the TF mediated transcriptional control, epigenetic modifications control the gene expression in cold stress mainly by chromatin remodeling altering the accessibility of chromatin for the transcription machinery [12, 13]. Besides the transcriptional control, gene regulation involves regulatory processes at the post-transcriptional and post-translational level [14]. An important post-transcriptional control of gene expression is mediated by non-coding RNAs (ncRNAs) that cannot be translated into functional proteins. ncRNAs are classified into long non-coding RNAs (lncRNAs) that contribute to the control of gene expression involving transcriptional and post-transcriptional pathways [15] and sRNAs binding to reverse complementary target RNAs to confer target RNA cleavage or translational inhibition [16] or they interfere with transcription via epigenetic mechanisms such as RNA-directed DNA methylation (RdDM) [17].

lncRNAs are longer than 200 nt and possess 5' capping and 3' polyadenylation similar to mRNAs [18–20]. lncRNAs exert their function by different modes of action, for instance lncRNAs restrain the accessibility of regulatory proteins to nucleic acids by serving as decoys [21]. Another mechanism is presented by the well characterized lncRNA Induced by Phosphate Starvation1 (*IPS1*), that acts as a non-cleavable competitor for the *Phosphate 2* (*PHO2*) mRNA that is targeted by miR399 for degradation [22]. lncRNAs also cause epigenetic alterations such as histone modifications as identified in the vernalization process where prolonged cold stress leads to epigenetic silencing of the Flowering locus C (*FLC*) that controls flowering time [23, 24]. Here, the lncRNA cold induced long antisense intragenic RNA (*COOLAIR*) interacts with a polycomb repressive complex (PRC2) and subsequently causes histone methylation and silencing of the *FLC* locus. lncRNAs also assist in de novo methylation of DNA cytosine residues and cause transcriptional silencing of genes by RdDM [25, 26].

Small RNAs (sRNA) are 21–24 nt in size and efficiently regulate mRNA transcript levels, translation and also mediate epigenetic silencing [27]. The two main sRNA classes are microRNA (miRNAs) that are processed from single stranded precursors forming a partially double-stranded hairpin structure and small interfering RNAs (siRNAs) that are generated from double-stranded RNA precursors. miRNA biogenesis occurs in a multi-step fashion starting with the transcription of nuclear encoded *MIR* genes by RNA polymerase II to produce a 5' capped and polyA-tailed primary miRNA transcript (pri-miRNA) [28]. The dicing complex containing Dicer-like1 (DCL1) and its accessory proteins Hyponastic Leaves 1 (HYL1) and Serrate (SE) excise a miRNA duplex from the double stranded hairpin structure that is translocated to the cytoplasm by the exportin Hasty (HST). The mature miRNA is loaded into an argonaute protein within the RNA-induced silencing complex to mediate the cleavage of target mRNAs via reverse complementary binding of the miRNA [29].

Plant miRNAs play important roles in a wide range of biological processes including development and stress adaptation [30]. To uncover the stress-regulated miRNA repertoire, sRNA libraries were generated from plants subjected to diverse stress conditions and analyzed by RNA sequencing approaches [31–34]. Previous studies in *A. thaliana* identified members of the miR171 family to be upregulated by low as well as elevated temperatures [35] targeting *SCARECROW-LIKE6-III* (*SCL6-III*) and *SCL6-IV* that belong to the *GRAS* family of TFs [36, 37]. MiR408 was recognized to be induced by cold and other abiotic stresses. It regulates transcripts encoding phytochrome family proteins (cupredoxin, plantacyanin and uclacyanin) which act as electron transfer shuttles between proteins [38] and transcripts of phytophenol oxidases called Laccases [39] which are known to oxidize flavonoids during seed development and environmental stress [40]. These are essential to maintain cell wall functions and are important to regulate biological pathways necessary for abiotic stress responses [41]. Recent investigations validated miR394 and its target *LEAF CURLING RESPONSIVENESS* (*LCR*) to regulate leaf development [42, 43] and to be involved in an ABA-dependent manner in responses to cold, salt and drought stress [44, 45]. In *A. thaliana*, miR397 was shown to positively regulate cold tolerance via the CBF-dependent signaling pathway and overexpression of *MIR397a* caused increased *CBF* transcript levels leading to induction of cold responsive *COR* genes [46].

In contrast to miRNAs, siRNAs are generated from dsRNA molecules and are sub-classified based on their specific biogenesis pathways. *Trans*-acting siRNAs (ta-siRNAs) are endogenous plant-specific small RNAs that are capable of acting in *trans* and have the potential to

repress distinct mRNA transcripts. The production of ta-siRNAs is triggered by miRNA-mediated cleavage of primary *TAS* transcripts to generate 21 nt ta-siRNAs in a phased manner [47, 48]. Ta-siRNAs have been shown to regulate plant development [49]. Recent studies suggest their role in environmental stress adaptation, for example, 14 hypoxia-responsive ta-siRNAs have been identified in *A. thaliana* that are processed from *TAS1a, b, c*, *TAS2* and *TAS3a* precursors [50]. The expression of a *TAS1*-derived ta-siRNA and its target transcript *heat-induced TAS1 target (HTT4)* were shown to be regulated by temperature shifts [51]. Furthermore, the generation of *TAS4*-derived ta-siRNAs was shown to be triggered by miR828 under phosphate deficiency [52].

Another subset of siRNAs are natural antisense transcript derived short interfering RNAs (nat-siRNAs) which are produced from overlapping regions of RNA polymerase II derived antisense transcripts [53]. The NATs can be classified into two types depending on the genomic location of the overlapping transcripts. Either both transcripts are encoded on opposite DNA strands within the same genomic region to produce overlapping transcripts (*cis*-NATs) or both transcripts derive from separate genomic regions (*trans*-NATs), but are able to pair with each other. A high salinity responsive nat-siRNA was first identified in *A. thaliana* where the constitutively expressed gene transcript *delta-pyrroline-5-carboxylate dehydrogenase (P5CDH)* and the salt induced gene transcript *Similar to Radicle Induced Cell Death One 5 (SRO5)* encoded on opposing strands of an overlapping genomic region form a dsRNA and DCL2 processes a distinct 24 nt nat-siRNA from the dsRNA region. The generated nat-siRNA cleaves the *P5CDH* transcript and suppresses proline degradation thereby inducing salinity tolerance [54]. In addition to nat-siRNAs produced from *cis*-NATs, *trans*-NATs can be generated when antisense-mediated pairing of transcripts occurs that are derived from non-overlapping genes [55]. The formation of these dsRNAs takes place in diverse *trans*-combinations i.e. between long non-coding RNAs, protein coding transcripts, homologous pseudogenes and transposable elements (TE) [56, 57]. For example, the class of *trans*-NATs that are produced from pseudogenes can regulate their homologous protein encoding transcripts levels [58].

A large number of TE-derived siRNAs were observed in *Decreased DNA methylation 1 (DDM1)* mutants of *A. thaliana* and are referred to as epigenetically activated siRNAs (ea-siRNAs). These siRNAs are produced from transposon-encoded transcripts that are cleaved in a miRNA-dependent manner and become converted into dsRNAs that are further processed by DCL4 into 21 nt ea-siRNAs. These ea-siRNAs were shown to be mainly required for silencing of TE by targeting their intrinsic

transcripts whereas a subset of these siRNAs also targets protein coding mRNAs to reduce their expression levels [59]. In addition, similar to *MIR* precursors some TE-derived transcripts can form a stem loop structure from which siRNAs can be processed [60]. TE also encode lncRNAs and there is rising evidence that environmental factors lead to altered chromatin organization and the expression of lncRNAs that may have functions in the adaptation to altered environmental conditions and can even be inherited. A study in *A. thaliana* reports on a TE-derived TE-lincRNA1195 that was shown to be involved in the ABA response and to contribute to abiotic stress adaptation [61].

In our study we have used RNA sequencing to uncover the cold responsive non-coding RNA repertoire in *A. thaliana* and to study their role in the regulation of various target RNAs. We sequenced mRNAs and sRNAs libraries from *A. thaliana* plants subjected to cold acclimation conditions for 3 h, 6 h and 2 d and analyzed putative correlations between differentially expressed sRNAs and their protein coding targets. To gain additional insight into the cold-responsive interconnection of miRNA-regulated direct targets and indirect targets that are regulated by TFs, we generated a gene regulatory network (GRN) using information on miRNA-targets and publicly available TF-related database the generated network allows to identify connectivities and regulatory impacts of miRNAs under cold acclimation.

Results

Altered expression of sRNAs during cold acclimation in *A. thaliana*

To analyze cold-responsive changes in the sRNA repertoire we subjected *A. thaliana* seedlings to 4 °C cold treatment for 3 h, 6 h and 2 d time points. Previous studies related to cold acclimation observed a rapid inhibition of photosynthetic machinery when shifted from normal temperatures to 4 °C [62]. In addition, studies revealed that abundant cold-responsive genes were differentially expressed at early time points i.e. 3 h and 6 h as well as at later time points i.e. 48 h [33, 34, 62]. Thus, in order to study the sRNAs that could possibly regulate these cold-altered genes, the 3 h, 6 h and 2 d time points were chosen for RNA sequencing analyses. The RNA of treated and control samples were used to perform transcriptome profiling yielding a minimum of 7 million reads per library. The sRNA reads were mapped to the *A. thaliana* reference genome and in all samples on average about 10% reads mapped to miRNA loci, 10% to *trans*- and 2% to *cis*-nat-siRNA loci, 4% reads mapped to lncRNAs, 3% to ta-siRNA producing regions and 0.3% to pha-siRNAs (Additional file 1: Table S2). Only about 1% of the total reads mapped to loci encoding the most abundant RNAs such as ribosomal RNA, snoRNA, tRNA

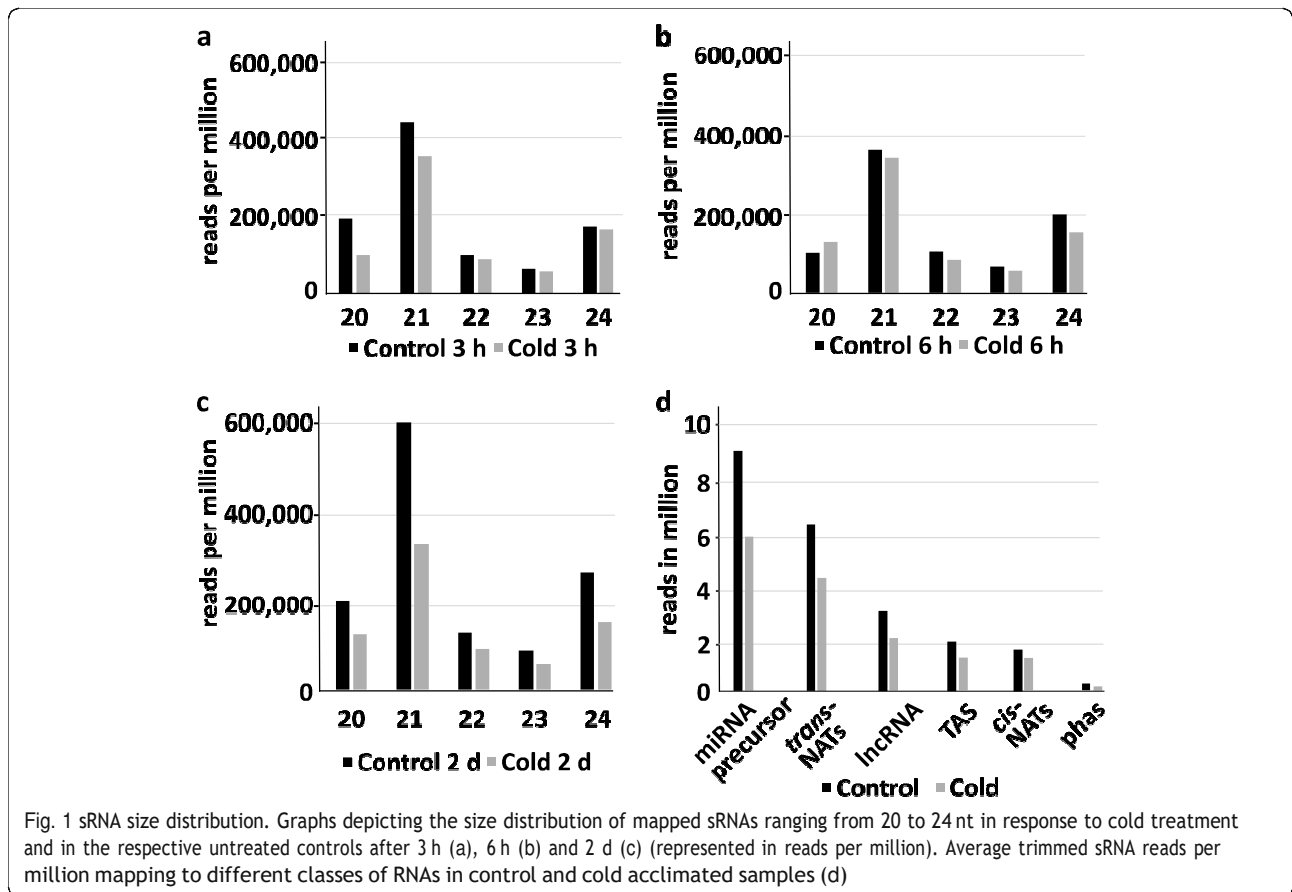
and snRNA which indicates a good quality of the sRNA libraries. The remaining proportion of reads mostly mapped to other RNA classes such as TE and repeat associated regions which are known to be involved in epigenetic pathways.

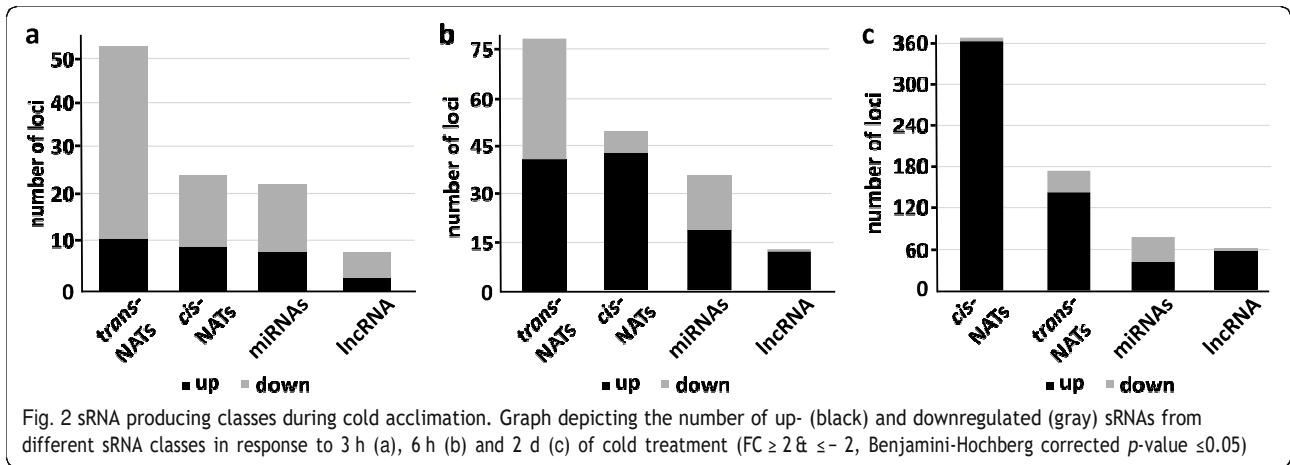
The size distribution of sRNAs ranging from 21 to 24 nt showed two distinct peaks at 21 nt indicating an enrichment of miRNAs, nat-siRNAs and ta-siRNA and at 24 nt corresponding to sRNAs derived from repetitive/intergenic RNAs, inverted repeats and TE (Fig. 1a, b, c, Additional file 1: Table S3). We observed an overall reduction of sRNAs in response to cold acclimation as compared to the control. The distribution of sRNA reads mapping to different sRNA producing loci including miRNAs, nat-siRNAs, ta-siRNAs, phasiRNAs and sRNAs produced from lncRNAs indicated that miRNAs and trans-nat-siRNAs are the two major sRNA classes detected in our data set (Fig. 1d) To identify differentially expressed (DE) sRNAs between cold treated samples and the respective untreated controls (fold change ≥ 2 & ≤ -2 and a Benjamini-Hochberg corrected p -value ≤ 0.05), the relative expression of mature miRNAs and siRNAs was calculated on the basis of the number of normalized reads. Over the analyzed time course cold stress mainly affected sRNAs produced from trans- and

cis-NATs-pairs followed by the class of miRNAs and sRNAs derived from lncRNA (Fig. 2a, b, c). Moreover, we observed an increasing number of up- and downregulated sRNAs from all sRNA classes during the time course reaching the highest numbers after 2 d of the cold treatment (Fig. 2c). To evaluate the reliability of the sRNA sequencing results, we performed stem-loop qRT-PCRs for selected sRNAs belonging to all analyzed sRNA classes to validate and confirm their expressional changes during the time course of cold treatment (Fig. 3). miR162a-3p, miR3434-5p, cis-nat-siRNA produced from *AT3G05870-AT3G05880* transcripts, a trans-nat-siRNA generated from *AT1G10522-AT5G53905* transcripts and a sRNA derived from lncRNA AT5G04445 were found to be induced over the course of cold treatment confirming our sRNA sequencing results.

Expression profiling of cold acclimation responsive miRNAs

The sRNA sequencing method allows to distinguish between individual miRNAs with even a single nucleotide difference. After precise read mapping, sequence reads were analyzed to identify differentially regulated miRNAs (FC ≥ 2 & ≤ -2 , Benjamini-Hochberg corrected p -value ≤ 0.05) (Table 2, Additional file 2: Table S4). We

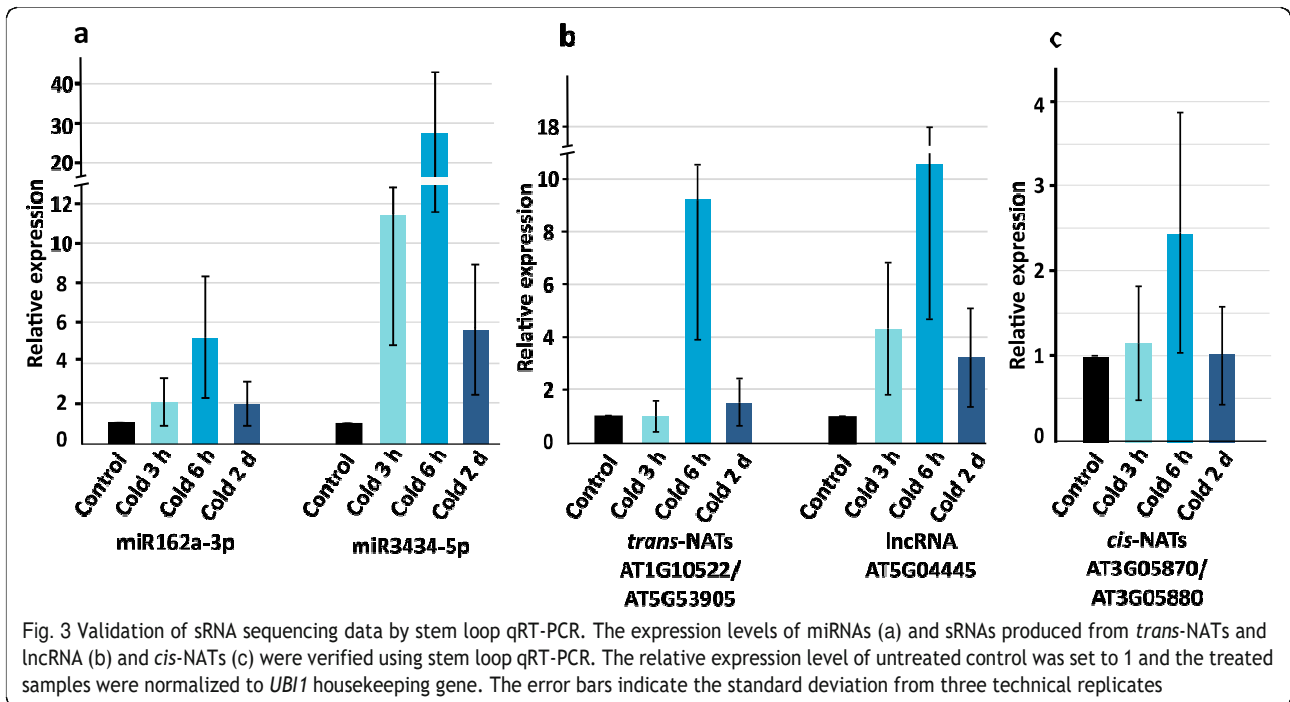




observed a general trend in all the samples that around 10% of the detected miRNAs possessed very high normalized read counts (> 1000 reads per sample), about 50% showed moderate expression (< 1000 and > 20 normalized reads), 11% showed reduced read counts (< 20 and > 5 normalized reads) and 27% showed very low expression (< 5 normalized reads) (Additional file 2: Table S5). In response to cold treatment we observed 22 miRNAs (8 up and 14 down) that were DE after 3 h, 36 mature DE miRNAs (19 up and 17 down) after 6 h and 79 DE mature miRNAs (42 up and 37 down) after 2 d. We found miRNAs showing differential expression at specific time points as well as miRNAs with differential expression at two or all three time points. Two DE miRNAs were found throughout the course of cold

treatment, 13 DE miRNAs were detected at 6 h and 2 d, 8 DE miRNAs were common after 3 h and 2 d, and 4 DE miRNAs were found at the 3 h and 6 h time point. We also observed 7, 17 and 55 DE miRNAs that were specifically regulated at the 3 h, 6 h, and 2 d time points (Fig. 4). We detected an increasing number of DE individual miRNAs over the time course of cold treatment suggesting that alterations in miRNA levels seem to be an important step during cold acclimation.

In recent years, 22 miRNA families were identified to be conserved between *A. thaliana*, *Oryza sativa* and *Populus trichocarpa* [63-65] and some of them were shown to have important roles in abiotic stress adaptation since they predominantly regulate targets encoding TFs or enzymes that promote tolerance to stresses [66-68]. Out of these



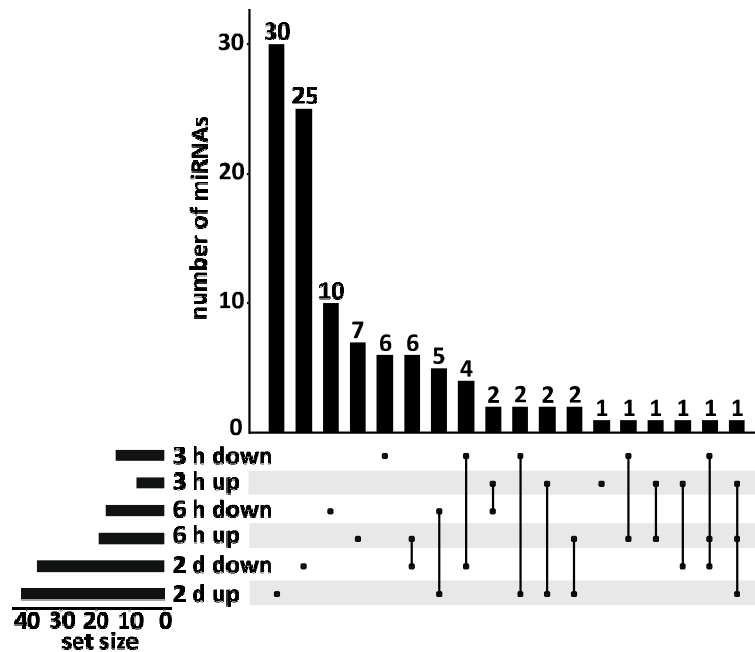


Fig. 4 UpSet plot depicting the number of DE miRNAs. The plot depicts the global comparison of up- and downregulated DE miRNAs after 3 h, 6 h and 2 d of cold treatment ($FC \geq 2$ & ≤ -2 , Benjamini-Hochberg corrected p -value ≤ 0.05)

22 miRNA families, we detected individual members of 16 families to be differentially expressed corresponding to 15, 20 and 43 DE mature miRNAs at 3 h, 6 h and 2 d, respectively (Fig. 5, Additional file 2: Table S6). In total, we found 107 non-redundant mature miRNAs to be differentially expressed throughout the course of cold treatment and 36 mature miRNAs out of these belonging to 9 conserved miRNA families have been known to be cold regulated in other plant species (Additional file 2: Table S6) [35, 69, 70]. Out of 107 miRNAs, 14 have been previously known to be cold responsive in *A. thaliana* and our study shows similarity in the induction or repression pattern of these miRNAs compared to other cold stress related studies [35, 71, 72]. The remaining 93 DE mature miRNAs that belong to 55 miRNA families have not been reported before to be cold-regulated in *A. thaliana* (Additional file 2: Table S6). We identified several miRNAs with a varying expression pattern i.e. up- and downregulation at different time points. For example, miR156f-5p and miR157b-3p were downregulated at 3 h and upregulated at 2 d, miR166f was upregulated at 3 h and downregulated at the 2 d time point, miR447b and miR5653 were upregulated at 3 h, but downregulated at 6 h time point whereas miR157b-5p was downregulated at 3 h and upregulated at 6 h. Similarly, 12 miRNAs showed inconsistent regulation at 6 h and 2 d, whereas we observed consistent upregulation of miR408-5p, miR395e, miR159c, miR169h and downregulation of miR160a-

5p, miR160b, miR398a-5p, miR8175, miR319b in at least two time points. This indicates that the regulatory pattern of a miRNA can vary at different time points of cold treatment and the steady-state level of mature miRNAs depends on the physiological need of plants subjected to stress conditions.

Differentially expressed miRNA targets

Since miRNAs and mRNA/lncRNA were sequenced from the same RNA samples we were able to compare changes in miRNA expression with the changes of their cognate targets. To identify the targets of miRNAs that were found to be differentially expressed during the time course of cold treatment we have used the psRNAtarget prediction tool with a stringent expectation cut-off of 2.5 and allowed miRNA accessibility to its mRNA target with a maximum energy to unpair the target site of 25 [73]. Applying these stringent parameters, the prediction tool revealed putative targets for 93 DE miRNAs out of 107. The target prediction for the 93 non-redundant DE miRNAs identified 338 mRNAs and 14 non-coding RNAs as putative targets (Additional file 3: Table S7, S8). The 18 DE miRNAs at 3 h (5 up- and 13 downregulated) can target 96 non-redundant mRNAs and 3 non-coding transcripts. The 33 DE miRNAs at 6 h (18 up- and 15 downregulated) can target 173 non-redundant mRNAs and 3 non-coding RNA targets and the 69 DE miRNAs after 2 d (34 up- and 35 downregulated) are able to target 267 non-redundant mRNAs and 12 non-coding RNA targets (Additional file 3: Table S7, S8). To

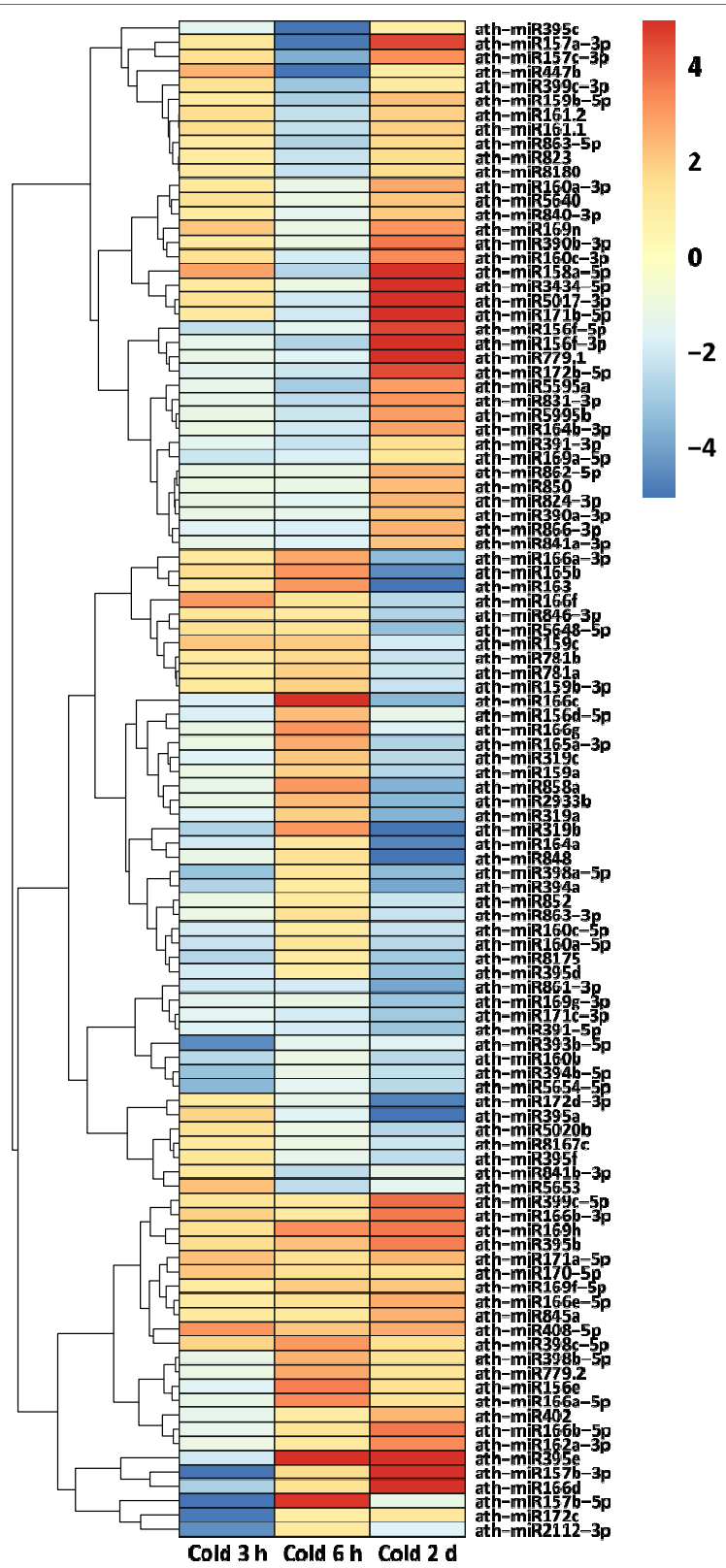


Fig. 5 Hierarchically clustered heatmap depicting miRNAs differentially expressed in at least one of the analyzed time points in response to cold treatment

analyze how the regulation of these targets correlates with the expression of miRNAs, we used our mRNA and lncRNA transcriptome sequencing data generated from the identical RNA pools as the sRNA data set for the 3 h, 6 h and 2 d cold treatments and their respective untreated controls (Additional file 4: Table S9, S10). We used the mRNA/lncRNA transcriptome data to examine the expression levels of all 338 transcripts targeted by the 93 differentially regulated miRNAs in order to correlate the target transcript expression to the expression of their cognate miRNAs (Additional file 3: Table S7). In frequent cases we observed that one transcript can be targeted by various isoforms of a miRNA family, but in a few cases target transcripts can also be cleaved by different miRNAs that are unrelated in sequence. In general, we considered all individual DE miRNAs and their cognate protein-coding targets (mRNAs) as miRNA:mRNA pairs and identified 111, 246 and 376 of these pairs for the 3 h, 6 h and 2 d time points of cold treatment, respectively (Additional file 3: Table S7). For each time point we classified the miRNA:mRNA target pairs into different subgroups according to the correlation of their expression with the expression of their cognate miRNA. These miRNA:mRNA target pair subgroups were classified as inversely correlated when they show an anticorrelation of mRNA and miRNA expression, showing same tendency of expression when the miRNA and its target are either upregulated or downregulated, and the miRNA is regulated, but the target remains unchanged or undetected (Table 1). We observed 2, 12 and 27 anticorrelated miRNA:mRNA target pairs at 3 h, 6 h and 2 d, respectively, with a total number of 39 non-redundant anticorrelated miRNA:mRNA target pairs pointing to a role of these miRNAs in controlling the transcriptome upon cold treatment (Additional file 3: Table S7). Apart from the mRNA targets, the target prediction tool also identified 14 putative non-coding RNA targets of DE miRNAs, but the expression levels of ncRNA target transcripts was less than 5 reads or they were not differentially expressed.

Table 1 Number of putative miRNA:mRNA target pairs and their relative expression pattern after 3 h, 6 h and 2 d of cold treatments

miRNA:mRNA pairs	3 h	6 h	2 d
↑ ↓	2	12	27
↑ ↑	0	9	15
↓ ↓	1	1	12
↑ — or ↓ —	7	15	32
↑ ○ or ↓ ○	29	137	99

The first arrow corresponds to miRNA regulation and the second to the regulation of its target mRNA transcripts and the arrows represent the correlation expression as follows: ↑ = upregulated, ↓ = downregulated, — = unchanged, ○ = undetected.

On the basis of Araport (Version 11; <https://araport.org/>) annotation, we observed 54 targets of DE miRNAs from all the four subgroups to be consistently present at all the time points (Additional file 5: Table S11). These mainly encode TFs and DNA binding domain containing proteins and include MYB domain containing proteins, nuclear factor Y subunit genes, heat shock TFs (HsFs), TCP domain proteins and Squamosa promoter binding (SPLs) proteins. We also examined the functions of the miRNA targets that were specific for each time point. Specifically, at 6 h time point we found several PPR proteins that are known to be important for RNA maturation in various organelles, TPR encoding genes required in plant signaling and organellar import and genes encoding membrane multi-antimicrobial extrusion [22] efflux proteins that act in the transport of xenobiotic compounds. At the 2 d time point we found abundant transcripts coding for factors involved in transcriptional regulation and protein phosphorylation that control intracellular signaling in response to stress. Taken together, we found a remarkable overrepresentation of genes encoding transcription factors, proteins associated with transcriptional regulation, and proteins involved in RNA processing and translational control.

We found 39 miRNAs and their putative targets showing an inverse correlation, for example, after 3 h of cold treatment we noticed a strong downregulation of miR172c (FC = -4.86) and an upregulation of its predicted target TARGET OF EARLY ACTIVATION TAGGED (EAT, FC = 2.18) which is known to be reduced in *A. thaliana ice1* mutants [33]. In addition, EAT also showed increased expression levels in roots and leaves at 4 °C in *A. thaliana* [74]. After 6 h of cold treatment we observed downregulation of miR395c (FC = -19.27) and a concomitant upregulation of its target transcript encoding the magnesium-chelatase subunit H which presents the GUN5 gene (FC = 2.18) that was shown to be an important component of plastid to nucleus signal transduction. Another miRNA, miR5595a showed reduced expression levels (FC = - 2.88) whereas its target encoding a methyl esterase 9 was upregulated (FC = 3.58) and is known to be a plant core environmental stress responsive gene (PCESR) [75]. Additionally, after 2 d of cold treatment, we observed three isoforms of miR319 to be downregulated and an upregulation of one of their target transcript encoding a TCP2 TF (FC = 2.56). A previous study revealed an upregulation of the TCP2 transcript after shifting *A. thaliana* plants to cold conditions with 100 μE light conditions, but not in dark conditions and it was speculated that light-dependent signals derived from the chloroplast at low temperature are important for increased TCP2 levels that might be important for the control of photosynthesis related genes [76, 77]. After 2 d of cold treatment we also detected downregulation of miR159 isoforms (FC = -2.53) resulting in elevated levels of

one of their target transcripts *Translocase Inner Membrane Subunit 44 (TIM44)*-related encoding a subunit of the mitochondrial inner membrane translocase complex subunit (FC = 2.80).

Gene ontology analysis of predicted miRNA targets

To obtain information about the possible role of DE cold responsive miRNAs and their targets, we performed gene ontology (GO) analysis of all putative targets using the David bioinformatics tool [78]. Based on the three categories; biological processes, cellular component and molecular function, we observed an enrichment of GO terms for all three time points with Benjamini-Hochberg corrected *p*-values obtained from Fisher’s test (Fig. 6, Additional file 6: Table S12). At the 3 h time point the significant biological processes included regulation of transcription (47), transcription (41), cell differentiation (12), ethylene-activated signaling pathway (7) and auxin-activated signaling pathway (7) indicating a major impact

of miRNAs on an early response of genes that code for proteins mainly acting in signaling and gene transcription. Concerning the category cellular component, we identified the highest number of targets associated with the nucleus (63) which nicely correlates with the overrepresentation of TFs before. Furthermore, in the category molecular functions, the TF activity, sequence-specific DNA binding (46), DNA binding (44) and auxin binding functions were most significant also pointing to an overrepresentation of transcripts that code for regulatory proteins and factors involved in gene transcription. For the 6 h time point significant biological processes with the highest number of genes included regulation of transcription (62 target genes), response to salicylic acid (8), regulation of secondary cell wall biogenesis (5) and positive regulation of programmed cell death. We also found S-adenosylmethionine-dependent methyltransferase activity (7) to be significantly enriched in the molecular function category. Similar to 3 h time point, we

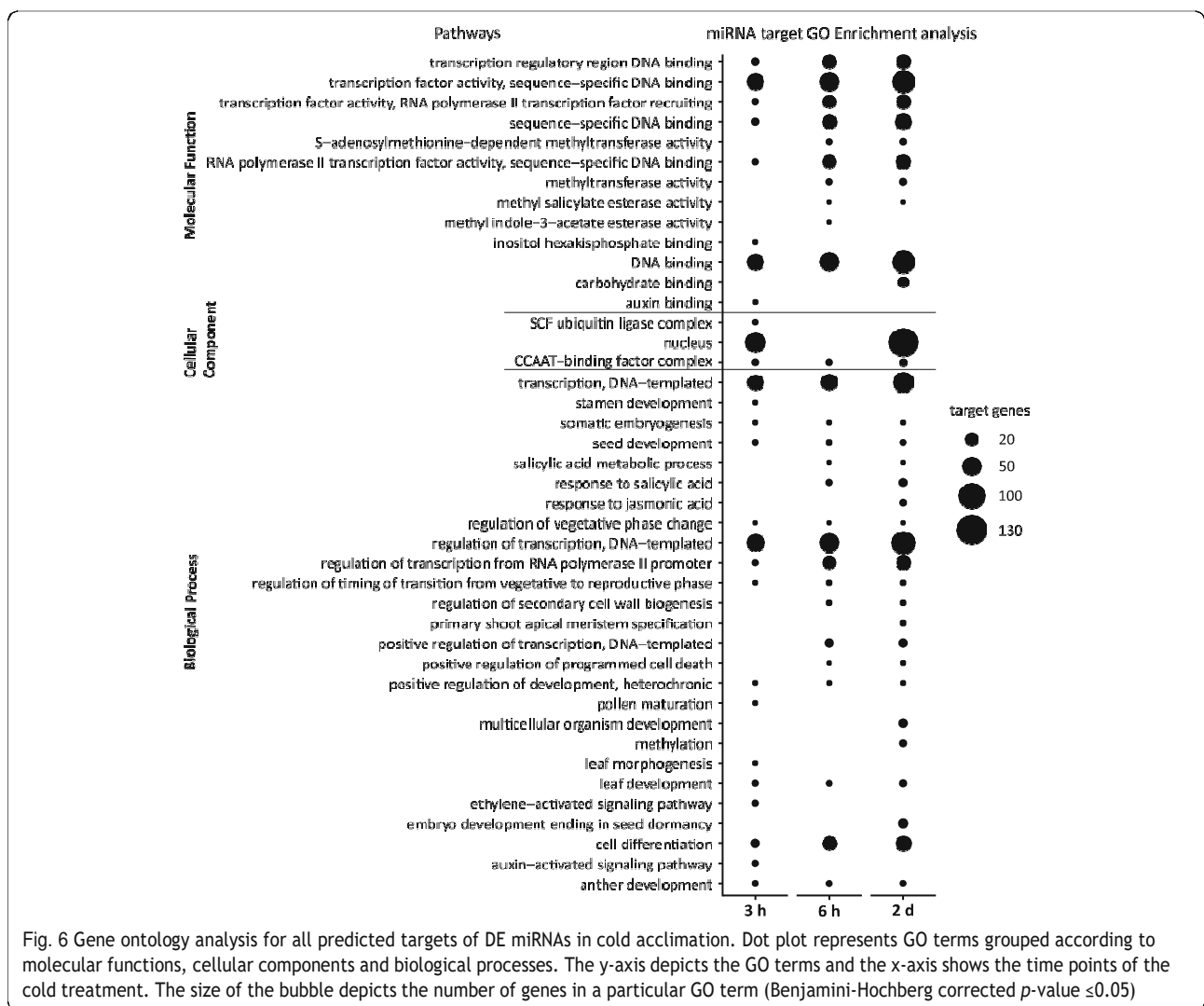


Fig. 6 Gene ontology analysis for all predicted targets of DE miRNAs in cold acclimation. Dot plot represents GO terms grouped according to molecular functions, cellular components and biological processes. The y-axis depicts the GO terms and the x-axis shows the time points of the cold treatment. The size of the bubble depicts the number of genes in a particular GO term (Benjamini-Hochberg corrected *p*-value ≤ 0.05)

observed an enrichment of transcription related genes at the 6 h time point. Along with these, the overrepresentation of methyltransferase activity related genes indicates epigenetic modifications related to abiotic stress and the genes that may act in secondary cell wall biogenesis could lead to strengthening of the cell wall and reduction in pore size in stress conditions. At the 2 d time point, significant biological processes included regulation of transcription (89), embryo development ending in seed dormancy (15), multicellular organism development (13), methylation (9) and response to jasmonic acid (8). At all the three time points, we observed an enrichment of genes encoding TFs which indicates that these are key regulators of a set of genes involved in transcriptional reprogramming during cold acclimation. Concerning the category cellular components, we observed the highest number of targets associated with the nucleus (136 target genes) which is in line with the categories outlined before and underlines the massive processes of transcriptional regulation in response to cold acclimation (Fig. 6).

Construction of a gene regulatory network (GRN)

To understand the possible interactions and contributions of the major gene regulatory classes, we reconstructed a miRNA and TF regulatory network (Additional file 7, Data S1). The network comprises direct miRNA-mediated target control, miRNAs that regulate transcripts encoding TFs regulating their downstream targets (indirect targets), and TFs which are not miRNA-controlled but regulating miRNA regulated downstream targets (direct targets). To construct the final network, we considered the generated miRNA and mRNA expression data and analyzed all miRNA targets that were predicted using the psRNATarget tool together with publicly available information of TF binding sites (TFBS) and downstream targets. We included experimentally validated regulatory connections from Arabidopsis Transcriptional Regulatory Map [79] and Agris [80]. Further, we included TF target interactions with high confidence from PlantRegMap [81] only considering TFs with different criteria of binding site conservation. First criterion includes TFs and their targets whose binding sites lie within conserved elements of different plant species (CE) whereas the second criterion includes TFs and targets whose binding sites were found to be conserved in different plant species when scanned for conservation of TFBS (FunTFBS).

The validity of the connections in the network was tested by predicting miRNA- and TF-controlled target mRNA expression levels based on miRNA or TF expression levels at a given time point. Here, the prediction power is used as an indicator for the reliability of regulatory links in the network and is calculated by Pearson

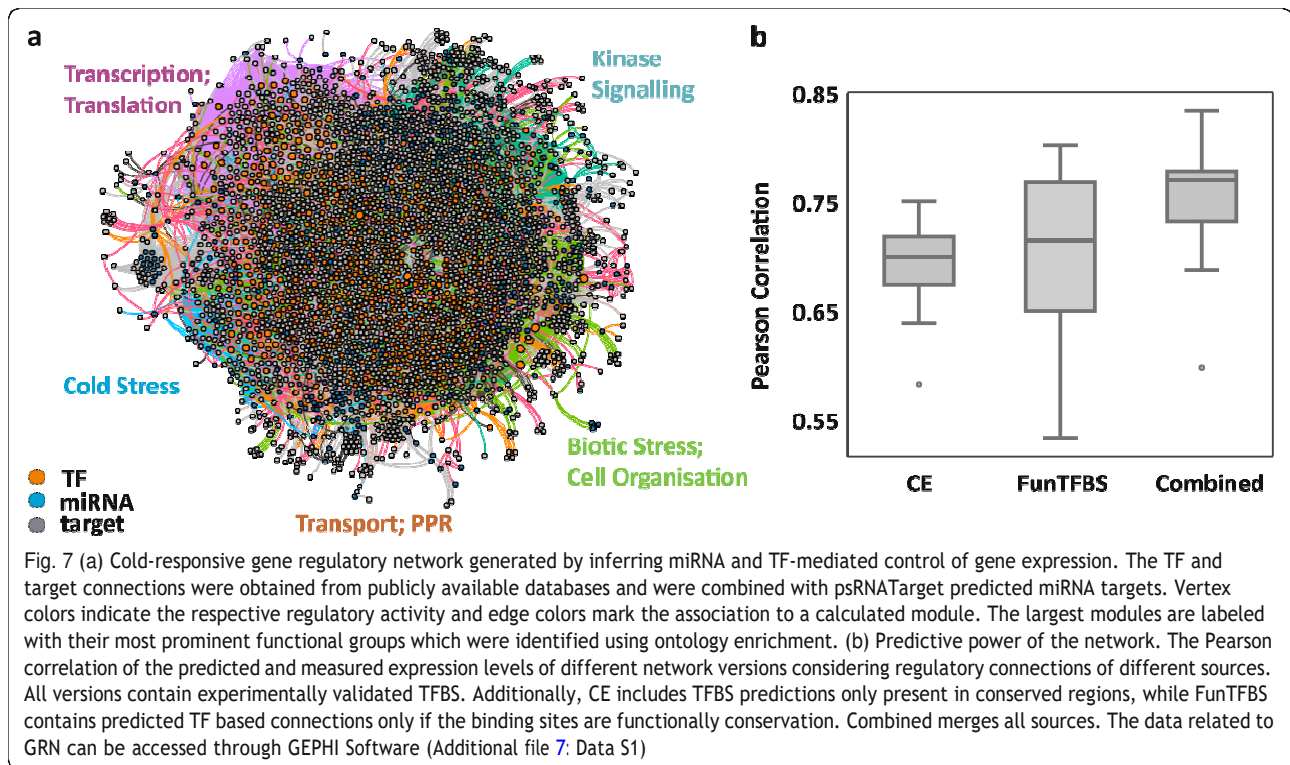
correlation between the predicted and the measured mRNA expression level (Fig. 7 b). We tested the predictive power of the three different network versions to ensure maximal information in the model. Here, the combined version is able to explain on average 77% of the change in target gene expression (0.77 Pearson correlation coefficient) and was considered for further investigation.

This resulting network model contains 350 miRNAs classified into 166 families and consisting a total of 657 TFs belonging to 38 families that either activate or repress 2420 downstream target genes. In total, there are 36,523 regulatory relationships out of which 3846 are miRNA based whereas the remaining 32,677 are TF-based (Fig. 7 a, Additional file 7: Data S1, Additional file 8: Fig. S1).

After validation of the network reconstruction we analyzed the network modularity. Modules are clusters of nodes which are closely connected to each other compared to other nodes in the network. In biological systems, nodes of one module are often co-regulated and closely associated in function. Modules can therefore be interpreted as the functional units of the cell [82]. By using the community detection method [83], we found 17 modules. Functional enrichment using GO and MapMan ontology revealed signaling, transport, cold and biotic stress components, RNA and protein synthesis and cellular organization to be overrepresented in five major network modules.

A cold responsive subnetwork (Fig. 8 a, Additional file 7: Data S2, Additional file 9: Fig. S2) comprising targets of differentially expressed miRNA and targets encoding TFs and their downstream targets was extracted from the GRN. The depicted targets are differentially expressed in at least one of the time points and the extracted network is comprised of 830 nodes and 1332 edges. We observed 103 mature miRNAs and 58 TFs to be involved in the regulation of 669 direct and indirect targets. The functional enrichment revealed a predominant regulation of genes related to cold acclimation, transcription/translation, biotic stress/cell organization, signaling/protein degradation and cell wall/lignin synthesis.

We selected two subnetworks, for miR319 which was DE at all the three time points and miR858 found to be DE at 6 h and 2 d. The miRNA-TF subnetwork of these two miRNAs was extracted from the whole network (Fig. 8 b, c) and the depicted targets in the network are DE in at least one of the analyzed time points (Additional file 10: Fig. S3 and Additional file 11: Fig. S4). The miR858 subnetwork consists of 30 nodes and 51 edges. Among its targets miR858 controls the expression of *Tryptophan synthase (TSBI, AT5G54810)* catalyzing tryptophan synthesis that is the precursor of the auxin indole-3-acetic acid [84]. MiR858 also controls a transcript encoding the TF MYB111 (AT5G49330) which modulates the salt stress response by regulating



flavonoid biosynthesis [85] and the heat shock factor *HSFA4A* (AT4G18880) involved in the response to heat stress. We found 25 nodes and 43 edges to be linked with miR319 that mediates regulation of transcripts such as *TRANSPARENT1 TESTA 8* (TT8, AT4G09820) encoding a TF regulating anthocyanin biosynthesis by the control of *dihydroflavonol 4-reductase* [86]. MiR319 also regulates mRNA for the thermotolerance related heat shock factor *HSFB-2b* (AT4G11660) and a transcript coding for Probable pectinesterase/pectinesterase inhibitor 25 (PME25, AT3G10720) that could facilitate cell wall modifications in cold stress.

Differentially expressed sRNAs derived from various other RNA classes

We used our sRNA sequencing data not only to analyze miRNA regulation in response to cold, but also to identify sRNAs derived from other RNA classes which could provide links to their role in cold acclimation. We mapped sRNA reads to publicly available reference databases of lncRNAs, *trans*- and *cis*-NATs pairs, *TAS* and *PHAS* [57, 87–89] and we were able to associate a high number of DE sRNAs to these RNA classes.

sRNAs derived from non-overlapping lncRNAs

Here we define non-overlapping lncRNAs as transcripts with a size larger than 200 nt that are single stranded RNA and do not overlap with protein coding transcripts or other non-coding transcripts. In our sRNA data, we

observed 15 non-redundant non-overlapping lncRNA loci that produce DE sRNAs and 13 of these upregulated sRNA production whereas the remaining two downregulated sRNAs in response to cold (Additional file 12: Table S13). However, even if these lncRNAs generate DE sRNAs, the transcript levels of the lncRNAs remained unchanged across the analyzed samples. We found one lncRNA at 3 h, another lncRNA at 6 h and 7 lncRNAs at the 2 d time point of cold treatment that produced DE sRNAs. In addition, we found two lncRNAs differentially producing sRNAs at 3 h as well as 6 h out of which AT5G07745 reduced sRNA production and the other (AT5G04445) upregulated sRNAs at both time points. At 6 h and 2 d we detected four common lncRNAs producing sRNAs with elevated expression levels. The lncRNA AT5G05455 was the only one that produced reduced amounts of sRNAs at the 2 d time point whereas others were upregulated. Single stranded transcripts have the capability to produce fold back structures forming dsRNA which can be processed into small RNAs, but we observed sRNAs produced from sense as well as antisense strands of these lncRNA transcripts. Since these lncRNAs do not overlap with any other transcript and do not have any pairing partners in other genomic loci, it probably indicates that RNA dependent RNA polymerases are involved in the formation of dsRNA from these lncRNA in a primer independent manner that are later converted to sRNAs [9, 90].

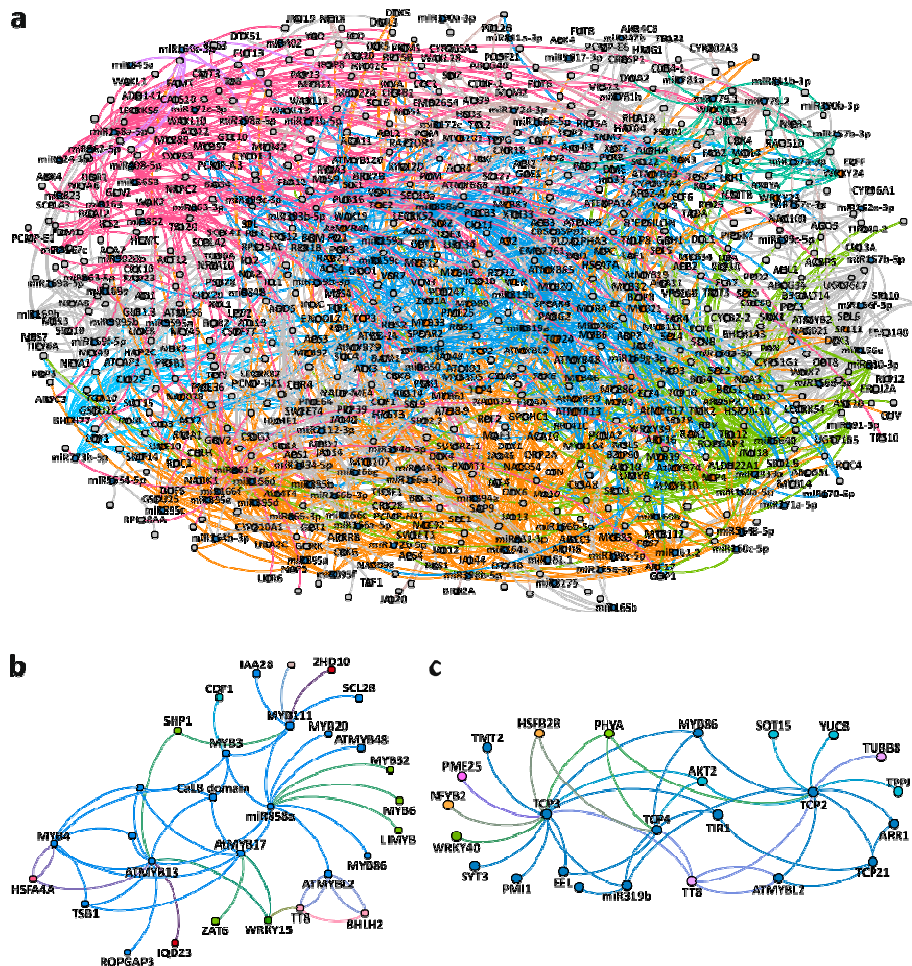


Fig. 8 The extracted cold responsive GRN comprising of direct and indirect targets of DE miRNAs. (a) Network of miRNAs and targets that are differentially expressed at any one of the analyzed time points ($FC \geq 2$ & ≤ -2 , Benjamini-Hochberg corrected p -value ≤ 0.05). Functional modules associated with cold acclimation, kinase signaling, transcription; translation and transport are represented by blue, dark green, pink, and orange color, respectively. (blue nodes = miRNAs, orange nodes = TFs, gray nodes = targets) (b) Subnetwork of miR58. (c) Subnetwork of miR319. In (b) and (c) direct and indirect targets of miRNAs are differentially expressed in at least one of the analyzed time points ($FC \geq 2$ & ≤ -2 , Benjamini-Hochberg corrected p -value ≤ 0.05). Curved edges indicate regulatory connections of a regulator and its target. The node colors depict the inferred function based on GO enrichment analyses. Green: biotic stress, cell organization; blue: cold stress; pink: transcription, translation; orange: transport, PPR; dark blue: cell wall, lignin synthesis; red: signaling, protein degradation. The data related to GRN can be accessed through GEPHI Software (Additional file 7: Data S2)

sRNAs derived from NATs

NATs are pairs of transcripts either non-coding (nc) or protein coding (pc) genes that overlap and form dsRNAs due to sequence complementarity. The pairing of transcripts is possible between nc-nc, nc-pc and pc-pc transcripts and the resulting paired transcript serve as targets for DCL-mediated processing into sRNAs. We found the majority of *cis*- and *trans*-NAT pairs to be produced from pc:pc or pc:nc transcript pairs. In case of pc:nc, the nc pairing partner mostly represents pre-tRNAs or transcripts from TE which also have the capacity to produce sRNAs individually [91-93]. It is known that pre-tRNA and TE-derived sRNAs have the capacity to regulate other transcripts by sequence complementarity which could

indicate their contribution in regulation of cold acclimation related network [92, 94]. Our data set revealed that transcript pairs producing elevated levels of sRNAs in response to cold can have different expression patterns. They can show anticorrelation (one transcript upregulated and the other downregulated), a same tendency of expression (both transcripts either upregulated or down regulated) or no correlation (one transcript regulated and the other remains unchanged). During stress conditions, reverse sequence complementary transcripts of a stress-induced gene and a constitutively expressed gene pair to each other and produce 24 nt and 21 nt siRNAs. The siRNAs produced have the capability to cleave the constitutively expressed transcript resulting in its downregulation

to facilitate stress acclimation. This mechanism represents the classical expression pattern of NATs [54]. The pair is characterized by induced differential expression of nat-siRNAs and anticorrelated expression pattern of the sense and antisense transcripts. We observed abundant sRNAs that were regulated, but their transcript levels remained unchanged. The second most abundant case was an upregulation or downregulation of one of the transcripts whereas the other transcript remained unchanged (Table 2).

Most of the *trans*-NATs gene pairs produced large amounts of sRNAs after 2 d of cold treatment and showed a decrease or no change in the gene transcript levels deduced from the mRNA data. This indicates the possible pairing of both transcripts which are further processed into nat-siRNAs and higher production of these nat-siRNA in the cold acclimation could be required to keep at least one of transcripts at steady levels.

cis-nat-siRNAs

We found 5, 20 and 100 *cis*-NATs loci (104 non-redundant pairs) at 3 h, 6 h and 2 d, respectively, that produced DE sRNAs from two overlapping transcripts one of which is up- or downregulated whereas the other one remains unchanged (Table 2) (Additional file 12: Table S14). In addition, we detected 24, 34 and 278 *cis*-NATs (308 non-redundant pairs) at 3 h, 6 h and 2 d time point that produced DE sRNAs, but where the cognate overlapping transcripts remained unchanged or could not be detected. Prevalently, we observed that most of the pairs producing *cis*-nat-siRNA were pc:pc transcript

Table 2 Overview of DE nat-siRNAs including expression analysis of the underlying *cis*- or *trans*-transcript pairs

Time points	sRNA clusters	↑↑	↑—	↓—	— —	↑↓
3h <i>cis</i> -NATs	up	1	5		3	
	down				21	
6h <i>cis</i> -NATs	up	1	20		26	1
	down				8	
2d <i>cis</i> -NATs	up	15	93	7	270	9
	down				8	
Non-redundant		16	104		308	9
3h <i>trans</i> -NATs	up				8	
	down				33	
6h <i>trans</i> -NATs	up		6		24	
	down	2	7		15	
2d <i>trans</i> -NATs	up		9	11	75	
	down		1	13	13	
Non-redundant		2	14	18	95	

The two symbols in the five columns at the right represent the pairing *cis*- or *trans*-transcript partners and indicate their expression as follows: ↑ = upregulated, ↓ = downregulated, — = unchanged (unchanged refers to FDR > 0.05 and/or fold change FC ≥ 2 & ≤ -2).

pairs. We found one NATs pair at 6 h and 9 pairs at 2 d resembling the classical mechanism of antisense transcript regulation by nat-siRNAs (Table 3) [54]. We detected a gene pair that gives rise to an increased production of nat-siRNAs and comprises a cold-induced transcript coding for a RAS-Related GTP-Binding Nuclear Protein (*RAN2*, AT5G20020) and a concomitant downregulation of its pairing transcript encoding a Plant Tudor-like RNA-binding protein (AT5G20030). Until now, functional studies on the Plant Tudor-like RNA binding protein are lacking, but *RAN2* is known to be necessary for nuclear translocation of proteins and for RNA export [95]. Another transcript of a salt stress responsive gene encoding an Oleosin-B3-like protein (AT1G13930) [96] which is known to be ABA-induced [97] was also induced by cold in our data and its transcript is able to pair with the transcript of a T-box TF (AT1G13940) to induce production of *cis* nat-siRNAs. Apart from the above mentioned expression patterns of transcripts that differentially regulate siRNA production, we found sRNA producing loci showing same tendency of transcript expression denoted by the upregulation of both pairing transcripts (16 non-redundant pairs; 1, 1 and 15 at 3 h, 6 h and 2 d, respectively) leading to induced sRNA biogenesis. In this category we observed enrichment of pc:pc as well as pc:nc transcript pairs. Prominent examples from our results include the stress-induced pc:pc transcripts *RARE-COLD-INDUCIBLE 2A* (AT3G05880) and *anaphase-promoting complex/cyclosome 11* (AT3G05870) which cause increased *cis*-nat-siRNA production. We also found a cold-induced pc:nc transcript pair coding for a chloroplast beta amylase and a lncRNA, and this upregulated *cis*-nat-siRNAs production consistently at all the three time points. The beta amylase promotes starch degradation into sugars which may act as osmolytes to maintain osmotic balance under cold stress conditions [98].

trans-nat-siRNAs

We found 38 non-redundant *trans*-NAT pairs (5, 14 and 26 at 3 h, 6 h and 2 d, respectively) that generated DE *trans*-nat-siRNAs from each transcripts. The transcript levels of these 38 gene pairs showed that one of the pairing transcript was either upregulated (5 transcript pairs) or both were unchanged (33 transcript pairs). Out of these 38, we detected four *trans*-NATs gene pairs that generated DE *trans*-nat-siRNA and were common after 3 h (both gene transcripts unchanged) as well as after 6 h (one transcript upregulated and the other one unchanged). We observed 41, 39 and 88 (95 non-redundant) *trans*-NATs gene pairs at 3 h, 6 h and 2 d, respectively, that gave rise to DE *trans*-nat-siRNAs from the overlapping region of two transcripts having unchanged or undetected transcript levels (Table 2). We

Table 3 Examples of cold acclimation induced *cis*-NATs pairs that produce siRNAs resembling the classical *nat*-siRNA expression

Gene 1	sense transcript	FC	Gene 2	antisense transcript	FC
6h					
AT2G22080	Transmembrane protein	4.75	AT2G22090	UBP1-associated proteins 1A	-1.41
2 d					
AT5G20020	RAS-related GTP-binding nuclear protein 2	2.58	AT5G20030	Plant Tudor-like RNA-binding protein	-2.17
AT3G11830	TCP-1/cpn60 chaperonin family protein	2.86	AT3G11840	Plant U-box 24	-2.9
AT1G03090	Methylcrotonyl-CoA carboxylase alpha chain, mitochondrial / 3-methylcrotonyl-CoA carboxylase 1 (MCCA)	-2.5	AT1G03100	Pentatricopeptide repeat (PPR) superfamily protein	2.47
AT1G72030	Acyl-CoA N-acyltransferases (NAT) superfamily protein	-2.3	AT1G72040	Deoxyribonucleoside kinase	2.44
AT2G40420	Transmembrane amino acid transporter family protein	-2.3	AT2G40430	SMALL ORGAN 4	2.32
AT5G52440	HIGH CHLOROPHYLL FLUORESCENCE 106	-1.7	AT5G52450	MATE efflux family protein	2.9
AT3G16800	E GROWTH-REGULATING 3	-1.4	AT3G16810	Pumilio 24	5.5
AT2G22080	Transmembrane protein	3.13	AT2G22090	UBP1-associated proteins 1A	-1.51
AT1G13930	Oleosin-B3-like protein	4.53	AT1G13940	T-box transcription factor, putative (DUF863)	-1.31

Sense transcript and antisense transcript fold change ≥ 2 or ≤ -2 , Benjamini-Hochberg corrected p -value ≤ 0.05 and siRNA expression fold change ≥ 2 , Benjamini-Hochberg corrected p -value ≤ 0.05 .

observed 2, 5 and 23 *trans*-NAT pairs comprising overlapping pc:pc transcript that generate DE *trans*-nat-siRNAs. We found one pc:pc NAT pair that produced reduced *nat*-siRNAs at 3 h, but increased *nat*-siRNAs at 6 h and 2 d time points. Both transcripts encode ZED related kinases (ZRK 1, AT3G57710 and ZRK 7, AT3G57770) that are known to be induced at high temperature and to inhibit the immune response in the absence of plant pathogens [99]. In our data, the transcript levels of these two genes were unchanged, but the generation of *trans*-nat-siRNAs from the two overlapping transcripts might be important to keep the transcripts at a steady-state level. After 2 d of cold treatment, we found a pc:pc *trans*-NAT pair that led to increased *trans*-nat-siRNA production from transcripts encoding Plastid Redox Insensitive (PRIN2, AT1G10522) and prolamins like protein (AT5G53905), but the transcript levels for these two genes remained unchanged. It is known that PRIN2 is a plastid protein involved in redox-mediated retrograde signaling and is required for light-activated PEP-dependent transcription. Another similar example comprises a ncRNA (AT1G70185) and a transcript for a hypothetical protein (AT5G53740) that produce high amounts of *trans*-nat-siRNAs, but their transcript levels were unchanged. Apart from pc:pc pairs, we detected pc transcripts that are able to pair with distinct pre-tRNA. In particular, 7 pc transcripts pairing with 36 pre-tRNA transcripts produced DE

trans-nat-siRNAs at 3 h, 10 pc transcripts paired with 46 pre-tRNAs at 6 h and 15 pc paired with 82 pre-tRNAs after 2 d of cold treatment. The majority of the *trans*-NAT gene pairs comprised a nc transcript partner encoding a pre-tRNA or RNA deriving from TE. We found a large number of pc:nc pairs that generated DE sRNAs (41, 37 and 65 loci at 3 h, 6 h and 2 d, respectively) where the transcripts levels were undetected or unchanged. There is a possibility that these pc:nc NATs pairs produce sRNA from the double stranded region of two completely or partially overlapping transcripts, which can be referred as *trans*-nat-siRNAs or these could be derived from single stranded region of two partially overlapping tRNA or TE transcripts (Additional file 12: Table S15). In particular, we observed 1, 8 and 17 pc:nc *trans*-NATs pairs at 3 h, 6 h and 2 d, respectively, that produced DE sRNAs from TE transcripts. One widely known example for a TE-derived siRNA is siRNA854 which shows partial complementarity to the 3' UTR of its target encoding an RNA-binding protein involved in stress granule formation known as UBPIb transcript [100]. We also detected TE-derived sRNAs that are able to target mRNA transcripts to promote cold treatment adaptation. Concerning the *trans*-nat-siRNA producing loci we found 13 transcript pairs after 6 h and 34 pairs after 2 d time that produced DE *trans*-nat-siRNAs where one of the transcripts from each pair was either up- or downregulated and the pairing

partner remained unchanged. The time profile revealed that the highest number of DE *trans*-nat-siRNAs were identified after 2 d indicating *trans*-nat-siRNA mediated regulation of gene expression seems to be most important for the late response to cold acclimation.

Pha-siRNA

At 6 h time point we identified upregulated sRNAs that were derived from a transcript coding for a mitochondrial PPR protein (AT1G63070) and this was already shown to produce pha-siRNAs [101] (Additional file 12: Table S16). Despite the increasing abundance of the pha-siRNAs we were not able to detect the respective PPR transcript in the mRNA data. The most abundant sRNAs were 21 nt in size followed by 22 nt sRNAs generated from this PPR transcript. The 21 nt pha-siRNAs are known to be loaded into the argonaute and RNA-induced silencing complex to mediate cleavage of mRNA targets. We performed a target prediction for the 21 nt pha-siRNA with psRNATarget applying stringent parameters and identified putative target transcripts that encode other PPR and TPR proteins, the photosystem II subunit QA (AT4G21280), RNA processing factor 2 (AT1G62670) and HVA22 Homologue A (AT1G74520). The RNA processing factor 2 also belongs to a class of PPR protein which facilitates RNA processing in mitochondria [102]. The photosystem II subunit QA is a component of the electron transport chain and the HVA22 Homologue A protein with an unknown function was previously shown to be ABA and stress inducible [103]. In agreement with the observed upregulation of the pha-siRNA we found the transcript levels of one of the putative targets encoding a PPR protein (AT1G18485) to be significantly downregulated.

Discussion

Our study aims to provide insights into the cold-responsive regulation of different classes of sRNAs and their impact on the control of either the transcripts underlying sRNA production or the control of transcripts targeted by the sRNAs. We combined sRNA sequencing together with sequencing of mRNAs and lncRNAs to correlate changes in mRNA/lncRNA steady state levels to changes in sRNA expression. We observed classical cold stress related marker genes to be upregulated in the mRNA sequencing data which were found to be differentially expressed in a previous study (Lee et al. 2005) (Additional file 13: Table S17). Over the time course of cold treatment, we observed an overall reduction of sRNAs produced from RNA classes such as miRNAs, *trans*- and *cis*-NATs-pairs and lncRNAs. To exclude that these changes are not caused by altered levels of the major components involved in sRNA biogenesis we analyzed the levels of transcripts encoding

sRNA biogenesis associated proteins such as Hua Enhancer 1 (HEN1), RNA dependent RNA polymerase (ATRDR1-6), DCL1-4, HST1, HYL1, Serrate and Suppressor of Gene Silencing 3 (SGS3). Their levels remained unaffected during the time course of cold treatment and we speculate that the reduced sRNA production could be due to a reduced transcription of sRNA precursor transcripts in response to cold acclimation.

Analysis of miRNAs and their putative targets

We analyzed DE miRNAs since these are powerful regulators of gene expression and are involved in the control of nearly all cellular pathways [104]. We found 107 DE miRNAs over the time course of the treatment and compared our results to previously reported cold-responsive miRNAs in *A. thaliana* [32, 35, 71]. Baev et al. (2014) treated plants at 4 °C for 24 h and sequenced the RNA from rosette leaves and detected 44 DE miRNAs. We found an overlap of 7 miRNAs following the same expression pattern and the majority of these were DE after 2 d of cold treatment. Similarly, Liu et al. (2008) subjected plants to 4 °C, isolated RNA from whole plant tissues and detected 11 DE miRNAs through microarray experiments. We detected 5 of these 11 miRNAs following the same expression pattern. Sunkar et al. (2004) studied DE miRNAs from whole plants treated at 0 °C for 24 h and two miRNAs were also identified as DE miRNAs in our study. We found 14 out of 107 DE miRNAs to be previously identified in *A. thaliana* in cold stress and these comparisons show that there is limited overlap between the different studies which might be due to the applied temperature, duration of the treatment or plant tissue types used in the studies. Several miRNAs such as miR167c, miR168, miR397, miR389, miR400, miR837-5p, miR838, and miR857 were reported to be cold stress responsive in other studies, but were not identified to be differentially expressed in this study [32, 35, 71].

We analyzed the psRNATarget tool predicted putative miRNA targets of the DE miRNAs and found 96, 173 and 267 miRNA target pairs at 3 h, 6 h and 2 d time points, respectively, which reflects the importance of miRNAs in regulating the transcriptome at prolonged cold treatment. Typically, the alterations in miRNA expression affect the abundance of target genes via cleavage of the target transcript after complementary pairing. The responses of several abiotic stresses are regulated by common mediators that facilitate cross talk of multiple signaling pathways [105]. To maintain the temporal and spatial expression of stress-related genes, the regulatory factors comprising TFs and sRNAs are extremely essential. Among the predicted targets of the DE miRNAs, we found mRNAs encoding TFs such as NFY, MYB, TCP

and HSFs. The GO enrichment of all predicted miRNA targets showed that the highest number of targets are associated with the nucleus (136 mRNAs) and 85 of these encode TFs. Some miRNAs were not associated with anticorrelated targets, but their expression pattern supports the findings of previous cold-related studies such as miR161.1 and miR159b, which were found to be downregulated at the 6 h time point. Studies with *SNRK1* overexpression lines showed reduced miR161 and miR159b promoter activity and lowered transcript levels of the respective *MIR* precursors that is likely to cause reduced miR161 and miR159b levels [106]. Plants have a multitude of TFs that are necessary for growth and stress responses and we predicted 85 targets of DE miRNA that encode TFs. We predicted TCP2 (AT4G18390) and TCP4 (AT3G15030) to be targeted by miR319 and which is consistent with previous studies in *A. thaliana* and sugarcane [107]. All miR319 isoforms were downregulated after 2 d of cold treatment which is consistent with a study in rice, where miR319 was downregulated and its target *TCP21* was upregulated by cold treatment [108]. We observed a similar downregulation of miR319 and concomitant upregulation of its targets *TCP2* and *TCP4* after 2 d of cold treatment.

MYB TFs are known to facilitate cell proliferation and to control phenylpropanoid metabolism and hormone responses [109]. We observed upregulation of miR858 and a corresponding downregulation of its putative targets *MYB48*, *MYB34* and *MYB20*. Apart from TFs, targets of miRNAs also comprise transcripts for epigenetic regulators such as methyl transferases. miR163 was upregulated after 6 h and downregulated after 2 d of cold treatment. One of its targets coding for a S-adenosyl-L-methionine-dependent methyltransferases superfamily protein (AT1G15125) was downregulated after 6 h and another target encoding a N2, N2-dimethylguanosine tRNA methyltransferase (AT5G15810) was upregulated after 2 d of cold treatment. The tRNA methyltransferase (AT5G15810) was shown to cause stress-related N2, N2-dimethylguanosine (m²G) modification in tRNAs of *A. thaliana* [110]. Usually, tRNA nucleotide modifications occur within tRNAs during their maturation and processing and these modifications are biomarkers of specific stresses and were observed to be induced in response to oxidizing agents [111]. It is also known that stress-induced epitranscriptomic changes regulate tRNA stability, translation initiation, and microRNA-based regulation of transcripts [111].

miR159 alters mitochondrial protein import and ethylene biosynthesis

Similarly, miR159 isoforms were upregulated at 3 h, but downregulated after 2 d of cold treatment. The putative target transcript of miR159 encoding a mitochondrial

translocase TIM-44 related protein (AT5G27395) was anticorrelated with 1.4 fold downregulation at 3 h and 2.8 fold upregulation after 2 d. Since mitochondrial proteins are translated in the cytosol and require import into the mitochondria, our results suggest miRNA-mediated regulation of TIM-44 that may lead to altered mitochondrial protein import during cold treatment. It is known that environmental stresses inhibit and stimulate protein import [112]. TIM44 recruits mitochondrial HSP70 and facilitates the import of proteins containing a transit peptide from the inner membrane into the mitochondrial matrix [113]. miR159 is also known to target RNAs coding for MYB TFs, an aminocyclopropane-1-carboxylate synthase (ACC synthase) and proteins of the *Small Auxin-Up RNA (SAUR)* family [114]. Consistent with the previous findings, the upregulation of miR159 was accompanied by a downregulation of 13 *SAUR* mRNAs and a transcript for an ACC synthase (AT4G37770) that is required for ethylene biosynthesis which is known to be a negative regulator of freezing tolerance [115]. Thus, miR159-mediated downregulation of *ACC synthase* observed in our study suggests a reduced ethylene biosynthesis and increased transcription of *CBF* genes.

miR395c targets an mRNA for a mg chelatase that promotes thermogenesis in cold acclimation

miR395c was found to be downregulated after 6 h of cold treatment and its putative target coding for the Mg chelatase subunit H was concomitantly upregulated. The Mg chelatase is a multifunctional protein involved in chlorophyll synthesis catalyzing the insertion of Mg²⁺ ions into protoporphyrin IX to produce Mg protoporphyrin IX (Mg-Proto-IX) [116]. A recent study confirmed the role of Mg-Proto-IX-derived signals in inducing the gene Alternative oxidase 1a (*AOX1a*) [117]. *AOX1a* reduces O₂ to H₂O without pumping protons from the matrix to the inter-membrane space and in turn dissipates excess energy in the form of heat. The generated heat plays a role in thermogenesis during cold stress conditions and promotes stress tolerance. Moreover, the Mg-Proto-IX signals also lead to increased activities of antioxidant enzymes that add to the maintenance of redox equilibrium in cold stress [118].

A putative target of miR408 coding for a galactose oxidase/kelch repeat protein could induce acclimation in an ABA-dependent manner

Interestingly, miR408-5p was upregulated at all analyzed time points. A chickpea *MIR408* overexpression line subjected to drought stress showed reduced levels of its target coding for plastocyanin. The lack of plastocyanin caused an accumulation of copper and increased levels of copper were shown to cause

upregulation of drought responsive genes such as DREB factors and induced their downstream genes *COR47/RD17* and Low Temperature-Induced 78/Responsive to desiccation 29A (*LTI78/RD29A*) [119]. Similarly, we observed upregulation of miR408-5p, transcripts of DREBs and their downstream transcripts *COR47/RD17* and *LTI78/RD29A* [120, 121]. Further, *MIR408* overexpression lines showed an increased efficiency of photosystem II, reduced electrolyte leakage and lipid peroxidation and increased chlorophyll fluorescence resulting in enhanced cold tolerance due to reduced ROS levels [122]. We predicted a miR408-5p target coding for a galactose oxidase/kelch repeat superfamily protein (AT1G67480) that was found to be downregulated at 6 h and 2 d time points indicating cleavage of the mRNA transcript. Song et al. (2013) studied miR394 and one of its targets coding for the galactose oxidase kelch family protein LCR (Leaf Curling Responsiveness) in *A. thaliana* *MIR394* overexpression and *lcr* mutant lines. They demonstrated upregulation of miR394 and downregulation of *LCR* in the presence of ABA indicating their regulation in salt and drought stress. Other galactose oxidase kelch family proteins such as ZEITLUPE (AT5G57360) have been observed to be reduced at low temperatures [123] and KISS ME DEADLY (AT1G80440) was downregulated to induce UV tolerance [124]. There is a possibility that the putative target galactose oxidase/kelch repeat superfamily protein (AT1G67480) could also mediate cold tolerance in an ABA-dependent manner by its downregulation through miR408-5p [45].

miRNA-mediated inhibition of chlorophyll biosynthesis and flowering in cold

miR171-3p was downregulated at the 2 d time point and its cognate mRNA target encoding the GRAS domain TF Scarecrow-Like 27 (AT2G45160) was upregulated. It is known that *SCL27* binds to the promoter of the *PORC* gene (protochlorophyllide oxidoreductase) through GT *cis*-element repeats and represses its expression causing reduced chlorophyll synthesis [125]. The upregulation of *SCL27* due to reduction in miR171 levels could facilitate the cold treatment imposed inhibition of chlorophyll biosynthesis.

We detected miR156/157 isoforms to be upregulated at the 2 d time point accompanied with downregulation of their target *SPL3* (Squamosa Promoter Binding Protein-Like 3). It has been shown that overexpression of *MIR156a* maintains reduced levels of *SPL3* transcripts which leads to delayed flowering in *A. thaliana* [126]. In contrast, miR172c was downregulated and its putative target encoding RAP2.7 also known as Target of Early Activation Tagged 1 (TOE1) was upregulated. *A. thaliana* *TOE1* overexpression lines also showed delayed

flowering [127] and it is possible that miR156 and miR172c regulate transcript levels of *SPL3* and *TOE1* under cold treatment to inhibit flowering.

A cold-responsive gene regulatory network indicates importance of miRNA-TF-mRNA interaction

By combining the temporal miRNA and mRNA expression data with publicly available knowledge about regulatory binding behavior of miRNAs, TFs and their downstream target genes, we were able to construct a cold-related GRN of *A. thaliana*. In the resulting GRN we observed different modes of target regulation with respect to miRNAs and TFs both regulating direct targets and miRNAs that regulate TF transcripts and thus control additional targets in an indirect manner. A large number of connections was observed between miRNAs and their direct targets, but the number of affected targets increased when miRNA-targeted TFs were included into the network. This indicates that TFs act as the central nodes for relaying information from miRNAs to several TF-affected targets. The extracted cold responsive GRN revealed an overrepresentation of distinct functional modules such as cold stress, biotic stress and cell organization, transcription and translation, transport and PPR, cell wall and lignin synthesis, signaling and protein degradation. This indicates that miRNA-regulation seems to be important to control major cellular pathways that are known to be involved in cold adaptation. The complete GRN as well as specific subnetworks can be used to study the regulatory relationships of miRNA, TFs and their direct and indirect targets to explore putative novel interacting regulatory components that facilitate cold acclimation.

Differentially expressed sRNAs derived from other RNA classes

We further investigated sRNAs derived from other RNA classes such as lncRNA, *cis*- and *trans*-NATs, *TAS* and *PHAS*. We found 15 non-redundant, non-overlapping lncRNAs that produced DE sRNAs during the course of cold treatment. Since 12 of these lncRNA transcripts were not detected by RNAseq and 3 were not DE, we speculate that the lncRNA transcripts are efficiently processed into sRNAs to repress their transcript levels. Such an autoregulatory mechanism has been shown in rice where the lncRNA *Long day specific male fertility associated RNA (LDMAR)* was able to produce *Psi-LDMAR* siRNAs that were able to repress their parent *LDMAR* transcript by RNA-dependent DNA methylation (RdDM) [128].

Besides non-overlapping lncRNAs, we found 429 non-redundant *cis*-NATs and 179 non-redundant *trans*-NATs pairs producing DE siRNAs with a high proportion of pc:nc and pc:pc transcript pairs. DE sRNAs

derived from *cis*-NATs have been identified in *A. thaliana* subjected to drought, cold and salt stress treatments [87]. Zhang et al. (2012) grew seedlings for 29 days at 23 °C and shifted them to 5 °C for 24 h and we detected three *cis*-NATs pairs that were reported in this study to give rise to cold-induced nat-siRNAs. One transcript pair, AT5G15845 (ncRNA) and AT5G15850 (CONSTANS-like 1) showed the same pattern of nat-siRNA production as reported for cold and salt stress and the transcript levels of both genes as well as the nat-siRNAs were upregulated [87]. Another transcript pair, AT5G19220 (ADP-glucose pyrophosphorylase) and AT5G19221 (ncRNA) showed unchanged transcript levels, but elevated nat-siRNA production. The second pair showed less normalized reads in untreated samples compared to cold, salt and drought stress in Zhang et al. (2012). Another NATs pair comprising AT3G22120 (Cell wall-plasma membrane linker protein homolog) and AT3G22121 (ncRNA) led to increased nat-siRNA production. The same gene pair was found to generate reduced nat-siRNA in the previous study in response to cold, but produced elevated nat-siRNAs under salt stress [87].

We observed a predominance of pc:nc gene pairs with pre-tRNA or TE as the non-coding transcript partner. We found a large number of pre-tRNA transcripts pairing with protein coding transcripts and producing siRNAs from one or both pairing transcripts. Several pre-tRNA transcripts are able to pair with an mRNA encoding a Gly-Asp-Ser-Leu (GDSL)-like Lipase/Acylhydrolase superfamily protein (AT5G55050) and a GDSL type lipase gene in pepper has been shown to be involved in drought tolerance, the expression of ABA-inducible genes and oxidative stress signaling [129]. Transcripts encoding F-Box containing proteins (AT2G33655, AT1G11270, AT2G16365) that are known to be co-expressed with several abiotic stress related genes [130] or to activate stress-responsive genes [131] showed pairing with pre-tRNA transcripts to produce *trans*-nat-siRNAs. With respect to the expression pattern of the pairing transcripts and the resulting nat-siRNA it is possible that the siRNAs are produced from the pre-tRNA alone or they are processed from a dsRNA formed by pairing of pre-tRNA and the protein coding transcript. tRNA-derived small RNAs (tsRNAs) were initially thought to be degradation products of endonucleases, but recent advances suggest their functional role in the maintenance of genome stability, epigenetic inheritance, stress response and cell proliferation [132]. Studies in other organisms suggest that the expression of these sRNAs referred to as transfer RNA-derived fragments (5'tRF and 3'tRF) can be related to the quality control of protein synthesis [133, 134]. Previous experiments in *A.thaliana* and human suggest that the tRNA-derived sRNA biogenesis depends on the miRNA pathway [135] and tRFs target transcripts of TE to promote genome

stability [91, 136]. A recent study confirmed the loading of 19-25 nt tRFs into AGO proteins suggesting a role of tRNA produced sRNAs in post-transcriptional gene silencing [94, 137-140]. German et al. (2017) observed the accumulation of 19 nt tRNA-derived sRNAs from the 5' end of mature tRNA transcripts in *A. thaliana* pollen. It was concluded that tRFs are processed similar to miRNAs since there was a reduction in tRF accumulation in a *ddm1/dcl1* double mutant. tRFs and TE-derived sRNAs have been observed to be DE in barley in the presence and absence of phosphorous [141] and in response to phosphate deficiency in *A.thaliana* [142]. Moreover, recently a new class of DCL-independent siRNAs termed sidRNAs were identified that are incorporated into AGO4 and trigger de novo methylation in *A. thaliana* [143] suggesting similarity to tRFs. Besides tRNAs, we detected differential regulation of *trans*-nat-siRNAs derived from transposons containing Ty3 Gypsy, CACTA and Ty1 Copia elements. TE-derived siRNAs can cause DNA methylation or induce repressive histone tail modifications to repress TE loci [144]. Furthermore, in *A. thaliana* TE-derived siRNAs can also target protein coding genes. For example the TE-derived siRNA854 was found to control *UBP1* transcript level that encodes Upstream Binding Protein 1a component of plant stress granules [100]. We found 4, 6 and 26 hypothetical protein coding transcripts pairing with TE encoded transcripts, pseudogene RNAs, mRNA and non-coding RNA transcripts at 3 h, 6 h and 2 d time point, respectively, indicating an involvement of several RNA classes in the adaptation to cold treatment.

In addition to nat-siRNAs derived from pc:nc pairing transcripts, we also identified pc:pc *cis*- and *trans*-NATs pairs that produced siRNAs and we observed an increasing number of nat-siRNAs over the time course of the treatment. We detected elevated expression of nat-siRNAs from 9 *cis*-NAT pairs in response to cold where the overlapping transcripts underlying nat-siRNA production follow the classical expression pattern of a nat-siRNA regulon [54]. This is characterized by an increased expression of nat-siRNAs in response to a stimulus due to an elevated transcription of one of the pairing partners that causes downregulation of the cognate partner transcript. We observed cold-induced upregulation of one transcript together with the repression of its cognate pairing transcript and these gene pairs comprised the transcripts *RAN2 GTPase* (AT5G20020) and *Plant Tudor-like RNA-binding protein* (AT5G20030), *TCP-1 chaperonin family protein* (AT3G11830) and *plant U-box 24* (AT3G11840) and *PPR* (AT1G03100) pairing with *mitochondrial/3-methylcrotonyl-CoA carboxylase 1* (AT1G03090). The inverse expression pattern of these pairing transcripts was accompanied by the induction of *cis*-nat-siRNAs in cold treatment. An ideal example is represented by the cold

responsive upregulation of an mRNA encoding a MATE efflux protein (AT5G52450) that is involved in xenobiotic detoxification, disease resistance, and the control of phytohormones and its pairing partner *High Chlorophyll Fluorescence 106* (*HCF106*, AT5G52440) that displays a concomitant downregulation. Until now, functional studies on the putative MATE efflux protein are lacking whereas the overlapping transcript encoding HCF106 protein is well characterized. HCF106 is a chloroplast thylakoid protein and imports proteins into the thylakoid lumen. The *hcf106* knockout mutants are albino mutants and seedling-lethal, whereas weaker T-DNA alleles are paler in color and display reduced stomatal aperture and reduced water loss and hence cause elevated dehydration tolerance [145]. The production of nat-siRNAs from the two transcripts resulting in elevated levels of the *MATE* transcript and downregulation of *HCF106* transcript suggests a cold-responsive regulatory mechanism which could act in cold acclimation.

Based on our results, we conclude that cold treatment leads to considerable changes in sRNA levels that are likely to contribute to changes in gene expression that underlie cold acclimation in *A. thaliana*. The combination of multilevel high throughput sequencing and bioinformatics analysis proved to be a powerful tool to create a regulatory network of sRNAs and mRNAs responsive to cold stress. A high number of miRNAs were DE and their predicted targets include a large number of mRNAs encoding TFs, PPR and TPR proteins that act in the regulation of gene expression and protein biosynthesis, respectively, and transcripts encoding important enzymes that act in cold acclimation. Along with miRNAs, large numbers of sRNAs were produced from lncRNAs and transcripts of *cis*- and *trans*-NATs pairs indicating a strong impact of all sRNA classes in cold adaptation.

Conclusions

According to this study in *A. thaliana*, miRNAs and sRNAs derived from, *cis*- and *trans*-NAT gene pairs and from lncRNAs play an important role in regulating gene expression in cold acclimation. The gene regulatory network constructed provides substantial information related to the interaction of miRNA and their associated direct and indirect targets. Overall, this study provides a fundamental database to deepen our knowledge and understanding of regulatory networks in cold acclimation.

Methods

Plant material and stress treatment

Seeds of *A. thaliana* ecotype Columbia (*Col-0*) were sown at a high density (ca. 50 seeds on 9 × 9 cm pots) with soil substrate and stratified at 4 °C for 2 d in the dark. Following stratification, the pots were transferred to LED-41 HIL2 cabinets (Percival, Perry, USA) and

cultivated under control conditions with a light / dark regime of 16 h light (80 μmol photons m⁻² s⁻¹; corresponding to 18% of blue and red channel) at 22 °C followed by 8 dark at 18 °C for 14 d. Plants serving as controls remained under these condition whereas plants subjected to cold treatment were transferred 4 h after the onset of light at continuous 4 °C with diurnal light intensity of 35 μmol photons m⁻² s⁻¹. The cold treatment was performed in three independent subsequent experimental replicates using the same growth chamber with identical settings. The aerial tissues from three experimental replicates of cold-treated as well as control samples were harvested after 3 h, 6 h, and 48 h (2 d).

RNA isolation and sRNA sequencing

The total RNA from the biological triplicates of each sample were isolated using TRI-Reagent (Sigma) according to the manufacturer's instructions. For each mRNA and lncRNA library including polyA-tailed lncRNAs, 10 μg total RNA was vacuum dried with RNA stable (Sigma-Aldrich). The libraries were prepared by Novogene (China) using the Next Ultra RNA Library Prep Kit (NEB). The libraries were strand-specifically sequenced as 150 bp paired-end on a HiSeq-2500 platform with at least 15 million read pairs per library.

For each sRNA library 50 μg of total RNA was separated on a 15% native polyacrylamide gel. The ZR small-RNA Ladder (Zymo Research) served as RNA size marker and sRNAs corresponding to 17-29 nt were excised from the gel. The gel pieces were transferred into a LoBind Eppendorf tube and crushed using a disposable polypropylene pestle. 0.3 M NaCl was added to immerse the gel pieces and the tubes were frozen for 15 min at -80 °C and RNA was subsequently eluted overnight at 4 °C. The buffer was transferred into a Spin-X centrifuge tube filter (COSTAR) and centrifuged for 1 min at 4 °C to remove the gel pieces. RNA was precipitated by adding 2.5 volume of 100% (v/v) ethanol, 1/10 volume of 3 M NaOAc (pH 5) and 1 μl of glycogen (10 mg/ml) and incubation at -80 °C for 4 h. The samples were centrifuged for 30 min with 17,000 × g at 4 °C and the RNAs were washed twice with 80% ethanol, dried at room temperature and resuspended in 7 μl of nuclease free water. RNA concentrations were measured spectrophotometrically and the sRNA fractions were used for library preparation using the NEBNext multiplex small RNA library prep kit Illumina following the manufacturer's protocol with minor modifications. The 3' SR adapter was ligated at 16 °C overnight and the SR reverse transcription primer was hybridized to an excess of 3' SR adapter to prevent adapter dimer formation. After ligation of the 3' SR adapter, the 5' SR adapter was ligated to the RNA and incubated for 1.5 h at 25 °C. PCR amplification of the libraries was performed using

specific index primers for 12 cycles and the cDNA amplicons were separated on a 6% native acrylamide gel at 120 V. The gel was stained with SYBR gold and RNAs with a size between 138 and 150 nt corresponding to adapter-ligated sRNAs with a size between 18 and 30 nt were excised. Gel elution of the DNA was performed as described above except the addition of 1 μ l linear acrylamide (5 mg/ml) prior to precipitation to increase the DNA pellet mass. The cDNA library with concentration of at least 8 ng/ μ l was considered optimum for sequencing. The sRNA libraries were sequenced with an Illumina deep sequencing platform (Illumina HiSeq 1500) with a read length of 50 nt and a minimum of 7 million reads per library.

Bioinformatic analyses of transcriptomes

The mRNA/lncRNA sequencing data for the triplicates of 3 h, 6 h and 2 d cold-acclimated samples together with the respective controls were analyzed using open web based platform GALAXY (<https://usegalaxy.org/>) [146]. The adapter sequences were trimmed using the FASTQ Trimmomatic tool using the default parameters. To map the raw reads against *A. thaliana* reference genome (<https://www.arabidopsis.org>, release: TAIR10), Tophat tool was used with a maximum intron length parameter of 3000 nt. The Araport11 annotation [147] was used to annotate the transcripts and ncRNA transcripts longer than 200 bp were considered as lncRNAs. We used the FeatureCounts tool to count the number of reads mapped to the reference genome (Additional file 1: Table S1). Using the count file as an input for the DeSeq2 tool of GALAXY, we obtained the final list of genes. All genes were classified based on Araport11 reference annotation (<https://araport.org/>).

The sRNA raw reads were mapped to the TAIR10 (<https://www.arabidopsis.org>, release: TAIR10) reference genome using the Shortstack software [148]. Approximately 80% of the obtained reads efficiently mapped to it (Additional file 1: Table S2). We generated a reference annotation database for sRNAs derived from RNA classes such as miRNA (miRBase version 22.1), lncRNA (Araport11), *trans*- and *cis*-nat-siRNA [57, 87–89], ta-siRNA and phasiRNA [101] that was used to generate read counts of sRNAs obtained from these RNA classes. The counts generated from the triplicates were used for the analysis of differential expression using the DeSeq2 tool in GALAXY and sRNAs having a FC ≥ 2 & ≤ -2 , Benjamini-Hochberg corrected *p*-value ≤ 0.05 were considered to be DE. Global comparisons of DE miRNAs were generated using UpSetR package (<https://CRAN.R-project.org/package=UpSetR>).

cDNA synthesis for stem loop qRT-PCR

cDNA was synthesized using 300 ng of RNA from three biological replicates of treated and untreated samples

[149]. The RNA was treated with DNase I (2 U, NEB) at 37 °C for 30 min to eliminate genomic DNA contamination, the enzyme was heat-inactivated at 65 °C for 10 min and the RNA was reverse transcribed into cDNA by M-MuLV Reverse transcriptase (200 U, NEB) at 42 °C for 30 min. Specific stem loop primers and a universal reverse primer were used for cDNA synthesis (Additional file 14: Table S18). During cDNA synthesis, we added *UBI1* (AT4G36800) specific reverse primer and monitored the successful cDNA synthesis through PCR by using *UBI1* specific gene primers.

Stem loop qRT-PCR

The Real-time PCR was performed using EvaGreen and sRNA-specific primers (Additional file 14: Table S18). For each sample, the qRT-PCR was performed in three technical replicates and each reaction contained cDNA amounts equivalent to 20 ng/ μ l of initial RNA. The qRT-PCR program was adjusted to initial denaturation at 95 °C for 2 min followed by 40 cycles of amplification with 95 °C for 12 s, annealing for 30 s and 72 °C for 15 s. The SYBR green signals were measured after each cycle and melting curves were monitored to confirm primer specificities. The C_t values were used to calculate the expression levels by using $\Delta\Delta C_t$ method [150]. The expression levels were normalized using *UBI1* housekeeping gene (AT4G36800).

miRNA target prediction

MiRNA targets were predicted using the psRNATarget prediction tool (2017 Update) [73]. DE miRNAs were used as a query to search against *A. thaliana* protein coding and non-coding transcripts of Araport11 keeping default parameters and allowing calculation of target accessibility (maximum energy to unpair the target site = 25). We used a stringent cut off value 2.5 as the maximum expectation score for selecting our potential targets.

Gene ontology of miRNA targets

GO analyses were performed with the DAVID Bioinformatics tool [78]. The list of miRNA target genes was provided as an input and the output list contained genes categorized into biological process, cellular compartment and molecular function. We filtered for significant GO terms with Benjamini-Hochberg corrected *p*-value ≤ 0.05 which was obtained from Fisher's test in all the categories. The dot plot visualizing the GO terms was generated using ggplot2 package (<https://CRAN.R-project.org/package=ggplot2>).

Construction and validation of the regulatory network model

The gene regulatory network (GRN) was constructed using high confidence experimentally validated regulatory connection from ATRM [79] and Agris [80]. We

did not include all the connections available in PlantReg-Map [151] but the ones which fulfill the criteria of conservation of binding motifs. First criterion includes TF connections whose binding sites lie in the conserved elements of different plant species (motif_CE) and the second criterion included TF connections whose binding sites were found to be conserved in different plant species when scanned for conservation of TFBSs (FunTFBS) [81]. The TF based regulatory connections following these two criteria were merged with the psRNATarget tool predicted miRNA targets to obtain the full network model. The prediction of target gene expression was performed using the Fast Tree Regression learner from Dotnet.ML version 0.8 [152]. The outcome variable was the FPKM of target gene expressions at the separate time points 3 h, 6 h, and 2 d. As input variables, we used the time point, the expression levels for each regulator familywise aggregated at the respective time and the counts of binding sites of the target gene. Both family assignments for each TF and binding site information for each target were taken from the AtTFDB database [153]. The data related to GRN can be accessed through free visualization Software GEPHI available for download at <https://gephi.org/> (Additional file 7: Data S1, S2).

Heatmap clustering

The heatmap function (<https://cran.r-project.org/web/packages/heatmap/index.html>) of the R package ‘Pheatmap’ was used to create a heatmap showing hierarchical clustering of differentially expressed miRNAs at the three time points of cold treatment.

Supplementary information

Supplementary information accompanies this paper at <https://doi.org/10.1186/s12870-020-02511-3>.

Additional file 1 Table S1: Total mRNA sequencing reads mapping to the *A. thaliana* reference genome after adapter trimming in control and cold treated samples (biological triplicates). Table S2: Total sRNA sequencing reads mapping to different sRNA producing RNA classes for control and cold treated samples. Table S3: sRNA size distribution in reads per million. The size distribution of total sRNAs derived from control and cold treated samples after adapter trimming.

Additional file 2 Table S4: Differentially expressed miRNAs during cold acclimation. The three sub-tables depict DE miRNAs at 3 h, 6 h and 2 d, respectively. The miRNAs highlighted in orange belong to evolutionarily conserved miRNA families. Table S5: Normalized read counts and fold changes of all miRNAs during cold acclimation. The three sub-tables depict all miRNAs at 3 h, 6 h and 2 d, respectively. Table S6: Differentially expressed cold-responsive miRNAs in *A. thaliana*. Fold changes of miRNAs after 3 h, 6 h and 2 d of cold treatment, considered DE when $\log_2FC \geq 1$ & ≤ -1 , Benjamini-Hochberg corrected p -value ≤ 0.05 , Conserved miRNAs are highlighted in bold.

Additional file 3 Table S7: List of miRNA-targeted mRNAs predicted using psRNATarget. The sub-tables depict all predicted targets of DE miRNAs at the three time points. A stringent expectation value of 2.5 was used to filter the targets. N/A = No significant fold change Table S8: List of miRNA-targeted ncRNAs predicted using psRNATarget. The sub-tables depict all predicted ncRNA targets of DE miRNAs at the three time points.

A stringent expectation value of 2.5 was used to filter the targets. N/A = No significant fold change .

Additional file 4 Table S9: List of all mRNAs generated from mRNA sequencing data. The three sub-tables depict normalized read counts (triplicates) from control and cold treated samples at 3 h, 6 h and 2 d. Table S10: List of all significant DE mRNAs generated from mRNA sequencing data. The sub-tables present all the details from control and cold treated samples after 3 h, 6 h and 2 d.

Additional file 5 Table S11: List of 54 targets of differentially expressed miRNAs from all the four subgroups found to be consistently present at all the three time points. The Venn diagram depicts all targets of differentially expressed miRNAs observed after 3 h, 6 h and 2 d.

Additional file 6 Table S12: Gene Ontology term enrichment analysis for predicted targets of differentially expressed miRNAs. The sub-tables depict GO terms after 3 h, 6 h and 2 d of cold acclimation.

Additional file 7. The data file that can be accessed using free software GEPHI available at <https://gephi.org/> comprising of Data S1: Gene regulatory network in cold acclimation, Data S2: Cold responsive network of the differentially expressed miRNAs.

Additional file 8 Fig. S1: Complete gene regulatory network (GRN) of cold acclimation. Overview of the GRN for cold acclimation. All predicted miRNA targets in cold were selected and TFs regulating these targets were inferred. Vertex colors indicate the respective regulatory activity and edge colors mark the association to a calculated module. The biggest modules are labeled with their most prominent functional groups which were identified using ontology enrichment.

Additional file 9 Fig. S2: Cold responsive gene regulatory network comprising of direct and indirect targets of DE miRNAs. The miRNAs and the targets are differentially expressed at any one of the analyzed time points ($FC \geq 2$ & ≤ -2 , Benjamini-Hochberg corrected p -value ≤ 0.05). Functional modules associated with cold stress; kinase signaling; transcription, translation and transport are represented by blue, dark green, pink, and orange color, respectively.

Additional file 10 Fig. S3: Subnetwork of miR858a extracted from the complete network. The direct and the indirect targets of miRNAs are differentially expressed in at least one of the analyzed time points ($FC \geq 2$ & ≤ -2 , Benjamini-Hochberg corrected p -value ≤ 0.05).

Additional file 11 Subnetwork of miR319b extracted from the complete network. The direct and the indirect targets of miRNAs are differentially expressed in at least one of the analyzed time points ($FC \geq 2$ & ≤ -2 , Benjamini-Hochberg corrected p -value ≤ 0.05).

Additional file 12 Table S13: Differentially expressed sRNAs produced from non-overlapping lncRNAs. The sub-tables depict detailed sRNA and lncRNA transcript sequencing data at 3 h, 6 h and 2 d. Table S14: Differentially expressed sRNAs produced from *cis*-NAT pairs. The sub-tables depict detailed sRNA and *cis*-NAT sequencing data at 3 h, 6 h and 2 d. Table S15: Differentially expressed sRNAs produced from *trans*-NAT pairs. The sub-tables depict detailed sRNA and *trans*-NAT sequencing data at 3 h, 6 h and 2 d. Table S16: Differentially expressed sRNAs produced from *PHAS* pairs. The sub-tables depict detailed sRNA and *PHAS* transcript sequencing data at 3 h, 6 h and 2 d.

Additional file 13 Table S17: List of classical cold responsive genes that were found to be differentially expressed in Lee et al. 2005 and are also differential expression in our study.

Additional file 14 Table S18: Sequences of oligonucleotides used in this study to perform stem loop qRT-PCR.

Abbreviations

sRNAs/ siRNAs: Small RNAs/ small interfering RNAs; miRNA: MicroRNA; ncRNA: Non-coding RNA; lncRNA: Long non-coding RNA; ta-siRNA: Trans-acting siRNA; *cis/trans*-NAT: *Cis/trans*-natural antisense transcript; NAT: Natural antisense transcript; DEG: Differentially expressed gene; TE: Transposable element; TF: Transcription factor; pc: Protein coding; nc: Non-coding; GO: Gene Ontology; OST1: OPEN STOMATA 1; ABA: Abscisic acid; ICE1: Inducer of CBF expression; CBF: C-repeat binding factors; DREB: Dehydration responsive element binding factors; CRT/DRE: Cold response sensitive transcription factors/dehydration responsive elements;

COR: Cold-responsive; **ABFs:** ABRE-binding factors; **RdDM:** RNA-directed DNA methylation; **FLC:** Flowering locus C; **DCL1:** DICER-LIKE1; **LCR:** *LEAF CURLING RESPONSIVENESS*; **P5CDH:** Delta-pyrroline-5-carboxylate dehydrogenase; **SRO5:** Similar to Radicle Induced Cell Death One 5; **DDM1:** Decreased DNA methylation 1; **ea-siRNA:** Epigenetically activated siRNA; **TCP:** Teosinte Branched 1, Cycloidea and Pcf Transcription Factor 2; **TIM:** Translocase Inner Membrane Subunit; **RAN2:** RAS-Related GTP-Binding Nuclear Protein; **PPR:** Pentatricopeptide repeat superfamily protein; **NFY:** Nuclear Factor-Y; **HSF:** Heat shock factors; **ACC synthase:** Amino-cyclopropane-1-carboxylate synthase; **MATE:** Multi-antimicrobial extrusion protein; **tRF:** tRNA-derived RNA fragments

Acknowledgements

We thank Martin Simon for technical support and advice regarding sRNA library preparations and Oguz Top for helpful comments on the manuscript.

Authors' contributions

WF and MAA designed the research; BT performed the research with the help of MAA and KH; BT, MAA, KH and WF analyzed the data; AGM and TK provided the 3 h and 2 d mRNA/lncRNA mRNA sequencing raw data; miRNA-TF network was constructed by HLW and TM; and BT, MAA, HLW and WF wrote the paper. The authors read and approved the final manuscript.

Funding

The funding for the research conducted was provided by the German Research Foundation (SFB-TRR 175, grants to W.F. project C03, T.M. project D02, and T.K. project C01). The Funding body was not involved in the design of the study and analysis or interpretation of the data and in writing of the manuscript.

Availability of data and materials

The raw Illumina sRNA and mRNA sequencing data is deposited in NCBI SRA database with the ID PRJNA592037. All raw data used for the analyses in this study is available for reviewers at <https://dataview.ncbi.nlm.nih.gov/object/PRJNA592037?reviewer=lhkljqn6c6q67vp6p70ra9159>.

Ethics approval and consent to participate

Not applicable.

Consent for publication

Not applicable.

Competing interests

The authors declare that they have no competing interests.

Author details

¹Department of Biology I, Plant Molecular Cell Biology, Ludwig-Maximilians-Universität München, LMU Biocenter, Großhaderner Str. 2-4, 82152 Planegg-Martinsried, Germany. ²Computational Systems Biology, Technische Universität Kaiserslautern, Paul-Ehrlich-Straße 23, 67663 Kaiserslautern, Germany. ³Department of Biology I, Plant Molecular Cell Biology, Ludwig-Maximilians-Universität München, LMU Biocenter, Großhaderner Str. 2-4, 82152 Planegg-Martinsried, Germany.

Received: 26 February 2020 Accepted: 22 June 2020

Published online: 29 June 2020

References

- Gornall J, Betts R, Burke E, Clark R, Camp J, Willett K, et al. Implications of climate change for agricultural productivity in the early twenty-first century. *Philos Trans R Soc Lond B Biol Sci.* 2010;365(1554):2973–89.
- Zhu JK. Abiotic stress signaling and responses in plants. *Cell.* 2016;167(2):313–24.
- Solanke AU, Sharma AK. Signal transduction during cold stress in plants. *Physiol Mol Biol Plants.* 2008;14(1–2):69–79.
- Thomashow MF. Role of cold-responsive genes in plant freezing tolerance. *Plant Physiol.* 1998;118(1):1–8.
- Abla M, Sun H, Li Z, Wei C, Gao F, Zhou Y, et al. Identification of miRNAs and their response to cold stress in *Astragalus Membranaceus*. *Biomolecules.* 2019;9(5):182.
- Ding Y. OST1 kinase modulates freezing tolerance by enhancing ICE1 stability in *Arabidopsis*. *Dev Cell.* 2015;32(3):278–89.
- Chinnusamy V, Zhu JK, Sunkar R. Gene regulation during cold stress acclimation in plants. *Methods Mol Biol.* 2010;639:39–55.
- Cuevas-Velazquez CL, Rendon-Luna DF, Covarrubias AA. Dissecting the cryoprotection mechanisms for dehydrins. *Front Plant Sci.* 2014;5:583.
- Devert A, Fabre N, Floris M, Canard B, Robaglia C, Crete P. Primer-dependent and primer-independent initiation of double stranded RNA synthesis by purified *Arabidopsis* RNA-dependent RNA polymerases RDR2 and RDR6. *PLoS One.* 2015;10(3):e0120100.
- Wang DZ, Jin YN, Ding XH, Wang WJ, Zhai SS, Bai LP, et al. Gene regulation and signal transduction in the ICE-CBF-COR signaling pathway during cold stress in plants. *Biochemistry.* 2017;82(10):1103–17.
- Lee SJ, Kang JY, Park HJ, Kim MD, Bae MS, Choi HI, et al. DREB2C interacts with ABF2, a bZIP protein regulating abscisic acid-responsive gene expression, and its overexpression affects abscisic acid sensitivity. *Plant Physiol.* 2010;153(2):716–27.
- Lamke J, Baurle I. Epigenetic and chromatin-based mechanisms in environmental stress adaptation and stress memory in plants. *Genome Biol.* 2017;18(1):124.
- Banerjee A, Wani SH, Roychoudhury A. Epigenetic control of plant cold responses. *Front Plant Sci.* 2017;8:1643.
- Palusa SG, Ali GS, Reddy AS. Alternative splicing of pre-mRNAs of *Arabidopsis* serine/arginine-rich proteins: regulation by hormones and stresses. *Plant J Cell Mol Biol.* 2007;49(6):1091–107.
- Chekanova JA. Long non-coding RNAs and their functions in plants. *Curr Opin Plant Biol.* 2015;27:207–16.
- Li S, Castillo-Gonzalez C, Yu B, Zhang X. The functions of plant small RNAs in development and in stress responses. *Plant J Cell Mol Biol.* 2017;90(4):654–70.
- Ku YS, Wong JW, Mui Z, Liu X, Hui JH, Chan TF, et al. Small RNAs in plant responses to abiotic stresses: regulatory roles and study methods. *Int J Mol Sci.* 2015;16(10):24532–54.
- Ransohoff JD, Wei Y, Khavari PA. The functions and unique features of long intergenic non-coding RNA. *Nat Rev Mol Cell Biol.* 2018;19(3):143–57.
- Wang XQ, Crutchley JL, Dostie J. Shaping the genome with non-coding RNAs. *Curr Genomics.* 2011;12(5):307–21.
- Di C, Yuan J, Wu Y, Li J, Lin H, Hu L, et al. Characterization of stress-responsive lncRNAs in *Arabidopsis thaliana* by integrating expression, epigenetic and structural features. *Plant J Cell Mol Biol.* 2014;80(5):848–61.
- Wang KC, Chang HY. Molecular mechanisms of long noncoding RNAs. *Mol Cell.* 2011;43(6):904–14.
- Franco-Zorrilla JM, Valli A, Todesco M, Mateos I, Puga MI, Rubio-Somoza I, et al. Target mimicry provides a new mechanism for regulation of microRNA activity. *Nat Genet.* 2007;39(8):1033–7.
- Swiezewski S, Liu F, Magusin A, Dean C. Cold-induced silencing by long antisense transcripts of an *Arabidopsis* Polycomb target. *Nature.* 2009;462(7274):799–802.
- Csorba T, Questa JI, Sun Q, Dean C. Antisense COOLAIR mediates the coordinated switching of chromatin states at FLC during vernalization. *Proc Natl Acad Sci.* 2014;111(45):16160–5.
- Matzke MA, Mosher RA. RNA-directed DNA methylation: an epigenetic pathway of increasing complexity. *Nat Rev Genet.* 2014;15(6):394–408.
- Phil Chi Khang Au ESD. Analysis of Argonaute 4-associated long non-coding RNA in *Arabidopsis thaliana* sheds novel insights into gene regulation through RNA-directed DNA methylation. *Genes.* 2017;8(8):198.
- Mallory AC, Vaucheret H. Functions of microRNAs and related small RNAs in plants. *Nat Genet.* 2006;38(Suppl):S31–6.
- Gusta LV, Trischuk R, Weiser CJ. Plant cold acclimation: the role of abscisic acid. *J Plant Growth Regul.* 2005;24(4):308–18.
- Chen X. MicroRNA biogenesis and function in plants. *FEBS Lett.* 2005;579(26):5923–31.
- de Lima JC, Löss-Morais G, Margis R. MicroRNAs play critical roles during plant development and in response to abiotic stresses. *Genet Mol Biol.* 2012;35(4):1069–77.
- Song G, Zhang R, Zhang S, Li Y, Gao J, Han X, et al. Response of microRNAs to cold treatment in the young spikes of common wheat. *BMC Genomics.* 2017;18(1):212.
- Baev V, Milev I, Naydenov M, Vachev T, Apostolova E, Mehterov N, et al. Insight into small RNA abundance and expression in high- and low-temperature stress response using deep sequencing in *Arabidopsis*. *Plant Physiol Biochem.* 2014;84:105–14.

33. Lee BH, Henderson DA, Zhu JK. The *Arabidopsis* cold-responsive transcriptome and its regulation by ICE1. *Plant Cell*. 2005;17(11):3155–75.
34. Lee H, Xiong L, Ishitani M, Stevenson B, Zhu JK. Cold-regulated gene expression and freezing tolerance in an *Arabidopsis thaliana* mutant. *Plant J Cell Mol Biol*. 1999;17(3):301–8.
35. Liu HH, Tian X, Li YJ, Wu CA, Zheng CC. Microarray-based analysis of stress-regulated microRNAs in *Arabidopsis thaliana*. *Rna*. 2008;14(5):836–43.
36. Mahale B, Fakrudin B, Ghosh S, Krishnaraj PU. LNA mediated in situ hybridization of miR171 and miR397a in leaf and ambient root tissues revealed expressional homogeneity in response to shoot heat shock in *Arabidopsis thaliana*. *J Plant Biochem Biotechnol*. 2013;23(1):93–103.
37. Zhang Y, Zhu X, Chen X, Song C, Zou Z, Wang Y, et al. Identification and characterization of cold-responsive microRNAs in tea plant (*Camellia sinensis*) and their targets using high-throughput sequencing and degradome analysis. *BMC Plant Biol*. 2014;14:271.
38. De Rienzo F, Gabdoulline RR, Menziani MC, Wade RC. Blue copper proteins: a comparative analysis of their molecular interaction properties. *Protein Sci*. 2000;9(8):1439–54.
39. Pilon SEA-GaM. MicroRNA-mediated systemic Down-regulation of copper protein expression in response to low copper availability in *Arabidopsis*. *J Biol Chem*. 2008;283(23):15932–45.
40. Pourcel L, Routaboul J-M, Cheynier V, Lepiniec L, Debeaujon I. Flavonoid oxidation in plants: from biochemical properties to physiological functions. *Trends Plant Sci*. 2007;12(1):29–36.
41. Liang M, Haroldsen Y, Cai X, Wu Y. Expression of a putative laccase gene, ZmLAC1, in maize primary roots under stress. *Plant Cell Environ*. 2006;29(5):746–53.
42. Song JB, Huang SQ, Dalmay T, Yang ZM. Regulation of LEAF morphology by microRNA394 and its target LEAF CURLING RESPONSIVENESS. *Plant Cell Physiol*. 2012;53(7):1283–94.
43. Knauer S, Holt AL, Rubio-Somoza I, Tucker EJ, Hinze A, Pisch M, et al. A protodermal miR394 signal defines a region of stem cell competence in the *Arabidopsis* shoot meristem. *Dev Cell*. 2013;24(2):125–32.
44. Song JB, Gao S, Wang Y, Li BW, Zhang YL, Yang ZM. miR394 and its target gene LCR are involved in cold stress response in *Arabidopsis*. *Plant Gene*. 2016;5:56–64.
45. Song JB, Gao S, Sun D, Li H, Shu XX, Yang ZM. miR394 and LCR are involved in *Arabidopsis* salt and drought stress responses in an abscisic acid-dependent manner. *BMC Plant Biol*. 2013;13:210.
46. Dong C-H, Pei H. Over-expression of miR397 improves plant tolerance to cold stress in *Arabidopsis thaliana*. *J Plant Biol*. 2014;57(4):209–17.
47. Peragine A, Yoshikawa M, Wu G, Albrecht HL, Poethig RS. SGS3 and SGS2/SDE1/RDR6 are required for juvenile development and the production of trans-acting siRNAs in *Arabidopsis*. *Genes Dev*. 2004;18(19):2368–79.
48. Vazquez F, Vaucheret H, Rajagopalan R, Lepers C, Gascioli V, Mallory AC, et al. Endogenous trans-acting siRNAs regulate the accumulation of *Arabidopsis* mRNAs. *Mol Cell*. 2004;16(1):69–79.
49. Guan C, Wu B, Yu T, Wang Q, Krogan NT, Liu X, et al. Spatial auxin signaling controls leaf flattening in *Arabidopsis*. *Curr Biol*. 2017;27(19):2940–50.
50. Moldovan D, Spriggs A, Yang J, Pogson BJ, Dennis ES, Wilson IW. Hypoxia-responsive microRNAs and trans-acting small interfering RNAs in *Arabidopsis*. *J Exp Bot*. 2010;61(1):165–77.
51. Kohei K. TAS1 trans-acting siRNA targets are differentially regulated at low temperature, and TAS1 trans-acting siRNA mediates temperature-controlled At1g51670 expression. *Biosci Biotechnol Biochem*. 2010;74(7):1435–40.
52. Hsieh L-C. Uncovering small RNA-mediated responses to phosphate deficiency in *Arabidopsis* by deep sequencing; 2009.
53. Kumar M, Carmichael GG. Antisense RNA: function and fate of duplex RNA in cells of higher eukaryotes. *Microbiol Mol Biol Rev*. 1998;62(4):1415–34.
54. Borsani O, Zhu J, Verslues PE, Sunkar R, Zhu JK. Endogenous siRNAs derived from a pair of natural cis-antisense transcripts regulate salt tolerance in *Arabidopsis*. *Cell*. 2005;123(7):1279–91.
55. Wight M, Werner A. The functions of natural antisense transcripts. *Essays Biochem*. 2013;54:91–101.
56. Wang XJ, Gaasterland T, Chua NH. Genome-wide prediction and identification of cis-natural antisense transcripts in *Arabidopsis thaliana*. *Genome Biol*. 2005;6(4):R30.
57. Yuan C, Wang J, Harrison AP, Meng X, Chen D, Chen M. Genome-wide view of natural antisense transcripts in *Arabidopsis thaliana*. *DNA Res*. 2015;22(3):233–43.
58. Zhang X, Lii Y, Wu Z, Polishko A, Zhang H, Chinnusamy V, et al. Mechanisms of small RNA generation from cis-NATs in response to environmental and developmental cues. *Mol Plant*. 2013;6(3):704–15.
59. Creasey KM, Zhai J. miRNAs trigger widespread epigenetically-activated siRNAs from transposons in *Arabidopsis*. *Nature*. 2014;508:411–5.
60. Piriyaopongsa J, Jordan IK. Dual coding of siRNAs and miRNAs by plant transposable elements. *Rna*. 2008;14(5):814–21.
61. Wang D, Qu Z, Yang L, Zhang Q, Liu ZH, Do T, et al. Transposable elements (TEs) contribute to stress-related long intergenic noncoding RNAs in plants. *Plant J Cell Mol Biol*. 2017;90(1):133–46.
62. Fowler S, Thomashow MF. *Arabidopsis* transcriptome profiling indicates that multiple regulatory pathways are activated during cold acclimation in addition to the CBF cold response pathway. *Plant Cell*. 2002;14(8):1675–90.
63. Zhang B, Pan X, Cannon CH, Cobb GP, Anderson TA. Conservation and divergence of plant microRNA genes. *Plant J*. 2006;46(2):243–59.
64. Pelaez P, Trejo MS, Iniguez LP, Estrada-Navarrete G, Covarrubias AA, Reyes JL, et al. Identification and characterization of microRNAs in *Phaseolus vulgaris* by high-throughput sequencing. *BMC Genomics*. 2012;13:83.
65. Bonnet E, Wuyts J, Rouze P, Van de Peer Y. Detection of 91 potential conserved plant microRNAs in *Arabidopsis thaliana* and *Oryza sativa* identifies important target genes. *Proc Natl Acad Sci U S A*. 2004;101(31):11511–6.
66. Khaksefidli RE, Mirolohi S, Khalaji F, Fakhari Z, Shiran B, Ebrahimie E. Differential expression of seven conserved microRNAs in response to abiotic stress and their regulatory network in *Helianthus annuus*. *Front Plant Sci*. 2015;6:741.
67. Yu Y, Ni Z, Wang Y, Wan H, Hu Z, Jiang Q, et al. Overexpression of soybean miR169c confers increased drought stress sensitivity in transgenic *Arabidopsis thaliana*. *Plant Sci*. 2019;285:68–78.
68. Qin Z, Li C, Mao L, Wu L. Novel insights from non-conserved microRNAs in plants. *Front Plant Sci*. 2014;5:586.
69. Megha S, Basu U, Kav NNV. Regulation of low temperature stress in plants by microRNAs. *Plant Cell Environ*. 2018;41(1):1–15.
70. Lv DK, Bai X, Li Y, Ding XD, Ge Y, Cai H, et al. Profiling of cold-stress-responsive miRNAs in rice by microarrays. *Gene*. 2010;459(1–2):39–47.
71. Sunkar R, Zhu JK. Novel and stress-regulated microRNAs and other small RNAs from *Arabidopsis*. *Plant Cell*. 2004;16(8):2001–19.
72. Khraiweh B, Zhu JK, Zhu J. Role of miRNAs and siRNAs in biotic and abiotic stress responses of plants. *Biochim Biophys Acta*. 2012;1819(2):137–48.
73. Dai X, Zhuang Z, Zhao PX. psRNATarget: a plant small RNA target analysis server (2017 release). *Nucleic Acids Res*. 2018;46(W1):W49–54.
74. Kreps JA, Wu Y, Chang HS, Zhu T, Wang X, Harper JF. Transcriptome changes for *Arabidopsis* in response to salt, osmotic, and cold stress. *Plant Physiol*. 2002;130(4):2129–41.
75. Hahn A, Kilian J, Mohrholz A, Ladwig F, Peschke F, Dautel R, et al. Plant core environmental stress response genes are systemically coordinated during abiotic stresses. *Int J Mol Sci*. 2013;14(4):7617–41.
76. Bresso EG, Chorostecki U, Rodriguez RE, Palatnik JF, Schommer C. Spatial control of gene expression by miR319-regulated TCP transcription factors in leaf development. *Plant Physiol*. 2018;176(2):1694–708.
77. Soitamo AJ, Piippo M, Allahverdiyeva Y, Battchikova N, Aro EM. Light has a specific role in modulating *Arabidopsis* gene expression at low temperature. *BMC Plant Biol*. 2008;8:13.
78. Jiao X, Sherman BT, Huang da W, Stephens R, Baseler MW, Lane HC, et al. DAVID-WS: a stateful web service to facilitate gene/protein list analysis. *Bioinformatics*. 2012;28(13):1805–6.
79. Jin J, He K, Tang X, Li Z, Lv L, Zhao Y, et al. An *Arabidopsis* transcriptional regulatory map reveals distinct functional and evolutionary features of novel transcription factors. *Mol Biol Evol*. 2015;32(7):1767–73.
80. Palaniswamy SK, James S, Sun H, Lamb RS, Davuluri RV, Grotwold E. AGRIS and AtRegNet. A platform to link cis-regulatory elements and transcription factors into regulatory networks. *Plant Physiol*. 2006;140(3):818–29.
81. Tian F, Yang DC, Meng YQ, Jin J, Gao G. PlantRegMap: charting functional regulatory maps in plants. *Nucleic Acids Res*. 2019;48(D1):D1104–13.
82. Hartwell LH, Hopfield JJ, Leibler S, Murray AW. From molecular to modular cell biology. *Nature*. 1999;402(6761 Suppl):C47–52.
83. Blondel VD, Guillaume J-L, Lambiotte R, Lefebvre E. Fast unfolding of communities in large networks. *J Stat Mech*. 2008;10:P10008.
84. Bouzroud S, Gouiaa S, Hu N, Bernadac A, Mila I, Bendaou N, et al. Auxin response factors (ARFs) are potential mediators of auxin action in tomato response to biotic and abiotic stress (*Solanum lycopersicum*). *PLoS One*. 2018;13(2):e0193517.
85. BaozhuLi RF, Guo S, Wang P, Zhu X. The *Arabidopsis* MYB transcription factor, MYB111 modulates salt responses by regulating flavonoid biosynthesis. *Environmental and Experimental Botany*. 166. 103807. <https://doi.org/10.1016/j.envexpbot.2019.103807>.

86. Petridis A, Doll S, Nichelmann L, Bilger W, Mock HP. Arabidopsis thaliana G2-LIKE FLAVONOID REGULATOR and BRASSINOSTEROID ENHANCED EXPRESSION1 are low-temperature regulators of flavonoid accumulation. *New Phytol.* 2016;211(3):912–25.
87. Zhang X, Xia J, Lii YE. Genome-wide analysis of plant nat-siRNAs reveals insights into their distribution, biogenesis and function. *Genome Biol.* 2012;13:R20.
88. Wang H, Chung PJ, Liu J, Jang I-C, Kean MJ, Xu J, et al. Genome-wide identification of long noncoding natural antisense transcripts and their responses to light in *Arabidopsis*. *Genome Res.* 2014;24(3):444–53.
89. Jin H, Vacic V, Girke T, Lonardi S, Zhu JK. Small RNAs and the regulation of cis-natural antisense transcripts in *Arabidopsis*. *BMC Mol Biol.* 2008;9:6.
90. Tang G, Reinhart BJ, Bartel DP, Zamore PD. A biochemical framework for RNA silencing in plants. *Genes Dev.* 2003;17(1):49–63.
91. Martinez G, Choudury SG, Slotkin RK. tRNA-derived small RNAs target transposable element transcripts. *Nucleic Acids Res.* 2017;45(9):5142–52.
92. Cho J. Transposon-derived non-coding RNAs and their function in plants. *Front Plant Sci.* 2018;9:600.
93. Creasey KM, Zhai J, Borges F, Van Ex F, Regulski M, Meyers BC, et al. miRNAs trigger widespread epigenetically activated siRNAs from transposons in *Arabidopsis*. *Nature.* 2014;508(7496):411–5.
94. Loss-Morais G, Waterhouse PM, Margis R. Description of plant tRNA-derived RNA fragments (tRFs) associated with argonaute and identification of their putative targets. *Biol Direct.* 2013;8:6.
95. Ma L, Hong Z, Zhang Z. Perinuclear and nuclear envelope localizations of Arabidopsis ran proteins. *Plant Cell Rep.* 2007;26(8):1373–82.
96. Du J, Huang YP, Xi J, Cao MJ, Ni WS, Chen X, et al. Functional gene-mining for salt-tolerance genes with the power of Arabidopsis. *Plant J Cell Mol Biol.* 2008;56(4):653–64.
97. Leonhardt N, Kwak JM, Robert N, Waner D, Leonhardt G, Schroeder JI. Microarray expression analyses of Arabidopsis guard cells and isolation of a recessive abscisic acid hypersensitive protein phosphatase 2C mutant. *Plant Cell.* 2004;16(3):596–615.
98. Kaplan F, Guy CL. Beta-amylase induction and the protective role of maltose during temperature shock. *Plant Physiol.* 2004;135(3):1674–84.
99. Wang Z, Cui D, Liu J, Zhao J, Cheng L, Xin W, et al. Arabidopsis ZED1-related kinases mediate the temperature-sensitive intersection of immune response and growth homeostasis. *New Phytol.* 2017;215:711–24.
100. McCue AD, Slotkin RK. Transposable element small RNAs as regulators of gene expression. *Trends Genet.* 2012;28(12):616–23.
101. Howell MD, Fahlgren N, Chapman EJ, Cumbie JS, Sullivan CM, Givan SA, et al. Genome-wide analysis of the RNA-DEPENDENT RNA POLYMERASE6/DICER-LIKE4 pathway in *Arabidopsis* reveals dependency on miRNA- and tasiRNA-directed targeting. *Plant Cell.* 2007;19(3):926–42.
102. Binder S, Stoll K, Stoll B. P-class pentatricopeptide repeat proteins are required for efficient 5' end formation of plant mitochondrial transcripts. *RNA Biol.* 2013;10(9):1511–9.
103. Guo W-J, Ho T-HD. An abscisic acid-induced protein, HVA22, inhibits gibberellin-mediated programmed cell death in cereal aleurone cells. *Plant Physiol.* 2008;147(4):1710–22.
104. Samad AFA, Sajad M, Nazaruddin N, Fauzi IA, Murad AMA, Zainal Z, et al. MicroRNA and transcription factor: key players in plant regulatory network. *Front Plant Sci.* 2017;8:565.
105. Atkinson NJ, Urwin PE. The interaction of plant biotic and abiotic stresses: from genes to the field. *J Exp Bot.* 2012;63(10):3523–43.
106. Confraria A, Martinho C, Elias A, Rubio-Somoza I, Baena-Gonzalez E. miRNAs mediate SnRK1-dependent energy signaling in Arabidopsis. *Front Plant Sci.* 2013;4:197.
107. Thiebaut F, Rojas CA, Almeida KL, Grativol C, Domiciano GC, Lamb CR, et al. Regulation of miR319 during cold stress in sugarcane. *Plant Cell Environ.* 2012;35(3):502–12.
108. Wang ST, Sun XL, Hoshino Y, Yu Y, Jia B, Sun ZW, et al. MicroRNA319 positively regulates cold tolerance by targeting OsPCF6 and OsTCP21 in rice (*Oryza sativa* L.). *PLoS One.* 2014;(3). <https://doi.org/10.1371/journal.pone.0091357>.
109. Ambawat S, Sharma P, Yadav NR, Yadav RC. MYB transcription factor genes as regulators for plant responses: an overview. *Physiol Mol Biol Plants.* 2013;19(3):307–21.
110. Wang Y, Pang C, Li X, Hu Z, Lv Z, Zheng B, et al. Identification of tRNA nucleoside modification genes critical for stress response and development in rice and Arabidopsis. *BMC Plant Biol.* 2017;17(1):261.
111. Huber SM, Leonardi A, Dedon PC, Begley TJ. The versatile roles of the tRNA Epitranscriptome during cellular responses to toxic exposures and environmental stress. *Toxics.* 2019;7(1):17.
112. Taylor NL, Rudhe C, Hulett JM, Lithgow T, Glaser E, Day DA, et al. Environmental stresses inhibit and stimulate different protein import pathways in plant mitochondria. *FEBS Lett.* 2003;547(1–3):125–30.
113. Krimmer T, Rassow J, Kunau WH, Voos W, Pfanner N. Mitochondrial protein import motor: the ATPase domain of matrix Hsp70 is crucial for binding to Tim44, while the peptide binding domain and the Carboxy-terminal segment play a stimulatory role. *Mol Cell Biol.* 2000;20(16):5879–87.
114. Hong Ren M, Gray W. SAUR proteins as effectors of hormonal and environmental signals in plant growth. *Mol Plant.* 2015;8(8):1153–64.
115. Shi Y, Tian S, Hou L, Huang X, Zhang X, Guo H, et al. Ethylene signaling negatively regulates freezing tolerance by repressing expression of CBF and type-a ARR genes in Arabidopsis. *Plant Cell.* 2012;24(6):2578–95.
116. Masuda T. Recent overview of the mg branch of the tetrapyrrole biosynthesis leading to chlorophylls. *Photosynth Res.* 2008;96(2):121–43.
117. Zhang ZW, Yuan S, Xu F, Yang H, Chen YE, Yuan M, et al. Mg-protoporphyrin, haem and sugar signals double cellular total RNA against herbicide and high-light-derived oxidative stress. *Plant Cell Environ.* 2011;34(6):1031–42.
118. Zhang Z-W, Wu Z-L, Feng L-Y, Dong L-H, Song A-J, Yuan M, et al. Mg-Protoporphyrin IX signals enhance Plant's tolerance to cold stress. *Front Plant Sci.* 2016;7:1545.
119. Sakuma Y, Maruyama K, Osakabe Y, Qin F, Seki M, Shinozaki K, et al. Functional analysis of an Arabidopsis transcription factor, DREB2A, involved in drought-responsive gene expression. *Plant Cell.* 2006;18(5):1292–309.
120. Hajyazadeh M, Turktas M, Khawar KM. Unver T: miR408 overexpression causes increased drought tolerance in chickpea. *Gene.* 2015;555(2):186–93.
121. Jiang Q, Sun X, Niu F, Hu Z, Chen R, Zhang H. GmdREB1 overexpression affects the expression of microRNAs in GM wheat seeds. *PLoS One.* 2017;(5). <https://doi.org/10.1371/journal.pone.0175924>.
122. Ma C, Burd S. Lers a: miR408 is involved in abiotic stress responses in Arabidopsis. *Plant J.* 2015;84(1):169–87.
123. Kwon YJ, Park MJ, Kim SG, Baldwin IT, Park CM. Alternative splicing and nonsense-mediated decay of circadian clock genes under environmental stress conditions in Arabidopsis. *BMC Plant Biol.* 2014;14:136.
124. Zhang X, Gou M, Guo C, Yang H, Liu CJ. Down-regulation of Kelch domain-containing F-box protein in Arabidopsis enhances the production of (poly) phenols and tolerance to ultraviolet radiation. *Plant Physiol.* 2015;167(2):337–50.
125. Ma Z, Hu X, Cai W, Huang W, Zhou X, Luo Q, et al. Arabidopsis miR171-targeted scarecrow-like proteins bind to GT cis-elements and mediate gibberellin-regulated chlorophyll biosynthesis under light conditions. *PLoS Genet.* 2014. <https://doi.org/10.1371/journal.pgen.1004519>.
126. Wu G, Poethig RS. Temporal regulation of shoot development in Arabidopsis thaliana by miR156 and its target SPL3. *Development.* 2006;133(18):3539–47.
127. Aukerman MJ, Sakai H. Regulation of flowering time and floral organ identity by a MicroRNA and its APETALA2-like target genes. *Plant Cell.* 2003;15(11):2730–41.
128. Ding J, Shen J, Mao H, Xie W, Li X, Zhang Q. RNA-directed DNA methylation is involved in regulating photoperiod-sensitive male sterility in rice. *Mol Plant.* 2012;5(6):1210–6.
129. Hong JK, Choi HW, Hwang IS, Kim DS, Kim NH, Choi DS, et al. Function of a novel GDSL-type pepper lipase gene, CaGLIP1, in disease susceptibility and abiotic stress tolerance. *Planta.* 2008;227(3):539–58.
130. Gonzalez LE, Keller K, Chan KX, Gessel MM, Thines BC. Transcriptome analysis uncovers Arabidopsis F-BOX STRESS INDUCED 1 as a regulator of jasmonic acid and abscisic acid stress gene expression. *BMC Genomics.* 2017;18:533.
131. Li Q, Wang W, Wang W, Zhang G, Yang L, Wang Y, et al. Wheat F-box protein gene TaFBA1 is involved in plant tolerance to heat stress. *Front Plant Sci.* 2018;9:521.
132. Zhu L, Ow DW, Dong Z. Transfer RNA-derived small RNAs in plants. *Sci China Life Sci.* 2018;61(2):155–61.
133. Wang Q, Li T, Xu K, Zhang W, Wang X, Quan J, et al. The tRNA-derived small RNAs regulate gene expression through triggering sequence-specific degradation of target transcripts in the oomycete pathogen *Phytophthora sojae*. *Front Plant Sci.* 2016;7:1938.

134. Qin C, Xu PP, Zhang X, Zhang C, Liu CB, Yang DG, et al. Pathological significance of tRNA-derived small RNAs in neurological disorders. *Neural Regen Res.* 2020;15(2):212–21.
135. Cole C, Sobala A, Lu C, Thatcher SR, Bowman A, Brown JW, et al. Filtering of deep sequencing data reveals the existence of abundant Dicer-dependent small RNAs derived from tRNAs. *Rna.* 2009;15(12):2147–60.
136. Haussecker D, Huang Y, Lau A, Parameswaran P, Fire AZ, Kay MA. Human tRNA-derived small RNAs in the global regulation of RNA silencing. *Rna.* 2010;16(4):673–95.
137. Alves CS, Vicentini R, Duarte GT, Pinoti VF, Vincentz M, Nogueira FT. Genome-wide identification and characterization of tRNA-derived RNA fragments in land plants. *Plant Mol Biol.* 2017;93(1–2):35–48.
138. Yeung ML, Bennasser Y, Watashi K, Le SY, Houzet L, Jeang KT. Pyrosequencing of small non-coding RNAs in HIV-1 infected cells: evidence for the processing of a viral-cellular double-stranded RNA hybrid. *Nucleic Acids Res.* 2009;37(19):6575–86.
139. Garcia-Silva MR, Cabrera-Cabrera F, Guida MC, Cayota A. Hints of tRNA-derived small RNAs role in RNA silencing mechanisms. *Genes (Basel).* 2012;3(4):603–14.
140. Kescu C, Kumar P, Kiran M, Su Z, Malik A, Dutta A. tRNA fragments (tRFs) guide ago to regulate gene expression post-transcriptionally in a Dicer-independent manner. *Rna.* 2018;24(8):1093–105.
141. Hackenberg M, Huang PJ, Huang CY, Shi BJ, Gustafson P, Langridge P. A comprehensive expression profile of microRNAs and other classes of non-coding small RNAs in barley under phosphorous-deficient and -sufficient conditions. *DNA Res.* 2013;20(2):109–25.
142. Hsieh LC, Lin SI, Shih AC, Chen JW, Lin WY, Tseng CY, et al. Uncovering small RNA-mediated responses to phosphate deficiency in *Arabidopsis* by deep sequencing. *Plant Physiol.* 2009;151(4):2120–32.
143. Ye R, Chen Z, Bi L, Jordan Rowley M, Xia N, Chai J, et al. A Dicer-independent route for biogenesis of siRNAs that direct DNA methylation in *Arabidopsis*. *Mol Cell.* 2016;61(2):222–35.
144. Xie M, Yu B. siRNA-directed DNA methylation in plants. *Curr Genomics.* 2015;16(1):23–31.
145. Wang Z, Wang F, Hong Y, Huang J, Shi H, Zhu JK. Two chloroplast proteins suppress drought resistance by affecting ROS production in guard cells. *Plant Physiol.* 2016;172(4):2491–503.
146. Afgan E, Baker D, van den Beek M, Blankenberg D, Bouvier D, Cech M, et al. The Galaxy platform for accessible, reproducible and collaborative biomedical analyses: 2016 update. *Nucleic Acids Res.* 2016;44(W1):W3–W10.
147. Cheng CY, Krishnakumar V, Chan AP, Thibaud-Nissen F, Schobel S, Town CD. Araport11: a complete reannotation of the *Arabidopsis thaliana* reference genome. *Plant J Cell Mol Biol.* 2017;89(4):789–804.
148. Axtell MJ. ShortStack: comprehensive annotation and quantification of small RNA genes. *Rna.* 2013;19(6):740–51.
149. Kramer MF. Stem-loop RT-qPCR for miRNAs. In: *Current protocols in molecular biology*; 2011. Chapter 15:Unit 15 10.
150. Livak KJ, Schmittgen TD. Analysis of relative gene expression data using real-time quantitative PCR and the 2^{(-Delta Delta C(T))} method. *Methods.* 2001;25(4):402–8.
151. Jin J, Tian F, Yang DC, Meng YQ, Kong L, Luo J, et al. PlantTFDB 4.0: toward a central hub for transcription factors and regulatory interactions in plants. *Nucleic Acids Res.* 2017;45(D1):D1040–5.
152. Rashmi KV, Gilad-Bachrach R. DART: dropouts meet multiple additive regression trees. 2015. Available online at <http://www.arxiv.org/pdf/150501866v1>.
153. Yilmaz A, Mejia-Guerra MK, Kurz K, Liang X, Welch L, Grotewold E. AGRIS: the *Arabidopsis* gene regulatory information server, an update. *Nucleic Acids Res.* 2011;39(Database issue):D1118–22.

Publisher's Note

Springer Nature remains neutral with regard to jurisdictional claims in published maps and institutional affiliations.

Ready to submit your research? Choose BMC and benefit from:

- fast, convenient online submission
- thorough peer review by experienced researchers in your field
- rapid publication on acceptance
- support for research data, including large and complex data types
- gold Open Access which fosters wider collaboration and increased citations
- maximum visibility for your research: over 100M website views per year

At BMC, research is always in progress.

Learn more [biomedcentral.com/submissions](https://www.biomedcentral.com/submissions)



2.2 Publication 2 (Habermann et al. 2020)

Identification of small non-coding RNAs responsive to GUN1 and GUN5 related retrograde signals in *Arabidopsis thaliana*.

Kristin Habermann, Bhavika Tiwari, Maria Krantz, Stephan O. Adler, Edda Klipp, M. Asif Arif & Wolfgang Frank

The Plant Journal, Volume 104, Issue 1, Page 138 – 155 (2020)

<https://doi.org/10.1111/tpj.14912>

Identification of small non-coding RNAs responsive to *GUN1* and *GUN5* related retrograde signals in *Arabidopsis thaliana*

Kristin Habermann¹ , Bhavika Tiwari¹, Maria Krantz², Stephan O. Adler², Edda Klipp², M. Asif Arif^{1,*} and Wolfgang Frank^{1,*}

¹Plant Molecular Cell Biology, Department Biology I, Ludwig-Maximilians-Universität München, LMU Biocenter, Planegg-Martinsried 82152, Germany, and

²Department Biologie, Bereich Theoretische Biophysik, Humboldt-Universität Berlin, Berlin 10115, Germany

Received 19 August 2019; revised 10 June 2020; accepted 17 June 2020; published online 8 July 2020.

*For correspondence (e-mails wolfgang.frank@lmu.de; asif.arif@lmu.de).

SUMMARY

Chloroplast perturbations activate retrograde signalling pathways, causing dynamic changes of gene expression. Besides transcriptional control of gene expression, different classes of small non-coding RNAs (sRNAs) act in gene expression control, but comprehensive analyses regarding their role in retrograde signalling are lacking. We performed sRNA profiling in response to norflurazon (NF), which provokes retrograde signals, in *Arabidopsis thaliana* wild type (WT) and the two retrograde signalling mutants *gun1* and *gun5*. The RNA samples were also used for mRNA and long non-coding RNA profiling to link altered sRNA levels to changes in the expression of their cognate target RNAs. We identified 122 sRNAs from all known sRNA classes that were responsive to NF in the WT. Strikingly, 142 and 213 sRNAs were found to be differentially regulated in both mutants, indicating a retrograde control of these sRNAs. Concomitant with the changes in sRNA expression, we detected about 1500 differentially expressed mRNAs in the NF-treated WT and around 900 and 1400 mRNAs that were differentially regulated in the *gun1* and *gun5* mutants, with a high proportion (~30%) of genes encoding plastid proteins. Furthermore, around 20% of predicted miRNA targets code for plastid-localised proteins. Among the sRNA–target pairs, we identified pairs with an anti-correlated expression as well pairs showing other expressional relations, pointing to a role of sRNAs in balancing transcriptional changes upon retrograde signals. Based on the comprehensive changes in sRNA expression, we assume a considerable impact of sRNAs in retrograde-dependent transcriptional changes to adjust plastidic and nuclear gene expression.

Keywords: small non-coding RNA, non-coding RNA, gene regulation, retrograde signalling, *gun1*, *gun5*, *Arabidopsis thaliana*.

INTRODUCTION

Both mitochondria and chloroplasts are characteristic organelles of eukaryotes that have evolved through the endosymbiosis of distinct prokaryotic progenitors (Goksoyr, 1967). Cyanobacteria gave rise to plastids, and the majority of the endosymbiotic cyanobacterial genome was transferred into the nuclear DNA of the host organism. Consequently, most multiprotein complexes within the plastids are formed by organellar- and nuclear-encoded proteins, requiring a well-coordinated expression of both genomes (Zimorski *et al.*, 2014; Zhao *et al.*, 2019a). The nuclear gene expression is controlled by plastid-to-nucleus retrograde signalling (Kleine and Leister, 2016; Chan *et al.*, 2016), which is proposed to be mediated by several factors. For example, norflurazon (NF), a specific inhibitor of the

enzyme phytoene desaturase, which produces b-carotenoids from phytoene, causes repression of photosynthesis-associated nuclear genes (*PhANGs*) (Woodson *et al.*, 2011). Carotenoids are part of the light-harvesting complexes and protect the cells from photooxidative damage (Kim and Apel, 2013). In the presence of NF the chloroplast suffers from photooxidation, leading to characteristic bleaching symptoms of the green plant tissues caused by the degradation of chlorophyll (Breitenbach *et al.*, 2001). Several decades ago *Arabidopsis thaliana* mutant screens were performed to identify factors which specifically block the expression of *PhANGs* under conditions of chloroplast developmental prevention (Susek *et al.*, 1993; Mochizuki *et al.*, 2001; Meskauskiene *et al.*, 2001; Larkin *et al.*, 2003; Gray *et al.*, 2003; Gutierrez-Nava *et al.*, 2004; Ball *et al.*,

2004; Rossel *et al.*, 2006; Saini *et al.*, 2011). Several GENOME UNCOUPLED (*gun*) mutants were identified with disturbed retrograde signalling leading to a de-repression of *PhANGs*. Interestingly, five different *gun* mutants, *gun2* to *gun6*, are affected in the tetrapyrrole biosynthesis pathway (TPB). The *gun5* mutant has a defective regulatory CHLH subunit of the magnesium-chelatase (Mochizuki *et al.*, 2001). The *gun4* mutation also affects the subunit of the magnesium-chelatase, leading to an increased efficiency. The *gun2*, *gun3* and *gun6* mutants are impaired in heme oxygenase, phytylchelatase and Fe-chelatase, respectively (Woodson *et al.*, 2011; Woodson *et al.*, 2013). Based on these studies, it has been proposed that chloroplast metabolites may act as retrograde signals (Kakizaki *et al.*, 2009). The *gun1* mutant is not related to the remaining *gun* mutants since *GUN1* encodes a member of the chloroplast-localised pentatricopeptide repeat proteins, which usually act in post-transcriptional processes (Tadini *et al.*, 2016). The *gun1* mutant is able to perceive signals from the TPB, plastid gene expression and redox state, but the mode of action of *GUN1* in retrograde signalling remains unknown (Kleine and Leister, 2016). Microarray studies have been performed to compare transcriptional changes of *A. thaliana* wild type (WT) and *gun1* and *gun5* mutants in response to NF, revealing a strong correlation between the *gun1* and the *gun5* mutant because a large number of genes were consistently regulated in both mutants, including de-repression of *PhANGs*.

To date, all studies analysing gene expression in various retrograde signalling mutants focused on the analysis of protein-coding genes. However, it is well known that classes of non-coding RNAs (ncRNAs), including long ncRNAs (lncRNAs) as well as small ncRNAs (sRNAs), have important functions in diverse biological processes because they mainly act in the control of gene expression (Wang and Chekanova, 2017; Huang *et al.*, 2019).

lncRNAs with a size larger than 200 nucleotides were shown to have important functions in the control of gene expression (Wierzbicki *et al.*, 2008; Dinger *et al.*, 2009) and to exert their function by various mechanisms. One specific role of lncRNAs is the regulation of mRNA splicing, where they can either activate or inhibit specific splicing events (Ma *et al.*, 2014). They also mediate epigenetic modifications and act in microRNA (miRNA) target mimicry, where the lncRNA harbours a miRNA binding site, causing miRNA binding and sequestration (Franco-Zorrilla *et al.*, 2007; Swiezewski *et al.*, 2009; Heo and Sung, 2011). A specific gene regulatory class of ncRNA comprises sRNAs with a size of 20–24 nucleotides. They can interfere with nuclear transcription by regulating epigenetic modifications (Khraiweh *et al.*, 2010; Bannister and Kouzarides, 2011; Holoch and Moazed, 2015) or they can act post-transcriptionally by targeting RNAs, mediating RNA cleavage or translational inhibition (Meister and Tuschl, 2004; Bartel,

2004; Kim, 2005). sRNAs can be divided into two classes on the basis of their origin: hairpin RNA (hpRNA) and small interfering RNA (siRNA) (Axtell, 2013a). One of the most important classes of hpRNA are miRNAs, which are processed from stem-loop transcripts by DICER-LIKE1 enzymes (Park *et al.*, 2002; Meyers *et al.*, 2008) and guided through ARGONAUTE1 and RNA-induced silencing complex to their target RNAs by sequence complementarity to mediate their cleavage or translational inhibition (Wierzbicki *et al.*, 2008; Voinnet, 2009). Until now only one recent study reported on a functional role of miRNAs in retrograde signalling (Fang *et al.*, 2018). It was shown that tocopherols positively regulate the accumulation of 3⁰-phosphoadenosine 5⁰-phosphate (PAP), which is an inhibitor of exonuclease 2 (XRN2), which negatively regulates mRNA and pri-miRNA levels by degradation of 5' uncapped mRNA. Moreover, miR395 mediates cleavage of the mRNA encoding ATP sulfurylase (APS), the enzyme catalysing the initial step of PAP synthesis (Fang *et al.*, 2018).

Two other sRNA classes are formed from double stranded RNAs (dsRNAs), which are derived from endogenous transcripts and generate natural antisense transcript-derived siRNA (nat-siRNA) or trans-acting siRNA (ta-siRNA), based on their specific biogenesis pathways. Nat-siRNAs are generated from two genes encoding overlapping transcripts in antisense orientation, leading to the formation of dsRNA molecules (Borsani *et al.*, 2005). Nat-siRNAs are processed from these dsRNAs and mediate subsequent cleavage of one of the initial overlapping transcripts. According to their genomic location, NAT pairs can be distinguished into *cis*-NAT pairs, generated from opposing DNA strands within an identical genomic region, and *trans*-NAT pairs, produced from transcripts encoded by separated genomic regions (Lapidot and Pilpel, 2006; Yuan *et al.*, 2015). The first identified nat-siRNA was shown to have an important function in salt stress adaptation of *A. thaliana* (Borsani *et al.*, 2005), where it is involved in the regulation of proline biosynthesis. Unlike nat-siRNAs, ta-siRNA generation is triggered by miRNAs, since ta-siRNA precursor transcripts are cleaved in a miRNA-dependent manner and further processed into phased 21 nt ta-siRNA duplexes to control target RNAs (Chen, 2009). The role of sRNAs in retrograde signalling has not been analysed yet and information on the role of lncRNAs in retrograde control is completely lacking. To gain information whether these classes of ncRNA act in retrograde signalling, we made use of two well-characterised mutants affecting plastid-to-nucleus signalling events. *A. thaliana gun1* and *gun5* mutants were grown under standard conditions and in the presence of NF, and RNA expression profiles were compared to WT controls to identify functional sRNA–RNA target pairs that are modulated by retrograde signals.

RESULTS

De novo sRNA sequencing after norflurazon treatment

To identify sRNAs that may act in retrograde signalling pathways, seedlings of *A. thaliana* WT and the two retrograde signalling mutants *gun1* and *gun5* were treated for 4 days with 5 μ M NF under continuous light (Figure S1a) and sRNA sequencing was performed from six independent biological replicates samples, yielding a minimum of 5 million reads per replicate. The length distribution of all sRNA reads was analysed and we observed an enrichment of reads with a length of 21 and 24 nt (Figure S1b–d). The 21 nt peak corresponds to an expected enrichment of miRNAs, ta-siRNAs and nat-siRNAs, whereas the 24 nt peak complies with enriched repeat-associated sRNAs. The ShortStack sRNA analysis software has been used to map the sRNA data set against different reference databases (Table S1).

DeSeq2 was used to calculate the differential expression (2-fold regulation and false discovery rate [FDR] ≤ 0.05) of sRNAs between the samples, with a special focus on sRNAs that were differentially expressed in NF-treated samples with respect to their untreated controls, and in NF-treated *gun* mutants compared to the NF-treated WT (Table S2). Specific sRNA clusters arising from different ncRNA classes were found to be differentially expressed (Figure 1). These classes include mature miRNAs, *cis*-nat-siRNAs and *trans*-nat-siRNA, as well as sRNAs derived from lncRNAs. Upon growth on normal media, we identified only a small number of differentially regulated sRNAs in the *gun* mutants as compared to the WT, whereas the number of differentially regulated sRNAs between the mutants and WT strongly increased upon NF treatment (Table S3).

NF treatment caused an increased number of differentially expressed sRNAs in WT and both *gun* mutants, indicating a considerable sRNA regulation by retrograde signals. Furthermore, we observed a higher number of

differentially expressed sRNAs in both NF-treated *gun* mutants compared to NF-treated WT, pointing to a strong regulation of sRNAs that underlies specific retrograde signals in these mutants. Most of the changes affect miRNA and nat-siRNA expression levels, and we mainly focused on these sRNA classes with regard to their differential expression and further target analysis to predict the regulatory functions of these sRNAs (Figure 1 and Table S3).

Analysis of differentially expressed miRNAs

Because beside a recent analysis of tocopherol-responsive miRNAs (Fang *et al.*, 2018) little is known about the role of miRNAs in retrograde signalling, we analysed changes in miRNA expression in response to NF in *A. thaliana* WT and in the *gun1* and *gun5* mutants. The comparison of differentially expressed miRNAs between the samples is shown in a hierarchically clustered heatmap (Figure 2a). Only a low number of differentially expressed miRNAs was observed in the untreated mutants compared to the WT control. In the *gun1* mutant (*gun1*/WT), only six differentially expressed miRNAs were detected, and only five miRNAs were detected in the untreated *gun5* mutant compared to the WT control (*gun5*/WT).

We hypothesised that miRNAs can play a role in retrograde signalling that should be reflected by an enrichment of differentially expressed miRNAs after NF treatment. Indeed, we observed a remarkable increase in the number of differentially expressed miRNAs in response to NF treatment with a similar number of NF-responsive miRNAs in the three analysed genotypes (Figure 2b). In total, we observed 22 miRNAs to be differentially regulated in the NF-treated WT compared to the untreated control (WT NF/WT). Twenty-four miRNAs were differentially expressed in the NF-treated *gun1* compared to the untreated *gun1* mutant (*gun1* NF/*gun1*), and 18 miRNAs were differentially regulated in the NF-treated *gun5* mutant compared to the untreated *gun5* control (*gun5* NF/*gun5*).

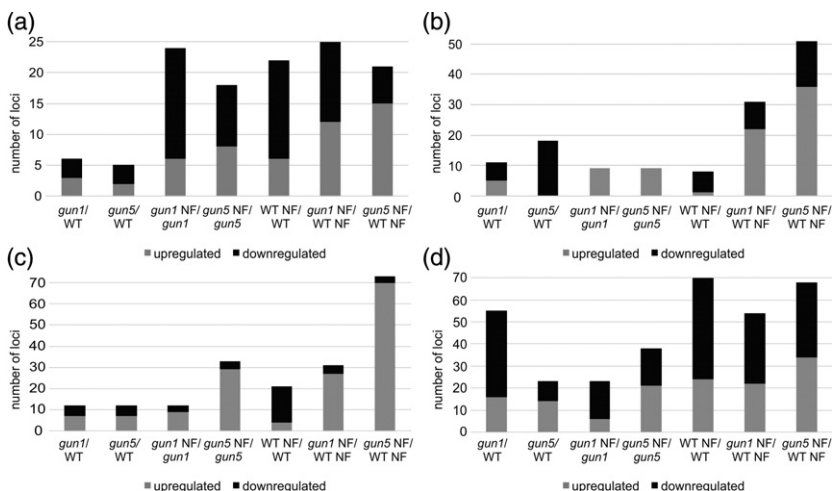
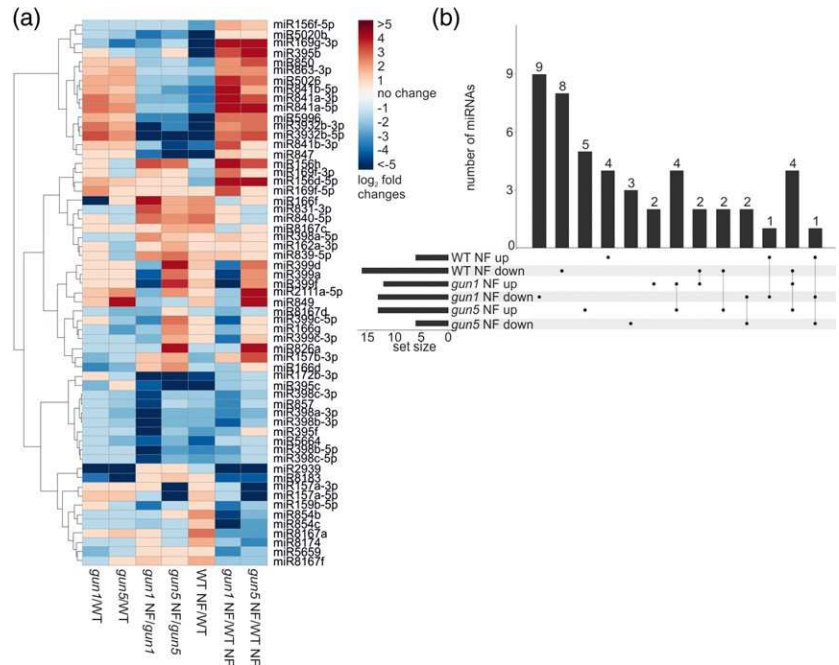


Figure 1. Differentially expressed sRNAs within the different samples. Overview of differentially regulated sRNAs between the different samples ($\log_2(\text{FC}) \leq -2$ or $\geq +2$; FDR ≤ 0.05) subdivided into specific sRNA classes. (a) miRNAs, (b) sRNAs derived from lncRNA, (c) *cis*-NAT pairs and (d) *trans*-NAT pairs. The up- and downregulation of the members of each class are depicted by grey (up) and black (down) partitions of the respective bars.

Figure 2. Behaviour of the differentially expressed miRNAs. (a) Hierarchically clustered (UPGMA) heat-map depicting miRNAs that are differentially regulated in at least one sample displaying normalised $\log_2(\text{FC})$ values. (b) UpSet plot depicting the number of differentially expressed miRNAs in response to NF in WT (WT NF/WT) and both *gun* mutants (*gun1* NF/WT NF and *gun5* NF/WT NF).



Interestingly, we further detected miRNAs that seem to be controlled by retrograde signals, as de-repressed miRNAs were observed in the *gun1* and *gun5* mutants in response to NF treatment, which is reminiscent of the de-repression of *PhANGs* in these mutants. We focused on miRNAs with altered expression levels in the treated WT (WT NF/WT) and correlated them with differentially expressed miRNAs in the NF-treated *gun* mutants (Figure 2b). In response to NF, two miRNAs (miR169g-3p and miR5996) showed patterns of de-repression in both *gun* mutants similar to de-repressed *PhANGs*, and one miRNA (miR3932-5p) was de-repressed only in the NF-treated *gun5* mutant compared to the treated WT (*gun5* NF/WT NF). Furthermore, five miRNAs were downregulated in the treated WT (WT NF/WT) and were upregulated in at least one NF-treated *gun* mutant (*gun* NF/WT NF). We also identified two miRNAs which seemed to be controlled by retrograde signals in an opposite manner. These two miRNAs were found to be upregulated in the treated WT (WT NF/WT) and downregulated in at least one of the treated *gun* mutants (*gun* NF/WT NF). In addition, we found miRNAs which showed a specific regulation restricted to NF-treated *gun* mutants when compared to the treated WT. Two miRNAs were found to be downregulated in both treated *gun* mutants (*gun* NF/WT NF). Moreover, nine miRNAs were specifically downregulated in the NF-treated *gun1* mutant compared to the treated WT (*gun1* NF/WT NF), and the expression of three miRNAs was reduced in the treated *gun5* mutant (*gun5* NF/WT NF). Furthermore, two miRNAs were upregulated in the treated *gun1* mutant and five miRNAs were upregulated in the treated *gun5* mutant (*gun* NF/

WT NF). We also detected four upregulated miRNAs common for both treated *gun* mutants (*gun* NF/WT NF).

Differentially regulated nat-siRNAs

To identify nat-siRNAs from our sRNA sequencing data we made use of different accessible databases (Table S1) comprising experimentally validated and computationally predicted *cis*- and *trans*-NAT pairs (Jin *et al.*, 2008; Zhang *et al.*, 2012; Yuan *et al.*, 2015).

We identified 12 various *cis*-NAT pairs producing differentially regulated nat-siRNA clusters in both untreated *gun1* and *gun5* mutants (*gun1*/WT and *gun5*/WT) (Figure 1c). Besides this, 57 and 23 *trans*-NAT pairs were detected to produce differentially regulated nat-siRNA in the *gun1* and *gun5* mutants, respectively (Figure 1d).

Upon NF treatment we detected 21 *cis*-NAT pairs (Figure S2a) and 70 *trans*-NAT pairs (Figure S2b) in the WT (WT NF/WT) producing differentially regulated nat-siRNA clusters from at least one transcript of these NAT pairs. In the treated *gun1* mutant (*gun1* NF/*gun1*), nat-siRNAs from 12 *cis*-NAT pairs were detected to be differentially expressed (Figure 1c) and 23 differentially regulated *trans*-NAT pairs producing nat-siRNA clusters were identified to be differentially regulated in the treated *gun1* mutant (*gun1* NF/*gun1*). In the NF-treated *gun5* mutant, we identified 33 *cis*-NATs and 38 *trans*-NATs generating differentially expressed nat-siRNAs (*gun5* NF/*gun5*) (Figure 1c,d).

The overlap and co-regulation as well as specific expression of the differentially expressed *cis*-NAT pairs and *trans*-NAT pairs producing differentially regulated nat-siRNA clusters were analysed between the samples and

are shown in an UpSet plot (Figure S2). We focused on the analysis of NF-responsive differentially expressed nat-siRNAs in the WT to provide information on nat-siRNAs that are controlled by retrograde signals. Moreover, we compared NF-treated WT with both NF-treated *gun* mutants to identify NF-responsive nat-siRNA misregulation that is caused by the perturbed retrograde signals in these mutants. We detected 31 *cis*-NAT pairs and 54 *trans*-NAT pairs producing differentially expressed nat-siRNAs in the NF-treated *gun1* mutant (*gun1* NF/WT NF). In the NF-treated *gun5* mutant we detected 73 *cis*-NAT pairs and 68 *trans*-NAT pairs that produce differentially regulated nat-siRNA clusters (*gun5* NF/WT NF). For both *gun* mutants the majority of *cis*-derived nat-siRNAs were upregulated, whereas the majority of *trans*-derived nat-siRNAs were downregulated in these mutants (Figure S2). We identified five *cis*-NAT pairs to be downregulated in the treated WT (WT NF/WT) and upregulated in both treated *gun* mutants (*gun* NF/WT NF), thus representing the *gun*-specific de-repression of nuclear-encoded *PhANGs* (Figure S2a). We also detected one nat-siRNA cluster produced from a *cis*-NAT pair displaying an opposing expression pattern (upregulated in WT NF/WT and downregulated in both *gun* NF/WT NF). Within *trans*-derived nat-siRNAs we identified 19 sRNA clusters that were differentially regulated in response to NF in WT (WT NF/WT) and showed further differential regulation in response to NF in both *gun* mutants (*gun* NF/WT NF) (Figure S2b). Five of them resemble the *gun*-specific de-repression, since they were downregulated in the WT (WT NF/WT) and upregulated in both mutants (*gun* NF/WT NF). Eleven *trans*-derived nat-siRNAs displayed an opposite expression and were upregulated in the treated WT (WT NF/WT) and downregulated in both treated *gun* mutants (*gun* NF/WT NF). In addition, two differentially expressed nat-siRNA from *trans*-NAT pairs were downregulated within all three samples and another one was upregulated in the treated WT (WT NF/WT) and in the treated *gun5* mutant (*gun5* NF/WT NF) and downregulated in the treated *gun1* mutant (*gun1* NF/WT NF).

Other differentially regulated sRNA classes

Besides the differentially expressed miRNAs and NAT pairs we also found differentially expressed sRNAs produced from lncRNAs and phased siRNA (phasiRNAs) precursors (Figure S3 and Table S3). Similar to miRNAs and nat-siRNAs, we detected only a small number of differentially regulated sRNA clusters derived from lncRNA precursors in the untreated genotypes (*gun*/WT). In total, 11 differentially expressed sRNA clusters produced from lncRNAs were noticed in the *gun1* mutant (*gun1*/WT) and all 18 differentially expressed sRNA clusters in the untreated *gun5* mutant were downregulated (*gun5*/WT).

When comparing the individual genotypes with and without NF treatment, we identified only a considerably

small number of differentially expressed sRNAs. In the treated WT, eight sRNA clusters processed from lncRNA precursors were identified to be differentially expressed (WT NF/WT). For both treated *gun* mutants, we observed nine different upregulated sRNA clusters (*gun* NF/*gun*).

Comparing the NF-treated *gun* mutants with the NF-treated WT we noticed an increase in the number of differentially expressed sRNAs (Figure S3). Generally, we observed a higher number of upregulated sRNA clusters produced from lncRNA precursors in both treated *gun* mutants (*gun* NF/WT NF). Of 31 differentially expressed sRNA clusters, 22 were detected to be upregulated in the NF-treated *gun1* mutant (*gun1* NF/WT NF). For the treated *gun5* mutant, 36 out of 51 differentially expressed sRNA clusters were found to be upregulated (*gun5* NF/WT NF). We detected only one sRNA cluster derived from a lncRNA precursor that was downregulated in the treated WT (WT NF/WT) and upregulated in both NF-treated *gun* mutants (*gun* NF/WT NF). Two sRNA clusters were downregulated in the treated WT (WT NF/WT) and upregulated in the treated *gun1* mutant (*gun1* NF/WT NF). Another two sRNA clusters derived from lncRNA precursors were downregulated in the treated WT (WT NF/WT) and upregulated in the treated *gun5* mutant (*gun5* NF/WT NF). Furthermore, 11 sRNA clusters produced from lncRNA precursors were similarly regulated in both treated *gun* mutants (*gun* NF/WT NF), with six of them upregulated and five downregulated (Figure S3).

In addition to the lncRNA-derived sRNA clusters, we identified two differentially expressed phasiRNAs. One phasiRNA derived from locus AT1G63070 was 5.8-fold upregulated in the untreated *gun1* mutant (*gun1*/WT) and 4.1-fold upregulated in the NF-treated *gun1* mutant (*gun1* NF/WT NF). The second phasiRNA produced from the locus AT5G38850 was 2.6-fold downregulated in the treated WT (WT NF/WT) and 3.5-fold downregulated in the treated *gun1* mutant (*gun1* NF/*gun1*).

Analysis of lncRNA and mRNA in the *gun* mutants

Besides sRNA sequencing, we also sequenced mRNAs and lncRNAs to gain more information about NF-dependent regulation of lncRNAs and to examine the correlation of sRNAs with their targets.

The samples were mapped against the *A. thaliana* genome deposited in Araport11 (Table S4) and differential expression of mRNA and lncRNA between the samples (Tables S5 and S6) was calculated with Cuffdiff. Representative transcripts belonging to different RNA classes showing differential expression levels in the RNA sequencing data were selected for expression analyses by quantitative real-time PCR (qRT-PCR), which confirmed the mRNA and lncRNA sequencing data (Figure S4). We selected various genes which were detected to be differentially expressed in the treated WT as well as in both NF-treated *gun* mutants. Furthermore, we selected two transcripts each

that displayed a low, moderate and high abundance, respectively. In addition, we included one lncRNA that was found to be differentially regulated in all three samples.

Classification of differentially expressed ncRNAs detected via ribosomal depleted RNA sequencing

We identified differentially expressed transcripts belonging to distinct ncRNA classes (Tables S5 and S6), including lncRNAs, which may act in regulatory processes of gene expression, as well as tRNA, rRNA and small nucleolar RNA (snoRNA), which act in protein translation and splicing and usually have few regulatory functions. Under normal growth conditions we identified 10 differentially expressed ncRNAs in each of the *gun* mutants as compared to the untreated WT (Table 1 and Figure S5a). The number of differentially expressed ncRNAs increased upon NF treatment, indicating potential roles upon plastid perturbations that trigger retrograde signalling. In total, we identified 34 differentially expressed ncRNAs in the NF-treated WT compared to the untreated control (Table 1). In the NF-treated *gun1* and *gun5* mutants (*gun* NF/*gun*), we identified 32 and 70 differentially expressed ncRNAs, respectively. Interestingly, in the NF-treated *gun* mutants we observed 20 and 45 differentially expressed ncRNAs in the *gun1* and *gun5* mutants (*gun* NF/WT NF), respectively.

An UpSet plot (Figure S5b) depicts the distribution of differentially expressed ncRNAs between various samples (WT NF/WT, *gun1* NF/WT NF and *gun5* NF/WT NF). We identified two interesting lncRNAs (AT1G05562 and AT4G13495), which represent the classical *gun*-related expression as these show a downregulation in response to NF treatment in WT, but are upregulated in both NF-treated *gun* mutants. Furthermore, three lncRNAs (AT3G01835, AT5G07325 and AT5G07745) were identified to be upregulated in the NF-treated WT (WT NF/WT) and downregulated in the treated *gun1* mutant (*gun1* NF/WT NF).

Another interesting lncRNA (AT4G13495) was de-repressed in both NF-treated *gun* mutants with 7.2-fold and

3.4-fold upregulation in *gun1* and *gun5* mutants (*gun* NF/WT NF), respectively, whereas this lncRNA was highly downregulated (fold change [FC] of -10.5) in the treated WT (WT NF/WT). From our sRNA data we already detected sRNAs arising from this lncRNA and in agreement with the expression level of this lncRNA, the total sRNAs generated from this transcript were downregulated in the treated WT (FC of -2.8 ; WT NF/WT) and 3.4-fold upregulated in the treated *gun1* mutant (*gun1* NF/WT NF). Interestingly, this lncRNA overlaps with three individual miRNA precursors (miR5026, miR850 and miR863) in sense direction, suggesting that these miRNAs can be processed from the individual precursors as well as from the overlapping lncRNA. In line with this hypothesis, we observed a consistent differential expression of the lncRNA and the three individual miRNAs within the analysed samples (Table 2).

In addition, we identified two differentially regulated lncRNAs overlapping with mRNA transcripts in antisense that may act as precursors for the generation of nat-siRNAs. One lncRNA (AT1G05562) that may act as a natural antisense transcript was downregulated in the treated WT (FC of -3.7 ; WT NF/WT) and upregulated in the treated *gun1* and *gun5* mutants with a FC of 3.9 and 4.2 (*gun* NF/WT NF), respectively. This lncRNA transcript is able to overlap with an mRNA encoding an UDP-glucose transferase (AT1G05560). Furthermore, the overlapping mRNA transcript was downregulated in the treated WT (FC of -5.8 ; WT NF/WT) and upregulated in both treated mutants (FC of 3.6 for *gun1* NF/WT NF; FC of 3.1 for *gun5* NF/WT NF). We also detected differentially expressed sRNA clusters processed from this region in the sRNA sequencing data in the treated WT (FC of -4.4 for WT NF/WT) as well as in the treated *gun1* mutant (FC of 6.6 for *gun1* NF/WT NF). Thus, the regulation of nat-siRNAs correlates with the expression of the respective lncRNA–mRNA transcript pair and the differential expression seems to be regulated by specific retrograde signalling pathways.

Table 1 Overview of differentially expressed ncRNAs in response to NF in *A. thaliana* WT and *gun1* and *gun5* mutants

	<i>gun1</i> / WT	<i>gun5</i> / WT	WT NF/ WT	<i>gun1</i> NF/ <i>gun1</i>	<i>gun5</i> NF/ <i>gun5</i>	<i>gun1</i> NF/ WT NF	<i>gun5</i> NF/ WT NF
lncRNAs	6	5	15	13	34	11	20
snRNAs	0	0	3	0	8	1	5
snoRNAs	0	0	3	3	11	2	4
rRNAs	0	0	2	0	1	1	0
tRNAs	0	0	3	4	1	2	1
pseudogenes	4	5	5	6	9	2	10
transcript regions	0	0	2	5	3	1	4
MIR precursors	0	0	1	1	2	0	0
antisense RNAs	0	0	0	0	1	0	1
Total	10	10	34	32	70	20	45

Table 2 Expression data for the lncRNA AT4G13495 that overlaps in sense with the individual miRNA precursors miR5026, miR850 and miR863

ID	FC WT NF/WT		FC <i>gun1</i> NF/WT		FC <i>gun5</i> NF/WT	
	FC	FDR	FC	FDR	FC	FDR
AT4G13495	-10.54	0.001	7.17	0.001	3.36	0.001
miR5026	-2.63	0.085	4.08	0.004	3.08	0.042
miR850	-2.58	0.077	2.61	0.068	3.81	0.007
miR863-5p	-1.7	0.561	1.29	0.941	2.34	0.467
miR863-3p	-1.51	0.538	2.7	0.025	2.61	0.045

In addition, we identified a *TAS3* precursor transcript (AT3G17185) that was downregulated in the NF-treated WT (FC of -2.9 for WT NF/WT) and de-repressed in the treated *gun5* mutant (FC of 2.6 for *gun5* NF/WT NF). Ta-siRNAs produced from the *TAS3* transcript control the expression of transcripts coding for auxin response factors such as *ARF2*, *ARF4* and *ETT*. However, we detected neither differentially expressed *TAS3*-derived ta-siRNAs nor differential expression of their cognate targets between the analysed samples.

Differentially regulated nuclear- and organellar-encoded mRNAs after NF treatment

In parallel to sRNA and lncRNA, we analysed the data obtained from the ribosomal depleted nuclear- (Figure 3) and organellar-encoded (Figure 4) RNA sequencing to identify protein-coding mRNAs that are regulated by retrograde signalling pathways. Furthermore, to categorise putative functions of differentially regulated RNAs after NF treatment, Gene Ontology (GO) enrichment terms were explored (Table S8 and Figure S6). We detected only a low number of differentially expressed genes (DEGs), with 212 and 165 differentially expressed transcripts in the untreated *gun1* and *gun5* mutants (*gun*/WT), respectively (Figure 3a). However, when we analysed differential gene expression in response to NF, we observed a remarkable increase in the number of DEGs (Figure 3b). We identified 1557 DEGs in the WT in response to NF (WT NF/WT). For both treated mutants compared to their respective untreated controls, we identified slightly lower numbers of DEGs. In total, 1361 DEGs were identified in the treated *gun1* mutant (*gun1* NF/*gun1*) and 1177 DEGs were detected in the treated *gun5* mutant (*gun5* NF/*gun5*). In addition, we compared mRNA expression between the NF-treated *gun* mutants and the NF-treated WT. We identified 905 DEGs in

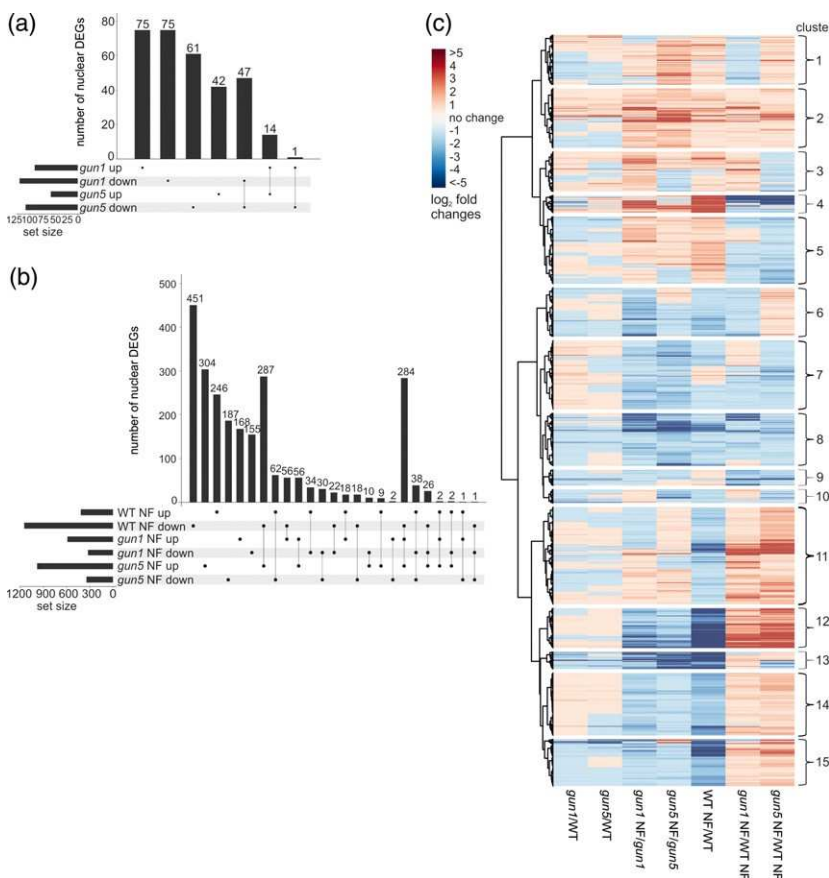


Figure 3. Distribution of nuclear DEGs in the untreated and NF-treated samples. (a) UpSet plot showing the distribution of differentially regulated mRNAs in the untreated *gun* mutants compared to the WT. (b) UpSet plot depicting the distribution of differentially regulated mRNAs in response to NF in WT (WT NF/WT) and both *gun* mutants (*gun1* NF/WT NF and *gun5* NF/WT NF). (c) Hierarchically clustered (UPGMA) heatmap of normalised $\log_2(FC)$ values from nuclear-encoded DEGs with 15 clusters based on co-expression patterns.

the NF-treated *gun1* mutant (*gun1* NF/WT NF) and 1319 DEGs in the treated *gun5* mutant (*gun5* NF/WT). We generated a hierarchically clustered heatmap from all 3352 nuclear-encoded mRNAs that were differentially regulated in at least one sample (Figure 3c). Based on the co-expression of DEGs we were able to separate 15 specific clusters of differentially regulated nuclear-encoded genes (Table S7). We identified 1557 DEGs in the treated WT (WT NF/WT) and 75% of the mRNAs were downregulated. As expected, the NF-treated *gun* mutants behaved in an opposite manner, as the majority of the RNAs were upregulated, with 65% and 75% upregulated DEGs in the treated *gun1* and *gun5* mutants (*gun* NF/WT NF), respectively.

To identify the most interesting candidates regulated by retrograde signals, we analysed the overlap between the treated WT (WT NF/WT) and both treated *gun* mutants (*gun* NF/WT NF) to detect those genes that display a typical *gun*-related expression in both mutants (Figure 3b). We identified 284 DEGs in response to NF in WT (WT NF/WT) as well as in both *gun* mutants (*gun* NF/WT NF). These DEGs seem to be controlled by retrograde signalling pathways, because they are repressed by NF in the WT and de-repressed in the *gun* mutants. Furthermore, we detected 56 DEGs with a specific de-repression in the treated *gun1* mutant (*gun1* NF/WT NF) and another 287 DEGs

specifically de-repressed in the *gun5* mutant (*gun5* NF/WT NF). Most likely, the regulation of the genes requires specific retrograde signals, as we identified genes showing a specific de-repression restricted to only one of the *gun* mutants.

Besides the analysis of nuclear-encoded genes, we investigated organellar gene expression and studied the expression of genes encoded by the plastidic and mitochondrial genomes in the WT and both *gun* mutants in the absence or presence of NF. We generated two hierarchically clustered heatmaps for plastidic (Figure 4a) and mitochondrial (Figure 4b) genes that were differentially expressed in at least one of the samples. As expected, we only detected eight mitochondrial genes with differential expression in at least one of the samples, as NF treatment affects carotenoid biosynthesis in the plastids and should not directly affect mitochondrial gene expression. Furthermore, the low number of affected genes in the mitochondria indicates an insignificant crosstalk between plastids and mitochondria triggered by plastid-derived retrograde signals.

In contrast, we detected a considerable high number of differentially regulated plastid-encoded genes. Upon growth in the absence of NF, none of the plastid-encoded genes were differentially expressed in the *gun5* mutant

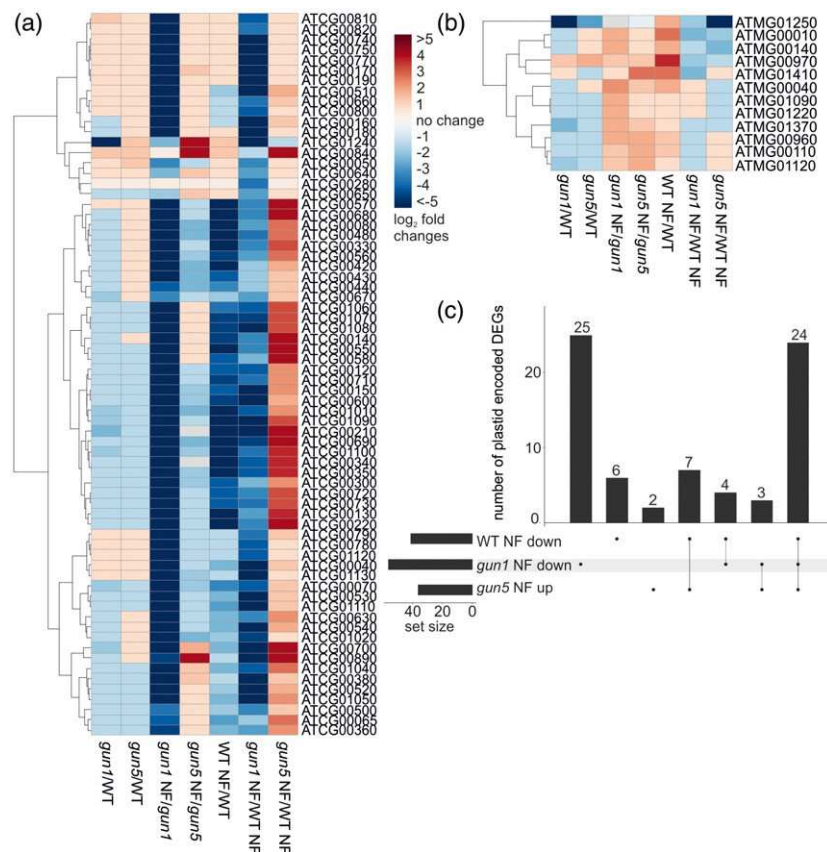


Figure 4. Distribution of differentially expressed plastidic and mitochondrial DEGs in the untreated and NF-treated samples. Hierarchically clustered (UPGMA) heatmap depicting (a) plastidic and (b) mitochondrial genes that are differentially expressed in at least one of the samples displaying normalised $\log_2(\text{FC})$ values. (c) UpSet plot depicting the expression of plastid-encoded DEGs detected in the NF-treated *gun* mutants (*gun1* NF/WT NF and *gun5* NF/WT NF) and in the NF-treated WT (WT NF/WT).

and only one plastid-encoded gene was differentially expressed in the *gun1* mutant (*gun*/WT). However, after NF treatment we detected 41, 56 and 36 differentially expressed plastid-encoded genes in the treated WT (WT NF/WT) and *gun1* and *gun5* mutants (*gun* NF/WT NF), respectively. Furthermore, we noticed a highly interesting phenomenon: Almost all plastid-encoded differentially expressed mRNAs were downregulated in the NF-treated *gun1* mutant (*gun1* NF/WT NF) and upregulated in the NF-treated *gun5* mutant (*gun5* NF/WT NF). Thus, based on the plastidic gene expression, both mutants respond in an almost completely opposed manner to NF treatment, suggesting specific perturbations in the NF-triggered organellar signalling pathways. We observed 27 differentially expressed plastid-encoded mRNAs in response to NF in both the *gun1* and the *gun5* mutant (Figure 4c) compared to the NF-treated WT, but they were regulated in an opposing manner: They were all downregulated in the treated *gun1* mutant, but upregulated in the treated *gun5* mutant.

miRNA target analysis

We performed miRNA target prediction with 'psRNATarget' using all protein-coding and non-coding transcripts

from Araport11 to correlate the expression of miRNAs with putative target RNA transcripts (Table S9). For each predicted miRNA target, we considered its expression changes to subclassify the miRNA–RNA pairs. For the differentially regulated miRNAs, which were detected in WT NF/WT, *gun1* NF/WT NF and *gun5* NF/WT NF, we were able to predict 218 protein-coding targets as well as 16 non-coding target RNAs, and some of these can be targeted by several miRNAs. We generated a non-redundant list of miRNA targets and excluded transcripts with low fragments per kilobase of transcript per million reads (FPKM) values (≥ 5). Applying these parameters, we obtained 119 predicted miRNA targets that were categorised into three different classes based on their expression. It has to be noted that a specific miRNA–RNA pair can be grouped into different categories since the miRNA as well as the cognate RNA target can be differently regulated between the analysed samples. The first category comprises miRNA–RNA pairs that are 'unchanged' according to the FC of the RNA transcript (but not the miRNA) and includes 101 miRNA–RNA pairs. The second category contains seven miRNA–RNA pairs that show an anticorrelated expression pattern, and the third category encompasses 16 miRNA–RNA pairs

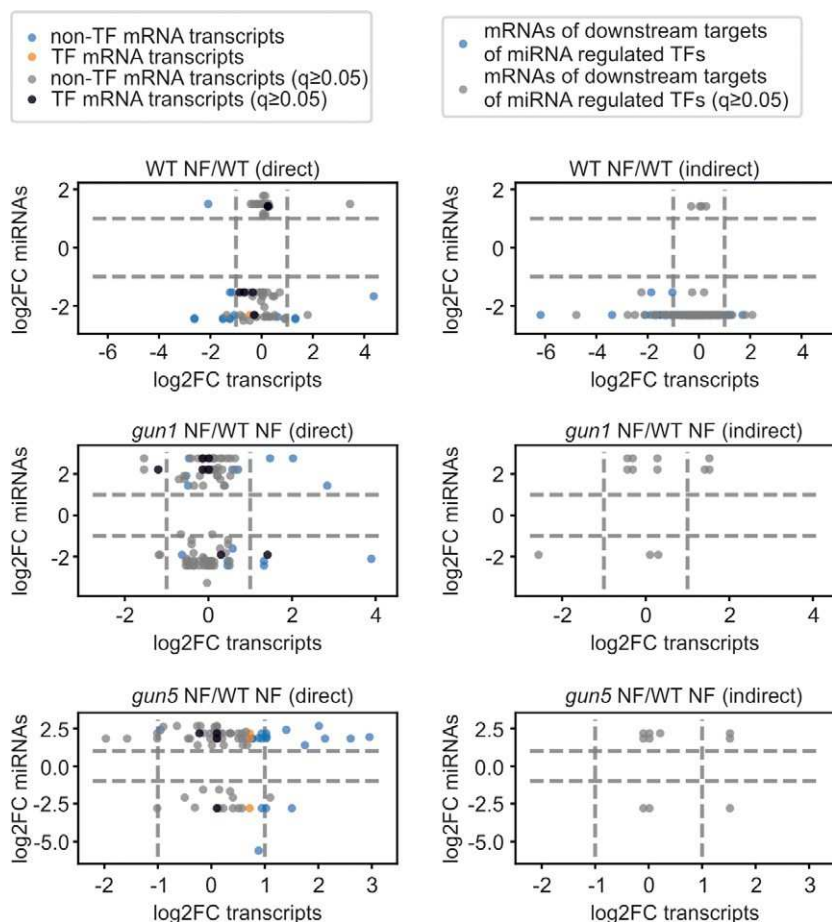


Figure 5. Scatter plots of differentially expressed miRNAs and their targets. Only miRNAs with $FDR \leq 0.05$ were included. The direct plots (left panel) depict all differentially expressed miRNAs and their direct predicted target transcripts. MiRNA target transcripts encoding transcription factors are shown in orange ($FDR \leq 0.05$) and black ($FDR \geq 0.05$). MiRNA target transcripts encoding other proteins are shown in blue ($FDR \leq 0.05$) and grey ($FDR \geq 0.05$). The indirect plots (right panel) depict downstream targets of transcription factors that are miRNA-regulated. Here, the mRNAs of these downstream genes are plotted against the miRNAs controlling their respective transcription factor mRNAs. The blue dots correspond to $FDR \leq 0.05$ and the grey dots to $FDR \geq 0.05$.

where the miRNA and the predicted target show the same direction of their differential expression (both up- or both downregulated). Two different miRNAs together with at least two of their targets were validated by qRT-PCR, confirming their anticorrelated expression pattern (Figure S7a, b). Scatter plots (Figure 5) were created to show the distribution of the differentially regulated miRNAs and their correlating targets and were divided into 'direct' and 'indirect' scatter plots. The direct plots show the correlation of miRNAs and their cognate RNA targets either coding for transcription factors or coding for other proteins. The indirect scatter plots depict the expression of downstream genes that are controlled by miRNA-regulated transcription factors. From the direct scatter plot, it is obvious that most differentially expressed miRNA targets do not encode transcription factors. Nevertheless, we identified transcription factor transcripts which are controlled by miRNAs, and their effect on the transcription factor targets can be seen in the indirect plots. For example, the indirect plot shows many differentially expressed transcripts coding for transcription factors, which are controlled by miRNAs in the NF-treated WT (WT NF/WT).

We identified one miRNA–RNA target pair (Table S9) that has been shown to play a role in the acclimation to phosphate deficiency. MiR399a was downregulated in the treated *gun1* mutant (*gun1* NF/WT NF), whereas the expression of its target *PHO2* (AT2G33770), encoding a ubiquitin-conjugating E2 enzyme, remained unchanged in the treated *gun1* mutant (*gun1* NF/WT NF). MiR850 and its cognate target, encoding a chloroplast RNA-binding protein (AT1G09340), belong to the category of miRNA–target pairs showing the same expression (Table S9) since both were upregulated in the treated *gun5* mutant (*gun5* NF/WT NF). This chloroplast RNA-binding protein is necessary for the proper function of the chloroplast and mutations in this gene cause growth deficiency (Fettke *et al.*, 2011). Furthermore, we also identified miR157a-5p (FC of -7 in *gun5* NF/WT NF), displaying an anticorrelated expression to its target PHOTOSYSTEM II REACTION CENTRE PSB28 PROTEIN (AT4G28660), which is 2.9-fold upregulated (*gun5* NF/WT NF). PSB28 is highly conserved in photosynthetic eukaryotes and lack of *PSB28* results in a pale-green phenotype in rice, pointing to a role in the assembly of chlorophyll-containing proteins such as CP47 (Lu, 2016).

Nat-siRNA target analysis

We detected a larger number of differentially expressed sRNAs arising from predicted NAT pairs than from any other sRNA class in the treated WT (WT NF/WT) as well as in both NF-treated *gun* mutants (*gun* NF/WT NF). Filtering the differentially expressed nat-siRNAs with at least five normalised reads in one of six samples (WT, WT NF, *gun1*, *gun1* NF, *gun5* and *gun5* NF) led to a total number of 73 non-redundant *cis*-NATs and 193 non-redundant *trans*-NAT

pairs. These pairs were further analysed and we only selected the nat-siRNA producing transcript pairs with at least five normalised reads for one of the two overlapping transcripts. This reduced the number to 64 non-redundant *cis*-NAT and 40 non-redundant *trans*-NAT pairs (Table S10). The expression changes of two nat-siRNAs together with their overlapping transcripts in NF-treated WT and the NF-treated *gun5* mutant were confirmed by qRT-PCR (Figure S7c,d).

For many *trans*-NAT pairs, we observed that one of the transcripts was derived from a transposable element or a pre-tRNA, whereas the second overlapping transcript represented a protein-coding gene. Among these *trans*-NAT pairs, we only detected one overlapping transcript encoding a plastid-localised protein, suggesting a low impact of *trans*-NAT pairs in the adjustment of plastid and nuclear gene expression in response to NF. The *trans*-nat-siRNA generated from this pair was found to be downregulated in the treated WT (WT NF/WT) and upregulated in both treated *gun* mutants (*gun* NF/WT NF). The first overlapping transcript codes for the plastid-localised UDP-glucosyl transferase 75B2 (AT1G05530), which is able to bind UDP-glucose, important for cellulose and callose synthesis (Hong *et al.*, 2001). Its expression was unchanged in the treated WT (WT NF/WT) as well as in both treated *gun* mutants (*gun* NF/WT NF). The second overlapping transcript represented a lncRNA (AT1G05562) that was downregulated in the treated WT (WT NF/WT) and upregulated in both treated *gun* mutants (*gun* NF/WT NF).

Interestingly, out of 64 *cis*-NAT pairs that give rise to differentially regulated nat-siRNAs, we detected 31 individual transcripts which encode plastid proteins, indicating a considerable role of *cis*-NAT pairs in the direct control of genes coding for plastid proteins via NF-triggered retrograde signals. Moreover, within the *cis*-NAT pairs we identified 35 individual transcripts encoding nuclear-localised proteins, pointing to a large impact of these in the indirect adjustment of nuclear gene expression via nuclear regulatory proteins. One sRNA processed from a *cis*-NAT pair was detected to be downregulated in the treated WT (WT NF/WT). Interestingly, both overlapping transcripts were identified to encode plastid-localised proteins. The expression of the first overlapping transcript (AT1G29900), which codes for a subunit of carbamoyl phosphate synthetase, which is presumed to be necessary for the conversion of ornithine to citrulline in the arginine biosynthesis pathway (Molla-Morales *et al.*, 2011), was unchanged (WT NF/WT). In agreement with the expression of the nat-siRNAs, the second overlapping transcript (AT1G29910) was downregulated by NF in the WT (WT NF/WT). This transcript encodes a chlorophyll A/B-binding protein, which is the major protein of the light-harvesting complex and is required for absorbing light during photosynthesis.

Network analysis

In order to gain a comprehensive picture of the role of miRNAs in retrograde signalling and to analyse possible downstream effects, we investigated a miRNA–RNA–target network that also comprises related transcription factor to target gene connections. The results were combined in a complex interaction network (Data S1), since one miRNA can control many mRNAs encoding transcription factors, which in turn control several downstream genes, but also one miRNA target can be controlled by numerous miRNAs (Figure S8 and Table S12). Within the considered network, most miRNAs regulate just a small number of target transcripts (Figure S8a), but there are some miRNAs regulating up to 140 targets. In contrast, the majority of miRNA targets are regulated by only a few miRNAs, but there are still some targets that can be regulated by up to 15 miRNAs (Figure S8b). We observed that miRNAs controlling the highest number of targets mainly regulate mRNAs that do not encode transcription factors (Figure S8c), while the distribution of miRNA targets encoding transcription factors indicates that most miRNAs regulate only a small number of such targets, with the highest number being eight (Figure S8d). Some motifs are recurrent in the miRNA–RNA target network (Figure 6). We explored the network for different characteristic relations of regulatory linkage and behaviour. Here, we found simple expected patterns where a miRNA, miR157a-5p, was downregulated and its target

mRNA transcript encoding a plastid-localised protein (AT4G28660) in turn was upregulated, or vice versa (Figure 6a), but we also observed many miRNA targets that did not show any differential expression on the mRNA level, although corresponding miRNAs were differentially expressed. The effect of these miRNAs might be visible on the protein level due to inhibition of translation. If the target mRNA encodes a transcription factor, we should see the miRNA-dependent regulation in the expression of downstream targets of this transcription factor (Figure 6b), as reported before (Megraw *et al.*, 2016). As an example, the transcription factor AT4G36920 can act as an activator or repressor on its targets, and furthermore, the transcription factor can control other transcription factors or downstream targets like AT2G33380, which is a *CALEOSIN 3* transcript and important for stress responses (Sham *et al.*, 2015). In addition, the downstream transcription factors can also target other transcription factors or downstream targets, which increases the network complexity. Furthermore, this points to a sophisticated interaction between miRNAs and their targets, because miRNAs indirectly regulate genes encoding plastid proteins through the direct control of transcription factor mRNAs. Besides transcription factor mRNAs, many miRNAs are able to regulate transcripts of genes that do not encode transcription factors, but also these transcripts do not always show the expected behaviour. For instance, miR395c is predicted to control

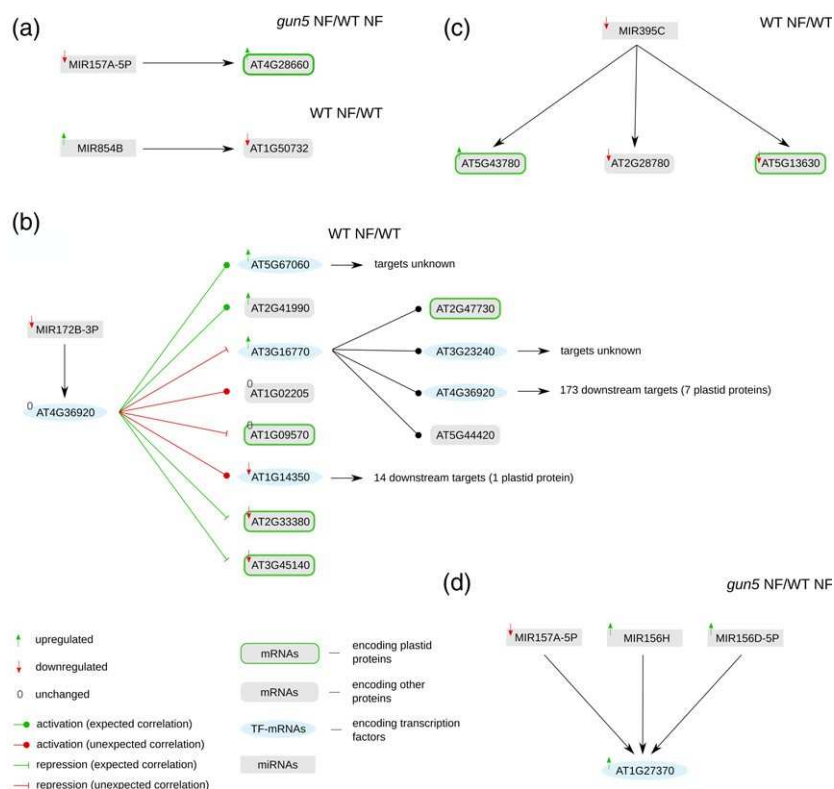


Figure 6. Illustration of different network motifs which we observed in the miRNA–RNA target network in connection with relative changes of RNA levels between treatments. (a) Examples of expected regulations where a miRNA and its target mRNA exhibit inverted differential expression. (b) The interaction between a miRNA regulating the mRNA of a transcription factor, and the interactions of this transcription factor with its downstream target genes. (c) A downregulated miRNA which regulates four different targets. (d) An example of three miRNAs that regulate a single mRNA. The whole network can be accessed through the supporting Data S1 in GML format.

four different mRNA targets, including three transcripts encoding plastid-localised proteins (Figure 6c). Further, we found examples where several miRNAs are able to control the transcript of a single transcription factor (Figure 6d). These cases show possible interactions between miRNAs and their targets and suggest a wide range of direct and indirect impacts of miRNAs to regulate gene expression. Nevertheless, behavioural predictions are impossible without additional information on the exact mode of action of each miRNA and the magnitude of its influence.

DISCUSSION

Until now, it is not known whether ncRNAs and sRNAs are regulated by retrograde signalling in response to NF treatment and how they contribute to the control of nuclear gene expression in response to plastid-derived signals. To better understand these biological processes, we combined sRNA sequencing with mRNA/lncRNA sequencing of *A. thaliana* WT seedlings and the two retrograde signalling mutants, *gun1* and *gun5*, to identify ncRNAs and mRNAs regulated by retrograde signals.

Generally, after NF treatment we detected nearly the same number of DEGs in all treated samples compared to the untreated WT. Further, we observed an overall tendency that more DEGs were downregulated than upregulated in response to NF treatment. In addition, we could observe an overrepresentation of DEGs encoding plastid-localised proteins in all three samples and detected more DEGs to be upregulated in the treated *gun* mutants compared to the treated WT.

Previous studies with different *gun* mutants were performed using *A. thaliana* microarrays lacking probes for ncRNAs (Strand *et al.*, 2003; Koussevitzky *et al.*, 2007; Woodson *et al.*, 2013). Koussevitzky *et al.* (2007) analysed changes in mRNA levels in WT (*Col-0*), *gun1* and *gun5* mutant seedlings grown on media with and without NF. About 43% of upregulated and 67% of downregulated DEGs in the present study overlap with those of Koussevitzky *et al.* (2007) in response to NF (Figure S9a,b). Generally, more downregulated DEGs and larger changes in the NF-treated *gun5* mutant than in the other mutant were identified in both studies. A good overlap of DEGs was found in both *gun* mutants. About 56% of the DEGs detected in *gun1-102* (*gun1* NF/WT NF) in our study were also detected in the treated *gun1-9* mutant by Koussevitzky *et al.* (2007) (Figure S9c), and about 50% of the DEGs identified in the treated *gun5* mutant (*gun5* NF/WT NF) in our study were also identified by Koussevitzky *et al.* (2007) (Figure S9d). However, in our data set we identified also 44% (*gun1* NF/WT NF) and 50% (*gun5* NF/WT NF) of DEGs that have not been shown to be controlled by *gun*-related retrograde signalling pathways before, which might be due to the differences between the two methods (RNA

sequencing versus microarrays) and the varying duration of the NF treatment between the studies (5 versus 4 days). Recently, another RNA sequencing study reported NF-responsive transcriptome changes in a different *gun1* mutant (*gun1-1*) (Richter *et al.*, 2020); 55% and 49% of the DEGs detected in the NF-treated *gun1* and *gun5* mutant compared to the NF-treated WT overlapped with DEGs in our study (Figure S9e,f). RNA sequencing was also performed in the *gun1-9* mutant grown in the presence of NF (Zhao *et al.*, 2019b) with an overlap of 65% of DEGs compared to our data (Figure S9g). Taken together, we observed a considerably high overlap with other transcriptome studies despite the differences between the studies regarding growth conditions, available mutants and analysis methods.

In our study, we observed an opposite regulation of differentially expressed plastid-encoded transcripts in both *gun* mutants, while the nuclear-encoded DEGs showed large overlap between the *gun1* and *gun5* mutants. Surprisingly, in response to NF all differentially expressed plastid-encoded transcripts were downregulated in the *gun1* mutant, whereas they were upregulated in the treated *gun5* mutant. These observations are in line with the model suggesting that plastid gene transcription is controlled by retrograde signalling networks, including sigma factors (SIG2 and SIG6) and plastid-encoded RNA polymerase (PEP), which might be crucial for proper plastid RNA transcription (Woodson *et al.*, 2013). It seems that *GUN1* activates PEP (Maruta *et al.*, 2015) and a perturbed PEP activation in the *gun1* mutant may prevent the upregulation of the plastid-encoded genes compared to WT upon NF treatment.

We identified an interesting lncRNA (AT4G13495) showing classical de-repression in both *gun* mutants (*gun* NF/WT NF) (Table 2). This lncRNA overlaps in sense direction with three different miRNA precursors (*MIR5026*, *MIR850* and *MIR863*) and all three miRNAs were differentially expressed in at least one treatment (WT NF/WT, *gun1* NF/WT NF and *gun5* NF/WT NF). We assume that all three miRNAs can be produced either from the three individual miRNA precursor transcripts or from the lncRNA. We did not find any predicted target for miR5026 according to the applied psRNATarget parameters. MiR850 was upregulated in the *gun5* mutant (*gun5* NF/WT NF), and two predicted cognate target RNAs, encoding a chloroplast RNA-binding protein (AT1G09340) and a threonine-tRNA ligase (AT2G04842), respectively, were upregulated as well. MiR863 targets the *SERRATE* transcript (AT2G27100), encoding an accessory protein essential for the miRNA biogenesis pathway, and thus may influence the regulation of several miRNAs (Meng *et al.*, 2012). MiR863 was upregulated in both treated *gun* mutants (*gun* NF/WT NF), but we did not detect significant changes of the *SERRATE* transcript in the two treated *gun* mutants.

Concerning the overall regulation of differentially expressed sRNAs belonging to different classes (miRNAs, nat-siRNAs and other sRNA producing loci), we detected more downregulated sRNAs in the treated WT (WT NF/WT), whereas both treated *gun* mutants exhibited a higher number of upregulated sRNAs (*gun* NF/WT NF). Principally, this suggests an increased sRNA processing in response to NF in both *gun* mutants, resembling the de-repression of nuclear-encoded genes, and we assume that these sRNAs might have an impact on retrograde-controlled nuclear gene expression. sRNAs are able to affect nuclear transcripts regulated by retrograde signals and they may regulate mRNA transcripts, affecting plastid-localised proteins. Among all sRNA classes, we observed in all treatments the highest number of differentially regulated sRNAs within the nat-siRNA class. Furthermore, all differentially regulated sRNAs have been associated to their corresponding putative differentially expressed RNA targets (Table S13) and we could detect high numbers of differentially regulated sRNAs. Besides an effect of sRNAs on their direct targets, we expect based on our network analyses a considerable indirect regulation by sRNAs through transcription factors (Data S1).

Interestingly, we found that miR169g-3p, a heat- and salt stress-responsive miRNA (Szyrajew *et al.*, 2017; Pegler *et al.*, 2019), is the most strongly downregulated miRNA in the treated WT (−151.6-fold; WT NF/WT), and the most strongly upregulated one in the treated *gun5* mutant (38.2-fold; *gun5* NF/WT NF). We did not find any predicted target for miR169g-3p according to our parameters.

Unexpectedly, after miRNA target prediction the expression of most of the targets was not anticorrelated to the expression changes of their cognate miRNA, leading us to conclude that miRNAs might not be involved in the expression of genes controlled by retrograde signalling pathways, or the expressional changes of miRNAs somehow balance transcriptional changes of their targets to maintain constant steady-state levels. Another possibility could be that they act as translational repressors and do not have a direct effect on the transcript abundance of their target RNAs. However, we predicted 20 miRNA targets coding for transcription factors and 22 targets encoding plastid-localised proteins to be targeted by 23 differentially regulated miRNAs. Thus, we assume that miRNAs may have important functions in the control of transcripts that code for regulatory proteins that are directly involved in transcriptional control and may contribute to the manifold changes of gene expression in response to retrograde signals. Further, nuclear transcripts that code for plastid-localised proteins are targets of miRNAs, suggesting that these specific miRNA–mRNA pairs can play an important role in the retrograde signalling pathway, and thus may contribute to the adjustment of plastidic and nuclear gene expression. One interesting case involves miR395b and

miR395c, which target the mRNA for the magnesium-chelatase subunit *GUN5* (AT5G13630). In the NF-treated WT, both miRNAs and the target mRNA are downregulated compared to the untreated control, whereas in the treated *gun5* mutant both miRNAs and the target are upregulated. Even though the expression of this miRNA–mRNA pair is not anticorrelated, the enhanced miRNA levels may balance an increased transcription rate of the target mRNA to keep physiologically relevant steady-state levels. Magnesium-chelatase is required in the chlorophyll biosynthesis pathway, where it catalyses the insertion of Mg²⁺ into protoporphyrin IX, and the *gun5* mutant is characterised by a single nucleotide substitution resulting in a defective magnesium-chelatase. In the WT, the *GUN5* transcript level decreases in response to NF-triggered retrograde signalling, whereas the transcript level in the *gun5* mutant remains high and cannot be efficiently downregulated by the increased miRNA levels. The seven detected classical anticorrelated miRNA–mRNA pairs point to regulatory functions of specific miRNAs in the retrograde signalling pathway, because we assume efficient miRNA-mediated target cleavage followed by a reduced mRNA steady-state level. In this category of anticorrelated pairs, we identified the mRNA for the transcription factor SPL10, representing a validated target of miR157a, suggesting miR157 acts in retrograde signalling by affecting the levels of a transcriptional regulator and its downstream targets. Another anticorrelated predicted miRNA–mRNA pair is miR398, targeting the transcript of the multidrug and toxic compound extrusion (MATE) efflux protein (AT2G04050). We found miR398 to be downregulated in the treated WT compared to the untreated control, and the target was slightly upregulated. This MATE efflux protein belongs to a huge class of membrane proteins located in the plasma membrane and the chloroplast envelope membrane (Wang *et al.*, 2016) that are able to bind cytotoxic compounds like primary and secondary metabolites, xenobiotic organic cations (Omote *et al.*, 2006) and toxic substances such as pollutants and herbicides (Diener *et al.*, 2001) to eliminate them from the cell (Liu *et al.*, 2016). NF-triggered downregulation of miR398 most likely causes elevated transcript levels and increased levels of the encoded plasma membrane-located MATE efflux protein. We speculate that the regulated MATE efflux protein might be involved in the extrusion of the applied herbicide NF or the extrusion of toxic compounds accumulating within the cell in response to NF treatment. Another interesting target encodes a plastid protein that appeared to be upregulated in the NF-treated *gun5* mutant (*gun5* NF/WT NF) by decreased levels of the cognate miRNAs. *PSB28* (AT4G28660), targeted by miR157a, encodes a protein that is part of the photosystem II reaction centre and is suggested to function in the biogenesis and assembly of chlorophyll-containing proteins (Mabbitt *et al.*, 2014). NF treatment usually leads to the

downregulation of *PhANGs* and thus should cause decreased expression levels of the *PSB28* mRNA. However, miR157a contributes to the downregulation of *PSB28* mRNA levels post-transcriptionally and seems to be controlled by retrograde signals, as indicated by the misregulation of miR157a in the *gun5* mutant.

Fang *et al.* (2018) identified miR395 and miR398 to be important in retrograde signalling triggered by tocopherols, and we confirmed both miRNAs applying NF as another trigger of retrograde signalling. Additionally, the transcript encoding the enzyme APS, which catalyses the initial step in PAP synthesis (Klein and Papenbrock, 2004; Pornsiriwong *et al.*, 2017) was identified to be targeted by miR395 (Liang *et al.*, 2010). We found miR395b to be downregulated in the treated WT (WT NF/WT) and upregulated in the treated *gun5* mutant (*gun5* NF/WT NF). In the treated WT, reduced miR395b levels lead to increased APS transcript levels, causing elevated PAP synthesis, which acts as retrograde inhibitor of XRN3 and should provoke elevated pri-miRNA and mature miRNA levels. Besides, Fang *et al.* (2018) detected the downregulation of miR398 in the WT after NF treatment, which is in line with our sRNA sequencing data. The COPPER/ZINC SUPEROXIDE DISMUTASE 2 (*CSD2*) was previously found to be a target of miR398 (Guan *et al.*, 2013). After heat stress, Fang *et al.* (2018) found miR398, PAP and tocopherol levels to be increased and *CSD2* levels to be decreased in the WT, and they hypothesised that tocopherols and PAP are required for miR398 biogenesis under heat stress. The *CSD2* mRNA escaped our miRNA target prediction due to a considerably high number of mismatches within the miRNA binding site, causing a score value that was above our cut-off value. Still, we identified this miRNA as differentially expressed supporting the previous study by Fang *et al.* (2018).

Besides differentially expressed miRNAs, we identified an even higher number of differentially regulated nat-siRNAs in the treated WT (WT NF/WT) and both *gun* mutants (*gun* NF/WT NF). Most of the overlapping transcripts encode nuclear or plastid proteins, suggesting that nat-siRNAs have a considerable impact on the control of *PhANGs* encoding plastid proteins. For most of the *cis*-NAT pairs we observed similar correlations between RNA transcript and sRNA expression levels. For example, the levels of two overlapping transcripts (AT1G05560 and AT1G05562) and the related *cis*-nat-siRNA were decreased in the treated WT (WT NF/WT) and increased in both *gun* mutants (*gun* NF/WT NF). The gene AT1G05562 encodes an antisense lncRNA and overlaps with the gene AT1G05560, which codes for a UDP-glucose transferase. Another interesting *cis*-nat-siRNA and one of the overlapping transcripts encoding a chlorophyll binding protein (AT1G29930) were downregulated in the treated WT (WT NF/WT) and upregulated in the treated *gun5* mutant (*gun5* NF/WT NF),

whereas levels of the other overlapping transcript, coding for a nuclear RNA polymerase (AT1G29940), remained unchanged in both treatments.

Here, we could demonstrate that NF treatment and subsequent retrograde signals lead to comprehensive changes in the steady-state levels of non-coding sRNAs comprising all known sRNA classes. The majority of the identified differentially expressed sRNAs belong to the *cis*- and *trans*-nat-siRNAs, followed by miRNAs, representing the second most abundant class. Thus, we postulate that mainly these two sRNA classes act as important regulators of gene expression in retrograde signalling. We also identified a considerably high number of so far unknown nuclear-encoded DEGs and thus add to the knowledge about genes that are controlled by retrograde signalling. Finally, we were able to identify promising sRNA–RNA target pairs that may act in the adjustment of plastidic and nuclear gene expression in retrograde signalling pathways.

EXPERIMENTAL PROCEDURES

Plant material and growth conditions

Arabidopsis thaliana WT (*Col-0*) and the retrograde signalling mutants *gun1-102* and *gun5-1* were used in this study. *Gun1-102* (SAIL_290_D09) harbours a transfer DNA insertion within the AT2G31400 gene locus resulting in a loss-of-function allele (Tadini *et al.*, 2016). *Gun5-1* is an EMS mutant harbouring a point mutation within the gene AT5G13630 causing an Ala/Val substitution at residue 990 (A990V) resulting in deficient magnesium-protoporphyrin IX synthesis (Mochizuki *et al.*, 2001). Surface-sterilised seeds were incubated on ½ MS agar plates containing 1.5% sucrose. For treatments with NF, seeds were incubated on the same medium supplemented with 5 µM norflurazon (Sigma-Aldrich, Taufkirchen, Germany). After vernalisation (2 days at 4°C in darkness) the seeds were grown for 4 days under continuous light (115 µmol photons m⁻² sec⁻¹) at 22°C. Whole plants were harvested and immediately frozen in liquid nitrogen and stored at –80°C until RNA isolation. All control experiments and norflurazon treatments were performed in three biological replicates for each genotype.

RNA isolation

The plant material was ground in liquid nitrogen and RNA isolation was performed using TRIzol reagent (Invitrogen) according to the manufacturer's protocol. RNA integrity was monitored by agarose gel electrophoresis and RNA concentration and purity were determined spectrophotometrically (260 nm/280 nm and 260 nm/230 nm absorbance ratios).

sRNA purification

For sRNA sequencing 30 µg of total RNA were separated by 15% PAGE for 2 h at 120 V. The sRNA fractions with sizes ranging from 18 to 29 nucleotides were excised from the gel and eluted in 0.3 M NaCl overnight at 4°C with rotation. Remaining gel pieces were removed using a Spin-X centrifuge tube (Sigma-Aldrich) and 1 µl GlycoBlue (15 mg ml⁻¹, Thermo Fisher), 25 µl sodium acetate (3 M, pH 5.0) and 625 µl ethanol were added to the 250 µl flow-through and samples were incubated for 4 h at –80°C. After centrifugation for 30 min with 17 000 g at 4°C the RNA pellet was

washed twice with 80% ethanol, dried and dissolved in nuclease-free water.

Quantitative RT-PCR

Prior to cDNA synthesis, RNA samples were subjected to DNase I digestion (NEB, Ipswich, MA, USA) to remove residual genomic DNA. Total RNA (2 µg) was incubated at 37°C for 30 min together with DNase I (2 U; NEB). To inactivate the DNase I, 2.5 µl 50 mM EDTA was added and samples were incubated at 65°C for 10 min. The RNA was denatured for 5 min at 65°C in the presence of 100 pmol of an oligo-dT23VN oligonucleotide and 10 mM dNTPs and transferred to ice. Subsequently, cDNA synthesis was performed for 1 h at 42°C using M-MuLV reverse transcriptase (200 U; NEB) followed by heat inactivation at 80°C for 5 min. To monitor successful cDNA synthesis, we performed RT-PCR using gene-specific primers for the gene *UBI7* (AT3G53090) (Table S11).

For each qRT-PCR we used cDNA equivalent to 20 ng µl⁻¹ RNA with gene-specific primers and an EvaGreen qPCR mix. The samples were pre-heated for 2 min at 95°C and qRT-PCR cycling conditions were as follows: 12 sec at 95°C, 30 sec at 58°C and 15 sec at 72°C for 40 cycles. All qRT-PCRs were performed in three technical triplicates with the CFX Connect Real-Time PCR device (Bio-Rad, Feldkirchen, Germany). The Ct-values were used to calculate changes in gene expression by the 2^{-DDCt} method (Livak and Schmittgen, 2001). The values were normalised to the housekeeping gene *UBI1* (AT4G36800). Oligonucleotide sequences of all gene-specific primers are listed in Table S11.

Stem-loop qRT-PCR

Stem-loop qRT-PCRs were used for sRNA quantification as described previously (Kramer, 2011). RNA from three independent biological replicates (300 ng) was used for cDNA synthesis. RNA was denatured for 5 min at 65°C together with 100 pmol of stem-loop oligonucleotides (Table S11) and 10 mM dNTPs. cDNA synthesis was performed for 5 min at 25°C and 20 min at 42°C using M-MuLV reverse transcriptase (200 U; NEB), followed by heat inactivation at 80°C for 5 min. RT-PCR for the gene *UBI7* (AT3G53090) served as control (Table S11).

RNA sequencing

For the generation of mRNA libraries, including poly(A)-tailed lncRNAs, 10 µg total RNA from each sample was vacuum-dried in the presence of RNAsable (Sigma-Aldrich). The libraries were prepared using the Next Ultra RNA Library Prep Kit (NEB) by Novogene (China). The samples were sequenced strand-specifically as 150 bp paired-end reads on a HiSeq-PE150 platform with at least 15 million read pairs per library.

sRNA libraries for each RNA sample were generated twice following two slightly modified protocols. The first set of libraries was generated from 5 µg total RNA with the NEBNext Multiplex Small RNA Library Prep Set for Illumina according to the manufacturer's instructions and 1 h of 3' adapter ligation. The second set of sRNA libraries was prepared from purified sRNAs obtained from 30 µg of total RNA using the same kit as described above performing 3' adapter ligation for 18 h. For both libraries, excessive non-ligated 3' adapters were made inaccessible by converting them into dsRNA by hybridisation of complementary oligonucleotides. 5' adapter ligation was carried out at 25°C for 1.5 h, reverse transcription was performed by using the ProtoScript II reverse transcriptase and libraries were amplified by 12 PCR cycles. The PCR products were separated by 6% PAGE for 2 h at

60 V. The cDNA library fractions with a size ranging from 138 to 150 nucleotides were excised from the gel and eluted overnight. The sRNA libraries were sequenced as 50 bp single-end reads on an Illumina HiSeq1500 sequencer with approximately 10 million reads per library.

Analysis of mRNA and lncRNA

The mRNA and lncRNA sequencing results were analysed with the open source and web-based platform GALAXY (Afgan *et al.*, 2016). The FASTQ raw sequences were trimmed with the tool Trimmomatic to remove adapter sequences with their default parameters (Bolger *et al.*, 2014). Tophat (Kim *et al.*, 2013) was used to map the reads against the *A. thaliana* reference genome (<https://www.arabidopsis.org/>, release: TAIR10) with a maximum intron length parameter of 3000 nt. The transcripts were annotated in Araport11 (<https://apps.araport.org/thalemine/dataCategories.do>); we considered annotated ncRNAs longer than 200 bp as lncRNAs. Differential expression of transcripts was analysed by Cuffdiff (Trapnell *et al.*, 2010) to normalise the sequencing depth of each library and to calculate FPKM values. The FDR was used as a statistic indicator to exclude type I errors or rather false positives. Transcripts having FDR ≤ 0.05 and log₂(FC) ≤ -1 and ≥ +1 were considered as DEGs. The package pheatmap (<https://cran.r-project.org/web/packages/pheatmap/pheatmap.pdf>) was used to generate hierarchically (UPGMA) clustered heatmaps of differentially expressed RNAs (Kolde, 2019).

Gene ontology terms

GO enrichment terms were analysed using the DAVID Bioinformatics Resources 6.8 (<https://david.ncicrf.gov>) with default parameters (Huang *et al.*, 2009a,b) and results were visualised with the R package 'ggpubr' (Wickham, 2016).

Analysis of sRNA

NEBNext Kit adapter sequences were clipped from the sequencing reads using a custom script within GALAXY that identifies Illumina adapter sequences using a seed sequence of 10 nt. After adapter clipping FASTQ files of the raw reads with a length of 18–26 nt were loaded into the CLC Genomics Workbench 11.0.1 (Qiagen, Hilden, Germany) for further analyses. The ShortStack analysis package was used for advanced analysis of the sRNA sequences (Axtell, 2013b). The FASTQ files of the six biological replicates derived from each treatment were first mapped against the *A. thaliana* TAIR10 reference genome (<https://www.arabidopsis.org/>, release: TAIR10). The merged alignments were mapped against a file covering all *A. thaliana* mature miRNAs (<http://www.mirbase.org/>) and a second file comprising different RNA classes, namely nat-siRNAs, ta-siRNAs, phasiRNAs and lncRNAs. A nat-siRNA database (Table S1) was generated from previously annotated NAT pairs (Jin *et al.*, 2008; Zhang *et al.*, 2012; Yuan *et al.*, 2015), phasiRNAs were taken from Howell *et al.* (Howell *et al.*, 2007) and lncRNAs were downloaded from Araport11 (<https://apps.araport.org/thalemine/dataCategories.do>, release: Araport 11 Annotation). After mapping to the respective references, the individual raw reads for each replicate were used for normalisation and differential expression analysis based on a calculation with DeSeq2 (Love *et al.*, 2014). The sRNAs were filtered by fold changes between ≤ -2 and ≥ +2. The significance of the differentially expressed sRNAs was evaluated with FDR ≤ 0.05. miRNA target RNAs were identified using the psRNATarget (Dai *et al.*, 2018) prediction V2 tool (<http://plantgrn.noble.org/psRNATarget/>) from protein-coding and non-coding transcripts present in Araport11. An expectation value of less than 2.5 was considered as a cut-off

for true miRNA targets, where mRNAs harbouring a lower number of mismatches to the reverse and complementary miRNA obtain lower score values.

Network analysis

Using the sRNA and mRNA sequencing data together with the miRNA target prediction, we assembled an interaction network of miRNAs and their putative targets. For network analysis, we used the python package networkX (Hagberg *et al.*, 2008). We further investigated the miRNA targets that were predicted as described above using the psRNATarget tool to identify all miRNA targets that encode transcription factors. For this, we compared all miRNA targets with a reference database, containing *A. thaliana* transcription factors, which was generated using publicly available data (<http://atrm.cbi.pku.edu.cn>). Furthermore, this reference database was extended by incorporating available information about whether the transcription factors act as activators or repressors of gene expression together with available information about the individual target genes of the transcription factors (<https://agris-knowledgebase.org>). The data obtained from the RNA sequencing experiments were then used to generate a network of miRNAs and their targets, differentiating between miRNA targets encoding transcription factors and targets encoding other proteins. For network analyses connected to measurements, only RNAs with a FDR less than 0.05 were considered, unless indicated otherwise. Network analyses were performed to determine relationships between miRNAs and their targets with special focus on miRNA targets encoding transcription factors. In these network analyses we considered the impact of miRNAs on the transcripts coding for transcription factors and the impact of the expression of transcription factor mRNAs on downstream genes, regulated by these transcription factors. If the change of a miRNA results in an expected change of an mRNA coding for a transcription factor, or at least downstream genes show expected transcriptional changes, we classified this behaviour as 'expected'. For example, if miRNA expression was reduced and the target mRNA encoding a transcription factor was upregulated, the transcription factor acted as an activator and downstream genes of this transcription factor were consequently also upregulated, this would be considered as 'expected' behaviour. Furthermore, the scatter plots presented for all differentially expressed miRNAs (FDR \leq 0.05) were subdivided into two categories: plots depicting relations of miRNA and their direct target transcripts (direct) and plots depicting indirect relations comprising miRNAs that control mRNAs encoding transcription factors and their downstream target genes (indirect).

ACCESSION NUMBERS

ATG accession numbers: GUN1 (AT2G31400), GUN5 (AT5G13630). The raw Illumina sRNA and mRNA/lncRNA sequencing data are deposited in the NCBI SRA database with the ID PRJNA557616.

ACKNOWLEDGEMENTS

This work was supported by the German Research Foundation (SFB-TRR 175, grants to WF project C03 and EK project D03). We thank Martin Simon for technical support and advice regarding sRNA library preparations and Oguz Top for helpful comments on the manuscript. Open access funding enabled and organized by Projekt DEAL.

AUTHOR CONTRIBUTIONS

WF and MAA designed the research; KH performed the research with help from MAA and BT; KH, MAA, BT and WF analysed the data; network analysis was performed by SOA, MK and EK; and KH, MAA, MK, SOA and WF wrote the paper. All authors read and approved the final manuscript.

CONFLICT OF INTEREST

The authors declare no conflict of interest.

SUPPORTING INFORMATION

Additional Supporting Information may be found in the online version of this article.

Appendix S1. Figure and table captions.

Figure S1. Effect of NF on the plants and sRNA size distribution.

Figure S2. Distribution of differentially expressed *cis*- and *trans*-nat-siRNA in response to NF.

Figure S3. Distribution of differentially expressed sRNAs derived from lncRNAs in response to NF.

Figure S4. Validation of transcript levels by qRT-PCR.

Figure S5. Distribution of differentially expressed ncRNAs in the untreated and treated samples.

Figure S6. GO term enrichment analysis.

Figure S7. Validation of sRNAs and their associated transcripts.

Figure S8. Distributions of miRNA–RNA target interaction numbers.

Figure S9. Comparison of differentially expressed mRNAs from Koussevitzky *et al.* (2007), Richter *et al.* (2020), Zhao *et al.* (2019) and our study.

Table S1. Reference sequences for the *cis*- and *trans*-NAT pairs.

Table S2. sRNA sequencing and mapping results for each independent biological replicate.

Table S3. Lists of all significant differentially expressed sRNA classes.

Table S4. RNA mapping results after the analysis with Tophat for each independent biological replicate.

Table S5. Overview of all significant differentially expressed mRNAs and other RNA classes.

Table S6. Accession numbers of all significant differentially expressed mRNAs and other RNA classes.

Table S7. List of the individual clusters of the mRNA heatmap.

Table S8. GO term enrichment analysis for significant DEGs.

Table S9. Lists of miRNA target prediction.

Table S10. Lists of *cis*- and *trans*-nat-siRNAs and their target correlation.

Table S11. Sequences of oligonucleotides used in this study.

Table S12. Distributions of miRNA–RNA target interaction numbers.

Table S13. Overview of all significant differentially expressed (DE) sRNAs and their corresponding differentially expressed mRNA target.

Data S1. MiRNA–RNA target network in GML format that can be accessed with the free software 'Gephi' (Bastian *et al.*, 2009).

REFERENCES

- Afgan, E., Baker, D., van den Beek, M. *et al.* (2016) The Galaxy platform for accessible, reproducible and collaborative biomedical analyses: 2016 update. *Nucleic Acids Res.* 44, W3–W10.
- Axtell, M.J. (2013a) Classification and comparison of small RNAs from plants. *Annu. Rev. Plant Biol.* 64, 137–159.
- Axtell, M.J. (2013b) ShortStack: comprehensive annotation and quantification of small RNA genes. *RNA*, 19, 740–751.
- Ball, L., Accotto, G.P., Bechtold, U. *et al.* (2004) Evidence for a direct link between glutathione biosynthesis and stress defense gene expression in Arabidopsis. *Plant Cell*, 16, 2448–2462.
- Bannister, A.J. and Kouzarides, T. (2011) Regulation of chromatin by histone modifications. *Cell Res.* 21, 381–395.
- Bartel, D.P. (2004) MicroRNAs: genomics, biogenesis, mechanism, and function. *Cell*, 116, 281–297.
- Bastian, M., Heymann, S. and Jacomy, M. (2009) Gephi: an open source software for exploring and manipulating networks. *International AAAI Conference on Weblogs and Social Media*.
- Bolger, A.M., Lohse, M. and Usadel, B. (2014) Trimmomatic: a flexible trimmer for Illumina sequence data. *Bioinformatics*, 30, 2114–2120.
- Borsani, O., Zhu, J., Verslues, P.E., Sunkar, R. and Zhu, J.K. (2005) Endogenous siRNAs derived from a pair of natural cis-antisense transcripts regulate salt tolerance in Arabidopsis. *Cell*, 123, 1279–1291.
- Breitenbach, J., Zhu, C. and Sandmann, G. (2001) Bleaching herbicide norflurazon inhibits phytoene desaturase by competition with the cofactors. *J. Agric. Food Chem.* 49, 5270–5272.
- Chan, K.X., Phua, S.Y., Crisp, P., McQuinn, R. and Pogson, B.J. (2016) Learning the languages of the chloroplast: Retrograde signaling and beyond. *Annu. Rev. Plant Biol.* 67, 25–53.
- Chen, X. (2009) Small RNAs and their roles in plant development. *Annu. Rev. Cell Dev. Biol.* 25, 21–44.
- Dai, X., Zhuang, Z. and Zhao, P.X. (2018) psRNATarget: a plant small RNA target analysis server (2017 release). *Nucleic Acids Res.* 46, W49–W54.
- Diener, A.C., Gaxiola, R.A. and Fink, G.R. (2001) Arabidopsis ALF5, a multidrug efflux transporter gene family member, confers resistance to toxins. *Plant Cell*, 13, 1625–1638.
- Dinger, M.E., Pang, K.C., Mercer, T.R., Crowe, M.L., Grimmond, S.M. and Mattick, J.S. (2009) NRED: a database of long noncoding RNA expression. *Nucleic Acids Res.* 37, D122–D126.
- Fang, X., Zhao, G., Zhang, S., Li, Y., Gu, H., Li, Y., Zhao, Q. and Qi, Y. (2018) Chloroplast-to-nucleus signaling regulates microRNA biogenesis in Arabidopsis. *Dev Cell*, 48, 371–382.
- Fettke, J., Nunes-Nesi, A., Fernie, A.R. and Steup, M. (2011) Identification of a novel heteroglycan-interacting protein, HIP 1.3, from *Arabidopsis thaliana*. *J. Plant Physiol.* 168, 1415–1425.
- Franco-Zorrilla, J.M., Valli, A., Todesco, M., Mateos, I., Puga, M.I., Rubio-Somoza, I., Leyva, A., Weigel, D., Garcia, J.A. and Paz-Ares, J. (2007) Target mimicry provides a new mechanism for regulation of microRNA activity. *Nat. Genet.* 39, 1033–1037.
- Goksoyr, J. (1967) Evolution of eucaryotic cells. *Nature*, 214, 1161.
- Gray, J.C., Sullivan, J.A., Wang, J.H., Jerome, C.A. and Maclean, D. (2003) Coordination of plastid and nuclear gene expression. *Philos. Trans. R Soc. Lond B Biol. Sci.* 358, 135–145.
- Guan, Q., Lu, X., Zeng, H., Zhang, Y. and Zhu, J. (2013) Heat stress induction of miR398 triggers a regulatory loop that is critical for thermotolerance in Arabidopsis. *Plant J.* 74, 840–851.
- Gutierrez-Nava, M.D.L., Gillmor, C.S., Jimenez, L.F., Guevara-Garcia, A. and Leon, P. (2004) CHLOROPLAST BIOGENESIS genes act cell and noncell autonomously in early chloroplast development. *Plant Physiol.* 135, 471–482.
- Hagberg, A., Schult, D. and Swart, P. (2008). Exploring Network Structure, Dynamics, and Function using NetworkX. Proceedings of the 7th Python in Science conference (SciPy 2008). 11–15.
- Heo, J.B. and Sung, S. (2011) Vernalization-mediated epigenetic silencing by a long intronic noncoding RNA. *Science*, 331, 76–79.
- Holoch, D. and Moazed, D. (2015) RNA-mediated epigenetic regulation of gene expression. *Nat. Rev. Genet.* 16, 71–84.
- Hong, Z., Zhang, Z., Olson, J.M. and Verma, D.P. (2001) A novel UDP-glucose transferase is part of the callose synthase complex and interacts with phragmoplastin at the forming cell plate. *Plant Cell*, 13, 769–779.
- Howell, M.D., Fahlgren, N., Chapman, E.J., Cumbie, J.S., Sullivan, C.M., Givan, S.A., Kasschau, K.D. and Carrington, J.C. (2007) Genome-wide analysis of the RNA-DEPENDENT RNA POLYMERASE6/DICER-LIKE4 pathway in Arabidopsis reveals dependency on miRNA- and tasiRNA-directed targeting. *Plant Cell*, 19, 926–942.
- Huang, C.Y., Wang, H., Hu, P., Hamby, R. and Jin, H. (2019) Small RNAs - Big players in plant-microbe interactions. *Cell Host Microbe*, 26, 173–182.
- Huang, D.W., Sherman, B.T. and Lempicki, R.A. (2009a) Bioinformatics enrichment tools: paths toward the comprehensive functional analysis of large gene lists. *Nucleic Acids Res.* 37, 1–13.
- Huang, D.W., Sherman, B.T. and Lempicki, R.A. (2009b) Systematic and integrative analysis of large gene lists using DAVID bioinformatics resources. *Nat. Protoc.* 4, 44–57.
- Jin, H., Vacic, V., Girke, T., Lonardi, S. and Zhu, J.K. (2008) Small RNAs and the regulation of cis-natural antisense transcripts in Arabidopsis. *BMC Mol. Biol.* 9(6). <https://doi.org/10.1186/1471-2199-9-6>
- Kakizaki, T., Matsumura, H., Nakayama, K., Che, F.S., Terauchi, R. and Inaba, T. (2009) Coordination of plastid protein import and nuclear gene expression by plastid-to-nucleus retrograde signaling. *Plant Physiol.* 151, 1339–1353.
- Khraiwesh, B., Arif, M.A., Seumel, G.I., Ossowski, S., Weigel, D., Reski, R. and Frank, W. (2010) Transcriptional control of gene expression by microRNAs. *Cell*, 140, 111–122.
- Kim, C. and Apel, K. (2013) 1O2-mediated and EXECUTER-dependent retrograde plastid-to-nucleus signaling in norflurazon-treated seedlings of *Arabidopsis thaliana*. *Mol. Plant*, 6, 1580–1591.
- Kim, D., Perteau, G., Trapnell, C., Pimentel, H., Kelley, R. and Salzberg, S.L. (2013) TopHat2: accurate alignment of transcriptomes in the presence of insertions, deletions and gene fusions. *Genome Biol.* 14, R36.
- Kim, V.N. (2005) Small RNAs: classification, biogenesis, and function. *Mol. Cells*, 19, 1–15.
- Klein, M. and Papenbrock, J. (2004) The multi-protein family of Arabidopsis sulphotransferases and their relatives in other plant species. *J. Exp. Bot.* 55, 1809–1820.
- Kleine, T. and Leister, D. (2016) Retrograde signaling: organelles go networking. *Biochim. Biophys. Acta*, 1857, 1313–1325.
- Kolde, R. (2019) Pretty Heatmaps. 1.0. 12 ed. <https://cran.r-project.org/web/packages/pheatmap/pheatmap.pdf>
- Koussevitzky, S., Nott, A., Mockler, T.C., Hong, F., Sachetto-Martins, G., Surpin, M., Lim, J., Mittler, R. and Chory, J. (2007) Signals from chloroplasts converge to regulate nuclear gene expression. *Science*, 316, 715–719.
- Kramer, M.F. (2011) Stem-loop RT-qPCR for miRNAs. *Curr Protoc. Mol. Biol.* 95(1), 15.10.1–15.10.15. <https://doi.org/10.1002/0471142727.mb1510s95>
- Lapidot, M. and Pilpel, Y. (2006) Genome-wide natural antisense transcription: coupling its regulation to its different regulatory mechanisms. *EMBO Rep.* 7, 1216–1222.
- Larkin, R.M., Alonso, J.M., Ecker, J.R. and Chory, J. (2003) GUN4, a regulator of chlorophyll synthesis and intracellular signaling. *Science*, 299, 902–906.
- Liang, G., Yang, F. and Yu, D. (2010) MicroRNA395 mediates regulation of sulfate accumulation and allocation in *Arabidopsis thaliana*. *Plant J.* 62, 1046–1057.
- Liu, J., Li, Y., Wang, W., Gai, J. and Li, Y. (2016) Genome-wide analysis of MATE transporters and expression patterns of a subgroup of MATE genes in response to aluminum toxicity in soybean. *BMC Genom.* 17, 223.
- Livak, K.J. and Schmittgen, T.D. (2001) Analysis of relative gene expression data using real-time quantitative PCR and the 2^{-ΔΔC_T} Method. *Methods*, 25, 402–408.
- Love, M.I., Huber, W. and Anders, S. (2014) Moderated estimation of fold change and dispersion for RNA-seq data with DESeq2. *Genome Biol.* 15, 550.
- Lu, Y. (2016) Identification and roles of photosystem II assembly, stability, and repair factors in Arabidopsis. *Front. Plant Sci.* 7, 168.
- Ma, X., Shao, C., Jin, Y., Wang, H. and Meng, Y. (2014) Long non-coding RNAs: a novel endogenous source for the generation of Dicer-like 1-dependent small RNAs in *Arabidopsis thaliana*. *RNA Biol.* 11, 373–390.
- Mabbitt, P.D., Wilbanks, S.M. and Eaton-Rye, J.J. (2014) Structure and function of the hydrophilic Photosystem II assembly proteins: Psb27, Psb28 and Ycf48. *Plant Physiol. Biochem.* 81, 96–107.

- Maruta, T., Miyazaki, N., Nosaka, R. *et al.* (2015) A gain-of-function mutation of plastidic invertase alters nuclear gene expression with sucrose treatment partially via GENOMES UNCOUPLED1-mediated signaling. *New Phytol.* 206, 1013–1023.
- Megraw, M., Cumbie, J.S., Ivanchenko, M.G. and Filichkin, S.A. (2016) Small genetic circuits and microRNAs: big players in polymerase II transcriptional control in plants. *Plant Cell*, 28, 286–303.
- Meister, G. and Tuschl, T. (2004) Mechanisms of gene silencing by double-stranded RNA. *Nature*, 431, 343–349.
- Meng, Y., Shao, C., Ma, X., Wang, H. and Chen, M. (2012) Expression-based functional investigation of the organ-specific microRNAs in *Arabidopsis*. *PLoS One*, 7, e50870.
- Meskauskiene, R., Nater, M., Goslings, D., Kessler, F., op den Camp, R. and Apel, K. (2001) FLU: a negative regulator of chlorophyll biosynthesis in *Arabidopsis thaliana*. *Proc. Natl. Acad. Sci. USA*, 98, 12826–12831.
- Meyers, B.C., Axtell, M.J., Bartel, B. *et al.* (2008) Criteria for annotation of plant MicroRNAs. *Plant Cell*, 20, 3186–3190.
- Mochizuki, N., Brusslan, J.A., Larkin, R., Nagatani, A. and Chory, J. (2001) *Arabidopsis* genomes uncoupled 5 (GUN5) mutant reveals the involvement of Mg-chelatase H subunit in plastid-to-nucleus signal transduction. *Proc. Natl. Acad. Sci. USA*, 98, 2053–2058.
- Molla-Morales, A., Sarmiento-Manus, R., Robles, P., Quesada, V., Perez-Perez, J.M., Gonzalez-Bayon, R., Hannah, M.A., Willmitzer, L., Ponce, M.R. and Micol, J.L. (2011) Analysis of ven3 and ven6 reticulate mutants reveals the importance of arginine biosynthesis in *Arabidopsis* leaf development. *Plant J.* 65, 335–345.
- Omote, H., Hiasa, M., Matsumoto, T., Otsuka, M. and Moriyama, Y. (2006) The MATE proteins as fundamental transporters of metabolic and xenobiotic organic cations. *Trends Pharmacol. Sci.* 27, 587–593.
- Park, W., Li, J., Song, R., Messing, J. and Chen, X. (2002) CARPEL FACTORY, a Dicer homolog, and HEN1, a novel protein, act in microRNA metabolism in *Arabidopsis thaliana*. *Curr. Biol.* 12, 1484–1495.
- Pegler, J.L., Oultram, J.M.J., Grof, C.P.L. and Eamens, A.L. (2019) Profiling the abiotic stress responsive microRNA landscape of *Arabidopsis thaliana*. *Plants (Basel)*, 8, 58.
- Pornsiriwong, W., Estavillo, G.M., Chan, K.X. *et al.* (2017) A chloroplast retrograde signal, 3'-phosphoadenosine 5'-phosphate, acts as a secondary messenger in abscisic acid signaling in stomatal closure and germination. *Elife*, 6, e23361.
- Richter, A.S., Tohge, T., Fernie, A.R. and Grimm, B. (2020) The genomes uncoupled-dependent signalling pathway coordinates plastid biogenesis with the synthesis of anthocyanins. *Philos. Trans. R Soc. Lond. B Biol. Sci.* 375, 20190403.
- Rossel, J.B., Walter, P.B., Hendrickson, L., Chow, W.S., Poole, A., Mullineaux, P.M. and Pogson, B.J. (2006) A mutation affecting ASCORBATE PEROXIDASE 2 gene expression reveals a link between responses to high light and drought tolerance. *Plant Cell Environ.* 29, 269–281.
- Saini, G., Meskauskiene, R., Pijacka, W., Roszak, P., Sjogren, L.L., Clarke, A.K., Straus, M. and Apel, K. (2011) 'happy on norflurazon' (hon) mutations implicate perturbation of plastid homeostasis with activating stress acclimatization and changing nuclear gene expression in norflurazon-treated seedlings. *Plant J.* 65, 690–702.
- Sham, A., Moustafa, K., Al-Ameri, S., Al-Azzawi, A., Iratni, R. and Abuqamar, S. (2015) Identification of *Arabidopsis* candidate genes in response to biotic and abiotic stresses using comparative microarrays. *PLoS One*, 10, e0125666.
- Strand, A., Asami, T., Alonso, J., Ecker, J.R. and Chory, J. (2003) Chloroplast to nucleus communication triggered by accumulation of Mg-protoporphyrinIX. *Nature*, 421, 79–83.
- Susek, R.E., Ausubel, F.M. and Chory, J. (1993) Signal transduction mutants of *Arabidopsis* uncouple nuclear CAB and RBCS gene expression from chloroplast development. *Cell*, 74, 787–799.
- Swiezewski, S., Liu, F., Magusin, A. and Dean, C. (2009) Cold-induced silencing by long antisense transcripts of an *Arabidopsis* Polycomb target. *Nature*, 462, 799–802.
- Szyrajew, K., Bielewicz, D., Dolata, J., Wojcik, A.M., Nowak, K., Szczygiel-Sommer, A., Szweykowska-Kulinska, Z., Jarmolowski, A. and Gaj, M.D. (2017) MicroRNAs are intensively regulated during induction of somatic embryogenesis in *Arabidopsis*. *Front. Plant Sci.*, 8, 18.
- Tadini, L., Pesaresi, P., Kleine, T. *et al.* (2016) GUN1 controls accumulation of the plastid ribosomal protein S1 at the protein level and interacts with proteins involved in plastid protein homeostasis. *Plant Physiol.* 170, 1817–1830.
- Trapnell, C., Williams, B.A., Pertea, G., Mortazavi, A., Kwan, G., van Baren, M.J., Salzberg, S.L., Wold, B.J. and Pachter, L. (2010) Transcript assembly and quantification by RNA-Seq reveals unannotated transcripts and isoform switching during cell differentiation. *Nat. Biotechnol.* 28, 511–515.
- Voinnet, O. (2009) Origin, biogenesis, and activity of plant microRNAs. *Cell*, 136, 669–687.
- Wang, H.V. and Chekanova, J.A. (2017) Long Noncoding RNAs in Plants. *Adv. Exp. Med. Biol.* 1008, 133–154.
- Wang, L., Bei, X., Gao, J., Li, Y., Yan, Y. and Hu, Y. (2016) The similar and different evolutionary trends of MATE family occurred between rice and *Arabidopsis thaliana*. *BMC Plant Biol.* 16, 207.
- Wickham, H. (2016) *ggplot2 – Elegant Graphics for Data Analysis*. New York: Springer-Verlag.
- Wierzbicki, A.T., Haag, J.R. and Pikaard, C.S. (2008) Noncoding transcription by RNA polymerase Pol IVb/Pol V mediates transcriptional silencing of overlapping and adjacent genes. *Cell*, 135, 635–648.
- Woodson, J.D., Perez-Ruiz, J.M. and Chory, J. (2011) Heme synthesis by plastid ferrochelatase I regulates nuclear gene expression in plants. *Curr. Biol.* 21, 897–903.
- Woodson, J.D., Perez-Ruiz, J.M., Schmitz, R.J., Ecker, J.R. and Chory, J. (2013) Sigma factor-mediated plastid retrograde signals control nuclear gene expression. *Plant J.* 73, 1–13.
- Yuan, C., Wang, J., Harrison, A.P., Meng, X., Chen, D. and Chen, M. (2015) Genome-wide view of natural antisense transcripts in *Arabidopsis thaliana*. *DNA Res.* 22, 233–243.
- Zhang, X., Xia, J., Lii, Y.E. *et al.* (2012) Genome-wide analysis of plant natural siRNAs reveals insights into their distribution, biogenesis and function. *Genome Biol.* 13, R20.
- Zhao, C., Wang, Y., Chan, K.X. *et al.* (2019a) Evolution of chloroplast retrograde signaling facilitates green plant adaptation to land. *Proc. Natl. Acad. Sci. USA*, 116, 5015–5020.
- Zhao, X., Huang, J. and Chory, J. (2019b) GUN1 interacts with MORF2 to regulate plastid RNA editing during retrograde signaling. *Proc. Natl. Acad. Sci. USA*, 116, 10162–10167.
- Zimorski, V., Ku, C., Martin, W.F. and Gould, S.B. (2014) Endosymbiotic theory for organelle origins. *Curr. Opin. Microbiol.* 22, 38–48.

2.3 Publication 3 (Tiwari et al. 2021)

Identification of small RNAs during high light acclimation in *Arabidopsis thaliana*.

Bhavika Tiwari, Kristin Habermann, M. Asif Arif, Oguz Top & Wolfgang Frank

Submitted to *Frontiers in Plant Science*

Identification of small RNAs during high light acclimation in *Arabidopsis thaliana*

Bhavika Tiwari¹, Kristin Habermann¹, M. Asif Arif¹, Oguz Top¹, Wolfgang Frank^{1*}

¹Plant Molecular Cell Biology, Department of Biology I, LMU Biocenter, Ludwig Maximilian University of Munich, Germany

Submitted to Journal:
Frontiers in Plant Science

Specialty Section:
Plant Abiotic Stress

Article type:
Original Research Article

Manuscript ID:
656657

Received on:
21 Jan 2021

Journal website link:
www.frontiersin.org

In review

Conflict of interest statement

The authors declare that the research was conducted in the absence of any commercial or financial relationships that could be construed as a potential conflict of interest

Author contribution statement

WF designed the research; BT performed the research with the help of MAA and KH; BT, MAA, KH, OT and WF analyzed the data; and BT, OT and WF wrote the paper. All authors read and approved the final manuscript.

Keywords

Arabidopsis thaliana (Arabidopsis), high light acclimation, small non-coding RNA, gene regulation, RNA sequencing

Abstract

Word count: 235

The biological significance of non-coding RNAs (ncRNAs) has been firmly established to be important for the regulation of genes involved in stress acclimation. Light plays an important role for the growth of plants providing the energy for photosynthesis, however, excessive light conditions can also cause substantial defects. Small RNAs (sRNAs) are a class of non-coding RNAs that regulate transcript levels of protein-coding genes and mediate epigenetic silencing. Next generation sequencing facilitates the identification of small non-coding RNA classes such as miRNAs (microRNAs) and small-interfering RNAs (siRNAs), and long non-coding RNAs (lncRNAs), but changes in the ncRNA transcriptome in response to high light are poorly understood. We subjected Arabidopsis plants to high light conditions and performed a temporal in-depth study of the transcriptome data after 3 h, 6 h and 2 d of high light treatment. We identified a large number of high light responsive miRNAs and sRNAs derived from cis- and trans-NAT gene pairs, lncRNAs and TAS transcripts. We performed target predictions for differentially expressed miRNAs and correlated their expression levels through mRNA sequencing data. GO analysis of the targets revealed an overrepresentation of genes involved in transcriptional regulation. In *A. thaliana*, sRNA-mediated regulation of gene expression in response to high light treatment is mainly carried out by miRNAs and sRNAs derived from cis- and trans-NAT gene pairs, and from lncRNAs. This study provides a deeper understanding of sRNA-dependent regulatory networks in high light acclimation.

Contribution to the field

Dear Editors of Frontiers in Plant Science, Please find enclosed our manuscript entitled "Identification of small RNAs during high light acclimation in Arabidopsis thaliana" that we would like to submit as an Original Research Article to Frontiers in Plant Science. Light plays an important role for the growth of plants providing the energy for photosynthesis. However, excessive light conditions can also cause substantial defects. As a result, molecular, physiological, biochemical and even morphological adaptations contribute to the acquisition and adaptation to high light. Besides the classical control of gene expression governed by transcription factors, several classes of small non-coding RNAs as well as long non-coding RNAs contribute to altered steady-state levels of protein coding transcripts. In this study we have combined small RNA sequencing with sequencing of mRNAs and lncRNAs in Arabidopsis thaliana to characterize changes in their expression after 3 hours, 6 hours and 2 days of high light treatment. We identified a large number of high light responsive miRNAs and sRNAs derived from cis- and trans-NAT gene pairs, lncRNAs and TAS transcripts. We performed target predictions for differentially expressed miRNAs and correlated their expression levels through mRNA sequencing data. GO analysis of the targets revealed an overrepresentation of genes involved in transcriptional regulation. Our study provides a fundamental database to deepen our knowledge related to the importance of sRNAs in the high light responsive acclimation networks. We hereby confirm that the manuscript has not been submitted to any other journal and all the authors have approved the submission of this manuscript to Frontiers in Plant Science. The authors have no conflicts of interests to declare. Yours sincerely, Wolfgang Frank

Funding statement

The funding for the research conducted was provided by the German Research Foundation (SFB-TRR 175, grants to W.F. project C03). The Funding body was not involved in the design of the study and analysis or interpretation of the data and in writing of the manuscript.

Ethics statements

Studies involving animal subjects

Generated Statement: No animal studies are presented in this manuscript.

Studies involving human subjects

Generated Statement: No human studies are presented in this manuscript.

Inclusion of identifiable human data

Generated Statement: No potentially identifiable human images or data is presented in this study.

In review

Data availability statement

Generated Statement: The datasets presented in this study can be found in online repositories. The names of the repository/repositories and accession number(s) can be found in the article/supplementary material.

In review

Identification of small RNAs during high light acclimation in *Arabidopsis thaliana*

1 **Bhavika Tiwari¹, Kristin Habermann¹, M. Asif Arif¹, Oguz Top¹, Wolfgang Frank^{1,*}**

2 ¹Plant Molecular Cell Biology, Department of Biology I, LMU Biocenter, Ludwig-Maximilians-
3 University Munich, Planegg-Martinsried, Germany

4 *** Correspondence:**

5 Wolfgang Frank

6 wolfgang.frank@lmu.de

7 ORCID IDs: 0000-0003-2820-6505 (O.T.), 0000-0003-2424-0087 (W.F.)

8 **Keywords: *Arabidopsis thaliana*, high light acclimation, small non-coding RNA, gene**
9 **regulation, RNA sequencing**

10 **Abstract**

11 The biological significance of non-coding RNAs (ncRNAs) has been firmly established to be
12 important for the regulation of genes involved in stress acclimation. Light plays an important role for
13 the growth of plants providing the energy for photosynthesis, however, excessive light conditions can
14 also cause substantial defects. Small RNAs (sRNAs) are a class of non-coding RNAs that regulate
15 transcript levels of protein-coding genes and mediate epigenetic silencing. Next generation sequencing
16 facilitates the identification of small non-coding RNA classes such as miRNAs (microRNAs) and
17 small-interfering RNAs (siRNAs), and long non-coding RNAs (lncRNAs), but changes in the ncRNA
18 transcriptome in response to high light are poorly understood. We subjected *Arabidopsis* plants to high
19 light conditions and performed a temporal in-depth study of the transcriptome data after 3 h, 6 h and 2
20 d of high light treatment. We identified a large number of high light responsive miRNAs and sRNAs
21 derived from NAT gene pairs, lncRNAs and *TAS* transcripts. We performed target predictions for
22 differentially expressed miRNAs and correlated their expression levels through mRNA sequencing
23 data. GO analysis of the targets revealed an overrepresentation of genes involved in transcriptional
24 regulation. In *A. thaliana*, sRNA-mediated regulation of gene expression in response to high light
25 treatment is mainly carried out by miRNAs and sRNAs derived from NAT gene pairs, and from
26 lncRNAs. This study provides a deeper understanding of sRNA-dependent regulatory networks in high
27 light acclimation.

28 **1 Introduction**

29 Acclimation to changing abiotic and climatic conditions is a prerequisite for plants to survive. High
30 light stress is probably the most frequently experienced stress by plants and efficient light utilization
31 requires proper acclimation to light-limiting and light-excess conditions. To counter the effects of high
32 light, plants respond systemically by adjusting leaf orientation, depositing salt crystals on the leaf
33 surface or developing air-filled hairs (Ruban, 2009). On the cellular level, changes in the light spectral
34 quality are perceived by the chloroplasts and light absorption is regulated by chloroplast movements.
35 Far-red light and red light are perceived by phytochromes (PHY A-E) (Sharrock and Quail, 1989)
36 whereas cryptochromes (CRY1/CRY2/CRY3) and phototropins sense blue light or UV-A light (Lin et
37 al., 1998). The conversion of light energy into chemical energy requires the photosynthetic apparatus

38 comprising photosystem II (PSII) and photosystem I (PSI) that function sequentially. The two
39 photosystems have different absorption spectra and thus any fluctuations in light intensity could lead
40 to imbalanced excitation rates causing a loss in photosynthetic efficiency. Excess light is known to
41 reduce the efficiency of photosynthesis. During short-term fluctuations, the light state transition
42 mechanism regulates the distribution of imbalanced energy through reversible phosphorylation of the
43 light-harvesting complex II (LHCII) (Minagawa, 2013). When PSI is overexcited, the
44 unphosphorylated LHCII antennae binds the PSII whereas when PSII is overexcited, STN7
45 (Serine/Threonine protein kinase) phosphorylated LHCII binds the PSI to correct the light-shift-
46 imbalance (Bellafiore et al., 2005).

47 Under excess light photoinhibition provokes the production of reactive oxygen species (ROS) which
48 leads to inactivation of the PSII reaction center by photodamage (Norikazu Ohnishi et al., 2005; Murata
49 et al., 2007). In the last few years, studies revealed that plants have developed mechanisms to cope
50 with photodamage such as thermal dissipation of excess energy, xanthophyll cycle, cyclic electron flow
51 and photorespiratory pathways (Demmig et al., 1987; Park et al., 1996; Niyogi et al., 1998; Cornic et
52 al., 2000; Maxwell and Johnson, 2000; Wingler et al., 2000; Clarke and Johnson, 2001; Munekage et
53 al., 2004; Miyake et al., 2005; Jahns and Holzwarth, 2012).

54 When plants are exposed to high light, chloroplasts transmit retrograde signals to the nucleus (Nott et
55 al., 2006) in order to downregulate the expression of photosynthesis associated genes and to induce
56 defense related genes to prevent oxidative damage (Apel and Hirt, 2004; Van Breusegem et al., 2008).
57 Moreover, biosynthesis of the phytohormone abscisic acid (ABA) was induced in parenchyma cells
58 and initiated a signaling network in bundle sheath cells. The G protein complex, OPEN STOMATA 1
59 protein kinase and H₂O₂ together with redox signals, activated expression and accumulation of
60 Ascorbate peroxidase 2 (APX2). Thus, ABA was found to be essential to coordinate the expression of
61 high light responsive genes in coordination with retrograde signaling mechanisms (Valdivieso et al.,
62 2009). In response to high light, 3'-phosphoadenosine 5'-phosphate (PAP) accumulates in the
63 chloroplasts of *Arabidopsis* which is normally dephosphorylated to AMP by the SAL1 phosphatase.
64 SAL1 was found to be inhibited upon high light and drought stress leading to PAP accumulation and
65 the inhibition of exoribonucleases in the nucleus causing modulations in nuclear gene expression
66 (Estavillo et al., 2011). MEcPP (methylerythritol cyclodiphosphate) was shown to be a retrograde
67 signal that is converted into HMBPP (hydroxymethylbutenyl diphosphate) by the enzyme 1-hydroxy-
68 2-methyl-2-(E)-butenyl-4-diphosphate synthase (HDS). In high light, HDS was inhibited leading to the
69 accumulation of MEcPP and altered gene expression in the nucleus with an upregulation of *HPL*
70 (hydroperoxide lyase) via chromatin remodeling (Xiao et al., 2012). HPL is a nuclear-encoded and
71 plastid localized enzyme and the stress-responsive induction of the gene initiates the oxylipin
72 biosynthesis (Savchenko et al., 2017). During high light stress, singlet oxygen (¹O₂) which is generated
73 due to imbalanced redox potential induced the expression of β-cyclocitral, about 10 glutathione S-
74 transferase and 12 UDP-glycosyltransferases genes, respectively. These genes are known to be
75 involved in detoxification of endogenous compounds such as lipid peroxides and to confer stress
76 tolerance to ¹O₂ (Ledford et al., 2007). The alterations in gene expression mediated by β-cyclocitral
77 increased the photosynthetic efficiency and reduced lipid peroxidation in high light stress (Ramel et
78 al., 2012).

79 Due to excess light, the electron transport chain is over reduced and PSII can be affected by
80 photoinhibition. This imbalance of redox potential leads to the production of high amounts of ¹O₂ in
81 PSII that can cause the formation of irreversible reactive oxygen species (ROS), peroxides and radical
82 induced damages even though high levels of ROS have also been shown to act in signaling pathways
83 in response to high light (Karpinski et al., 2003). Plants have evolved mechanisms to protect themselves

84 from elevated ROS levels by ROS scavenging proteins such as ascorbate peroxidases (APX),
 85 superoxide dismutase (SOD), glutathione peroxidases (GPX), catalases (CAT), and peroxiredoxins
 86 (PRX). Fluorescence quenching (NPQ) was proven to be a potential initiator of retrograde signals and
 87 were shown to be the regulators of *APX1* and *APX2* encoding ascorbate peroxidases (Szechynska-
 88 Hebda et al., 2010). The non-enzymatic antioxidants include ascorbate and glutathione, flavones,
 89 carotenoids, tocopherols and anthocyanins (Birben et al., 2012). The constant process of ROS
 90 production and scavenging occurs in all cellular compartments and hence is tightly controlled by a
 91 ROS associated gene network (Mittler et al., 2004).

92 In addition to transcriptional changes of protein-coding genes light stress also causes changes in the
 93 expression of non-coding transcripts (Wang et al., 2014a). Non-coding RNAs (ncRNAs) are divided
 94 into two groups based on their size. ncRNAs shorter than 200 nt are considered as small ncRNAs
 95 whereas longer transcripts are referred to as long ncRNAs. Among the small ncRNAs miRNAs with a
 96 size of approximately 21 nt are prominent regulators of gene expression. miRNAs are transcribed as
 97 primary miRNAs from *MIR* genes by RNA polymerase II. The pri-miRNA folds back into a stem loop
 98 structure which is further processed into a pre-miRNA by DICER-LIKE1 (DCL1), HYPOPLASTIC
 99 LEAVES1 (HYL1) and SERRATE (SE) that is further processed to release the mature
 100 miRNA:miRNA* duplex (Voinnet, 2009). The duplex becomes 3' methylated by HUA ENHANCER1
 101 (HEN1) protecting the miRNA from degradation (Bin Yu et al., 2005). The mature miRNA strand
 102 binds to ARGONAUTE1 (AGO1) and is loaded into the RNA-induced silencing complex (RISC)
 103 guiding the complex to fully or partially reverse complementary target transcripts causing target
 104 cleavage or translational inhibition (Voinnet, 2009).

105 Studies in different plant species have been conducted to identify differentially expressed miRNAs in
 106 response to high light, UV-A and UV-B (Zhou et al., 2016). miR156/157, miR167, miR170/171 and
 107 miR159/319 are known to be red light and UV-B responsive in *Arabidopsis* (Zhou et al., 2007; Tsai et
 108 al., 2014; Zhenfei S. et al., 2018), *Oryza sativa* (Sun et al., 2015), *Glycine max* (Li et al., 2015) and
 109 *Triticum aestivum* (Wang et al., 2013). The expression levels of miR165/166, miR396, miR408 and
 110 miR169 were UV-B, white and red light regulated in *A. thaliana*, *O. sativa* and *G. max* (Casadevall et
 111 al., 2013). miR398, miR172, miR160, miR169, miR164, miR395, miR399, miR168, miR393, miR858,
 112 miR163, miR390 and miR397 were responsive to white and far red light, UV-A, UV-B and
 113 differentially expressed in *Arabidopsis phyB* (*phytochrome B*) and *pif4* (*phytochrome interacting factor*
 114 *4*) mutants (Chung et al., 2016; Sharma et al., 2016; Lin et al., 2017; Zhenfei S. et al., 2018). In addition,
 115 miR396 was found to be upregulated in response to UV-B light mediating the downregulation of its
 116 targets encoding *GROWTH REGULATING FACTOR1* (*GRF1*), *GRF2*, and *GRF3* that led to an
 117 inhibition of cell proliferation in leaves (Casadevall et al., 2013). miR163 was also found to be highly
 118 induced by red light in *Arabidopsis* targeting *PXMT1* encoding a 1,7-paraxanthine methyltransferase
 119 involved in methylation of phytohormones (Chung et al., 2016). In the early stages of development,
 120 this miRNA and its target were also found to regulate germination. Upregulation of miR156 was found
 121 to be important for increasing anthocyanin levels in *Arabidopsis*. miR156 targets *SPL* transcripts which
 122 are known to repress the anthocyanin biosynthesis pathway (Gou et al., 2011; Cui et al., 2014). In
 123 addition to miR156, miR858 is also considered a positive regulator of anthocyanin biosynthesis as it
 124 targets *MYBL2* coding for a repressor of the phenylpropanoid pathway (Sharma et al., 2016; Yulong
 125 Wang et al., 2016). ELONGATED HYPOCOTYL 5 (HY5) was also shown to be a positive regulator
 126 of the anthocyanin pathway as it downregulates MYBL2 (MYB-LIKE 2) (Nguyen et al., 2015).

127 lncRNAs can be transcribed from the positive as well as the negative strand of the genomic DNA
 128 generating overlapping sense and antisense transcripts referred to as natural antisense transcripts
 129 (NAT). When lncRNAs do not overlap with any protein coding gene, but are present between two

130 genes or in the intronic region, they are referred as long intergenic or intronic non-coding RNAs
 131 (lincRNAs) (Ma et al., 2013). Recent studies have found lincRNAs involved in light regulated
 132 processes, *HIDDEN TREASURE 1 (HIDI)* was found to act through PIF3 which is a key repressor of
 133 photomorphogenesis (Wang et al., 2014b) and *CDF5 LONG NONCODING RNA (FLORE)*, a NAT of
 134 *CDF5* repressed *CDF5* itself and promoted transcription of *FLOWERING LOCUS T (FT)* which
 135 induced flowering (Henriques et al., 2017). The RNA polymerase II derived NATs are able to produce
 136 siRNAs from overlapping regions referred to as nat-siRNAs. Depending on the genomic locations of
 137 the two overlapping transcripts, the NATs are classified as *cis*-NATs when the transcripts are encoded
 138 by complementary DNA strands at the same genomic region and referred to as *trans*-NATs when the
 139 transcripts are produced from two different regions in the genome (Wight and Werner, 2013). The first
 140 identified *cis*-nat-siRNA producing loci have an important role in response to high salinity stress. The
 141 constitutively expressed transcript *delta-pyrroline-5-carboxylate dehydrogenase (P5CDH)* and the salt
 142 induced transcript *Similar to Radicle Induced Cell Death One 5 (SRO5)* produce 24 nt *cis*-nat-siRNA
 143 from a dsRNA formed by both transcripts. siRNAs produced from this region are able to cleave the
 144 *P5CDH* transcript resulting a decreased proline degradation and improved salinity tolerance (Borsani
 145 et al., 2005). *trans*-nat-siRNAs are produced in a similar manner, but transcript pairing can take place
 146 in diverse combinations i.e. between lincRNAs, mRNAs, transposable elements (TE) and tRNA
 147 transcripts (Wang et al., 2005; Yuan et al., 2015). Another class of secondary siRNAs known as *trans*-
 148 acting siRNAs (ta-siRNAs) are produced from non-coding *TAS* transcripts. ta-siRNA production is
 149 initiated by miRNA assisted cleavage of *TAS* transcripts, subsequent dsRNA synthesis and phased
 150 processing to produce siRNAs in a specific head to tail arrangement. Another sRNA class, the
 151 phasiRNAs are similar to ta-siRNAs and also produced in a phased manner, but ta-siRNAs are able to
 152 act only in *trans* (Fei et al., 2013). The recently discovered class of 21 nt epigenetically activated
 153 siRNAs (ea-siRNAs) were found to be expressed from transposon-encoded transcripts in the
 154 *Decreased DNA Methylation 1 (DDMI)* mutant of *Arabidopsis*. These siRNAs are important to reduce
 155 or prevent transcription of TE-encoded RNAs and certain mRNA transcripts via siRNA-mediated
 156 silencing (K.M. Creasey and Zhai, 2014). A TE-derived lincRNA (TE-lincRNA1195) was also reported
 157 to be involved in the ABA response and found to be important for abiotic stress adaptation (Wang et
 158 al., 2017).

159 In our study we performed transcriptome sequencing to identify the ncRNA repertoire involved in the
 160 response to high light treatment in *Arabidopsis* and to analyze their impact on associated target
 161 mRNAs. We sequenced mRNA as well as sRNA libraries from *Arabidopsis* plants treated with high
 162 light acclimation conditions for 3 h, 6 h and 2 d and investigated putative correlations between
 163 differentially expressed sRNAs from all classes and their cognate target RNAs. We identified a large
 164 number of sRNAs belonging to all known sRNA classes which were differentially expressed during
 165 the high light treatment and these sRNAs are able to control a large set target RNAs. Most of these
 166 targets encode transcription factors pointing to their role in modulation of gene expression.

167 2 Materials and Methods

168 2.1 Plant material and stress treatment

169 Seeds of *A. thaliana* ecotype Columbia (*Col-0*), purchased from Nottingham Arabidopsis Stock Centre
 170 (NASC; UK), were sown at a high density (ca. 50 seeds on 9 x 9 cm pots) on a soil substrate and
 171 stratified for 2 d in the dark at 4°C. The pots were transferred into the light (LED-41 HIL2 cabinets,
 172 Percival, Perry, USA) following stratification and cultivated under control conditions with a light /
 173 dark regime of 16 h light (80 $\mu\text{mol photons m}^{-2} \text{s}^{-1}$; corresponding to 18% of blue and red channel) at
 174 22°C followed by 8 h dark at 18°C for 14 d. Plants serving as controls remained under these conditions

175 whereas plants subjected to high light treatment were transferred 4 h after the onset of light at 22°C
 176 with a light intensity of 450 $\mu\text{mol photons m}^{-2} \text{s}^{-1}$. Aerial tissues from 3 h, 6 h, and 48 h high light-
 177 treated as well as control samples were harvested.

178 2.2 RNA isolation and sequencing

179 The mRNA and sRNA sequencing data of untreated control samples obtained after 3 h, 6 h and 2 d
 180 time points are available from our previous study (Tiwari et al., 2020). The mRNA sequencing data of
 181 high light treated samples obtained after 3 h and 2 d were reported previously (Garcia-Molina et al.,
 182 2020). The mRNA sequencing data of high light treated samples obtained after 6 h as well as the sRNA
 183 sequencing data after 3 h, 6 h and 2 d time were generated in this study. Total RNA was isolated using
 184 TRI-Reagent (Sigma) following manufacturer's protocol. Library preparations and sequencing were
 185 performed according to our previous study (Tiwari et al., 2020). Briefly, the mRNA/lncRNA libraries
 186 were prepared using the Next Ultra RNA Library Prep Kit (NEB) and were sequenced strand-
 187 specifically as 150 bp paired-ends with at least 15 million read pairs per library on Illumina HiSeq-
 188 2500 platform. sRNA libraries were prepared from 50 μg of total RNA using the NEBNext Multiplex
 189 sRNA Library Prep Kit (NEB) for Illumina following manufacturer's instructions. The sRNA libraries
 190 were sequenced as 50 bp read length with a minimum of 7 million reads per library on Illumina HiSeq
 191 1500.

192 2.3 Bioinformatic analyses of transcriptomes

193 The 3 h, 6 h and 2 d high light-acclimated samples along with their respective controls were sequenced
 194 and the mRNA/lncRNA sequencing data was analyzed using open web based platform GALAXY
 195 (<https://usegalaxy.org/>) (Afgan et al., 2016). The adapter sequences were trimmed by FASTQ
 196 Trimmomatic tool using the default parameters. The Tophat tool mapped the raw reads against the *A.*
 197 *thaliana* TAIR10 reference genome (<https://www.arabidopsis.org>) with a maximum intron length
 198 parameter of 3,000 nt. The annotation of coding and non-coding RNA transcripts (≥ 200 bp) was
 199 performed using Araport11 annotation (Cheng et al., 2017). The FeatureCounts tool counted the
 200 number of reads mapped to the reference genome. The final list of genes was obtained by DeSeq2 tool
 201 of GALAXY using output from the FeatureCounts tool and classified using Araport11 reference
 202 annotation (<https://araport.org/>).

203 The TAIR10 reference genome was used to map sRNA raw reads using the Shortstack software (Axtell,
 204 2013). Approximately 80% of the obtained reads efficiently mapped to the reference. A reference
 205 annotation database was created from publicly available sources such as miRNA (miRBase version
 206 22.1), lncRNA (Araport11), *trans*- and *cis*-nat-siRNA (Jin et al., 2008; Zhang et al., 2012; Wang et al.,
 207 2014a; Yuan et al., 2015), ta-siRNA and phasiRNA (Howell et al., 2007). Using these sources, the read
 208 counts of different classes of sRNAs were calculated. The read counts of the triplicates of samples
 209 were later analyzed by the DeSeq2 tool and differentially expressed (DE) sRNAs with $\text{FC} \geq 2$ & ≤ -2
 210 (Benjamini-Hochberg corrected p-value ≤ 0.05) were identified. Further global comparisons of DE
 211 miRNAs were performed using UpSetR package (<https://CRAN.R-project.org/package=UpSetR>).

212 2.4 Prediction of putative miRNA targets

213 psRNATarget: A Plant Small RNA Target Analysis Server(2017 Update) was used to identify putative
 214 miRNA targets (Dai et al., 2018). DE miRNAs were used as a query to search against *A. thaliana*
 215 Araport11 transcript database using default parameters with changes in UPE (25) and maximum
 216 expectation (2.5) to ensure more stringent predictions.

217 2.5 Gene Ontology analyses of putative miRNA targets

218 We used the DAVID Bioinformatics tool (Jiao et al., 2012) to perform the GO analyses. The list of
 219 miRNA target genes was provided as an input and the output gene list was broadly classified into
 220 biological process, cellular compartment and molecular function. The significant GO terms were
 221 identified in all aforementioned categories (Fisher's test with Benjamini-Hochberg corrected p-value
 222 ≤ 0.05). The ggplot2 package (<https://CRAN.R-project.org/package=ggplot2>) was used for
 223 visualization of the output. the ggplot2 package was used.

224 2.6 cDNA synthesis for stem loop qRT-PCR

225 We used 300 ng of RNA from three biological replicates of treated and untreated samples as the starting
 226 material for cDNA synthesis. DNase I (2 U, NEB) was added to the RNA and incubated at 37 °C for
 227 30 min to eliminate genomic DNA contamination, and later was inactivated at 65 °C for 10 min.
 228 Reverse transcription of RNA into cDNA was performed by M-MuLV Reverse transcriptase (200 U,
 229 NEB) at 42 °C for 30 min. The stem loop primers specific for the sRNAs and a universal reverse primer
 230 were used for cDNA synthesis (**Supplementary Material 1, Table S1**). We used *UBI1* (*AT4G36800*)
 231 specific reverse primer during the reverse transcription and confirmed successful cDNA synthesis
 232 through RT-PCR by using *UBI1* specific gene primers.

233 2.7 Stem loop qRT-PCR

234 We performed qRT-PCR using EvaGreen and sRNA-specific primers (Kramer, 2011)
 235 (**Supplementary Material 1, Table S1**). The qRT-PCRs were performed in three technical replicates
 236 for each sample and each reaction contained cDNA amounts equivalent to 20 ng/ μ l of initial RNA. The
 237 qRT-PCR program was subjected to initial denaturation at 95 °C for 2 min followed by 40 cycles of
 238 amplification with 95 °C for 12 s, annealing for 30 s and 72 °C for 15 s. After each cycle, the EvaGreen
 239 signals were measured and melting curves were monitored to confirm primer specificities. The $\Delta\Delta C_t$
 240 method was used to calculate the expression levels following normalization against *UBI1*
 241 housekeeping gene.

242 3 Results

243 3.1 Changes in the sRNA repertoire during high light acclimation in *A. thaliana*

244 *A. thaliana* seedlings were subjected to high light treatments (450 μ mol photons $m^{-2} s^{-1}$ for 3 h, 6 h and
 245 2 d) to analyze high light-responsive changes in the sRNA repertoire. A minimum of 7 million reads
 246 per library of treated and control samples were generated for transcriptome profiling. For all samples,
 247 mapping of sRNA reads against the *A. thaliana* reference genome revealed an average of about 13%
 248 reads mapping to miRNA loci, 10% to *trans*- and 2% to *cis*-nat-siRNA loci. 5% of the remaining reads
 249 corresponded to lncRNAs, 3% to ta-siRNA producing regions and 0.3% to phasiRNAs
 250 (**Supplementary Material 2, Table S2,3**). Only approximately 1% of the reads accounted for loci
 251 encoding the most abundant RNAs such as rRNA, snoRNA, tRNA and snRNA validating high quality
 252 of the sRNA libraries. The remaining reads mostly mapped to other RNA classes involved in epigenetic
 253 regulations such as TE and repeat associated regions.

254 The size distribution of sRNAs showed two distinct peaks at 21 nt and 24 nt. The peak at 21 nt indicates
 255 an enrichment of miRNAs, nat-siRNAs and ta-siRNA whereas the peak at 24 nt represents sRNAs
 256 derived from repetitive/intergenic RNAs, inverted repeats and TE (**Figure 1A,B,C, Supplementary**
 257 **Material 2, Table S4**). We observed an increased sRNA biogenesis at the early time points (3 h and 6

258 h) and reduced production after 2 d compared to the control samples in response to high light
 259 acclimation. Our analyses revealed that miRNAs and *trans*-nat-siRNAs are the two major sRNA
 260 classes uncovered in our data set (**Figure 1D**). To identify DE sRNAs between treated samples and the
 261 controls, the values of normalized reads were used to calculate the relative expression of mature
 262 miRNAs and siRNAs ($FC \geq 2$ and ≤ -2 , Benjamini-Hochberg corrected p -value ≤ 0.05).

263 Over the analyzed time points, high light affected sRNAs were mainly generated from *trans*- followed
 264 by *cis*-NAT-pairs and miRNAs (**Figure 2A,B,C**). We observed an increasing number of upregulated
 265 *trans*-nat-siRNAs and *cis*-nat-siRNAs over the time course of high light treatment (**Figure 2A,C**). The
 266 differential expression of miRNAs substantially increased after 6 h of treatment (**Figure 2B**).

267 To confirm the reliability and validity of our sRNA sequencing data, we performed stem loop RT-
 268 PCRs to determine the steady-state levels for selected sRNAs produced from all analyzed RNA classes
 269 during the course of high light treatment (**Figure 3**). miR159c, miR166f, miR779.2, *trans*-nat-siRNAs
 270 produced from *AT4G20520-AT4G32200* and *AT1G31600-AT5G39660* transcripts, *cis*-nat-siRNAs
 271 derived from *AT1G48920-AT1G48930* were differentially expressed upon high light treatment and
 272 *AT1G11260-AT1G11270* were repressed after 6 h whereas sRNAs derived from lncRNA *AT5G07325*
 273 were downregulated after 3 h of high light treatment confirming our sequencing results.

274 3.2 Expression profiling of miRNAs during high light acclimation

275 Next generation sequencing distinguishes between individual miRNAs even with a single nucleotide
 276 polymorphism and obtained reads were analyzed to determine differentially regulated miRNAs ($FC \geq$
 277 2 and ≤ -2 , Benjamini-Hochberg corrected p -value ≤ 0.05) after precise read mapping (**Table 1**,
 278 **Supplementary Material 3, Table S5**). We observed a general trend in all samples that around 11 %
 279 of the detected miRNAs possessed very high normalized read counts ($> 1,000$ reads per sample), about
 280 38 % showed moderate expression ($< 1,000$ and > 20 normalized reads), 15 % showed reduced read
 281 counts (< 20 and > 5 normalized reads) and 36 % showed very low expression (< 5 normalized reads)
 282 (**Supplementary Material 3, Table S6**). In response to high light treatment, we observed 24 DE
 283 miRNAs (8 up and 16 down) after 3 h, 56 mature DE miRNAs (26 up and 30 down) after 6 h and 26
 284 DE mature miRNAs (14 up and 12 down) after 2 d.

285 Conserved miRNA families seem to have important functions since they mainly regulate targets
 286 encoding TFs or enzymes acting in abiotic stress adaptation (Qin et al., 2014; Khaksefidi et al., 2015;
 287 Yu et al., 2019). Over the last few years, 22 miRNA families were identified to be conserved between
 288 *A. thaliana*, *Oryza sativa* and *Populus trichocarpa* (Bonnet et al., 2004; Zhang et al., 2006; Pelaez et
 289 al., 2012). Out of these 22 miRNA families, members of 16 families were found to be differentially
 290 expressed upon high light; corresponding to 8, 11 and 13 DE mature miRNAs at 3 h, 6 h and 2 d,
 291 respectively (**Supplementary Material 3, Table S7**). It is known that miRNAs regulate the expression
 292 of TFs and are involved in phyB-mediated light signaling pathways and there are very few light
 293 responsive miRNAs identified in crop plants (Sun et al., 2015; Yang et al., 2019). In total, 92 non-
 294 redundant mature miRNAs were found to be differentially expressed throughout the course of high
 295 light treatment. Out of these 92 mature miRNAs, 38 mature miRNAs belonging to 14 conserved
 296 miRNA families are light stress regulated in other plant species (Casati, 2013) (**Table 1**) and 46 mature
 297 miRNAs have been previously known to be UV-B, white light, and red light responsive in *A. thaliana*.
 298 Our study shows similarity in the induction or repression pattern of these miRNAs compared to other
 299 light stress-related studies (Zhou et al., 2007; Shikata et al., 2014). The remaining 46 DE mature
 300 miRNAs belonging to 37 miRNA families such as miR447, miR861 and miR863 have not been
 301 reported before to be light-regulated in *A. thaliana* (**Supplementary Material 3, Table S7**). We

302 identified 5 miRNAs with a varying expression pattern i.e. up- and downregulation, and 7 miRNAs
 303 with consistent expression pattern (either up- or downregulated) in at least two of the analyzed time
 304 points. We found miR399a to be consistently upregulated at all the three time points. This miRNA was
 305 also found to be upregulated by red light in leaves of potatoes and in phosphorous deficient conditions
 306 in barley (Hackenberg et al., 2013; Qiao et al., 2017).

307 3.3 Differentially expressed miRNA targets

308 MiRNAs can mediate the cleavage of their mRNA targets or cause translation inhibition (Aukerman
 309 and Sakai, 2003). Plant miRNAs show perfect or partial sequence complementarity to their target
 310 sequences and often lead to mRNA cleavage between nucleotides 10 and 11 of the miRNA binding
 311 site (Bartel, 2004; Brodersen et al., 2008). We sequenced the sRNAs and mRNA/lncRNA from the
 312 same RNA samples and directly compared changes in miRNA expression with the changes of their
 313 cognate targets. We used the psRNATarget analysis server with stringent search criteria to determine
 314 the targets of DE miRNAs during the time course of high light treatment (Dai et al., 2018) and found
 315 putative targets for 88 of 92 DE miRNAs comprising 322 mRNAs and 15 ncRNAs (**Supplementary**
 316 **Material 4, Table S8,9**). The 25 DE miRNAs (14 up- and 11 downregulated) at 3 h of high light
 317 acclimation can target 100 non-redundant mRNAs and 3 non-coding transcripts. The 50 DE miRNAs
 318 (23 up- and 27 downregulated) at 6 h of treatment are able to target 220 non-redundant mRNAs and
 319 10 non-coding RNA targets and the 25 DE miRNAs (14 up- and 11 downregulated) after 2 d can target
 320 125 non-redundant mRNAs and 5 non-coding RNA targets (**Supplementary Material 4, Table S8,9**).
 321 To investigate how the regulation of these putative targets correlates with the changes in the miRNA
 322 repertoire, our mRNA as well as lncRNA transcriptome data generated from the identical RNA pools
 323 were further analyzed (**Supplementary Material 5, Table S10,11**). We investigated the correlation
 324 between the 88 DE miRNAs and their cognate 332 target transcripts (**Supplementary Material 4,**
 325 **Table S8**). Even though we mainly observed that one transcript can be targeted by various isoforms of
 326 a miRNA family, we found few cases in which target transcripts can also be cleaved by different
 327 miRNAs that are not related in sequence. By taking all individual DE miRNAs and their cognate
 328 protein-coding transcripts (mRNAs) as miRNA:mRNA pairs into consideration, we identified 128, 298
 329 and 175 miRNA:mRNA pairs for the 3 h, 6 h and 2 d time points of high light treatment, respectively
 330 (**Supplementary Material 4, Table S8**). We broadly classified the miRNA:mRNA target pairs of all
 331 time points into different categories based on the correlation between miRNAs and their cognate
 332 mRNA expressions. These broad categories are i. inverse correlation (when miRNA and mRNA show
 333 anticorrelation), ii. same tendencies (when both miRNA and mRNA either upregulated or
 334 downregulated), iii. steady (or undetected) levels of target mRNA despite changes in miRNA levels
 335 (**Table 1**). We observed 3, 6 and 2 inversely correlated pairs at 3 h, 6 h and 2 d, respectively, with a
 336 total number of 10 non-redundant inversely correlated miRNA:mRNA target pairs that modulate the
 337 mRNA repertoire upon high light treatment (**Supplementary Material 4, Table S8**). Apart from the
 338 mRNA targets, psRNATarget prediction server additionally predicted 17 putative non-coding RNA
 339 targets of DE miRNAs, but the expression levels of those ncRNA target transcripts were either
 340 unchanged or their levels were below detection limit (less than 5 reads).

341 **Table 1.** Putative miRNA:mRNA target pairs and their relative expression patterns upon 3 h, 6 h and
 342 2 d of high light treatments. The first arrow corresponds to miRNA regulation and the second to the
 343 regulation of its target mRNA transcripts and the arrows represent the correlation expression as
 344 follows: \uparrow = upregulated, \downarrow = downregulated, $-$ = unchanged, \circ = undetected.

miRNA:mRNA pairs 3 h 6 h 2 d

↑↓	3	6	2
↑↑	0	4	5
↓↓	3	1	1
↑— or ↓—	18	34	36
↑○ or ↓○	104	253	131

345 On the basis of Araport annotation (V11; <https://araport.org/>) (Cheng et al., 2017), we observed 30
346 targets of DE miRNAs from all the four subgroups to be consistently present throughout the course of
347 high light treatment (**Supplementary Material 4, Table S8**). These mRNAs mainly encode
348 transcription factors and integral membrane proteins. We also examined the putative function of
349 miRNA targets that were specifically observed in each time point. At the 6 h time point we found
350 several pentatricopeptide repeat proteins (PPR), important for RNA maturation in various organelles,
351 tetratricopeptide repeat (TPR) proteins acting in signaling and organellar import, and S-adenosyl-L-
352 methionine-dependent methyltransferases superfamily proteins, necessary for epigenetic regulation of
353 gene expression. At the 2 d time point we found transcripts encoding auxin response factors, GRAS
354 family transcription factors and MYB domain proteins that are involved in transcriptional regulation
355 in response to stress. We detected an inverse correlation between 10 miRNAs and their putative targets,
356 for example, after 3 h of high light treatment we noticed upregulation of miR864-3p (FC = 3.65) and
357 downregulation of its predicted target *DARK INDUCIBLE 4* (*DIN4*, FC = -2.31) which is known to be
358 induced in darkness in *A. thaliana* (Fujiki et al., 2000) and suggests that miR864-3p represses *DIN4*
359 expression in high light. At the same time point, we found miR172b-3p to be upregulated (FC = 2.47)
360 and its putative target *hydroxysteroid dehydrogenase 3* (*HSD3*, FC = -2.05) to be downregulated. It is
361 known that plant cell membranes contain sterols that are synthesized by hydroxysteroid
362 dehydrogenases/decarboxylases (Kim et al., 2012) and that light stress has an impact on the
363 composition of sterols in the cell membranes (Kuczynska et al., 2019). After 6 h of high light treatment
364 we observed upregulation of miR156d-5p (FC = 2.42) and a concomitant downregulation of its target
365 transcript encoding the Squamosa promoter binding protein-like 3 (*SPL3*, FC = -2.14). A previous
366 study has shown that constitutive expression of miR156 extended the transition from the juvenile to
367 vegetative phase resulting in delayed flowering (Wu and Poethig, 2006). Thus, it is likely that high
368 light leads to an upregulation of miR156 and a concomitant downregulation of *SPL3* to delay flowering.
369 Another miRNA, miR171c-5p showed reduced expression levels (FC = -2.53) after 6 h of high light
370 treatment whereas its target encoding APS reductase 3 was upregulated (FC = 2.26). APS reductase is
371 the key enzyme of sulfate assimilation and was previously reported to increase in response to sugar
372 and light (Kopriva et al., 1999) suggesting a regulatory role of miR171c-5p in this process.
373 Additionally, after 6 h and 2 d of high light treatment, we observed a downregulation of miR395a and
374 an upregulation of its target transcript encoding cellulose synthase like G3 which is responsible for
375 producing the polysaccharide cellulose, the main component of the plant cell wall.

376 3.4 Gene ontology analysis of predicted miRNA targets

377 We used the David bioinformatics tool (Jiao et al., 2012) to perform gene ontology (GO) analysis for
378 the putative targets of DE high light responsive miRNAs to obtain information about the possible role
379 of the targets. Based on the three categories of GO biological processes, cellular component and

380 molecular function, an enrichment of GO terms for all time points was observed (Fisher's test with
 381 Benjamini-Hochberg corrected p-values) (**Figure 4, Supplementary Material 6, Table S12**). After 3
 382 h time point the significant biological processes included regulation of transcription (32) and
 383 transcription (30). Within the cellular component category, the highest number of targets were
 384 associated with the CCAAT-binding factor complex (8). Furthermore, in the molecular functions
 385 category, regulatory proteins involved in gene transcription such as TF activity, sequence-specific
 386 DNA binding (33) and DNA binding (31) were significantly overrepresented. After 6 h of high light
 387 treatment, miRNA targets were mainly involved in regulation of transcription (68), cell differentiation
 388 (38), salicylic acid response (11), methylation (9) and jasmonic acid response (7), and similar to the 3
 389 h time point indicating an enrichment of genes associated with transcriptional control. We also found
 390 methyltransferase activity (9) to be significantly enriched in the category molecular function suggesting
 391 epigenetic modifications and a potential role in secondary cell wall biogenesis. At the 2 d time point,
 392 we detected an enrichment of significant biological processes including regulation of transcription (61),
 393 cell differentiation (34), multicellular organism development (11) and jasmonic acid response (8).
 394 Thus, at all the three time points, genes encoding proteins involved in transcriptional reprogramming
 395 upon high light acclimation were enriched. The category cellular components showed a striking
 396 enrichment of targets associated with the nucleus (78 target genes) nicely matching the enrichment of
 397 transcription-related biological processes and molecular functions that points to massive changes in
 398 transcriptional regulation in response to high light acclimation (**Figure 4**).

399 3.5 DE sRNAs derived from various other RNA classes

400 The sRNA sequencing data was used to analyze miRNA regulation as well as to identify sRNAs
 401 derived from other RNA classes in response to high light providing links to their role in high light
 402 acclimation. After mapping the sRNA reads against publicly available reference databases (Jin et al.,
 403 2008; Zhang et al., 2012; Wang et al., 2014a; Yuan et al., 2015), we revealed a high number of DE
 404 sRNAs associated to lncRNAs, *trans*- and *cis*-NATs pairs, *TAS* and *PHAS* RNAs.

405 3.6 sRNAs derived from non-overlapping lncRNAs

406 Non-overlapping lncRNA transcripts, ≥ 200 nt in size, do not overlap with protein encoding or other
 407 non-coding transcripts. In our sRNA data 11 non-redundant non-overlapping lncRNA loci which
 408 produce DE sRNAs were determined and two of these 11 lncRNA loci give rise to upregulated sRNAs
 409 whereas the remaining 11 generate downregulated sRNAs upon high light (**Supplementary Material**
 410 **7, Table S13**). The transcript levels of the lncRNAs remained unchanged across all analyzed samples,
 411 but we observed DE sRNAs generated from these lncRNAs. We found 5, 5 and 1 lncRNA at 3 h, 6 h
 412 and 2 d time point after high light treatment, respectively, that produced DE sRNAs. We found
 413 differentially expressed 24 nt sRNAs derived from lncRNA *AT4G05135* and *AT3G05925* and 21 nt
 414 sRNAs produced from lncRNA *AT5G07325* after 3 h time point. At 6 h time point, lncRNA
 415 *AT3G26612*, *AT3G04485* and *AT4G04965* gave rise to differentially expressed 24 nt sRNAs and
 416 *AT5G04445* produced increased 21 nt sRNAs. We found one ncRNA *AT1G06797* that generated
 417 reduced levels of 24 nt sRNAs after 2 d of treatment. There were 4 sense strand (*AT2G14878*,
 418 *AT5G04445*, *AT3G26612*, *AT5G06045*) and 3 antisense strand lncRNA transcripts (*AT5G07565*,
 419 *AT5G07325*, *AT4G04965*) that produced DE sRNAs, and strand specificity was undetected for the
 420 remaining 4 lncRNA loci. Furthermore, since the lncRNAs do not overlap with any other gene and do
 421 not have any trans pairing partner, we speculate that the sense strand lncRNAs are converted into
 422 dsRNA by RNA dependent RNA polymerases in a primer independent manner. The lncRNA antisense
 423 transcripts also have a capability to form stem-loop fold back structures which can produce sRNAs.

424 3.7 sRNAs derived from natural antisense transcripts

425 The NAT pairs can form dsRNAs due to sequence complementarity and can arise from overlapping
 426 non-coding (nc) or protein coding (pc) genes. The transcript pairing is possible between pc-pc, nc-pc
 427 and nc-nc transcripts and the resulting paired transcript can be targeted by DCL enzymes to produce
 428 nat-siRNAs. The majority of *cis*- and *trans*-NAT pairs were produced from pc:pc or pc:nc transcript
 429 pairs. In case of pc:nc, the nc pairing partner mostly represents tRNA or TE derived transcripts which
 430 also have the capacity to produce sRNAs individually (Creasey et al., 2014; Martinez et al., 2017; Cho,
 431 2018). The pre-tRNA and TE-derived sRNAs could contribute to the regulation of a high light
 432 acclimation related network by regulating their own as well as other transcripts by sequence
 433 complementarity (Loss-Morais et al., 2013; Cho, 2018). We revealed that transcript pairs producing
 434 elevated levels of sRNAs can have different expression patterns. We observed abundant transcript pairs
 435 that generate differentially expressed nat-siRNAs, but the transcripts were either undetected or
 436 unchanged in the mRNA data. We further identified pairs of transcripts where one transcript is
 437 regulated and the other remains unchanged, anticorrelated pairs with one transcript up- and the other
 438 transcript downregulated, and pairs showing the same changes in expression (both transcripts either
 439 upregulated or down regulated).

440 3.8 *cis*-nat-siRNAs

441 We found 56, 25 and 24 *cis*-NATs loci (90 non-redundant pairs) at 3 h, 6 h and 2 d, respectively, that
 442 produced DE *cis*-nat-siRNAs from two overlapping transcripts. We detected 7, 3 and 2 loci at 3 h, 6 h
 443 and 2 d, respectively, where one of the transcripts was either up- or downregulated and the other one
 444 remained unchanged (**Table 3**). At 3 h time point, we observed that all the 7 loci encoding pc:pc
 445 transcripts reduced the production of sRNAs with at least two-fold decrease in one of their parent
 446 transcripts. The decrease in one of the parent transcripts and thus the sRNAs could be due to transient
 447 changes in response to high light stress (**Supplementary Material 7, Table S14**). We detected 49, 21
 448 and 20 *cis*-NATs (76 non-redundant pairs) at 3 h, 6 h and 2 d time point, respectively, that produced
 449 DE sRNAs from cognate overlapping transcripts that remained unchanged or were undetectable
 450 (**Supplementary Material 7, Table S14**). At the 6 h time point, we observed upregulation of sRNAs
 451 from a *cis*-NAT transcript pair where one of the pairing transcripts encoding NUCLEOLIN LIKE 1
 452 was upregulated. This gene was also shown to be upregulated by salt stress and to play a role in
 453 ribosome biogenesis (Huang et al., 2018). We detected another transcript pair with reduced nat-siRNA
 454 production where one transcript encoding the ARABIDOPSIS HOMOLOGUE OF YEAST BRX1-1
 455 (AT3G15460) was upregulated and the other transcript encoding an aluminum induced protein with
 456 YGL and LRDR motifs (AT3G15450) was downregulated. It has been shown that AT3G15450 is
 457 regulated by ABA since an ABA hypersensitive mutant (*ahg2-1*) shows reduced levels of this gene in
 458 response to high light stress (Nishimura et al., 2005; Valdivieso et al., 2009). After 2 d of high light
 459 stress, we found two gene pairs generating elevated levels of nat-siRNAs where the pairing transcripts
 460 were also upregulated. In each pair, one transcript encodes a lncRNA (AT3G51238 and AT5G01595)
 461 and the other encodes flavanone 3-hydroxylase (AT3G51240) and FERRETIN 1 (AT5G01600),
 462 respectively. The upregulation of *flavanone 3-hydroxylase* is associated to the biosynthesis of
 463 flavonoids where it catalyzes the conversion of flavanones to dihydroflavonols whereas *FERRETIN 1*
 464 plays a role in iron homeostasis (Pelletier and Shirley, 1996; Briat et al., 2010). At the same time point,
 465 we found upregulated nat-siRNAs derived from two gene pairs where one transcript was upregulated
 466 and the other remained unchanged. Interestingly, the upregulated transcripts of these pairs encode for
 467 chalcone synthase (AT5G13930) known to be the rate-limiting enzyme involved in flavonoid synthesis
 468 (Fuglevand et al., 1996) and a MULTIDRUG RESISTANCE-ASSOCIATED PROTEIN 2
 469 (AT2G34660) which was shown to assist in vacuolar transport of anthocyanins and flavonoids
 470 (Behrens et al., 2019). This suggests a possible involvement of nat-siRNAs in regulation of these

471 transcripts in biosynthesis and transport of flavonoids which could play a major role in protection of
472 plant against high light stress.

473 3.9 trans-nat-siRNAs

474 We found 17 non-redundant *trans*-NAT pairs (0, 12 and 5 at 3 h, 6 h and 2 d, respectively) producing
475 differentially expressed *trans*-nat-siRNA. In this case, transcripts can produce sRNAs from their
476 overlapping region or from the single stranded region when partially overlapped. We observed 40, 124
477 and 52 (84 non-redundant loci) *trans*-NATs gene pairs at 3 h, 6 h and 2 d, respectively, that promote
478 DE *trans*-nat-siRNAs from the overlapping region of two transcripts having unchanged transcript
479 levels or levels below the detection limit (**Supplementary Material 7, Table S15**). We observed 3, 5
480 and 3 *trans*-NAT pairs comprising overlapping pc:pc transcripts that generate DE *trans*-nat-siRNAs.
481 The majority of the *trans*-NAT gene pairs comprise a nc transcript partner encoding a pre-tRNA or
482 RNA derived from a TE. Apart from the pc:pc pairs at 3 h, 6 h and 2 d time point, we found 34, 124
483 and 44 transcript pairs generating DE *trans*-nat-siRNAs which are comprised of one transcript
484 encoding a pre-tRNA and 7, 13 and 4 pairs where one of the transcripts is encoded by a TE transcript.
485 The profiling of *trans*-nat-siRNAs over time revealed that the highest number of DE *trans*-nat-siRNAs
486 were found after 6 h proposing the involvement of *trans*-nat-siRNA in modulating gene expression
487 during early stages of high light acclimation.

488 3.10 ta-siRNAs

489 After 2 d of high light treatment, we observed an upregulation of ta-siRNAs derived from the *TAS4*
490 precursor (**Supplementary Material 7, Table S15**) that requires miR828-mediated cleavage prior to
491 ta-siRNA biogenesis (Rajagopalan et al., 2006).

492 In response to sugar accumulation, *TAS4* expression is regulated through a signaling pathway involving
493 PRODUCTION OF ANTHOCYANIN PIGMENT 1 (PAP1) (Luo et al., 2012). The *TAS4* derived ta-
494 siRNAs are capable of targeting mRNAs encoding MYB transcription factors such as PAP1 and PAP2
495 which regulate the anthocyanin biosynthesis pathway. *MIR828* overexpression lines showed reduced
496 anthocyanin accumulation since miR828 is also known to target *PAP1* (Yang et al., 2013). We found
497 increasing levels of miR828 (FC = 20.9), *TAS4* transcript (AT3G25795, FC = 3.27), *ta-siRNAs* (FC =
498 6.32), *PAP1* (AT1G56650, FC = 5.20), *PAP2* (AT1G66390, FC = 6.77), and ELONGATED
499 HYPOCOTYL 5 (*HY5*, AT5G11260, FC = 1.67) that all play a role in anthocyanin biosynthesis. In
500 addition to the altered expression of these regulators, we also found increased amounts of downstream
501 anthocyanin biosynthetic enzymes i.e. DIHYDROFLAVONOL 4-REDUCTASE (*DFR*, AT5G42800,
502 FC = 12.1), CHALCONE SYNTHASE (*CHS*, AT5G13930, FC = 5.16) and ANTHOCYANIDIN
503 SYNTHASE (*ANS*, AT4G22880, FC = 14.7) (see also discussion, Fig 5). According to our sequencing
504 data, we can provide evidence that the regulation of the *PAP1* transcript in response to high light stress
505 is mediated by miR828 and *HY5*. The consequent increase in the components of the anthocyanin
506 biosynthetic pathway is likely to maintain the increased levels of anthocyanin production required to
507 protect plants from high light.

508 4 Discussion

509 Transcriptome studies by mRNA and sRNA sequencing in response to high light stress and white light,
510 respectively, have been conducted in several plant species, whereas a global transcriptome analysis of
511 sRNAs in response to high light acclimation has not been performed yet. Our study aims to provide
512 insights into the high light-responsive regulation of different classes of sRNAs and their effects on the
513 modulation of gene expression. We performed sRNA sequencing along with mRNA and lncRNA

514 sequencing from the same RNA samples to associate changes in target transcripts (mRNA/lncRNA)
 515 steady state levels to changes in sRNA repertoire upon high light. Over the time course of high light
 516 treatment, the number of DE sRNAs from all different classes showed a gradual increase during the
 517 early stages (3 h and 6 h) of high light treatment and a reduction after 2 d. We analyzed the miRNAs
 518 which are known to be important regulators of gene expression in eukaryotes and detected 92 DE
 519 miRNAs over the course of high light treatment and out of these, 44 DE miRNAs were shown before
 520 to be responsive to UV-B, white light or red light in *A. thaliana* (Bonnet et al., 2004; Zhang et al.,
 521 2006; Zhou et al., 2007; Pelaez et al., 2012; Shikata et al., 2014). To determine the impact of DE
 522 miRNAs on the transcriptome of *A. thaliana* we investigated their targets predicted by the
 523 psRNATarget tool and found 128, 298 and 175 potential miRNA:mRNA target pairs at 3 h, 6 h and 2
 524 d time point, respectively. The high number of putative miRNA targets at the early time points reflect
 525 the importance of miRNAs in regulating the gene expression at the initial stages of the high light
 526 treatment. At early time points, we observed targets encoding PPR and TPR proteins which could lead
 527 to alterations in the process of RNA maturation, stress signaling and organellar transport. The miRNA
 528 targets also include members of the S-adenosyl-L-methionine-dependent methyltransferase
 529 superfamily proteins indicating a possible epigenetic regulation of gene expression in response to high
 530 light. GO analysis revealed a large number of putative targets encoding transcription factors such as
 531 MYB, squamosa promoter binding proteins (SPBs), Teosinte Branched 1, Cycloidea, members of the
 532 PCF (TCP) TF family and members of the Homeodomain-like superfamily. The enrichment of these
 533 TFs clearly indicates their involvement in high light-induced regulation of gene expression. Studies on
 534 high light and salinity stress in *A. thaliana* have shown that MYB TFs are principal regulators of
 535 flavonoid biosynthesis. MYB112 was found to be induced by high light stress and to regulate
 536 anthocyanin biosynthesis. It mediates activation of *PAP1*, *MYB7* and *MYB32*, but downregulates
 537 *MYB12* and *MYB111* which are involved in the control of the flavonoid pathway, however the
 538 mechanism of this negative control has not been fully elucidated (Lotkowska et al., 2015). It can be
 539 hypothesized that the *MYB* transcripts targeted by miRNAs in our study are directly or indirectly
 540 involved in the regulation of anthocyanin biosynthesis to protect the plant against high light. Plants
 541 also require the crosstalk between phytohormones such as jasmonic acid (JA) and salicylic acid (SA)
 542 to acclimate to high light (Mateo et al., 2006; Balfagon et al., 2019). Studies in wheat and barley
 543 subjected to UV-B stress in the presence of exogenous JA reported an increased antioxidant signaling,
 544 enhanced proline levels and elevated ROS scavenging capabilities (Fedina et al., 2009; Liu et al., 2012).
 545 Similarly, the role of SA in response to high light and its role in redox homeostasis was elucidated in
 546 *A. thaliana* (Mateo et al., 2006). Our GO analysis for DE mRNAs revealed an enrichment of genes
 547 expressed in response to SA which may be involved in in the maintenance of redox homeostasis as
 548 well as protection of PSII and improvement of the photosynthetic capacity upon high light (Herrera-
 549 Vasquez et al., 2015; Chen et al., 2020). We also noticed an enrichment of *SPLs* which are known to
 550 be targeted by miR156/miR157 isoforms. miR156-*SPLs* affect the anthocyanin biosynthesis pathway
 551 and control development in stress conditions (Cui et al., 2014). After 6 h of high light treatment, we
 552 observed an upregulation of miR156d-5p and a concomitant downregulation of its target *SPL3*.
 553 Constitutive overexpression of miR156 caused an extended juvenile phase and delayed flowering (Wu
 554 and Poethig, 2006). On the other hand, it was shown that upregulation of *SPL3* leads to increased levels
 555 of *LEAFY (LFY)*, *FRUITFULL (FUL)*, and *APETALA1 (API)* all encoding TFs that promote flowering
 556 (Yamaguchi et al., 2009). Our results suggest that high light causes upregulation of miR156 that
 557 mediates downregulation of its cognate target *SPL3* to inhibit flowering under stress conditions.

558 After 6 h of treatment, miR171c-5p levels were reduced and associated with the upregulation of its
 559 target *APS reductase 3*. This enzyme was found in high amounts after 4 h of light treatment and when
 560 supplemented with 0.5% sucrose, its amount increased seven-fold (Kopriva et al., 1999). It is also
 561 known that continuous light treatments lead to increased sugar levels (Haque et al., 2015; Chen et al.,

2019) which could enhance the *APS reductase* expression. Studies have shown that APS reductase is needed to synthesize additional cysteine required for glutathione biosynthesis. During oxidative stress in *A. thaliana*, the amount of oxidized glutathione increases and the reduced form of glutathione decreases which drives the expression of *APS reductase* (Leustek, 2002). Considering the impact of enhanced oxidative stress during high light stress, our data point to an important role of miR171c-5p in the control of *APS3 reductase* transcript levels to promote the production of reduced glutathione.

At the same time point, the upregulation of miR163 led to downregulation of one of its target transcripts coding for a S-adenosyl-L-methionine-dependent methyltransferases superfamily protein (AT1G15125). It is known that SAM dependent carboxyl methyltransferases are a family of plant enzymes that act on a variety of substrates such as salicylic acid, jasmonic acid and 7-methylxanthine to produce their methyl compounds (Ross et al., 1999). In conditions of high light stress, it is likely that the plant maintains its levels of SA and JA by reducing the levels of methyltransferases that could be necessary for defense and development (Kemal Kazan and Manners, 2011; Svyatyna and Riemann, 2012; Khan et al., 2015). After 6 h and 2 d of treatment, miR395a was downregulated accompanied by elevated levels of one of its putative targets encoding cellulose synthase like G3. A previous study revealed differential regulation of this transcript in *cry1* mutants subjected to blue light (Folta et al., 2003) and in *phyB* mutants exposed to continuous monochromatic red light (Tepperman et al., 2004). Light receptors such as *cry1* and *phyB* perceive light and mediate growth control with the help of cellulose synthase which is involved in maintaining the strength and composition of cell walls (Bischoff et al., 2011; Le Gall et al., 2015). The upregulation of this transcript (6 h and 2 d) in response to high light treatment may lead to increased mechanical strength to withstand elevated turgor pressure. This hypothesis is supported by mutants that are defective in cellulose synthase like genes displaying an enhanced sensitivity to salt stress (Wang et al., 2016; Zhang et al., 2016).

We further investigated sRNAs derived from lncRNA, *cis*- and *trans*-NATs, *TAS* and *PHAS* RNAs. We found 11 non-redundant, non-overlapping lncRNAs which produced DE sRNAs during the course of high light treatment. The transcripts of all lncRNAs were undetectable in the sequencing data and two lncRNAs showed increased production of sRNAs. A study in rice may explain these observations where *Psi-LDMAR* siRNAs generated from the lncRNA *Long day specific male fertility associated RNA (LDMAR)* were able to downregulate the *LDMAR* transcript through RNA-dependent DNA methylation (RdDM) (Ding et al., 2012). Out of 11, the remaining 9 lncRNAs led to decreased sRNA production in high light samples compared to their respective controls and we speculate that the steady state levels of parent transcripts were maintained by the siRNAs.

We also found 90 non-redundant *cis*-NATs pairs and 104 *trans*-NATs pairs that led to the production of differentially expressed nat-siRNA over the time course of high light treatment. We detected 45 pc:pc and 45 pc:nc non-redundant *cis*-nat-siRNA producing loci, and 10 pc:pc and 94 pc:nc non-redundant *trans*-nat-siRNA producing loci. After 6 h of treatment, we observed *cis*-nat-siRNAs being produced from two pairing transcripts. The transcript encoding *NUCLEOLIN LIKE 1* was upregulated and *glycosyl hydrolase 9C1* transcript levels remained unchanged. Salt stress causes elevated *NUCLEOLIN LIKE 1* transcript levels pointing to its role in rRNA processing during salt stress adaptation (Huang et al., 2018). It has been demonstrated that stress affected plants show altered ribosome biogenesis (Huang et al., 2016; Palm et al., 2019). Similar results were obtained in our data indicating an involvement of this gene in response to high light treatment. Another *cis*-NATs pair reduced the production of nat-siRNAs. While the upregulated transcript encodes for ARABIDOPSIS HOMOLOGUE OF YEAST BRX1-1 (AT3G15460) that plays a role in the maturation of the large ribosomal subunit and facilitates pre-rRNA processing, its pairing transcript encoding aluminum induced protein with YGL and LRDR motifs (AT3G15450) was reduced. Studies have shown that

608 AT3G15450 is an auxin responsive transcript that was found to be downregulated by drought stress
 609 (Huang et al., 2008). Its downregulation is also observed in high light treatment, but the significance
 610 of its repression in stress remains unknown. After 2 d of high light treatment, lncRNA AT3G51238
 611 and AT5G01595 paired with a transcript encoding flavanone 3-hydroxylase (AT3G51240) and
 612 FERRETIN 1 (AT5G01600), respectively. Both pairing transcripts as well as the deriving nat-siRNAs
 613 were upregulated. It can be speculated that the upregulation of these transcripts is necessary for high
 614 light acclimation since flavanone 3-hydroxylase is known to promote flavonoid accumulation in high
 615 light (Pelletier and Shirley, 1996) and FERRETIN 1 is known to increase the photosynthetic
 616 performance of plants in response to oxidative stress (Briat et al., 2010). The upregulated levels of nat-
 617 siRNAs could be responsible for maintaining steady state levels of the parent transcripts produced in
 618 response to high light treatment. This may occur by maintaining an equilibrium between the rate of
 619 transcription of the parent transcripts and the rate of subsequent nat-siRNAs generation. The *trans*-nat-
 620 siRNAs were mostly produced from pc:nc transcript pairs with pre-tRNAs being the most prominent
 621 nc pairing partner. Studies have shown how sRNAs derived from tRNAs and mRNAs can regulate
 622 post-transcriptional gene expression (Garsin, 2016). At all the three time points, we found nat-siRNAs
 623 produced from single stranded regions of partially overlapping transcripts as well as from the double
 624 stranded regions of completely overlapping transcripts. The second most abundant nc pairing partner
 625 that led to differentially expressed *trans*-nat-siRNA were TE derived RNAs. TEs have the potential to
 626 mobilize and induce mutations in the host genome. Thus, plants have evolved special mechanisms to
 627 control the expression of TEs which are based on RNA silencing and chromatin modifications (Slotkin
 628 and Martienssen, 2007). Studies have confirmed that tRNA derived sRNAs can target endogenous TE
 629 (Martinez et al., 2017) and target other non-TE targets (Creasey et al., 2014; Cho, 2018).

630 We also detected differentially expressed genes and sRNAs that might regulate anthocyanin
 631 biosynthesis under high light conditions (**Figure 5**). For example, miR828 seems to be involved in two
 632 pathways regulating *PAP1* transcripts. In the indirect pathway, that was elucidated in sugar treated
 633 plants, miR828 triggers the production of *TAS4* derived ta-siRNAs which target and negatively control
 634 *MYB* transcription factors including *PAP1* and *PAP2* resulting in reduced anthocyanin production (Luo
 635 et al., 2012). In addition, in the direct pathway, miR828 is able to directly target the *PAP1* transcript
 636 and its overexpression causes reduced *PAP1* transcript levels and represses anthocyanin biogenesis
 637 (Yang et al., 2013). Moreover, we observed upregulation of *HY5* encoding a transcriptional regulator
 638 that enhances *PAP1* transcription by binding to G- and ACE-boxes in the *PAP1* promoter. In support
 639 of this positive regulation of *PAP1* by *HY5* and an anticipated increase in anthocyanin production, we
 640 observed increasing transcript levels of downstream genes encoding enzymes such as *DFR*, *CHS* and
 641 *ANS* that act in the anthocyanin biosynthetic pathway. Apart from its role in the sugar and high light
 642 response, miR828 is also known to trigger the production of *TAS4* derived ta-siRNAs in response to Pi
 643 deficiency (Hsieh et al., 2009). We found more than two-fold upregulation of members acting in the
 644 regulation of anthocyanin production: miR828, *TAS4* transcript, *TAS4*-derived ta-siRNAs, *PAP1* and
 645 *PAP2*, *HY5*, *DFR*, *CHS* and *ANS*. Taken together, our results support previously reported studies (Luo
 646 et al., 2012; Yang et al., 2013; Hsieh et al., 2009) and expand the current knowledge on regulatory
 647 components of the anthocyanin biosynthetic pathway by the identification of *HY5* and *PAP1* that may
 648 lead to elevated anthocyanin levels in response to high light.

649 Consequently, the proposed model for anthocyanin biosynthesis as well as the high number of
 650 identified miRNAs, sRNAs derived from *cis*- and *trans*-NAT gene pairs and from lncRNAs provide a
 651 fundamental base to elucidate sRNA-controlled gene regulatory networks underlying molecular
 652 adaptations of high light induced acclimation responses.

653 5 Data Availability Statement

654 The raw Illumina sRNA and mRNA sequencing data is deposited in NCBI SRA database with the ID
655 PRJNA653584. All raw data used for the analyses in this study is available for reviewers at

656 <https://dataview.ncbi.nlm.nih.gov/object/PRJNA653584?reviewer=pdhcbecm4g2ufc5pguk4f1hk2>

657 The original contributions presented in the study are included in the article/Supplementary Material,
658 further inquiries can be directed to the corresponding authors.

659 **6 Author Contributions**

660 WF designed the research; BT performed the research with the help of MAA and KH; BT, MAA, KH,
661 OT and WF analyzed the data; and BT, OT and WF wrote the paper. All authors read and approved
662 the final manuscript.

663 **7 Funding**

664 The funding for the research conducted was provided by the German Research Foundation (SFB-TRR
665 175, grants to W.F. project C03). The Funding body was not involved in the design of the study and
666 analysis or interpretation of the data and in writing of the manuscript.

667 **8 Conflict of Interest**

668 The authors declare that they have no competing interests.

669 **9 Supplementary Material**

670 **Supplementary Material 1: Table S1.** List of stem loop qPCR oligonucleotides used in this study.

671 **Supplementary Material 2: Table S2.** Mapped mRNA sequencing reads after adapter trimming in
672 control and high light treated samples (biological triplicates). **Table S3.** Mapped sRNA sequencing
673 reads from specific sRNA producing RNA classes in control and high light treated samples. **Table S4.**
674 The size distribution of sRNAs (reads per million) from control and high light treated samples after
675 adapter trimming.

676 **Supplementary Material 3: Table S5.** DE miRNAs upon 3 h, 6 h and 2 d of high light acclimation,
677 respectively. Evolutionarily conserved miRNA families are highlighted in orange. **Table S6.**
678 Normalized read counts and FC of all miRNAs upon 3 h, 6 h and 2 d of high light acclimation,
679 respectively. **Table S7.** High light-responsive DE miRNAs in *Arabidopsis*. MiRNAs were classified
680 as DE miRNAs when $\log_2FC \geq 1$ & ≤ -1 (Benjamini-Hochberg corrected p-value ≤ 0.05).

681 **Supplementary Material 4: Table S8.** Targets of all DE miRNAs at the three time points predicted
682 using psRNATarget Analysis Server. N/A = No significant fold change. **Table S9.** ncRNA targets of
683 all DE miRNAs at three time points predicted using psRNATarget Analysis Server. N/A = No
684 significant fold change.

685 **Supplementary Material 5: Table S10.** All mRNAs and their normalized read counts (triplicates)
686 acquired from mRNA sequencing data of control and high light treated samples at 3 h, 6 h and 2 d.
687 **Table S11.** Detailed list of all DE mRNAs acquired from mRNA sequencing data (control and 3h, 6 h
688 and 2d of high light treated samples).

689 **Supplementary Material 6: Table S12.** Gene Ontology term enrichment analysis for putative targets
690 of DE miRNAs after 3 h, 6 h and 2 d of high light acclimation.

691 **Supplementary Material 7: Table S13.** DE sRNAs derived from non-overlapping lncRNAs. The
692 sRNA and lncRNA sequencing data at different time points are shown in the sub-tables. **Table S14.**
693 DE sRNAs generated from *cis*-NAT pairs. The sRNA and *cis*-NAT sequencing data at different time
694 points are shown in the sub-tables. **Table S15.** DE sRNAs generated from *trans*-NAT pairs. The sRNA
695 and *trans*-NAT sequencing data at different time points are shown in the sub-tables. **Table S16.** DE
696 sRNAs generated from *TAS* transcripts. The sRNA and *trans*-NAT sequencing data at different time
697 points are shown in the sub-tables.

698 10 References

- 699 Afgan, E., Baker, D., Van Den Beek, M., Blankenberg, D., Bouvier, D., Cech, M., Chilton, J., Clements, D., Coraor, N., Eberhard, C.,
700 Gruning, B., Guerler, A., Hillman-Jackson, J., Von Kuster, G., Rasche, E., Soranzo, N., Turaga, N., Taylor, J., Nekrutenko,
701 A., and Goecks, J. (2016). The Galaxy platform for accessible, reproducible and collaborative biomedical analyses: 2016
702 update. *Nucleic Acids Res* 44, W3-W10. doi:10.1093/nar/gkw343
- 703 Apel, K., and Hirt, H. (2004). Reactive oxygen species: metabolism, oxidative stress, and signal transduction. *Annu Rev Plant Biol* 55,
704 373-399. doi:10.1146/annurev.arplant.55.031903.141701
- 705 Aukerman, M.J., and Sakai, H. (2003). Regulation of flowering time and floral organ identity by a MicroRNA and its APETALA2-like
706 target genes. *Plant Cell* 15, 2730-2741. doi:10.1105/tpc.016238
- 707 Axtell, M.J. (2013). ShortStack: comprehensive annotation and quantification of small RNA genes. *RNA* 19, 740-751.
708 doi:10.1261/rna.035279.112
- 709 Balfagon, D., Sengupta, S., Gomez-Cadenas, A., Fritschi, F.B., Azad, R.K., Mittler, R., and Zandalinas, S.I. (2019). Jasmonic acid is
710 required for plant acclimation to a combination of high light and heat stress. *Plant Physiol* 181, 1668-1682.
711 doi:10.1104/pp.19.00956
- 712 Bartel, D.P. (2004). MicroRNAs: Genomics, biogenesis, mechanism, and function. *Cell* 116, 281-297.
- 713 Behrens, C.E., Smith, K.E., Iancu, C.V., Choe, J.Y., and Dean, J.V. (2019). Transport of anthocyanins and other flavonoids by the
714 Arabidopsis ATP-binding cassette transporter AtABCC2. *Sci Rep* 9, 437. doi:10.1038/s41598-018-37504-8
- 715 Bellafiore, S., Barneche, F., Peltier, G., and Rochaix, J.D. (2005). State transitions and light adaptation require chloroplast thylakoid
716 protein kinase STN7. *Nature* 433, 892-895. doi:10.1038/nature03286
- 717 Bin Yu, Zhiyong Yang, Junjie Li, Svetlana Minakhina, Maocheng Yang, Richard W. Padgett, Ruth Steward, and Chen, X. (2005).
718 Methylation as a crucial step in plant microRNA biogenesis. *Science* 307, 932-935. doi:10.1126/science.1107130
- 719 Birben, E., Sahiner, U.M., Sackesen, C., Erzurum, S., and Kalayci, O. (2012). Oxidative stress and antioxidant defense. *World Allergy*
720 *Organ J* 5, 9-19. doi:10.1097/WOX.0b013e3182439613
- 721 Bischoff, V., Desprez, T., Mouille, G., Vernhettes, S., Gonneau, M., and Hofte, H. (2011). Phytochrome regulation of cellulose synthesis
722 in Arabidopsis. *Curr Biol* 21, 1822-1827. doi:10.1016/j.cub.2011.09.026
- 723 Bonnet, E., Wuyts, J., Rouze, P., and Van De Peer, Y. (2004). Detection of 91 potential conserved plant microRNAs in *Arabidopsis*
724 *thaliana* and *Oryza sativa* identifies important target genes. *Proc Natl Acad Sci USA* 101, 11511-11516.
725 doi:10.1073/pnas.0404025101
- 726 Borsani, O., Zhu, J., Verslues, P.E., Sunkar, R., and Zhu, J.K. (2005). Endogenous siRNAs derived from a pair of natural cis-antisense
727 transcripts regulate salt tolerance in *Arabidopsis*. *Cell* 123, 1279-1291. doi:10.1016/j.cell.2005.11.035
- 728 Briat, J.F., Ravet, K., Arnaud, N., Duc, C., Boucherez, J., Touraine, B., Cellier, F., and Gaymard, F. (2010). New insights into ferritin
729 synthesis and function highlight a link between iron homeostasis and oxidative stress in plants. *Ann Bot* 105, 811-822.
730 doi:10.1093/aob/mcp128
- 731 Brodersen, P., Sakvarelidze-Achard, L., Bruun-Rasmussen, M., Dunoyer, P., Yamamoto, Y.Y., Sieburth, L., and Voinnet, O. (2008).
732 Widespread translational inhibition by plant miRNAs and siRNAs. *Science* 320, 1185-1190. doi:10.1126/science.1159151
- 733 Casadevall, R., Rodriguez, R.E., Debernardi, J.M., Palatnik, J.F., and Casati, P. (2013). Repression of growth regulating factors by the
734 microRNA396 inhibits cell proliferation by UV-B radiation in Arabidopsis leaves. *Plant Cell* 25, 3570-3583.
735 doi:10.1105/tpc.113.117473
- 736 Casati, P. (2013). Analysis of UV-B regulated miRNAs and their targets in maize leaves. *Plant Signal Behav* 8(10), e26758.
737 doi:10.4161/psb.26758
- 738 Chen, X.L., Wang, L.C., Li, T., Yang, Q.C., and Guo, W.Z. (2019). Sugar accumulation and growth of lettuce exposed to different
739 lighting modes of red and blue LED light. *Sci Rep* 9, 6926. doi:10.1038/s41598-019-43498-8
- 740 Chen, Y.E., Mao, H.T., Wu, N., Mohi Ud Din, A., Khan, A., Zhang, H.Y., and Yuan, S. (2020). Salicylic acid protects photosystem II
741 by alleviating photoinhibition in *Arabidopsis thaliana* under high light. *International Journal of Molecular Sciences* 21(4),
742 1229. doi:10.3390/ijms21041229
- 743 Cheng, C.Y., Krishnakumar, V., Chan, A.P., Thibaud-Nissen, F., Schobel, S., and Town, C.D. (2017). Araport11: a complete
744 reannotation of the Arabidopsis thaliana reference genome. *Plant J* 89, 789-804. doi:10.1111/tbj.13415
- 745 Cho, J. (2018). Transposon-derived non-coding RNAs and their function in plants. *Front Plant Sci* 9, 600. doi:10.3389/fpls.2018.00600

- 746 Chung, P.J., Park, B.S., Wang, H., Liu, J., Jang, I.C., and Chua, N.H. (2016). Light-inducible mir163 targets PXMT1 transcripts to
747 promote seed germination and primary root elongation in *Arabidopsis*. *Plant Physiol* 170, 1772-1782. doi:10.1104/pp.15.01188
- 748 Clarke, J.E., and Johnson, G.N. (2001). In vivo temperature dependence of cyclic and pseudocyclic electron transport in barley. *Planta*
749 212, 808-816. doi:10.1007/s004250000432
- 750 Cornic, G., Bukhov, G.N., Wiese, C., Bligny, R., and Heber, U. (2000). Flexible coupling between light-dependent electron and vectorial
751 proton transport in illuminated leaves of C3 plants. Role of photosystem I-dependent proton pumping. *Planta* 210, 468-477.
- 752 Creasey, K.M., Zhai, J., Borges, F., Van Ex, F., Regulski, M., Meyers, B.C., and Martienssen, R.A. (2014). miRNAs trigger widespread
753 epigenetically activated siRNAs from transposons in *Arabidopsis*. *Nature* 508, 411-415. doi:10.1038/nature13069
- 754 Cui, L.G., Shan, J.X., Shi, M., Gao, J.P., and Lin, H.X. (2014). The miR156-SPL9-DFR pathway coordinates the relationship between
755 development and abiotic stress tolerance in plants. *Plant J* 80, 1108-1117. doi:10.1111/tpj.12712
- 756 Dai, X., Zhuang, Z., and Zhao, P.X. (2018). psRNATarget: a plant small RNA target analysis server (2017 release). *Nucleic Acids Res*
757 46, W49-W54. doi:10.1093/nar/gky316
- 758 Demmig, B., Winter, K., Kruger, A., and Czygan, F.C. (1987). Photoinhibition and zeaxanthin formation in intact leaves : a possible role
759 of the xanthophyll cycle in the dissipation of excess light energy. *Plant Physiol* 84, 218-224. doi:10.1104/pp.84.2.218
- 760 Ding, J., Shen, J., Mao, H., Xie, W., Li, X., and Zhang, Q. (2012). RNA-directed DNA methylation is involved in regulating photoperiod-
761 sensitive male sterility in rice. *Molecular Plant* 5, 1210-1216.
- 762 Estavillo, G.M., Crisp, P.A., Pornsiriwong, W., Wirtz, M., Collinge, D., Carrie, C., Giraud, E., Whelan, J., David, P., Javot, H., Brearley,
763 C., Hell, R., Marin, E., and Pogson, B.J. (2011). Evidence for a SAL1-PAP chloroplast retrograde pathway that functions in
764 drought and high light signaling in *Arabidopsis*. *Plant Cell* 23, 3992-4012. doi:10.1105/tpc.111.091033
- 765 Fedina, I., Nedeva, D., Georgieva, K., and Velitchkova, M. (2009). Methyl jasmonate counteract UV-B Stress in barley seedlings. *Journal*
766 *of Agronomy and Crop Science* 195, 204-212.
- 767 Fei, Q., Xia, R., and Meyers, B.C. (2013). Phased, secondary, small interfering RNAs in posttranscriptional regulatory networks. *Plant*
768 *Cell* 25, 2400-2415. doi:10.1105/tpc.113.114652
- 769 Folta, K.M., Pontin, M.A., Karlin-Neumann, G., Bottini, R., and Spalding, E.P. (2003). Genomic and physiological studies of early
770 cryptochrome 1 action demonstrate roles for auxin and gibberellin in the control of hypocotyl growth by blue light. *Plant J* 36,
771 203-214. doi:10.1046/j.1365-313x.2003.01870.x
- 772 Fuglevand, G., Jackson, J.A., and Jenkins, G.I. (1996). UV-B, UV-A, and blue light signal transduction pathways interact synergistically
773 to regulate chalcone synthase gene expression in *Arabidopsis*. *Plant Cell* 8, 2347-2357. doi:10.1105/tpc.8.12.2347
- 774 Fujiki, Y., Ito, M., Nishida, I., and Watanabe, A. (2000). Multiple signaling pathways in gene expression during sugar starvation.
775 Pharmacological analysis of din gene expression in suspension-cultured cells of *Arabidopsis*. *Plant Physiol* 124, 1139-1148.
776 doi:10.1104/pp.124.3.1139
- 777 Garcia-Molina, A., Kleiné, T., Schneider, K., Muhlhaus, T., Lehmann, M., and Leister, D. (2020). Translational Components Contribute
778 to Acclimation Responses to High Light, Heat, and Cold in *Arabidopsis*. *iScience* 23, 101331. doi:10.1016/j.isci.2020.101331
- 779 Garsin, N.R.D.L.a.D.A. (2016). The unmasking of "junk" RNA reveals novel sRNAs: from processed RNA fragments to marooned
780 riboswitches. *Curr Opin Microbiol*. doi: 10.1016/j.mib.2015.12.006, 16-21. doi:doi: 10.1016/j.mib.2015.12.006
- 781 Gou, J.Y., Felippes, F.F., Liu, C.J., Weigel, D., and Wang, J.W. (2011). Negative regulation of anthocyanin biosynthesis in *Arabidopsis*
782 by a miR156-targeted SPL transcription factor. *Plant Cell* 23, 1512-1522. doi:10.1105/tpc.111.084525
- 783 Hackenberg, M., Shi, B.J., Gustafson, P., and Langridge, P. (2013). Characterization of phosphorus-regulated miR399 and miR827 and
784 their isomirs in barley under phosphorus-sufficient and phosphorus-deficient conditions. *BMC Plant Biol* 13, 214.
785 doi:10.1186/1471-2229-13-214
- 786 Haque, M.S., Kjaer, K.H., Rosenqvist, E., and Ottosen, C.O. (2015). Continuous light increases growth, daily carbon gain, antioxidants,
787 and alters carbohydrate metabolism in a cultivated and a wild tomato species. *Front Plant Sci* 6, 522.
788 doi:10.3389/fpls.2015.00522
- 789 Henriques, R., Wang, H., Liu, J., Boix, M., Huang, L.F., and Chua, N.H. (2017). The antiphasic regulatory module comprising CDF5
790 and its antisense RNA FLORE links the circadian clock to photoperiodic flowering. *New Phytologist* 216, 854-867.
791 doi:10.1111/nph.14703
- 792 Herrera-Vasquez, A., Salinas, P., and Holuigue, L. (2015). Salicylic acid and reactive oxygen species interplay in the transcriptional
793 control of defense genes expression. *Front Plant Sci* 6, 171. doi:10.3389/fpls.2015.00171
- 794 Howell, M.D., Fahlgren, N., Chapman, E.J., Cumbie, J.S., Sullivan, C.M., Givan, S.A., Kasschau, K.D., and Carrington, J.C. (2007).
795 Genome-wide analysis of the RNA-DEPENDENT RNA POLYMERASE6/DICER-LIKE4 pathway in *Arabidopsis* reveals
796 dependency on miRNA- and tasiRNA-directed targeting. *Plant Cell* 19, 926-942. doi:10.1105/tpc.107.050062
- 797 Hsieh, L.C., Lin, S.I., Shih, A.C., Chen, J.W., Lin, W.Y., Tseng, C.Y., Li, W.H., and Chiou, T.J. (2009). Uncovering small RNA-
798 mediated responses to phosphate deficiency in *Arabidopsis* by deep sequencing. *Plant Physiology* 151, 2120-2132.
799 doi:10.1104/pp.109.147280
- 800 Huang, C.K., Shen, Y.L., Huang, L.F., Wu, S.J., Yeh, C.H., and Lu, C.A. (2016). The DEAD-Box RNA helicase AtRH7/PRH75
801 participates in pre-rRNA processing, plant development and cold tolerance in *Arabidopsis*. *Plant Cell Physiol* 57, 174-191.
802 doi:10.1093/pcp/pcv188
- 803 Huang, D., Wu, W., Abrams, S.R., and Cutler, A.J. (2008). The relationship of drought-related gene expression in *Arabidopsis thaliana*
804 to hormonal and environmental factors. *J Exp Bot* 59, 2991-3007. doi:10.1093/jxb/ern155
- 805 Huang, K.C., Lin, W.C., and Cheng, W.H. (2018). Salt hypersensitive mutant 9, a nucleolar APUM23 protein, is essential for salt
806 sensitivity in association with the ABA signaling pathway in *Arabidopsis*. *BMC Plant Biol* 18, 40. doi:10.1186/s12870-018-
807 1255-z
- 808 Jahns, P., and Holzwarth, A.R. (2012). The role of the xanthophyll cycle and of lutein in photoprotection of photosystem II. *Biochim*
809 *Biophys Acta* 1817, 182-193. doi:10.1016/j.bbabi.2011.04.012

- 810 Jiao, X., Sherman, B.T., Huang Da, W., Stephens, R., Baseler, M.W., Lane, H.C., and Lempicki, R.A. (2012). DAVID-WS: a stateful
811 web service to facilitate gene/protein list analysis. *Bioinformatics* 28, 1805-1806. doi:10.1093/bioinformatics/bts251
- 812 Jin, H., Vacic, V., Girke, T., Lonardi, S., and Zhu, J.K. (2008). Small RNAs and the regulation of cis-natural antisense transcripts in
813 *Arabidopsis*. *BMC Mol Biol* 9, 6. doi:10.1186/1471-2199-9-6
- 814 K.M. Creasey, and Zhai, J. (2014). miRNAs trigger widespread epigenetically-activated siRNAs from transposons in *Arabidopsis*. *Nature*
815 10.1038/nature13069, 411-415. doi:10.1038/nature13069
- 816 Karpinski, S., Gabrys, H., Mateo, A., Karpinska, B., and Mullineaux, P.M. (2003). Light perception in plant disease defence signalling.
817 *Curr Opin Plant Biol* 6, 390-396. doi:10.1016/s1369-5266(03)00061-x
- 818 Kemal Kazan, and Manners, J.M. (2011). The interplay between light and jasmonate signalling during defence and development. *Journal*
819 *of Experimental Botany* 62, 4087-4100. doi:https://doi.org/10.1093/jxb/err142
- 820 Khaksefidi, R., Mirlohi, S., Khalaji, F., Fakhari, Z., Shiran, B., and E., E. (2015). Differential expression of seven conserved microRNAs
821 in response to abiotic stress and their regulatory network in *Helianthus annuus*. *Front Plant Sci* 6. doi:10.3389/fpls.2015.00741
- 822 Khan, M.I., Fatma, M., Per, T.S., Anjum, N.A., and Khan, N.A. (2015). Salicylic acid-induced abiotic stress tolerance and underlying
823 mechanisms in plants. *Front Plant Sci* 6, 462. doi:10.3389/fpls.2015.00462
- 824 Kim, B., Kim, G., Fujioka, S., Takatsuto, S., and Choe, S. (2012). Overexpression of 3beta-hydroxysteroid dehydrogenases/C-4
825 decarboxylases causes growth defects possibly due to abnormal auxin transport in *Arabidopsis*. *Mol Cells* 34, 77-84.
826 doi:10.1007/s10059-012-0102-6
- 827 Kopriva, S., Muheim, R., Koprivova, A., Trachsel, N., Catalano, C., Suter, M., and Brunold, C. (1999). Light regulation of assimilatory
828 sulphate reduction in *Arabidopsis thaliana*. *Plant J* 20, 37-44. doi:10.1046/j.1365-313x.1999.00573.x
- 829 Kramer, M.F. (2011). Stem-loop RT-qPCR for miRNAs. *Current Protocols in Molecular Biology* Chapter 15, Unit 15 10.
830 doi:10.1002/0471142727.mb1510s95
- 831 Kuczynska, A., Cardenia, V., Ogradowicz, P., Kempa, M., Rodriguez-Estrada, M.T., and Mikolajczak, K. (2019). Effects of multiple
832 abiotic stresses on lipids and sterols profile in barley leaves (*Hordeum vulgare* L.). *Plant Physiol Biochem* 141, 215-224.
833 doi:10.1016/j.plaphy.2019.05.033
- 834 Le Gall, H., Philippe, F., Domon, J.M., Gillet, F., Pelloux, J., and Rayon, C. (2015). Cell Wall Metabolism in Response to Abiotic Stress.
835 *Plants (Basel)* 4, 112-166. doi:10.3390/plants4010112
- 836 Ledford, H.K., Chin, B.L., and Niyogi, K.K. (2007). Acclimation to singlet oxygen stress in *Chlamydomonas reinhardtii*. *Eukaryot Cell*
837 6, 919-930. doi:10.1128/EC.00207-06
- 838 Leustek, T. (2002). Sulfate metabolism. *Arabidopsis Book* 1, e0017. doi:10.1199/tab.0017
- 839 Li, W., Wang, P., Li, Y., Zhang, K., Ding, F., Nie, T., Yang, X., Lv, Q., and Zhao, L. (2015). Identification of micromRNAs in response to
840 different day lengths in soybean using high-throughput sequencing and qRT-PCR. *PLoS One* 10, e0132621.
841 doi:10.1371/journal.pone.0132621
- 842 Lin, C., Yang, H., Guo, H., Mockler, T., Chen, J., and Cashmore, A.R. (1998). Enhancement of blue-light sensitivity of *Arabidopsis*
843 seedlings by a blue light receptor cryptochrome 2. *Proc Natl Acad Sci USA* 95, 2686-2690. doi:10.1073/pnas.95.5.2686
- 844 Lin, M.C., Tsai, H.L., Lim, S.L., Jeng, S.T., and Wu, S.H. (2017). Unraveling multifaceted contributions of small regulatory RNAs to
845 photomorphogenic development in *Arabidopsis*. *BMC Genomics* 18, 559. doi:10.1186/s12864-017-3937-6
- 846 Liu, X., Chi, H., Yue, M., Zhang, X., Li, W., and Jia, E. (2012). The regulation of exogenous jasmonic acid on UV-B stress tolerance in
847 wheat. *Journal of Plant Growth Regulation* 31, 436-447.
- 848 Loss-Morais, G., Waterhouse, P.M., and Margis, R. (2013). Description of plant tRNA-derived RNA fragments (tRFs) associated with
849 argonaute and identification of their putative targets. *Biology Direct* 8, 6. doi:10.1186/1745-6150-8-6
- 850 Lotkowska, M.E., Tohge, T., Fernie, A.R., Xue, G.P., Balazadeh, S., and Mueller-Roeber, B. (2015). The *Arabidopsis* transcription factor
851 MYB112 promotes anthocyanin formation during salinity and under high light stress. *Plant Physiol* 169, 1862-1880.
852 doi:10.1104/pp.15.00605
- 853 Luo, Q.J., Mittal, A., Jia, F., and Rock, C.D. (2012). An autoregulatory feedback loop involving PAP1 and TAS4 in response to sugars
854 in *Arabidopsis*. *Plant Mol Biol* 80, 117-129. doi:10.1007/s11103-011-9778-9
- 855 Ma, L., Bajic, V.B., and Zhang, Z. (2013). On the classification of long non-coding RNAs. *RNA Biol* 10, 925-933. doi:10.4161/rna.24604
- 856 Martinez, G., Choudhury, S.G., and Slotkin, R.K. (2017). tRNA-derived small RNAs target transposable element transcripts. *Nucleic*
857 *Acids Research* 45, 5142-5152. doi:10.1093/nar/gkx103
- 858 Mateo, A., Funck, D., Muhlenbock, P., Kular, B., Mullineaux, P.M., and Karpinski, S. (2006). Controlled levels of salicylic acid are
859 required for optimal photosynthesis and redox homeostasis. *J Exp Bot* 57, 1795-1807. doi:10.1093/jxb/erj196
- 860 Maxwell, K., and Johnson, G.N. (2000). Chlorophyll fluorescence--a practical guide. *J Exp Bot* 51, 659-668. doi:10.1093/jxb/51.345.659
- 861 Minagawa, J. (2013). Dynamic reorganization of photosynthetic supercomplexes during environmental acclimation of photosynthesis.
862 *Front Plant Sci* 4, 513. doi:10.3389/fpls.2013.00513
- 863 Mittler, R., Vanderauwera, S., Gollery, M., and Van Breusegem, F. (2004). Reactive oxygen gene network of plants. *Trends Plant Sci* 9,
864 490-498. doi:10.1016/j.tplants.2004.08.009
- 865 Miyake, C., Horiguchi, S., Makino, A., Shinzaki, Y., Yamamoto, H., and Tomizawa, K. (2005). Effects of light intensity on cyclic
866 electron flow around PSI and its relationship to Non-photochemical Quenching of Chl fluorescence in tobacco leaves. *Plant*
867 *and Cell Physiology* 46, 1819-1830.
- 868 Munekage, Y., Hashimoto, M., Miyake, C., Tomizawa, K., Endo, T., Tasaka, M., and Shikanai, T. (2004). Cyclic electron flow around
869 photosystem I is essential for photosynthesis. *Nature* 429, 579-582. doi:10.1038/nature02598
- 870 Murata, N., Takahashi, S., Nishiyama, Y., and Allakhverdiev, S.I. (2007). Photoinhibition of photosystem II under environmental stress.
871 *Biochimica et Biophysica Acta* 1767, 414-421. doi:10.1016/j.bbabi.2006.11.019
- 872 Nguyen, N.H., Jeong, C.Y., Kang, G.H., Yoo, S.D., Hong, S.W., and Lee, H. (2015). MYBD employed by HY5 increases anthocyanin
873 accumulation via repression of MYBL2 in *Arabidopsis*. *Plant J* 84, 1192-1205. doi:10.1111/tpj.13077

- 874 Nishimura, N., Kitahata, N., Seki, M., Narusaka, Y., Narusaka, M., Kuromori, T., Asami, T., Shinozaki, K., and Hirayama, T. (2005).
875 Analysis of ABA hypersensitive germination2 revealed the pivotal functions of PARN in stress response in Arabidopsis. *Plant*
876 *J* 44, 972-984. doi:10.1111/j.1365-313X.2005.02589.x
- 877 Niyogi, K.K., Grossman, A.R., and Bjorkman, O. (1998). *Arabidopsis* mutants define a central role for the xanthophyll cycle in the
878 regulation of photosynthetic energy conversion. *Plant Cell* 10, 1121-1134. doi:10.1105/tpc.10.7.1121
- 879 Norikazu Ohnishi, Suleyman Allakhverdiev, Shunichi Takahashi, Shoichi Higashi, Masakatsu Watanabe, Yoshitaka Nishiyama, and
880 Murata, N. (2005). Two-step mechanism of photodamage to photosystem II: step 1 occurs at the oxygen-evolving complex
881 and step 2 occurs at the photochemical reaction center. *Biochemistry* 44, 8494-8499. doi:https://doi.org/10.1021/bi047518q
- 882 Nott, A., Jung, H.S., Koussevitzky, S., and Chory, J. (2006). Plastid-to-nucleus retrograde signaling. *Annu Rev Plant Biol* 57, 739-759.
883 doi:10.1146/annurev.arplant.57.032905.105310
- 884 Palm, D., Streit, D., Shanmugam, T., Weis, B.L., Ruprecht, M., Simm, S., and Schleiff, E. (2019). Plant-specific ribosome biogenesis
885 factors in *Arabidopsis thaliana* with essential function in rRNA processing. *Nucleic Acids Res* 47, 1880-1895.
886 doi:10.1093/nar/gky1261
- 887 Park, Y.I., Chow, W.S., Osmond, C.B., and Anderson, J.M. (1996). Electron transport to oxygen mitigates against the photoinactivation
888 of Photosystem II in vivo. *Photosynth Res* 50, 23-32. doi:10.1007/BF00018218
- 889 Pelaez, P., Trejo, M.S., Iniguez, L.P., Estrada-Navarrete, G., Covarrubias, A.A., Reyes, J.L., and Sanchez, F. (2012). Identification and
890 characterization of microRNAs in *Phaseolus vulgaris* by high-throughput sequencing. *BMC Genomics* 13, 83.
891 doi:10.1186/1471-2164-13-83
- 892 Pelletier, M.K., and Shirley, B.W. (1996). Analysis of flavanone 3-hydroxylase in Arabidopsis seedlings. Coordinate regulation with
893 chalcone synthase and chalcone isomerase. *Plant Physiol* 111, 339-345. doi:10.1104/pp.111.1.339
- 894 Qiao, Y., Zhang, J., Zhang, J., Wang, Z., Ran, A., Guo, H., Wang, D., and Zhang, J. (2017). Integrated RNA-seq and sRNA-seq analysis
895 reveals miRNA effects on secondary metabolism in *Solanum tuberosum* L. *Mol Genet Genomics* 292, 37-52.
896 doi:10.1007/s00438-016-1253-5
- 897 Qin, Z., Li, C., Mao, L., and Wu, L. (2014). Novel insights from non-conserved microRNAs in plants. *Front Plant Sci* 5, 586.
898 doi:10.3389/fpls.2014.00586
- 899 Rajagopalan, R., Vaucheret, H., Trejo, J., and Bartel, D.P. (2006). A diverse and evolutionarily fluid set of microRNAs in *Arabidopsis*
900 *thaliana*. *Genes and Development* 20, 3407-3425. doi:10.1101/gad.1476406
- 901 Ramel, F., Birtic, S., Ginies, C., Soubigou-Taconnat, L., Triantaphylides, C., and Havaux, M. (2012). Carotenoid oxidation products are
902 stress signals that mediate gene responses to singlet oxygen in plants. *Proc Natl Acad Sci USA* 109, 5535-5540.
903 doi:10.1073/pnas.1115982109
- 904 Ross, J.R., Nam, K.H., D'auria, J.C., and Pichersky, E. (1999). S-Adenosyl-L-methionine:salicylic acid carboxyl methyltransferase, an
905 enzyme involved in floral scent production and plant defense, represents a new class of plant methyltransferases. *Arch Biochem*
906 *Biophys* 367, 9-16. doi:10.1006/abbi.1999.1255
- 907 Ruban, A.V. (2009). Plants in light. *Commun Integr Biol* 2, 50-55. doi:10.4161/cib.2.1.7504
- 908 Savchenko, T., Yanykin, D., Khorobrykh, A., Terentyev, V., Klimov, V., and Dehesh, K. (2017). The hydroperoxide lyase branch of the
909 oxylipin pathway protects against photoinhibition of photosynthesis. *Planta* 245, 1179-1192. doi:10.1007/s00425-017-2674-z
- 910 Sharma, D., Tiwari, M., Pandey, A., Bhatia, C., Sharma, A., and Trivedi, P.K. (2016). MicroRNA858 Is a Potential Regulator of
911 Phenylpropanoid Pathway and Plant Development. *Plant Physiol* 171, 944-959. doi:10.1104/pp.15.01831
- 912 Sharrock, R.A., and Quail, P.H. (1989). Novel phytochrome sequences in *Arabidopsis thaliana*: structure, evolution, and differential
913 expression of a plant regulatory photoreceptor family. *Genes and Development* 3, 1745-1757. doi:10.1101/gad.3.11.1745
- 914 Shikata, H., Hanada, K., Ushijima, T., Nakashima, M., Suzuki, Y., and Matsushita, T. (2014). Phytochrome controls alternative splicing
915 to mediate light responses in Arabidopsis. *Proc Natl Acad Sci USA* 111, 18781-18786. doi:10.1073/pnas.1407147112
- 916 Slotkin, R.K., and Martienssen, R. (2007). Transposable elements and the epigenetic regulation of the genome. *Nat Rev Genet* 8, 272-
917 285. doi:10.1038/nrg2072
- 918 Sun, W., Xu, X.H., Wu, X., Wang, Y., Lu, X., Sun, H., and Xie, X. (2015). Genome-wide identification of microRNAs and their targets
919 in wild type and phyB mutant provides a key link between microRNAs and the phyB-mediated light signaling pathway in rice.
920 *Front Plant Sci* 6, 372. doi:10.3389/fpls.2015.00372
- 921 Svyatyna, K., and Riemann, M. (2012). Light-dependent regulation of the jasmonate pathway. *Protoplasma* 249 Suppl 2, S137-145.
922 doi:10.1007/s00709-012-0409-3
- 923 Szechynska-Hebda, M., Kruk, J., Gorecka, M., Karpinska, B., and Karpinski, S. (2010). Evidence for light wavelength-specific
924 photoelectrophysiological signaling and memory of excess light episodes in Arabidopsis. *Plant Cell* 22, 2201-2218.
925 doi:10.1105/tpc.109.069302
- 926 Tepperman, J.M., Hudson, M.E., Khanna, R., Zhu, T., Chang, S.H., Wang, X., and Quail, P.H. (2004). Expression profiling of phyB
927 mutant demonstrates substantial contribution of other phytochromes to red-light-regulated gene expression during seedling de-
928 teliation. *Plant J* 38, 725-739. doi:10.1111/j.1365-313X.2004.02084.x
- 929 Tiwari, B., Habermann, K., Arif, M.A., Weil, H.L., Garcia-Molina, A., Kleine, T., Muhlhaus, T., and Frank, W. (2020). Identification of
930 small RNAs during cold acclimation in *Arabidopsis thaliana*. *BMC Plant Biol* 20, 298. doi:10.1186/s12870-020-02511-3
- 931 Tsai, H.L., Li, Y.H., Hsieh, W.P., Lin, M.C., Ahn, J.H., and Wu, S.H. (2014). HUA ENHANCER1 is involved in posttranscriptional
932 regulation of positive and negative regulators in Arabidopsis photomorphogenesis. *Plant Cell* 26, 2858-2872.
933 doi:10.1105/tpc.114.126722
- 934 Valdivieso, G.G., Fryer, J.M., Lawson, T., Slattery, K., Truman, W., Smirnov, N., Asami, T., Davies, J.W., Jones, M.A., Baker, R.N.,
935 and Mullineaux, M.P. (2009). The high light response in Arabidopsis involves ABA signaling between vascular and bundle
936 sheath cells. *Plant Cell* 21, 2143-2162. doi:doi: 10.1105/tpc.108.061507
- 937 Van Breusegem, F., Bailey-Serres, J., and Mittler, R. (2008). Unraveling the tapestry of networks involving reactive oxygen species in
938 plants. *Plant Physiol* 147, 978-984. doi:10.1104/pp.108.122325

- 939 Voinnet, O. (2009). Origin, biogenesis, and activity of plant microRNAs. *Cell* 136, 669-687. doi:10.1016/j.cell.2009.01.046
- 940 Wang, B., Sun, Y.F., Song, N., Wang, X.J., Feng, H., Huang, L.L., and Kang, Z.S. (2013). Identification of UV-B-induced microRNAs
- 941 in wheat. *Genet Mol Res* 12, 4213-4221. doi:10.4238/2013.October.7.7
- 942 Wang, D., Qu, Z., Yang, L., Zhang, Q., Liu, Z.H., Do, T., Adelson, D.L., Wang, Z.Y., Searle, I., and Zhu, J.K. (2017). Transposable
- 943 elements (TEs) contribute to stress-related long intergenic noncoding RNAs in plants. *The Plant Journal* 90, 133-146.
- 944 doi:10.1111/tpj.13481
- 945 Wang, H., Chung, J.P., Liu, J., Jang, I., Kean, J.M., Xu, J., and N., C.H. (2014a). Genome-wide identification of long noncoding natural
- 946 antisense transcripts and their responses to light in *Arabidopsis*. *Genome Research* 24, 444-453. doi: 10.1101/gr.165555.113
- 947 Wang, T., Mcfarlane, H.E., and Persson, S. (2016). The impact of abiotic factors on cellulose synthesis. *J Exp Bot* 67, 543-552.
- 948 doi:10.1093/jxb/erv488
- 949 Wang, X.J., Gaasterland, T., and Chua, N.H. (2005). Genome-wide prediction and identification of *cis*-natural antisense transcripts in
- 950 *Arabidopsis thaliana*. *Genome Biology* 6, R30. doi:10.1186/gb-2005-6-4-r30
- 951 Wang, Y., Fan, X., Lin, F., He, G., Terzaghi, W., Zhu, D., and Deng, X.W. (2014b). *Arabidopsis* noncoding RNA mediates control of
- 952 photomorphogenesis by red light. *Proc Natl Acad Sci USA* 111, 10359-10364. doi:10.1073/pnas.1409457111
- 953 Wight, M., and Werner, A. (2013). The functions of natural antisense transcripts. *Essays in Biochemistry* 54, 91-101.
- 954 doi:10.1042/bse0540091
- 955 Wingler, A., Lea, P., Quick, W., and Leegood, R. (2000). Photorespiration: metabolic pathways and their role in stress protection. *Philos*
- 956 *Trans R Soc Lond B Biol Sci.* 355, 1517-1529. doi:doi: 10.1098/rstb.2000.0712
- 957 Wu, G., and Poethig, R.S. (2006). Temporal regulation of shoot development in *Arabidopsis thaliana* by miR156 and its target SPL3.
- 958 *Development* 133, 3539-3547. doi:10.1242/dev.02521
- 959 Xiao, Y., Savchenko, T., Baidoo, E.E., Chehab, W.E., Hayden, D.M., Tolstikov, V., Corwin, J.A., Kliebenstein, D.J., Keasling, J.D., and
- 960 Dehesh, K. (2012). Retrograde signaling by the plastidial metabolite MEcPP regulates expression of nuclear stress-response
- 961 genes. *Cell* 149, 1525-1535. doi:10.1016/j.cell.2012.04.038
- 962 Yamaguchi, A., Wu, M.F., Yang, L., Wu, G., Poethig, R.S., and Wagner, D. (2009). The microRNA-regulated SBP-Box transcription
- 963 factor SPL3 is a direct upstream activator of LEAFY, FRUITFULL, and APETALA1. *Dev Cell* 17, 268-278.
- 964 doi:10.1016/j.devcel.2009.06.007
- 965 Yang, B., Tang, J., Yu, Z., Khare, T., Srivastav, A., Datir, S., and Kumar, V. (2019). Light Stress Responses and Prospects for Engineering
- 966 Light Stress Tolerance in Crop Plants. *Journal of Plant Growth Regulation* 38, 1489-1506.
- 967 Yang, F., Cai, J., Yang, Y., and Liu, Z.H. (2013). Overexpression of microRNA828 reduces anthocyanin accumulation in *Arabidopsis*.
- 968 *Plant Cell, Tissue and Organ Culture* 115, 159-167. doi:doi.org/10.1007/s11240-013-0349-4
- 969 Yu, Y., Ni, Z., Wang, Y., Wan, H., Hu, Z., Jiang, Q., Sun, X., and Zhang, H. (2019). Overexpression of soybean miR169c confers
- 970 increased drought stress sensitivity in transgenic *Arabidopsis thaliana*. *Plant Sci* 285, 68-78. doi:10.1016/j.plantsci.2019.05.003
- 971 Yuan, C., Wang, J., Harrison, A.P., Meng, X., Chen, D., and Chen, M. (2015). Genome-wide view of natural antisense transcripts in
- 972 *Arabidopsis thaliana*. *DNA Research* 22, 233-243. doi:10.1093/dnares/dsv008
- 973 Yulong Wang, Yiqing Wang, Zhaoqing Song, and Zhang, H. (2016). Repression of MYBL2 by Both microRNA858a and HY5 Leads to
- 974 the Activation of Anthocyanin Biosynthetic Pathway in *Arabidopsis*. *Molecular Plant* 9, 1395-1405.
- 975 doi:10.1016/j.molp.2016.07.003
- 976 Zhang, B., Pan, X., Cannon H C., Cobb P G., and T., A.A. (2006). Conservation and divergence of plant microRNA genes. *Plant J.* 46,
- 977 243-259. doi:10.1111/j.1365-313X.2006.02697.x
- 978 Zhang, S.S., Sun, L., Dong, X., Lu, S.J., Tian, W., and Liu, J.X. (2016). Cellulose synthesis genes CESA6 and CSI1 are important for
- 979 salt stress tolerance in *Arabidopsis*. *J Integr Plant Biol* 58, 623-626. doi:10.1111/jipb.12442
- 980 Zhang, X., Xia, J., Lii, Y.E., Barrera-Figueroa, B.E., Zhou, X., Gao, S., Lu, L., Niu, D., Chen, Z., Leung, C., Wong, T., Zhang, H., Guo,
- 981 J., Li, Y., Liu, R., Liang, W., Zhu, J.K., Zhang, W., and Jin, H. (2012). Genome-wide analysis of plant nat-siRNAs reveals
- 982 insights into their distribution, biogenesis and function *Genome Biology* 13, R20.
- 983 Zhenfei S., Min L., Ying Z., and F., Y. (2018). Coordinated regulation of *Arabidopsis* microRNA biogenesis and red light signaling
- 984 through Dicer-like 1 and phytochrome-interacting factor 4. *PLoS Genet* 14, e1007247. doi:10.1371/journal.pgen.1007247
- 985 Zhou, B., Fan, P., Li, Y., Yan, H., and Xu, Q. (2016). Exploring miRNAs involved in blue/UV-A light response in *Brassica rapa* reveals
- 986 special regulatory mode during seedling development. *BMC Plant Biol* 16, 111. doi:10.1186/s12870-016-0799-z
- 987 Zhou, X., Wang, G., and Zhang, W. (2007). UV-B responsive microRNA genes in *Arabidopsis thaliana*. *Mol Syst Biol* 3, 103.
- 988 doi:10.1038/msb4100143

989 11 Figure Legends

990 **Figure 1.** The size distribution (20 to 24 nt) of mapped sRNAs after 3 h (A), 6 h (B) and 2 d (C) of

991 high light treatment (represented in reads per million). The distribution of trimmed sRNA reads from

992 different RNA classes (reads per million) in untreated and high light acclimated samples (D).

993 **Figure 2.** Number of detected sRNAs belonging to different sRNA classes during high light

994 acclimation. The number of up- (black) and downregulated (gray) sRNAs from *trans*-NATs (A),

995 miRNAs (B), *cis*-NATs (C), lncRNAs (D) and ta-siRNAs (E) in response to high light treatment after

996 3 h, 6 h and 2 d ($FC \geq 2$ & ≤ -2 , Benjamini-Hochberg corrected p-value ≤ 0.05).

997 **Figure 3.** Stem loop qRT-PCR based validation of sRNA sequencing data for miRNAs as well as
998 sRNAs derived from *trans*-NATs, *cis*-NATs and lncRNA. Expression values are normalized to *UBI1*
999 housekeeping gene and the untreated control was set to 1. The error bars indicate the standard deviation
1000 (n=3).

1001 **Figure 4.** Gene ontology analysis for all predicted targets of DE miRNAs in high light acclimation.
1002 The dot plot represents GO terms categorized into molecular functions, cellular components and
1003 biological processes. The GO terms and the time points of the high light treatment were depicted on
1004 the y- and x-axis, respectively. The bubble size represents the number of genes in that particular GO
1005 term (Benjamini-Hochberg corrected p-value ≤ 0.05).

1006 **Figure 5.** Our current model on the regulation of anthocyanin biosynthesis in response to high light.
1007 Increased PRODUCTION OF ANTHOCYANIN PIGMENT 1 (PAP1) can bind to the PAP1 *cis*-
1008 elements of the *TAS4* gene to induce *TAS4* transcription. In response to high light, miR828 is
1009 upregulated and triggers the production of *TAS4* derived ta-siRNAs. The ta-siRNAs can target *PAP1*
1010 and *PAP2* mRNAs and downregulate their transcript levels. Additionally, high light induced miR828
1011 can also downregulate *PAP1* transcripts. Furthermore, high light induces the transcription factor
1012 ELONGATED HYPOCOTYL 5 (HY5) that binds to the *PAP1* promoter and activates *PAP1*
1013 transcription that in turn provokes transcription of genes encoding enzymes involved in anthocyanin
1014 biosynthesis such as DIHYDROFLAVONOL 4-REDUCTASE (DFR), CHALCONE SYNTHASE
1015 (CHS) and ANTHOCYANIDIN SYNTHASE (ANS). After 2 d of high light treatment, the
1016 concomitant increase in the components of the proposed model were confirmed by our mRNA
1017 sequencing data which support previous findings (Luo et al., 2012; Yang et al., 2013; Hsieh et al.,
1018 2009).

Figure 1.JPEG

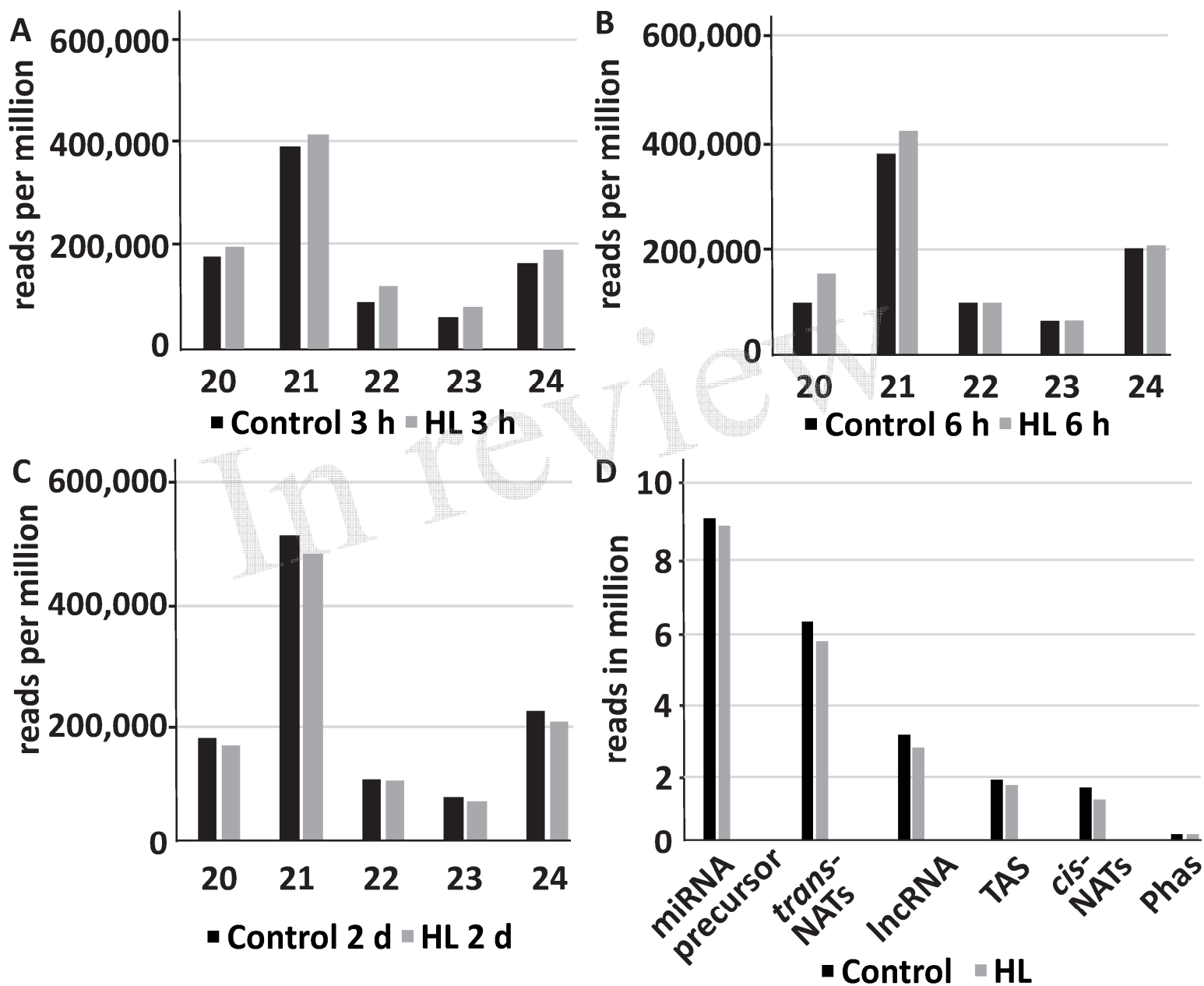


Figure 2.JPEG

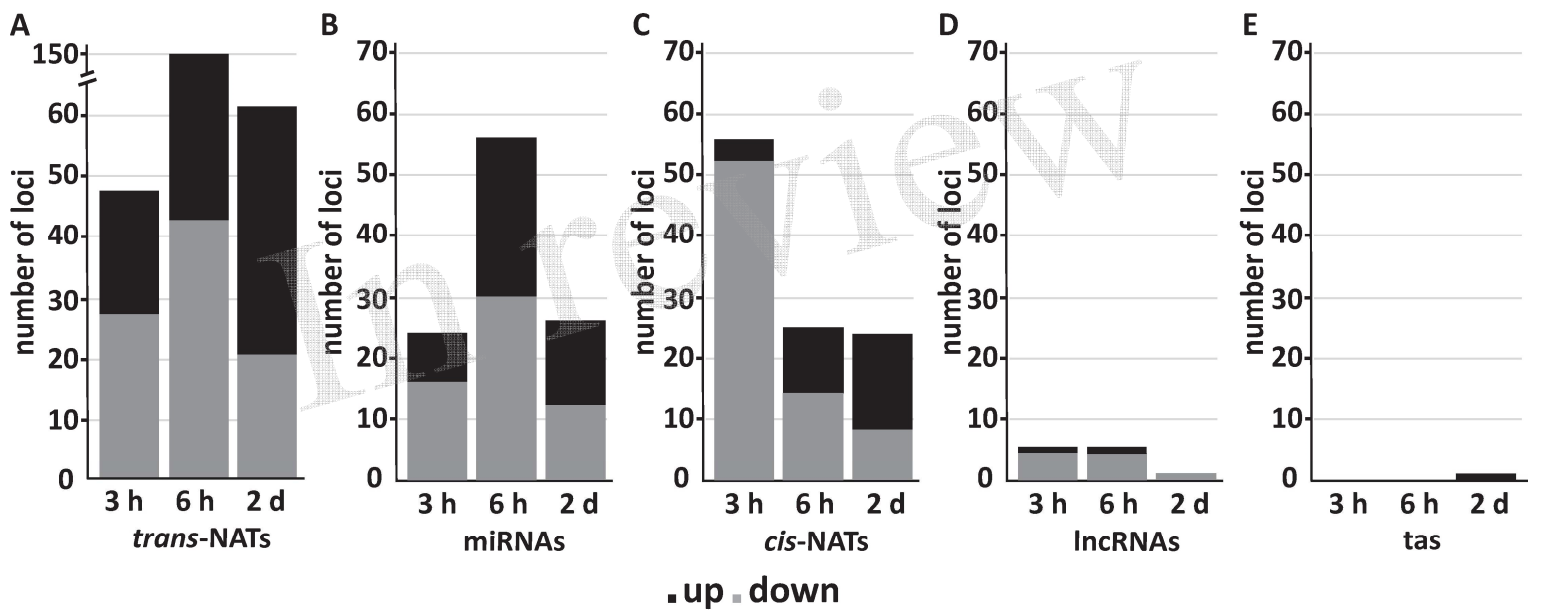


Figure 3.JPEG

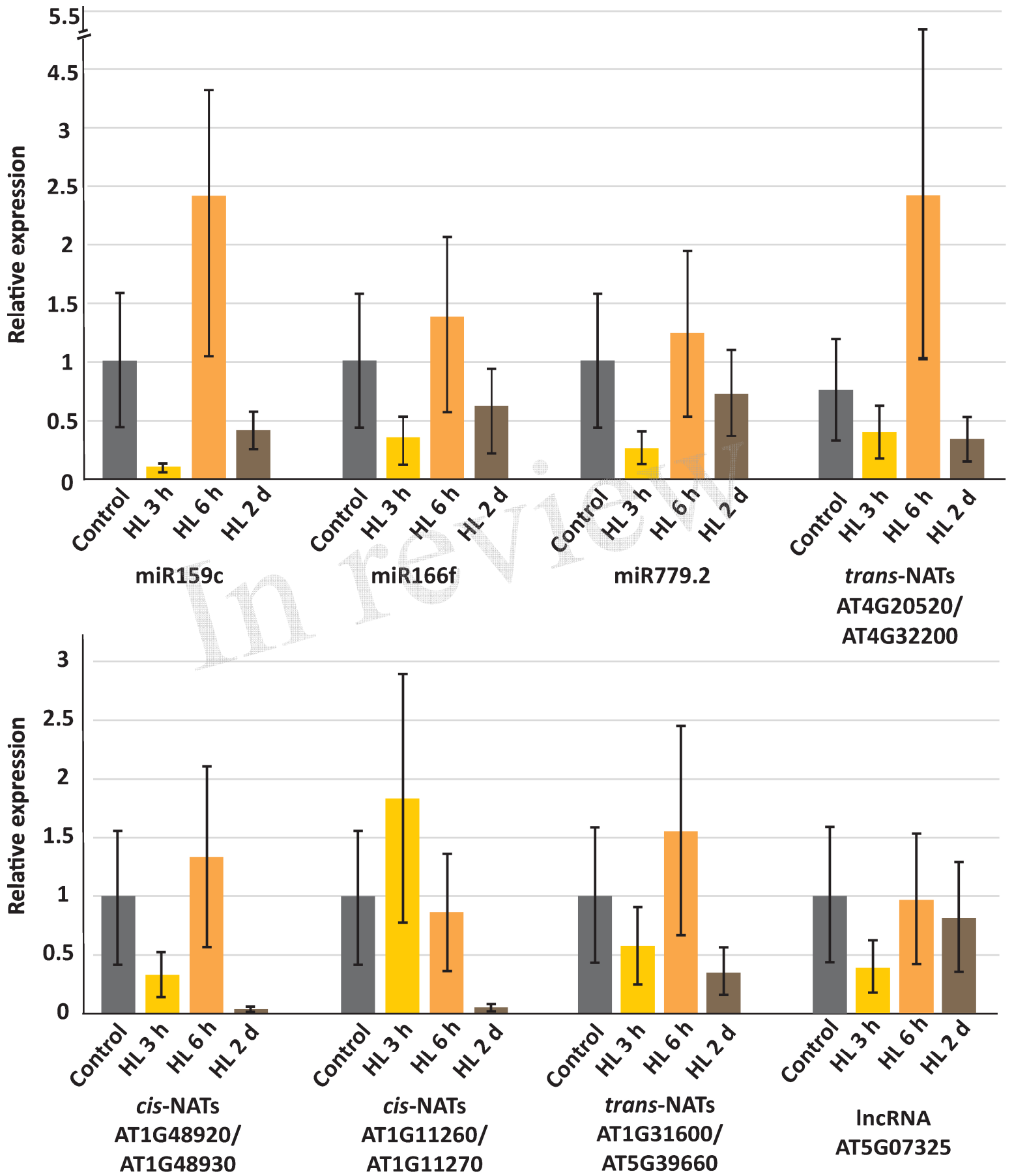


Figure 4.JPEG

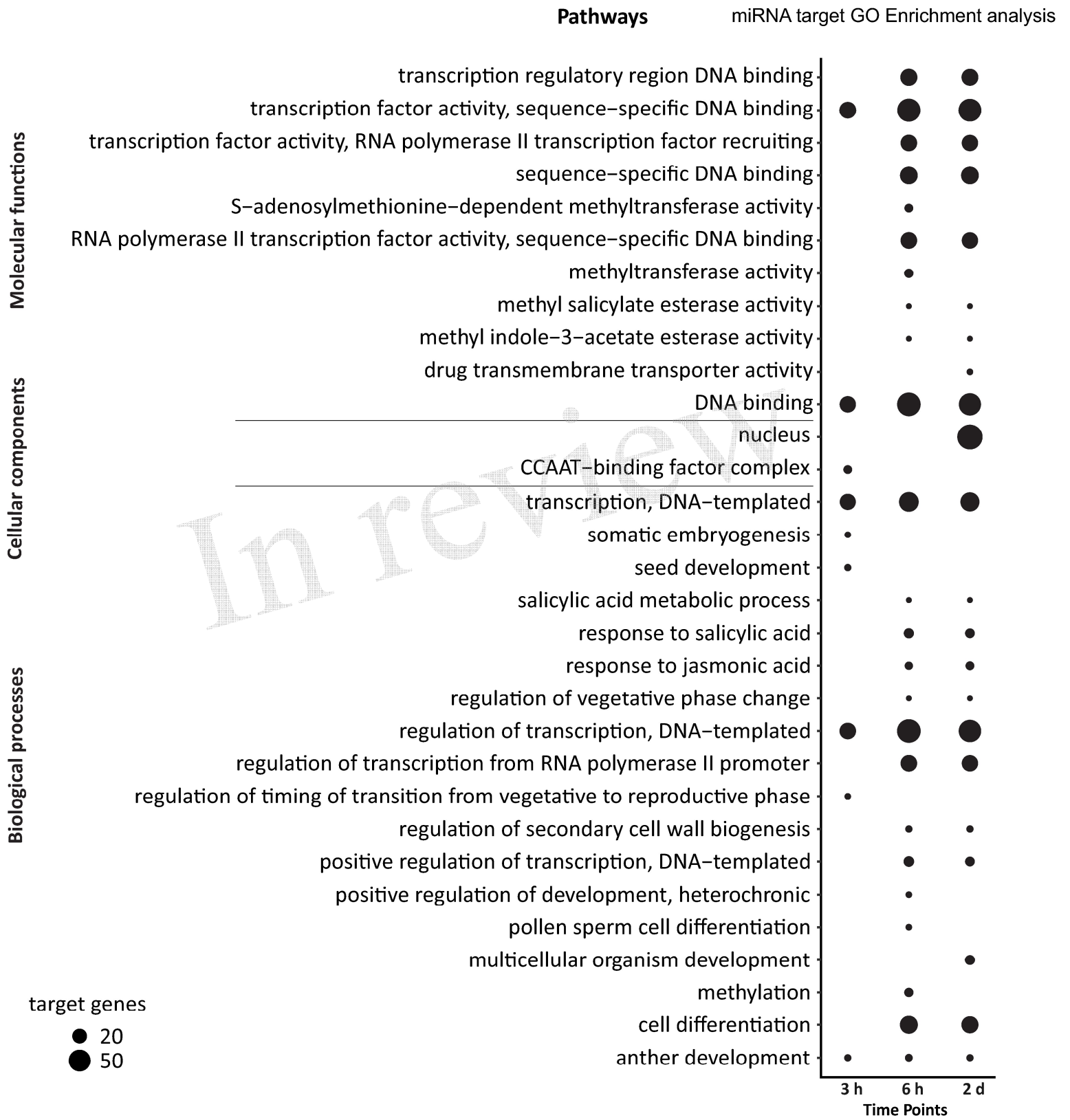
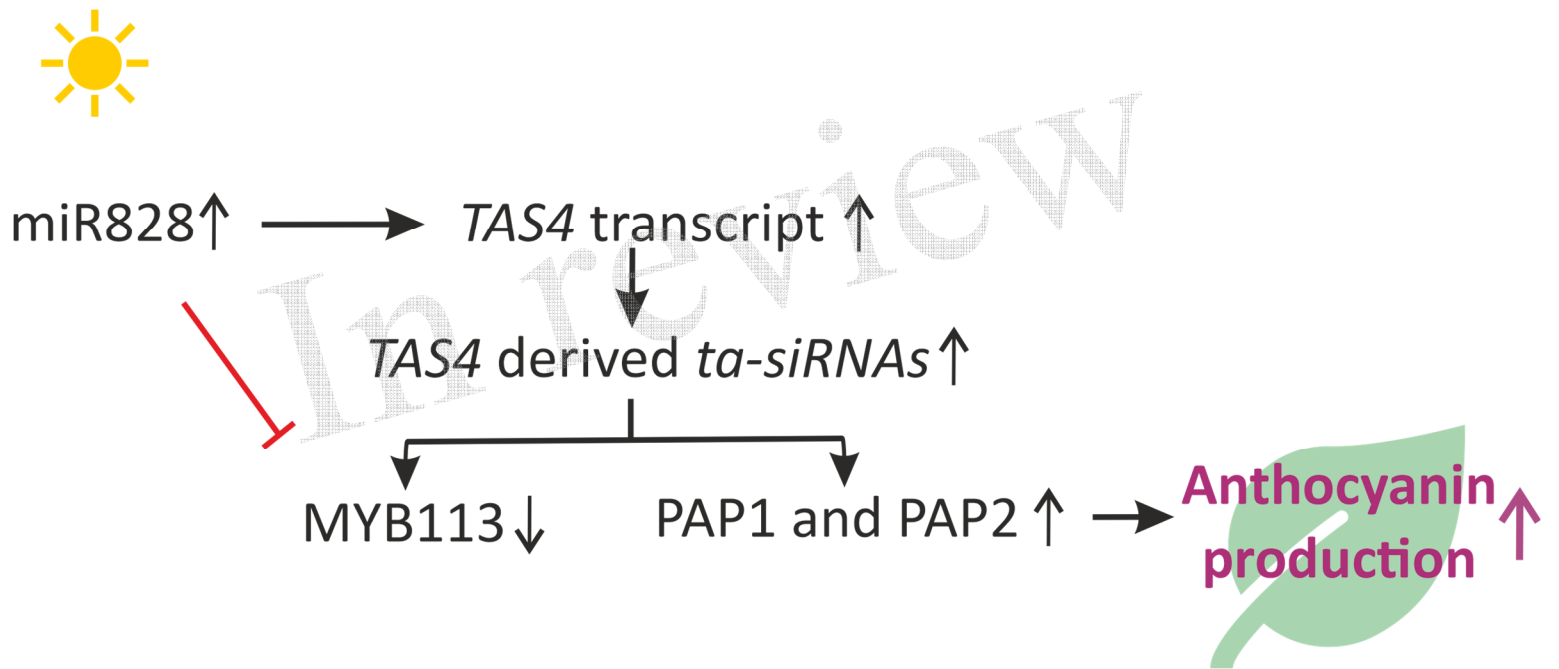


Figure 5.TIF



3 Discussion

The study presented here aims to provide an insight into the cold-, high light- and retrograde signaling-responsive small RNAs (sRNA) which could have an impact on the sRNA producing transcripts or the sRNA targeted transcripts. The sRNA and mRNA/lncRNA sequencing data were combined to study the correlations between the sRNAs and their corresponding parent and/or target mRNA/lncRNA transcripts. The development of high throughput transcriptome sequencing has enabled researchers to identify the miRNAs and their role in regulation of gene expression in response to environmental stress. Several studies have identified the differentially expressed cold and high light responsive miRNAs that could alter expression of stress acclimation related genes. But a comprehensive investigation to identify the sRNAs derived from lncRNAs, *cis*- and *trans*-NATs, *TAS* and *PHAS* has not been published yet. Over the years, it is unrevealed if non-coding RNAs are regulated by retrograde signaling in the presence of norflurazon (NF) treatment that perturbs the chloroplast development and restricts the plastid-derived signals. To study the sRNAs, WT *Arabidopsis* plants were subjected to cold (4 °C) and high light treatment (450 μE); to study the retrograde signaling responsive sRNAs, two additional mutants *gun1* and *gun5* together with WT were treated with NF.

The sequencing data for mRNA/lncRNA was analyzed using GALAXY software and the sRNA data with Shortstack software. We observed an approximate mapping of 10 - 13% reads mapping to miRNAs, 10% to *trans*- and 2% to *cis*-nat-siRNA loci, 4 - 5% reads mapped to lncRNAs, 3% to ta-siRNA producing regions and 0.3% to pha-siRNAs. The remaining reads mapped to transposable elements and repeat-associated regions. We observed differential expression of *cis*-nat-siRNAs and *trans*-nat-siRNAs followed by miRNAs in response to cold, high light and retrograde signaling treatments. Most of the changes were observed after 2 d of cold treatment and 6 h of high light treatment whereas a striking de-repression pattern of sRNAs was observed in NF treated *gun* mutants when compared to NF treated WT. There was a strong upregulation of *cis*-nat-siRNAs in NF treated *gun* mutants and downregulation of *trans*-nat-siRNAs and miRNAs. The results suggest a predominant role of nat-siRNAs and miRNAs in response to environmental stresses and in retrograde signaling.

3.1 Cold stress

The agricultural productivity is decreasing at an alarming rate due to the effects of various climatic conditions. Cold stress is one of the major factors that alters the physiology of plants and causes changes at molecular levels to attain acclimation.

Due to cold treatment, we observed an overall reduction of sRNAs produced from RNA classes such as miRNAs, *trans*- and *cis*-NATs-pairs and lncRNAs. The reason behind the reduction could be the reduced transcription of sRNA precursor transcripts in response to cold acclimation. With the help of our sequencing data, we found 107 DE miRNAs responsive to cold treatment and when compared to previously reported cold-responsive miRNAs in *A. thaliana*, we found an overlap of 14 DE miRNAs to be previously identified in *A. thaliana* in cold stress (Tiwari et al. 2020). To predict the genes that could be affected by the DE miRNAs, we used the psRNATarget tool to predict putative miRNA targets and found 96, 173 and 267 miRNA target pairs at 3 h, 6 h and 2 d time points, respectively. It reflects the importance of miRNAs in regulating the transcriptome at prolonged cold treatment. Prominently, we found mRNAs encoding TFs such as NFY, MYB, TCP and HSFs as the predicted targets of the DE miRNAs. The GO enrichment of all predicted miRNA targets showed that the highest number of targets are associated with the nucleus (136 mRNAs) and 85 of these encode TFs (Tiwari et al. 2020). Plants have a multitude of TFs that are necessary for growth and stress responses and we predicted 85 targets of DE miRNA that encode TFs.

With the help of our mRNA and sRNA sequencing results, we observed several miRNAs showing anti-correlated expression to their targets indicating cold acclimation related alterations (Table 1). In response to cold treatment, miRNAs could be involved in altering transcript levels of their target genes through sequence complementarity. Plants generally activate metabolic pathways that are necessary to protect cells from subjected stress and deactivate pathways that needs investment of energy. The target genes downregulated were found to be negative regulators of cold tolerance and the upregulated targets were involved in reducing chlorophyll synthesis or in delaying the flowering time.

The sRNA sequencing data was used to analyze miRNA regulation and to identify sRNAs derived from other RNA classes in response to cold treatment providing links to their role in acclimation.

miRNA	miRNA Expression	Target	Target Expression	Time point	Function in cold stress
miR159	↑	<i>TIM-44</i>	↓	3 h	Alters mitochondrial protein import in stress conditions
miR159	↓	<i>TIM-44</i>	↑	2 d	Alters mitochondrial protein import in stress conditions
miR159	↑	<i>ACC synthase</i>	↓	3 h	ACC synthase produces ethylene which is a negative regulator of freezing tolerance
miR395c	↓	<i>Mg chelatase</i>	↑	6 h	Mg chelatase produced Mg-Proto-IX which is known to signal the induction of <i>AOX1a</i> gene. <i>AOX1a</i> is involved in initiating thermogenesis during cold stress Mg-Proto-IX also increases activities of antioxidant enzymes and maintains redox equilibrium of cells in cold stress
miR408-5p	↑	Galactose oxidase/Kelch family protein	↓	6 h, 2 d	Expected to mediate cold stress in an ABA-dependent manner
miR171-3p	↓	<i>Scarecrow like 27</i>	↑	2 d	SCL 27 binds to <i>cis</i> -elements of <i>PORC</i> gene leading to reduced chlorophyll synthesis during stress conditions
miR156/157	↑	<i>SPL3</i>	↓	2 d	Involved in delayed flowering during cold stress
miR172c	↓	<i>TOE1</i>	↑	2 d	Involved in delayed flowering during cold stress

Table 1: Cold treatment responsive differentially expressed miRNAs and their anti-correlated protein coding gene targets ($FC \geq 2$ & ≤ -2 , Benjamini-Hochberg corrected p -value ≤ 0.05). The arrows represent the correlation expression as follows: \uparrow =upregulated, \downarrow =downregulated. Source: Tiwari et al. (2020).

The sRNAs derived from non-overlapping lncRNAs were differentially expressed, but their parent transcripts were undetected pointing to their efficient processing into sRNAs and

repression of parent transcripts. We observed a high number of sRNAs derived from *cis*-NATs followed by *trans*-NATs. We found protein-coding transcripts pairing with pre-tRNAs and/or TE transcripts producing sRNAs from one or both transcripts. Several F box related proteins (AT2G33655, AT1G11270, AT2G16365) known to be co-expressed with abiotic stress related genes (Gonzalez et al. 2017) were found to be pairing with tRNA transcripts to produce *trans*-nat-siRNAs. There is a possibility that the nat-siRNAs are produced from the pre-tRNA transcript alone or from the overlapping regions of the two transcripts. Recent studies revealed the role of sRNA derived from tRNA in maintenance of epigenetic inheritance, genome stability, cell proliferation and stress response (Zhu et al. 2018). We observed *trans*-nat-siRNAs produced from TE such as Ty3 Gypsy, CACTA and Ty1 Copia elements. TE derived sRNAs are known to repress TE transcripts via DNA methylation or histone tail modifications (Xie and Yu 2015)

The study concludes that cold stress considerably alters the sRNA expression that in turn alters the gene expression in order to induce cold acclimation. A large number of miRNAs and other classes of sRNAs were differentially expressed indicating their importance in regulation of gene expression.

3.2 High light stress

Light is the primary source of energy for plants and serves as an important factor for their growth and development. When the irradiance is far above the light saturation point of photosynthesis, it is considered as high light stress which induces acclimation responses linked to the photosynthetic machinery, xanthophyll cycle and photorespiratory pathways.

Over the time course of high light treatment, we observed an increase in the number of differentially expressed sRNAs during the 3 h and 6 h time points, but a reduction after 2 d. We found 92 miRNAs to be differentially expressed and 44 miRNAs have been previously reported in UV B, red light and white light related studies in *Arabidopsis* (Bonnet et al. 2004, Zhou et al. 2007, Zhou et al. 2016). The psRNATarget tool was used to identify the putative targets of differentially expressed miRNAs and we found 128, 298 and 175 potential miRNA:mRNA target pairs at 3 h, 6 h and 2 d time point, respectively. The number of targets indicate that the majority of the acclimation related alterations through miRNAs occurred during the early stages of treatment. Similar to the study of cold treatment, the GO analysis of differentially expressed miRNAs revealed association of transcription factors such as MYB, squamosa

promoter binding protein (SPLs) and Teosinte Branched 1, Cycloidea, and members of the PCF (TCP) TF family. The enrichment of TFs indicates their involvement in inducing stress tolerance since TFs can bind to *cis* - elements in the promoter regions of stress tolerance genes and modulate their expression.

miRNA	miRNA Expression	Target	Target Expression	Time point	Function in cold stress
miR156-5p	↑	<i>SPL3</i>	↓	6 h	Involved in delayed flowering during high light stress
miR171c-5p	↓	<i>APS reductase 3</i>	↑	6 h	Increases the amounts of reduced glutathione in stress affected plants
miR163	↑	S-adenosyl-L-methionine-dependent methyltransferases superfamily protein	↓	6 h	These enzymes convert substrates into their methyl compounds reducing levels of important substrates. These could be involved in maintaining levels of salicylic acid and jasmonic acids in high light stress
miR395a	↓	<i>cellulose synthase like G3</i>	↑	6 h, 2 d	Could lead to increased mechanical strength to withstand the turgor pressure in high light conditions

Table 2: High light treatment responsive differentially expressed miRNAs and their anti-correlated protein coding gene targets ($FC \geq 2$ & ≤ -2 , Benjamini-Hochberg corrected p-value ≤ 0.05). The arrows represent the correlation expression as follows: ↑=upregulated, ↓=downregulated. Source: Tiwari et al. (2021) (Submitted to *Frontiers in Plant Science*).

When we correlated the sRNA and the mRNA sequencing data, we observed anti-correlated pairs of miRNAs and their predicted targets (Table 2). During high light treatment, the levels of differential expression of these targets corresponds to their functions as expected. We found genes that could inhibit flowering in stress conditions, increase mechanical strength, and

maintain levels of salicylic acid and jasmonic acid found to be important in the high light stress signaling.

Similar to our data of the cold treatment, we found abundant sRNAs produced from *cis*-NATs and *trans*-NATs pairs in response to high light treatment. We found sRNAs to be produced from the single stranded regions as well as the overlapping regions of the two pairing transcripts. Out of the two transcripts, the non-coding transcripts comprised pre-tRNAs and/or TE pairing with a protein coding gene transcript. After 2 d of high light treatment, we identified ta-siRNAs derived from the *TAS4* precursor. A previous study in *Arabidopsis* explained an autoregulatory loop that involved *PAP1* and *TAS4* transcript in response to sugar accumulation and was also shown to regulate anthocyanin production in high light stressed plants (Luo et al. 2012). miR828 was found to trigger production of *TAS4* derived ta-siRNAs which were able to target transcripts of *PAP1* and *PAP2* MYB factors. It is known that the downregulation of these two TFs causes reduced anthocyanin biosynthesis (Yang et al. 2013). Another TF namely HY5 was upregulated in our sequencing data and it is known to enhance *PAP1* transcription. The positive regulation of *PAP1* by HY5 is supported by the increase in transcripts coding for enzymes of the anthocyanin biosynthesis pathway such as DFR, CHS and ANS. Another study confirmed that miR828 triggers production of *TAS4* derived ta-siRNAs in response to Pi deficiency (Hsieh et al. 2009). Our sequencing data revealed a two-fold increase in the levels of *miR828*, *TAS4* transcript, ta-siRNAs, *PAP1* and *PAP2*, *HY5*, *DFR*, *CHS* and *ANS*. We can conclude that HY5 and *PAP1* facilitate an increase in the production of anthocyanin production in response to high light treatment.

3.3 Retrograde Signaling

Until now, it is not known if sRNAs can be regulated by retrograde signaling in response to NF treatment. To better understand the role of sRNAs in modulating nuclear gene expression responsive to retrograde signals, the sRNA and mRNA sequencing of treated *Arabidopsis* samples and *gun* mutants were analyzed (Habermann et al. 2020).

The mRNA sequencing data was first evaluated and surprisingly, we found that in response to NF, plastid encoded DEGs were repressed in *gun1* mutant whereas the same set of genes were differentially upregulated in the *gun5* mutant. This observation is consistent with previous findings showing the control of plastid gene transcription via retrograde signaling networks (Kleine and Leister 2016). Another surprising observation was that the plastid encoded

transcripts in untreated *gun* mutants were oppositely regulated whereas the nuclear encoded transcripts were overlapping in large numbers in both the mutants.

Concerning the sRNA sequencing data, we detected large numbers of downregulated sRNAs in treated WT (WT NF/WT) whereas treated *gun* mutants exhibited upregulated sRNAs (*gun1/5* NF/WT NF). The increase of sRNAs in treated *gun* mutants suggests their de-repression and their potential role in retrograde-controlled nuclear gene expression. It is possible that these retrograde signal induced sRNAs modulate the mRNA transcript levels and therefore affect the plastid localized proteins. A large number of nat-siRNAs have been found to be differentially expressed in all the treatments (Habermann et al. 2020). We used psRNATarget to find putative targets of differentially expressed miRNAs and unexpectedly, there was no anticorrelation of targets to their cognate miRNAs. From this, we concluded that either the miRNAs are not directly involved in retrograde signal induced alteration of gene expression or they inhibit the initiation of translation thereby repressing translation of mRNA transcripts. Similar to cold and high light related studies, the target prediction tool found 20 miRNA targets encoding transcription factors and 22 targets encoding plastid-localized proteins, being targeted by 23 differentially regulated miRNAs. It can be concluded that miRNAs control transcripts of regulatory proteins which could in turn regulate the nuclear gene expression.

The chloroplast localizing protein transcripts that are targeted by specific miRNAs suggest their possible impact in response to retrograde signals. Our results found a validated target *SPL10* transcript to be regulated by miR157a, suggesting its possible role in retrograde signaling. Another pair showing anticorrelated regulation is comprised of miR398 targeting the transcript of multidrug and toxic compound extrusion (MATE) efflux protein. It mediates removal of the xenobiotic organic compounds out of the cell. The NF-triggered downregulation of miR398 would cause elevation of MATE efflux transcript pointing to its role in extrusion of NF herbicide or other toxic compounds accumulating in the cell. miR395b was downregulated in NF treated WT (WT NF/WT) whereas upregulated in treated *gun5* mutant (*gun5* NF/WT NF). Fang et al. (2019) found that reduced levels of miR395b causes increased PAP synthesis, which inhibits XRNs and prompt elevation of pri-miRNA and mature miRNA levels. Besides miRNAs, we observed a higher number of differentially expressed nat-siRNAs in the treated WT (WT NF/WT) and both *gun* mutants (*gun* NF/WT NF). Majority of pairing transcripts encode nuclear or plastid proteins suggesting a greater impact of nat-siRNAs in control of *PhANGs* encoding plastid proteins.

3.4 Comparison of cold stress, high light stress and retrograde signaling affected non-coding RNAs

It is known that high light and low temperature stress induce disturbances in the organellar gene expression (OGE) such as in chloroplast and mitochondria. The disturbances in the homeostasis trigger retrograde signals to cause nuclear gene expression (NGE) changes (Kleine and Leister 2016). To modulate changes at the transcript level, miRNAs either cleave the mRNA transcripts or repress their translation. Our results suggest involvement of 5 miRNAs differentially regulated in cold, high light and in response to norflurazon treatment (Figure 4). These miRNAs include miR166f, miR169g-3p, two isoforms of miR395b/c and miR398b-5p. The differential expression of these miRNAs clearly reflects their role in retrograde signaling. The differential regulation of the same set of miRNAs in response to cold and high light treatment indicates the trigger of retrograde signals in order to modulate nuclear gene expression in stress conditions.

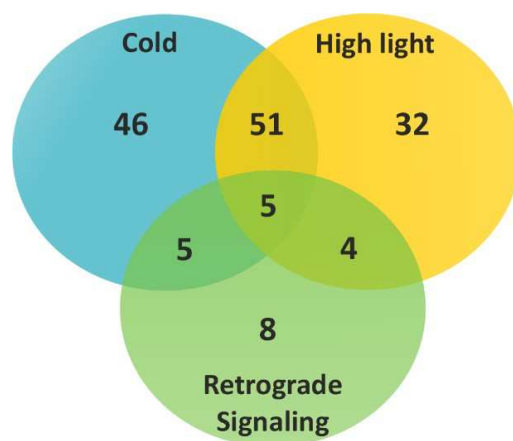


Figure 4. Venn diagram depicting the overlap of differentially expressed miRNAs in response to cold treatment, high light treatment and NF treatment in WT.

To unravel the putative protein-coding transcripts that could be regulated by the DE miRNAs, we used psRNATarget tool for the prediction of their targets. The gene ontology enrichment of all miRNA targets was performed for high light and cold affected miRNAs and we observed a striking overlap between the putative targets. There was an overrepresentation of transcription regulatory proteins and factors with DNA binding ability. Also genes coding for proteins with methyltransferase activity were enriched pointing to potential epigenetic

modifications upon environmental stress (Thiebaut et al. 2019). The genes associated with response to salicylic acid and jasmonic acid were enriched in cold as well as high light stress treatments. The genes associated with post-transcriptional processing such as TPR and PPR were also enriched and these proteins have a role in mediating RNA maturation, stress signaling and organellar transport to promote stress acclimation. The overlap of miRNA targets in high light and cold stress indicates common miRNAs that are potentially modulating gene expression in response to abiotic stresses.

We observed 51 miRNAs overlapping between cold and high light treatments and majority of them are conserved suggesting that miRNAs regulating gene expression alterations in response to environmental cues could be common. We explored the possibility of finding alterations in sRNA expression from all the other RNA classes and found expression of sRNAs from 6 *cis*-NAT loci and 28 *trans*-NAT loci being altered in cold, high light and in response to NF treatment in WT plants (Figure 5).

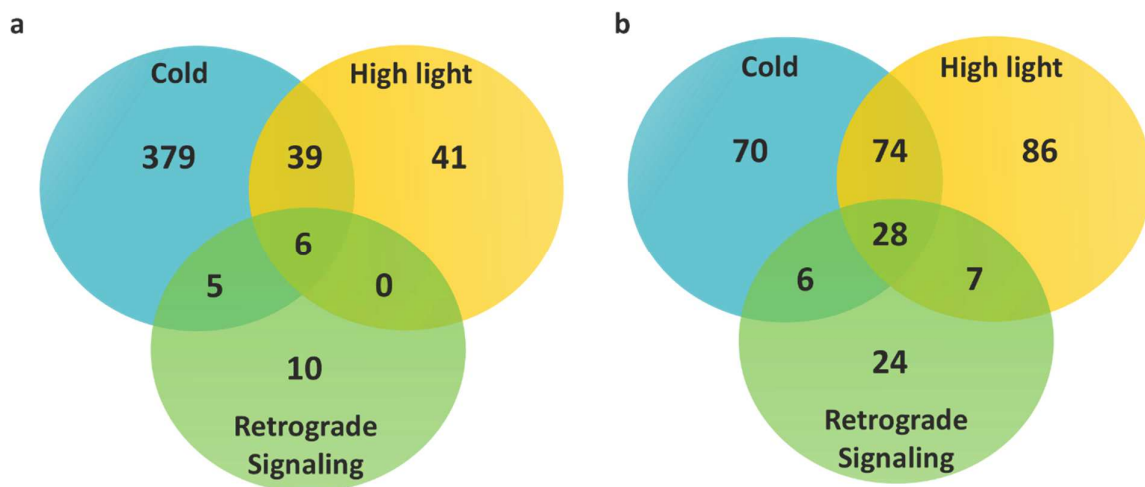


Figure 5. Venn diagram depicting the overlap of differentially expressed nat-siRNAs in response to cold treatment, high light treatment and NF treatment in WT. (a) *cis*-nat-siRNAs were differentially expressed in large numbers in response to cold treatment (b) the overlap of *trans*-nat-siRNAs differentially expressed in the three treatments were substantially high compared to the other classes of sRNAs.

There was a higher overlap between cold and high light related sRNAs produced from *cis*- and *trans*-NATs transcripts indicating their importance in regulating stress related genes. The *cis*-NATs gene pairs comprised of pairing between an mRNA transcript and a tRNA transcripts including tRNA-*Phe* (AT5G03452), tRNA-*His* (AT3G06665), tRNA-*Phe* (AT3G15585), tRNA-*Ser* (AT1G59570), tRNA-*His* (AT1G02600) and tRNA-*Gly* (AT5G11325). The 28 *trans*-nat-siRNAs

comprised of pairing between an mRNA transcript and a tRNA transcripts including tRNA-*Asp* (AT3G02335), tRNA-*Ser* (AT1G57030), tRNA-*Phe* (AT5G03452), tRNA-*Asp* (AT5G59055), tRNA-*Phe* (AT4G01865), tRNA-*Val* (AT3G59923), tRNA-*Asp* (AT1G75070), tRNA-*Ser* (AT1G72780), tRNA-*Asp* (AT3G27555). The sRNAs produced from single stranded tRNA-*Asp* transcript were found to be induced by Pi starvation in roots (Hsieh et al. 2009), from single tRNA-*His* transcript known to be induced by oxidative stress in *Arabidopsis* seedlings (Thompson et al. 2008) and from tRNA-*Phe* in the leaves (Nowacka et al. 2013). There was an overlap of 39 *cis*-NAT loci and 74 *trans*-NAT loci in high light and cold treatment. The results suggest a greater involvement of *trans*-nat-siRNAs and *cis*-nat-siRNAs followed by miRNAs in regulation of environmentally altered genes. We did not find an overlap of sRNAs derived from non-overlapping lncRNAs in response to NF when compared with cold and high light treatments, but 5 lncRNAs loci generated differentially expressed sRNAs in both stress treatments. In cold treatment, majority of lncRNAs generated upregulated sRNAs whereas in high light these were downregulated. Along with differential upregulation of sRNAs we found that the lncRNA transcripts were not differentially expressed in the mRNA data indicating potential processing of transcripts into sRNAs. In high light mRNA data, we found lncRNA AT5G07325 transcript to be differentially downregulated with a concomitant downregulation of sRNAs.

Apart from the sRNA data, we analyzed the overlap of mRNA genes differentially expressed ($FC \geq 2$ & ≤ -2 , Benjamini-Hochberg corrected p-value ≤ 0.01) in response to cold and high light treatments, and in NF treated WT plants (WT NF/WT). There was an overlap of 140 genes in all the three treatments, with 900 genes found in high light and cold treatment, 385 overlapping between cold treatment and WT NF/WT, and 82 overlapping between high light treatment and WT NF/WT. Out of the 140 genes found in all the three treatments, 31 genes encoded chloroplast localizing proteins and mainly comprised genes related to oxidation-reduction processes, response to UV and jasmonic acid, and flavonoid biosynthesis processes. With the cold treatment we observed genes mainly related to metabolic pathways, carbon metabolism, photosynthesis and chlorophyll metabolism.

A large number of genes were differentially up- or downregulated in response to abiotic stresses, as there is an increased generation of ROS indicating reduced photosynthetic efficiency and shut down of the photosynthetic machinery. Alterations in gene expression upon such stresses take place with the help of retrograde signals that modulates the *PhANGs* expression with the help of sRNAs and transcription factors (Figure 6).

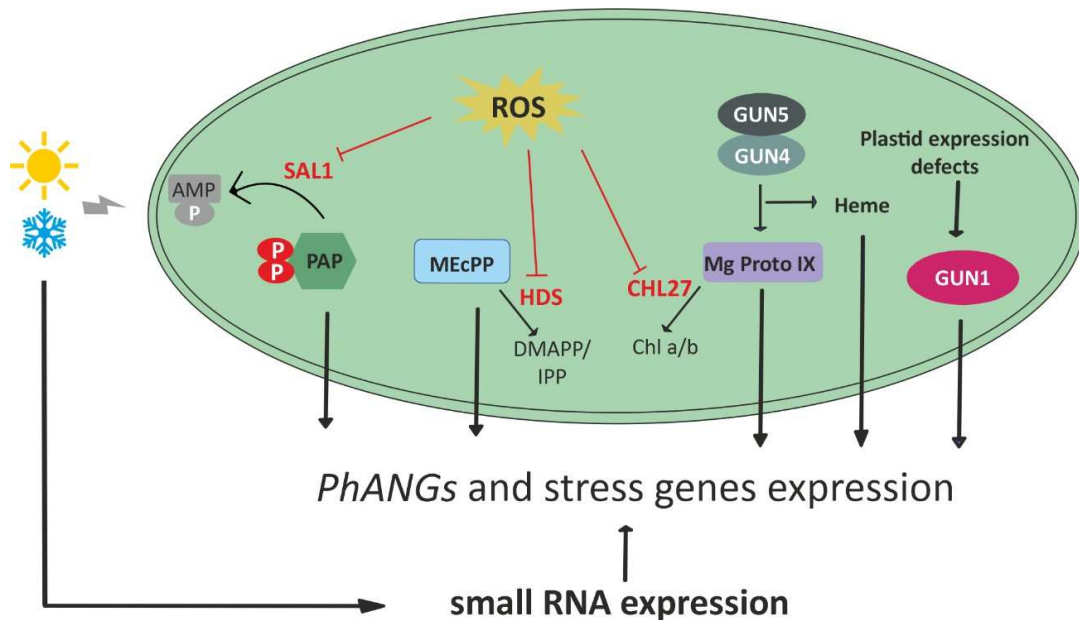


Figure 6. Impact of high light and cold stress on components of retrograde signaling pathways. High light and cold stress induce generation of reactive oxygen species via the electron transport chain. The ROS have an inhibiting effect on enzymes such as SAL1, HDS and CHL27 which lead to accumulation of the intermediate metabolites PAP, MEcPP and MG Proto IX. These intermediates are responsible for altering the *PhANGs* expression and stress responsive genes. SAL1: inositol polyphosphate 1-phosphatase, HDS: 1-hydroxy-2-methyl-2-E)-butenyl-4-diphosphate synthase, CHL27: Mg-protoporphyrin monomethylester aerobic cyclase, MEcPP: 2-C-methyl-D-erythritol 2,4-cyclodiphosphate, MgProtoIX(-ME): magnesium protoporphyrin 9 (and its monomethylester derivative), PAP: 3'-phosphoadenosine 5'-phosphate, *PhANGs*: photosynthesis-associated nuclear genes, ROS: reactive oxygen species.

The chloroplast can sense the fluctuations in the environment and in response to abiotic stresses, changes in nuclear gene expression are induced. The trigger of high light and cold treatment is known to generate large amounts of reactive oxygen species due to inefficient photosynthetic electron transport chain. The ROS causes inhibition of certain enzymes such as SAL1, HDS and CHL27 which use PAP, MEcPP and Mg Proto IX metabolites as substrates. The accumulation of these intermediate metabolites leads to their transport into the nucleus, altering expression of *PhANGs* and stress responsive genes with the help of transcription factors (Crawford et al. 2018). The abiotic stress directs modulation of nuclear gene expression leading to expression of small RNAs, which in turn regulate the expression of stress responsive genes.

3.5 Outlook

Our study provides a fundamental database showing the possible involvement of sRNAs in cold and high light acclimation and their potential role as regulators of gene expression in retrograde signaling. Using the accuracy of high throughput data generated via next-generation sequencing platform and bioinformatics tools for subsequent data analyses, we were able to find abundant of differentially expressed sRNAs in the aforementioned treatments. We were able to identify miRNAs and sRNAs derived from *cis*- and *trans*-NATs, lncRNAs, *PHAS* and *TAS* that can be further selected for functional analysis. The miRNAs affected in cold and high light treatment can be further studied in overexpression or knock out lines of miRNAs. We were able to transform the miRNA mimicry constructs of 4 miRNAs namely miR395, miR161.1, miR163 and miR169 into *Arabidopsis* plants. These transformed lines are considered as the knock-down lines as the miRNA transcripts are sequestered by binding to the miRNA mimicry sequence. The putative targets of these miRNAs can be validated for a concomitant upregulation in knock-out or knock-down lines and for downregulation in overexpression lines through RT-PCRs. Apart from the identification of miRNAs, our results provide miRNA-TF-mRNA networks that were constructed using bioinformatic tools and machine learning concepts. The specific miRNA subnetworks comprising TFs and their direct as well as indirect targets can be used to explore the regulatory relationships in abiotic stress acclimation. We identified cold treatment related *cis*-nat-siRNA producing *cis*-NATs pairs that can be further used for functional studies in cold treatments in *Arabidopsis*. Cold affected siRNAs derived from AT3G05870-AT3G05880 (ANAPHASE-PROMOTING COMPLEX/CYCLOSOME 11 - RARE-COLD-INDUCIBLE 2A), AT1G10522-AT5G53905 (PLASTID REDOX INSENSITIVE 2 - prolamin-like protein) and high light affected siRNAs from AT1G48920-AT1G48930 (NUCLEOLIN LIKE 1 - GLYCOSYL HYDROLASE 9C1) and AT1G11260 - AT1G11270 (SUGAR TRANSPORTER 1 - F-box and associated interaction domains-containing protein) have been validated to be differentially expressed through stem-loop RT-PCR through our studies. The identified *cis*-NATs can be functionally analyzed in treated WT or in gene knock out mutants.

Overall, the results of this PhD thesis can be used to unravel the regulators of gene expression in response to cold, high light and retrograde signaling. Most sRNAs act in post-transcriptional control of gene expression by binding to reverse complementary sequences within their target

RNA and thus our combined analyses facilitate direct correlations of altered small RNA expression to changes in mRNA transcripts. Furthermore, we identified a considerable high number of sRNAs that have not been associated with cold, high light and retrograde signaling-responsive transcriptional changes previously. We also included a modeling approach to generate a gene regulatory network that involves microRNAs and their direct targets as well as transcription factors that are miRNA-regulated and their respective downstream targets. The obtained network and cold-responsive subnetwork provide insights into regulatory gene interconnectivities that underlie adaptation processes to cold.

4 References

- Adams, B., K. Winter, A. Krüger and F. Czygan (1989). "Zeaxanthin Synthesis, Energy Dissipation, and Photoprotection of Photosystem II at Chilling Temperatures." Plant Physiology **90**(3): 894-898.
- Affymetrix, E. T. P. and E. T. P. Cold Spring Harbor Laboratory (2009). "Post-transcriptional processing generates a diversity of 5'-modified long and short RNAs." Nature **457**(7232): 1028-1032.
- Ahmad, M. and A. R. Cashmore (1993). "HY4 gene of *A. thaliana* encodes a protein with characteristics of a blue-light photoreceptor." Nature **366**(6451): 162-166.
- Allen, E., Z. Xie, A. M. Gustafson and J. C. Carrington (2005). "microRNA-directed phasing during trans-acting siRNA biogenesis in plants." Cell **121**(2): 207-221.
- Alsharafa, K., M. O. Vogel, M. L. Oelze, M. Moore, N. Stingl, K. König, H. Friedman, M. J. Mueller and K. J. Dietz (2014). "Kinetics of retrograde signalling initiation in the high light response of *Arabidopsis thaliana*." Philos Trans R Soc Lond B Biol Sci **369**(1640): 20130424.
- Alves, C. S., R. Vicentini, G. T. Duarte, V. F. Pinoti, M. Vincentz and F. T. Nogueira (2017). "Genome-wide identification and characterization of tRNA-derived RNA fragments in land plants." Plant Molecular Biology **93**(1-2): 35-48.
- Alyabyev A., N. L. Loseva., T. P. Jakushenkova., G. G. Rachimova., V. I. Tribunskih., R. I. Estrina. and V. Y. Petrov. (2002). "Comparative effects of blue light and red light on the rates of oxygen metabolism and heat production in wheat seedlings stressed by heat shock." Thermochimica Acta **394** 227–231.
- Anderson, L. E. (1971). "Chloroplast and cytoplasmic enzymes. II. Pea leaf triose phosphate isomerases." Biochimica et Biophysica Acta **235**(1): 237-244.
- Ankele, E., P. Kindgren, E. Pesquet and A. Strand (2007). "In vivo visualization of Mg-protoporphyrin IX, a coordinator of photosynthetic gene expression in the nucleus and the chloroplast." Plant Cell **19**(6): 1964-1979.
- Aro, E. M., M. Suorsa, A. Rokka, Y. Allahverdiyeva, V. Paakkari, A. Saleem, N. Battchikova and E. Rintamäki (2005). "Dynamics of photosystem II: a proteomic approach to thylakoid protein complexes." Journal of Experimental Botany **56**(411): 347-356.
- Aro, E. M., I. Virgin and B. Andersson (1993). "Photoinhibition of Photosystem II. Inactivation, protein damage and turnover." Biochimica et Biophysica Acta **1143**(2): 113-134.
- Au, P. and E. Dennis (2017). "Analysis of Argonaute 4-Associated Long Non-Coding RNA in *Arabidopsis thaliana* Sheds Novel Insights into Gene Regulation through RNA-Directed DNA Methylation." Genes **8**(8): 198.
- Baev, V., I. Milev, M. Naydenov, T. Vachev, E. Apostolova, N. Mehterov, M. Gozmanva, G. Minkov, G. Sablok and G. Yahubyan (2014). "Insight into small RNA abundance and expression in high- and low-temperature stress response using deep sequencing in *Arabidopsis*." Plant Physiology and Biochemistry **84**: 105-114.
- Baier, M. and K. Dietz (2005). "Chloroplasts as source and target of cellular redox regulation: a discussion on chloroplast redox signals in the context of plant physiology." Journal of Experimental Botany **56**(416): 1449-1462.

- Banerjee, A., S. H. Wani and A. Roychoudhury (2017). "Epigenetic control of plant cold responses." Frontiers in Plant Science **8**: 1643.
- Banerjee, R., E. Schleicher, S. Meier, R. M. Viana, R. Pokorny, M. Ahmad, R. Bittl and A. Batschauer (2007). "The signaling state of *Arabidopsis* cryptochrome 2 contains flavin semiquinone." Journal of Biological Chemistry **282**(20): 14916-14922.
- Bechtold, U., O. Richard, A. Zamboni, C. Gapper, M. Geisler, B. Pogson, S. Karpinski and P. M. Mullineaux (2008). "Impact of chloroplastic- and extracellular-sourced ROS on high light-responsive gene expression in *Arabidopsis*." Journal of Experimental Botany **59**(2): 121-133.
- Bellaïf, S., F. Barneche, G. Peltier and J. D. Rochaix (2005). "State transitions and light adaptation require chloroplast thylakoid protein kinase STN7." Nature **433**(7028): 892-895.
- Bin Yu, Zhiyong Yang, Junjie Li, Svetlana Minakhina, Maocheng Yang, Richard W. Padgett, Ruth Steward and X. Chen (2005). "Methylation as a crucial step in plant microRNA biogenesis." Science **307**(5711): 932-935.
- Bonnet, E., J. Wuyts, P. Rouze and Y. Van de Peer (2004). "Detection of 91 potential conserved plant microRNAs in *Arabidopsis thaliana* and *Oryza sativa* identifies important target genes." Proc Natl Acad Sci U S A **101**(31): 11511-11516.
- Borsani, O., J. Zhu, P. E. Verslues, R. Sunkar and J. K. Zhu (2005). "Endogenous siRNAs derived from a pair of natural cis-antisense transcripts regulate salt tolerance in *Arabidopsis*." Cell **123**(7): 1279-1291.
- Bowman, S. K., A. M. Deaton, H. Domingues, P. I. Wang, R. I. Sadreyev, R. E. Kingston and W. Bender (2014). "Histone occupancy-dependent and -independent removal of H3K27 trimethylation at cold-responsive genes in *Arabidopsis*." eLife **3**: e02833.
- Brown, B. A., C. Cloix, G. H. Jiang, E. Kaiserli, P. Herzyk, D. J. Kliebenstein and G. I. Jenkins (2005). "A UV-B-specific signaling component orchestrates plant UV protection." Proc Natl Acad Sci U S A **102**(50): 18225-18230.
- Brzezowski, P., A. S. Richter and B. Grimm (2015). "Regulation and function of tetrapyrrole biosynthesis in plants and algae." Biochimica et Biophysica Acta **1847**(9): 968-985.
- Busch, F. A., T. L. Sage, A. B. Cousins and R. F. Sage (2013). "C3 plants enhance rates of photosynthesis by reassimilating photorespired and respired CO₂." Plant, Cell and Environment **36**(1): 200-212.
- Carmell, M. A. (2002). "The Argonaute family: tentacles that reach into RNAi, developmental control, stem cell maintenance, and tumorigenesis." Genes and Development **16**(21): 2733-2742.
- Catala, R., J. Medina and J. Salinas (2011). "Integration of low temperature and light signaling during cold acclimation response in *Arabidopsis*." Proc Natl Acad Sci U S A **108**(39): 16475-16480.
- Chaves, I., R. Pokorny, M. Byrdin, N. Hoang, T. Ritz, K. Brettel, L. O. Essen, G. T. van der Horst, A. Batschauer and M. Ahmad (2011). "The cryptochromes: blue light photoreceptors in plants and animals." Annual Review of Plant Biology **62**: 335-364.
- Chekanova, J. A. (2015). "Long non-coding RNAs and their functions in plants." Current Opinion in Plant Biology **27**: 207-216.

- Chen, T. H. and L. V. Gusta (1983). "Abscisic Acid-induced freezing resistance in cultured plant cells." Plant Physiology **73**(1): 71-75.
- Chinnusamy, V., J. K. Zhu and R. Sunkar (2010). "Gene regulation during cold stress acclimation in plants." Methods in Molecular Biology **639**: 39-55.
- Cho, J. (2018). "Transposon-Derived Non-coding RNAs and Their Function in Plants." Frontiers in Plant Science **9**: 600.
- Christie, J. M. (2007). "Phototropin blue-light receptors." Annual Review of Plant Biology **58**: 21-45.
- Crawford, T., N. Lehotai and A. Strand (2018). "The role of retrograde signals during plant stress responses." Journal of Experimental Botany **69**(11): 2783-2795.
- Creasey, K. M., J. Zhai, F. Borges, F. Van Ex, M. Regulski, B. C. Meyers and R. A. Martienssen (2014). "miRNAs trigger widespread epigenetically activated siRNAs from transposons in *Arabidopsis*." Nature **508**(7496): 411-415.
- Csorba, T., J. Questa, Q. Sun and C. Dean (2014). "Antisense COOLAIR mediates the coordinated switching of chromatin states at FLC during vernalization." Proc Natl Acad Sci. **111**(45): 16160-16165.
- Cuevas-Velazquez, C. L., D. F. Rendon-Luna and A. A. Covarrubias (2014). "Dissecting the cryoprotection mechanisms for dehydrins." Frontiers in Plant Science **5**: 583.
- Dalal, V. K. and B. C. Tripathy (2018). "Water-stress induced downsizing of light-harvesting antenna complex protects developing rice seedlings from photo-oxidative damage." Scientific Reports **8**(1): 5955.
- Das, K. and A. Roychoudhury (2014). "Reactive oxygen species (ROS) and response of antioxidants as ROS-scavengers during environmental stress in plants." Frontiers in Environmental Science **2**: 53.
- Dau, H., I. Zaharieva and M. Haumann (2012). "Recent developments in research on water oxidation by photosystem II." Current Opinion in Chemical Biology **16**(1-2): 3-10.
- Demmig, B., K. Winter, A. Kruger and F. C. Czygan (1988). "Zeaxanthin and the heat dissipation of excess light energy in *Nerium oleander* exposed to a combination of high light and water stress." Plant Physiology **87**(1): 17-24.
- Devert, A., N. Fabre, M. Floris, B. Canard, C. Robaglia and P. Crete (2015). "Primer-dependent and primer-independent initiation of double stranded RNA synthesis by purified *Arabidopsis* RNA-dependent RNA polymerases RDR2 and RDR6." PLoS One **10**(3): e0120100.
- Di, C., J. Yuan, Y. Wu, J. Li, H. Lin, L. Hu, T. Zhang, Y. Qi, M. B. Gerstein, Y. Guo and Z. J. Lu (2014). "Characterization of stress-responsive lncRNAs in *Arabidopsis thaliana* by integrating expression, epigenetic and structural features." The Plant Journal **80**(5): 848-861.
- Ding, Y. (2015). "OST1 Kinase Modulates Freezing Tolerance by Enhancing ICE1 Stability in *Arabidopsis*." Developmental Cell **32**(3): 278-289.
- Dong, C.-H. (2006). "The negative regulator of plant cold responses, HOS1, is a RING E3 ligase that mediates the ubiquitination and degradation of ICE1."
- Dong, C. and H. Pei (2014). "Over-expression of miR397 improves plant tolerance to cold stress in *Arabidopsis thaliana*." Journal of Plant Biology **57**(4): 209-217.

- Dyall, S. D., M. T. Brown and P. J. Johnson (2004). "Ancient invasions: from endosymbionts to organelles." Science **304**(5668): 253-257.
- Effendi, Y., A. M. Jones and G. F. Scherer (2013). "AUXIN-BINDING-PROTEIN1 (ABP1) in phytochrome-B-controlled responses." Journal of Experimental Botany **64**(16): 5065-5074.
- Ensminger, I., F. Busch and N. Huner (2006). "Photostasis and cold acclimation: sensing low temperature through photosynthesis." Physiologia Plantarum **126**: 28-44.
- Erdal, S., M. Genisel, H. Turk, R. Dumlupinar and Y. Demir (2015). "Modulation of alternative oxidase to enhance tolerance against cold stress of chickpea by chemical treatments." Journal of Plant Physiology **175**: 95-101.
- Estavillo, G. M., P. A. Crisp, W. Pornsiriwong, M. Wirtz, D. Collinge, C. Carrie, E. Giraud, J. Whelan, P. David, H. Javot, C. Brearley, R. Hell, E. Marin and B. J. Pogson (2011). "Evidence for a SAL1-PAP chloroplast retrograde pathway that functions in drought and high light signaling in *Arabidopsis*." Plant Cell **23**(11): 3992-4012.
- Eulalio, A., E. Huntzinger and E. Izaurralde (2008). "Getting to the root of miRNA-mediated gene silencing." Cell **132**(1): 9-14.
- Evans, J. (1987). "The relationship between electron transport components and photosynthetic capacity in pea leaves grown at different irradiances." Australian Journal of Plant Physiology **14**(2): 157-170.
- Fang, X., G. Zhao, S. Zhang, Y. Li, H. Gu, Y. Li, Q. Zhao and Y. Qi (2019). "Chloroplast-to-nucleus signaling regulates microRNA biogenesis in *Arabidopsis*." Developmental Cell **48**(3): 371-382.
- Fey, V., R. Wagner, K. Brautigam, M. Wirtz, R. Hell, A. Dietzmann, D. Leister, R. Oelmüller and T. Pfannschmidt (2005). "Retrograde plastid redox signals in the expression of nuclear genes for chloroplast proteins of *Arabidopsis thaliana*." Journal of Biological Chemistry **280**(7): 5318-5328.
- Franco-Zorrilla, J. M., A. Valli, M. Todesco, I. Mateos, M. I. Puga, I. Rubio-Somoza, A. Leyva, D. Weigel, J. A. Garcia and J. Paz-Ares (2007). "Target mimicry provides a new mechanism for regulation of microRNA activity." Nature Genetics **39**(8): 1033-1037.
- Frankow-Lindberg, B. E. (2001). "Adaptation to winter stress in nine white clover populations: changes in non-structural carbohydrates during exposure to simulated winter conditions and 'spring' regrowth potential." Annals of Botany **88**: 745-751.
- Frigerio, S., C. Campoli, S. Zorzan, L. Fantoni, C. Crosatti, F. Drepper, W. Haehnel, L. Cattivelli, T. Morosinotto and R. Bassi (2007). "Photosynthetic antenna size in higher plants is controlled by the plastoquinone redox state at the post-transcriptional rather than transcriptional level." The Journal of Biological Chemistry **282**: 29457-29469.
- Gebetsberger, J., M. Zywicki, A. Künzi and N. Polacek (2012). "tRNA-derived fragments target the ribosome and function as regulatory non-coding RNA in *Haloferax volcanii*." Archaea **2012**: 11.
- Goksoyr, J. (1967). "Evolution of eucaryotic cells." Nature **214**(5093): 1161.
- Gombos, Z., H. Wada, E. Hideg and N. Murata (1994). "The unsaturation of membrane lipids stabilizes photosynthesis against heat stress." Plant Physiology **104**(2): 563-567.

- Gonzalez, L., K. Keller, K. Chan, M. Gessel and B. Thines (2017). "Transcriptome analysis uncovers *Arabidopsis* F-BOX STRESS INDUCED 1 as a regulator of jasmonic acid and abscisic acid stress gene expression." BMC Genomics **18**.
- Gornall, J., R. Betts, E. Burke, R. Clark, J. Camp, K. Willett and A. Wiltshire (2010). "Implications of climate change for agricultural productivity in the early twenty-first century." Philos Trans R Soc Lond B Biol Sci **365**(1554): 2973-2989.
- Gray, J. C., J. A. Sullivan, J. H. Wang, C. A. Jerome and D. MacLean (2003). "Coordination of plastid and nuclear gene expression." Philos Trans R Soc Lond B Biol Sci **358**(1429): 135-144; discussion 144-135.
- Greenberg, B. M., V. Gaba, O. Canaani, S. Malkin, A. K. Mattoo and M. Edelman (1989). "Separate photosensitizers mediate degradation of the 32-kDa photosystem II reaction center protein in the visible and UV spectral regions." Proc Natl Acad Sci U S A **86**(17): 6617-6620.
- Guan, C., B. Wu, T. Yu, Q. Wang, N. T. Krogan, X. Liu and Y. Jiao (2017). "Spatial auxin signaling controls leaf flattening in *Arabidopsis*." Current Biology **27**(19): 2940-2950.
- Gusta, L., R. Trischuk and C. Weiser (2005). "Plant cold acclimation: the role of abscisic acid." Journal of Plant Growth Regulation **24**(4): 308-318.
- Gy, I., V. Gascioli, D. Lauressergues, J. B. Morel, J. Gombert, F. Proux, C. Proux, H. Vaucheret and A. C. Mallory (2007). "*Arabidopsis* FIERY1, XRN2, and XRN3 are endogenous RNA silencing suppressors." Plant Cell **19**(11): 3451-3461.
- Habermann, K., B. Tiwari, M. Krantz, S. O. Adler, E. Klipp, M. A. Arif and W. Frank (2020). "Identification of small non-coding RNAs responsive to GUN1 and GUN5 related retrograde signals in *Arabidopsis thaliana*." Plant J.
- Hackenberg, M., P. J. Huang, C. Y. Huang, B. J. Shi, P. Gustafson and P. Langridge (2013). "A comprehensive expression profile of microRNAs and other classes of non-coding small RNAs in barley under phosphorous-deficient and -sufficient conditions." DNA Res **20**(2): 109-125.
- Hasler, D., G. Lehmann, Y. Murakawa, F. Klironomos, L. Jakob, F. A. Grasser, N. Rajewsky, M. Landthaler and G. Meister (2016). "The Lupus Autoantigen La prevents mischanneling of tRNA fragments into the human microRNA pathway." Molecular Cell **63**(1): 110-124.
- Havaux, M. and K. Kloppstech (2001). "The protective functions of carotenoid and flavonoid pigments against excess visible radiation at chilling temperature investigated in *Arabidopsis* npq and tt mutants." Planta **213**: 953-966.
- Hayyan, M., M. A. Hashim and I. M. AlNashef (2016). "Superoxide ion: Generation and chemical implications." Chemical Reviews **116**(5): 3029-3085.
- Henriques, R., H. Wang, J. Liu, M. Boix, L. F. Huang and N. H. Chua (2017). "The antiphase regulatory module comprising CDF5 and its antisense RNA FLORE links the circadian clock to photoperiodic flowering." New Phytologist **216**(3): 854-867.
- Hoecker, U. (2017). "The activities of the E3 ubiquitin ligase COP1/SPA, a key repressor in light signaling." Current Opinion in Plant Biology **37**: 63-69.
- Hohner, R., A. Aboukila, H. H. Kunz and K. Venema (2016). "Proton gradients and proton-dependent transport processes in the chloroplast." Frontiers in Plant Science **7**: 218.

- Hollosy, F. (2002). "Effects of ultraviolet radiation on plant cells." Micron **33**(2): 179-197.
- Howell, M. D., N. Fahlgren, E. J. Chapman, J. S. Cumbie, C. M. Sullivan, S. A. Givan, K. D. Kasschau and J. C. Carrington (2007). "Genome-wide analysis of the RNA-DEPENDENT RNA POLYMERASE6/DICER-LIKE4 pathway in *Arabidopsis* reveals dependency on miRNA- and tasiRNA-directed targeting." Plant Cell **19**(3): 926-942.
- Hsieh, L. C., S. I. Lin, A. C. Shih, J. W. Chen, W. Y. Lin, C. Y. Tseng, W. H. Li and T. J. Chiou (2009). "Uncovering small RNA-mediated responses to phosphate deficiency in *Arabidopsis* by deep sequencing." Plant Physiology **151**(4): 2120-2132.
- Hsu, P. K., Y. Takahashi, S. Munemasa, E. Merilo, K. Laanemets, R. Waadt, D. Pater, H. Kollist and J. I. Schroeder (2018). "Abscisic acid-independent stomatal CO₂ signal transduction pathway and convergence of CO₂ and ABA signaling downstream of OST1 kinase." Proc Natl Acad Sci U S A **115**(42): E9971-E9980.
- Hu, Y., L. Zhang, L. Zhao, J. Li, S. He, K. Zhou, F. Yang, M. Huang, L. Jiang and L. Li (2011). "Trichostatin A selectively suppresses the cold-induced transcription of the ZmDREB1 gene in maize." PLoS One **6**(7): e22132.
- Huang, W., S. B. Zhang and H. Hu (2014). "Sun leaves up-regulate the photorespiratory pathway to maintain a high rate of CO₂ assimilation in tobacco." Frontiers in Plant Science **5**: 688.
- Jarillo, J. A., H. Gabrys, J. Capel, J. M. Alonso, J. R. Ecker and A. R. Cashmore (2001). "Phototropin-related NPL1 controls chloroplast relocation induced by blue light." Nature **410**(6831): 952-954.
- Jiao, Y., O. S. Lau and X. W. Deng (2007). "Light-regulated transcriptional networks in higher plants." Nature Reviews Genetics **8**(3): 217-230.
- Kazuo Shinozaki and Kazuko Yamaguchi-Shinozaki (2000). "Molecular responses to dehydration and low temperature: differences and cross-talk between two stress signaling pathways." Current Opinion in Plant Biology **3**(3): 217-223.
- Kindgren, P., C. Dubreuil and A. Strand (2015). "The Recovery of Plastid Function Is Required for Optimal Response to Low Temperatures in *Arabidopsis*." PLoS ONE **10**(9): e0138010.
- Kleine, T. and D. Leister (2016). "Retrograde signaling: Organelles go networking." Biochimica et Biophysica Acta **1857**(8): 1313-1325.
- Kmiecik, P., M. Leonardelli and M. Teige (2016). "Novel connections in plant organellar signalling link different stress responses and signalling pathways." Journal of Experimental Botany **67**(13): 3793-3807.
- Knauer, S., A. L. Holt, I. Rubio-Somoza, E. J. Tucker, A. Hinze, M. Pisch, M. Javelle, M. C. Timmermans, M. R. Tucker and T. Laux (2013). "A protodermal miR394 signal defines a region of stem cell competence in the *Arabidopsis* shoot meristem." Developmental Cell **24**(2): 125-132.
- Kohei, K. (2010). "TAS1 *trans*-acting siRNA targets are differentially regulated at low temperature, and TAS1 *trans*-acting siRNA mediates temperature-controlled At1g51670 expression." Bioscience, Biotechnology and Biochemistry **74**(7): 1435-1440.
- Koussevitzky, S., A. Nott, T. C. Mockler, F. Hong, G. Sachetto-Martins, M. Surpin, J. Lim, R. Mittler and J. Chory (2007). "Signals from chloroplasts converge to regulate nuclear gene expression." Science **316**(5825): 715-719.

- Ku, Y. S., J. W. Wong, Z. Mui, X. Liu, J. H. Hui, T. F. Chan and H. M. Lam (2015). "Small RNAs in plant responses to abiotic stresses: Regulatory roles and study methods." International Journal of Molecular Sciences **16**(10): 24532-24554.
- Kumar, M. and G. G. Carmichael (1998). "Antisense RNA: function and fate of duplex RNA in cells of higher eukaryotes." Microbiology and Molecular Biology Reviews **62**(4): 1415-1434.
- Lamke, J. and I. Baurle (2017). "Epigenetic and chromatin-based mechanisms in environmental stress adaptation and stress memory in plants." Genome Biology **18**(1): 124.
- Larkin, R. M. (2014). "Influence of plastids on light signalling and development." Philos Trans R Soc Lond B Biol Sci **369**(1640): 20130232.
- Larkin, R. M., J. M. Alonso, J. R. Ecker and J. Chory (2003). "GUN4, a regulator of chlorophyll synthesis and intracellular signaling." Science **299**(5608): 902-906.
- Lau, K., R. Podolec, R. Chappuis, R. Ulm and M. Hothorn (2019). "Plant photoreceptors and their signaling components compete for COP1 binding via VP peptide motifs." The EMBO Journal **38**(18): e102140.
- Lavorgna, G., D. Dahary, B. Lehner, R. Sorek, C. M. Sanderson and G. Casari (2004). "In search of antisense." Trends in Biochemical Sciences **29**(2): 88-94.
- Lee, J., K. He, V. Stolc, H. Lee, P. Figueroa, Y. Gao, W. Tongprasit, H. Zhao, I. Lee and X. W. Deng (2007). "Analysis of transcription factor HY5 genomic binding sites revealed its hierarchical role in light regulation of development." Plant Cell **19**(3): 731-749.
- Lee, S. J., J. Y. Kang, H. J. Park, M. D. Kim, M. S. Bae, H. I. Choi and S. Y. Kim (2010). "DREB2C interacts with ABF2, a bZIP protein regulating abscisic acid-responsive gene expression, and its overexpression affects abscisic acid sensitivity." Plant Physiology **153**(2): 716-727.
- Leitsch, J., B. Schnettger, C. Critchley and G. Krause (1994). "Two mechanisms of recovery from photoinhibition in vivo: Reactivation of photosystem II related and unrelated to D1-protein turnover." Planta **194**: 15-21.
- Li, J. and A. A. Millar (2013). "Expression of a microRNA-resistant target transgene misrepresents the functional significance of the endogenous microRNA: target gene relationship." Molecular Plant **6**(2): 577-580.
- Li, S., C. Castillo-Gonzalez, B. Yu and X. Zhang (2017). "The functions of plant small RNAs in development and in stress responses." The Plant Journal **90**(4): 654-670.
- Liang, M., V. Haroldsen, X. Cai and Y. Wu (2006). "Expression of a putative laccase gene, *ZmLAC1*, in maize primary roots under stress." Plant, Cell and Environment **29**(5): 746-753.
- Lima, J. C., G. Loss-Morais and R. Margis (2012). "MicroRNAs play critical roles during plant development and in response to abiotic stresses." Genetics and Molecular Biology **35**(4): 1069-1077.
- Lin, C., H. Yang, H. Guo, T. Mockler, J. Chen and A. R. Cashmore (1998). "Enhancement of blue-light sensitivity of Arabidopsis seedlings by a blue light receptor cryptochrome 2." Proc Natl Acad Sci U S A **95**(5): 2686-2690.
- Liu, H. H., X. Tian, Y. J. Li, C. A. Wu and C. C. Zheng (2008). "Microarray-based analysis of stress-regulated microRNAs in *Arabidopsis thaliana*." RNA **14**(5): 836-843.

- Los, D. A. and N. Murata (2004). "Membrane fluidity and its roles in the perception of environmental signals." Biochimica et Biophysica Acta **1666**(1-2): 142-157.
- Loss-Morais, G., P. M. Waterhouse and R. Margis (2013). "Description of plant tRNA-derived RNA fragments (tRFs) associated with argonaute and identification of their putative targets." Biology Direct **8**: 6.
- Luo, Q. J., A. Mittal, F. Jia and C. D. Rock (2012). "An autoregulatory feedback loop involving PAP1 and TAS4 in response to sugars in Arabidopsis." Plant Mol Biol **80**(1): 117-129.
- Ma, C., S. Burd and A. Lers (2015). "miR408 is involved in abiotic stress responses in *Arabidopsis*." The Plant Journal **84**(1): 169-187.
- Mahale, B., B. Fakrudin, S. Ghosh and P. Krishnaraj (2013). "LNA mediated in situ hybridization of miR171 and miR397a in leaf and ambient root tissues revealed expressional homogeneity in response to shoot heat shock in *Arabidopsis thaliana*." Journal of Plant Biochemistry and Biotechnology **23**(1): 93-103.
- Mallory, A. C. and H. Vaucheret (2006). "Functions of microRNAs and related small RNAs in plants." Nature Genetics **38** S31-36.
- Marino, G., B. Naranjo, J. Wang, J. F. Penzler, T. Kleine and D. Leister (2019). "Relationship of GUN1 to FUG1 in chloroplast protein homeostasis." The Plant Journal **99**(3): 521-535.
- Martinez, G. (2018). "tRNA-derived small RNAs: New players in genome protection against retrotransposons." RNA Biology **15**(2): 170-175.
- Martinez, G., S. G. Choudury and R. K. Slotkin (2017). "tRNA-derived small RNAs target transposable element transcripts." Nucleic Acids Research **45**(9): 5142-5152.
- Matzke, M. A. and R. A. Mosher (2014). "RNA-directed DNA methylation: an epigenetic pathway of increasing complexity." Nature Reviews Genetics **15**(6): 394-408.
- McKenzie, R. L., P. J. Aucamp, A. F. Bais, L. O. Bjorn and M. Ilyas (2007). "Changes in biologically-active ultraviolet radiation reaching the Earth's surface." Journal of Photochemistry and Photobiology **6**(3): 218-231.
- Medina, J., M. Bargues, J. Terol, M. Pérez-Alonso and J. Salinas (1999). "The *Arabidopsis* CBF gene family is composed of three genes encoding AP2 Domain-containing proteins whose expression is regulated by low temperature but not by abscisic acid or dehydration." Plant Physiology **119**(2): 463-470.
- Mellenthin, M., U. Ellersiek, A. Borger and M. Baier (2014). "Expression of the *Arabidopsis* sigma factor SIG5 is photoreceptor and photosynthesis controlled." Plants (Basel) **3**(3): 359-391.
- Minagawa, J. (2013). "Dynamic reorganization of photosynthetic supercomplexes during environmental acclimation of photosynthesis." Frontiers in Plant Science **4**: 513.
- Miura, K., J. B. Jin, J. Lee, C. Y. Yoo, V. Stirm, T. Miura, E. N. Ashworth, R. A. Bressan, D. J. Yun and P. M. Hasegawa (2007). "SIZ1-mediated sumoylation of ICE1 controls CBF3/DREB1A expression and freezing tolerance in *Arabidopsis*." Plant Cell **19**(4): 1403-1414.
- Miyake, C., Y. Shinzaki, M. Miyata and K. Tomizawa (2004). "Enhancement of cyclic electron flow around PSI at high light and its contribution to the induction of non-photochemical quenching of chl fluorescence in intact leaves of tobacco plants." Plant Cell Physiology **45**(10): 1426-1433.

- Mizuno, M., M. Kamei and H. Tsuchida (1998). "Ascorbate peroxidase and catalase cooperate for protection against hydrogen peroxide generated in potato tubers during low-temperature storage." Biochemistry and Molecular Biology International **44**(4): 717-726.
- Mochizuki, N., J. A. Brusslan, R. Larkin, A. Nagatani and J. Chory (2001). "*Arabidopsis* genomes uncoupled 5 (GUN5) mutant reveals the involvement of Mg-chelatase H subunit in plastid-to-nucleus signal transduction." Proc Natl Acad Sci U S A **98**(4): 2053-2058.
- Moldovan, D., A. Spriggs, J. Yang, B. J. Pogson, E. S. Dennis and I. W. Wilson (2010). "Hypoxia-responsive microRNAs and trans-acting small interfering RNAs in *Arabidopsis*." Journal of Experimental Botany **61**(1): 165-177.
- Murata, N., S. Takahashi, Y. Nishiyama and S. I. Allakhverdiev (2007). "Photoinhibition of photosystem II under environmental stress." Biochimica et Biophysica Acta **1767**(6): 414-421.
- Nagashima, A., M. Hanaoka, T. Shikanai, M. Fujiwara, K. Kanamaru, H. Takahashi and K. Tanaka (2004). "The multiple-stress responsive plastid sigma factor, SIG5, directs activation of the psbD blue light-responsive promoter (BLRP) in *Arabidopsis thaliana*." Plant Cell Physiology **45**(4): 357-368.
- Niyogi, K., O. Björkman and A. Grossman (1997). "The roles of specific xanthophylls in photoprotection." PNAS **94** (25): 14162-14167.
- Niyogi, K. K., A. R. Grossman and O. Bjorkman (1998). "*Arabidopsis* mutants define a central role for the xanthophyll cycle in the regulation of photosynthetic energy conversion." Plant Cell **10**(7): 1121-1134.
- Nogues, S., D. J. Allen, J. I. Morison and N. R. Baker (1998). "Ultraviolet-B radiation effects on water relations, leaf development, and photosynthesis in droughted pea plants." Plant Physiology **117**(1): 173-181.
- Nowacka, M., P. M. Strozycki, P. Jackowiak, A. Hojka-Osinska, M. Szymanski and M. Figlerowicz (2013). "Identification of stable, high copy number, medium-sized RNA degradation intermediates that accumulate in plants under non-stress conditions." Plant Molecular Biology **83**(3): 191-204.
- Ogren, W. L. (1984). "Photorespiration: Pathways, Regulation, and Modification." Annual Review of Plant Physiology **35**: 415-442.
- Okegawa, Y., Y. Kobayashi and T. Shikanai (2010). "Physiological links among alternative electron transport pathways that reduce and oxidize plastoquinone in *Arabidopsis*." The Plant Journal **63**(3): 458-468.
- Oyama, T., Y. Shimura and K. Okada (1997). "The *Arabidopsis* HY5 gene encodes a bZIP protein that regulates stimulus-induced development of root and hypocotyl." Genes and Development **11**(22): 2983-2995.
- Palusa, S. G., G. S. Ali and A. S. Reddy (2007). "Alternative splicing of pre-mRNAs of *Arabidopsis* serine/arginine-rich proteins: regulation by hormones and stresses." The Plant Journal **49**(6): 1091-1107.
- Paredes, M. and M. J. Quiles (2015). "The Effects of Cold Stress on Photosynthesis in Hibiscus Plants." PLoS One **10**(9): e0137472.
- Park, S. Y., P. Fung, N. Nishimura, D. R. Jensen, H. Fujii, Y. Zhao, S. Lumba, J. Santiago, A. Rodrigues, T. F. Chow, S. E. Alfred, D. Bonetta, R. Finkelstein, N. J. Provart, D. Desveaux, P. L. Rodriguez, P.

- McCourt, J. K. Zhu, J. I. Schroeder, B. F. Volkman and S. R. Cutler (2009). "Abscisic acid inhibits type 2C protein phosphatases via the PYR/PYL family of START proteins." Science **324**(5930): 1068-1071.
- Peragine, A., M. Yoshikawa, G. Wu, H. L. Albrecht and R. S. Poethig (2004). "SGS3 and SGS2/SDE1/RDR6 are required for juvenile development and the production of trans-acting siRNAs in *Arabidopsis*." Genes and Development **18**(19): 2368-2379.
- Pilon, S. E. A.-G. a. M. (2008). "MicroRNA-mediated systemic down-regulation of copper protein expression in response to low copper availability in *Arabidopsis*." Journal of Biological Chemistry **283**(23): 15932-15945.
- Piriyapongsa, J. and I. K. Jordan (2008). "Dual coding of siRNAs and miRNAs by plant transposable elements." RNA **14**(5): 814-821.
- Pospíšil, P. (2016). "Production of reactive oxygen species by photosystem II as a response to light and temperature stress." Frontiers in Plant Science **7**: 1950.
- Pourcel, L., J. M. Routaboul, V. Cheynier, L. Lepiniec and I. Debeaujon (2007). "Flavonoid oxidation in plants: from biochemical properties to physiological functions." Trends in Plant Science **12**(1): 29-36.
- Powles, S. B. (1984). "Photoinhibition of Photosynthesis Induced by Visible Light." Annual Review of Plant Physiology **35**: 15-44.
- Pratt, A. and I. MacRae (2009). "The RNA-induced silencing complex: a versatile gene-silencing machine." Journal of Biological Chemistry **284**(27): 17897-17901.
- Rajagopalan, R., H. Vaucheret, J. Trejo and D. P. Bartel (2006). "A diverse and evolutionarily fluid set of microRNAs in *Arabidopsis thaliana*." Genes and Development **20**(24): 3407-3425.
- Ransohoff, J. D., Y. Wei and P. A. Khavari (2018). "The functions and unique features of long intergenic non-coding RNA." Nature Reviews Molecular Cell Biology **19**(3): 143-157.
- Ren, B., X. Wang, J. Duan and J. Ma (2019). "Rhizobial tRNA-derived small RNAs are signal molecules regulating plant nodulation." Science **365**(6456): 919-922.
- Reyes, T., A. Scartazza, A. Castagna, E. G. Cosio, A. Ranieri and L. Guglielminetti (2018). "Physiological effects of short acute UVB treatments in *Chenopodium quinoa* Willd." Scientific Reports **8**(1): 371.
- Rienzo, F., R. Gabdoulline, M. Menziani and R. Wade (2000). "Blue copper proteins: A comparative analysis of their molecular interaction properties." Protein Science **9**(8): 1439-1454.
- Rizzini, L., J. J. Favory, C. Cloix, D. Faggionato, A. O'Hara, E. Kaiserli, R. Baumeister, E. Schafer, F. Nagy, G. I. Jenkins and R. Ulm (2011). "Perception of UV-B by the *Arabidopsis* UVR8 protein." Science **332**(6025): 103-106.
- Rockwell, N. C., Y. S. Su and J. C. Lagarias (2006). "Phytochrome structure and signaling mechanisms." Annual Reviews Plant Biology **57**: 837-858.
- Roy, D., A. Paul, A. Roy, R. Ghosh, P. Ganguly and S. Chaudhuri (2014). "Differential acetylation of histone H3 at the regulatory region of OsDREB1b promoter facilitates chromatin remodelling and transcription activation during cold stress." PLoS One **9**(6): e100343.
- Rozema, J., A. Chardonnens, M. Tosserams, R. Hafkenscheid and S. Bruijnzeel (1997). "Leaf thickness and UV-B absorbing pigments of plants in relation to an elevational gradient along the Blue Mountains, Jamaica." Plant Ecology **128**: 151-159.

- Sakamoto, A. and N. Murata (2002). "The role of glycine betaine in the protection of plants from stress: clues from transgenic plants." Plant, Cell and Environment **25**(2): 163-171.
- Sakuma, Y., Q. Liu, J. G. Dubouzet, H. Abe, K. Shinozaki and K. Yamaguchi-Shinozaki (2002). "DNA-binding specificity of the ERF/AP2 domain of *Arabidopsis* DREBs, transcription factors involved in dehydration- and cold-inducible gene expression." Biochemical and Biophysical Research Communications **290**(3): 998-1009.
- Savitch, L., E. Leonardos, M. Krol, S. Jansson, B. Grodzinski, N. Huner and G. Öquist (2002). "Two different strategies for light utilization in photosynthesis in relation to growth and cold acclimation." Plant, Cell and Environment **25**: 761-771.
- Seo, E., H. Lee, J. Jeon, H. Park, J. Kim, Y. Noh and I. Leea (2009). "Crosstalk between cold response and flowering in *Arabidopsis* is mediated through the flowering-time gene SOC1 and its upstream negative regulator FLC." Plant Cell. **21**(10): 3185–3197.
- Sharma, P., A. Jha, R. Dubey and M. Pessaraki (2012). "Reactive oxygen species, oxidative damage, and antioxidative defense mechanism in plants under stressful conditions." Journal of Botany: 217037.
- Sharrock, R. A. and P. H. Quail (1989). "Novel phytochrome sequences in *Arabidopsis thaliana*: structure, evolution, and differential expression of a plant regulatory photoreceptor family." Genes and Development **3**(11): 1745-1757.
- Shi, Y., Y. Ding and S. Yang (2015). "Cold signal transduction and its interplay with phytohormones during cold acclimation." Plant Cell Physiol **56**(1): 7-15.
- Slotkin, R. K., M. Vaughn, F. Borges, M. Tanurdzic, J. D. Becker, J. A. Feijo and R. A. Martienssen (2009). "Epigenetic reprogramming and small RNA silencing of transposable elements in pollen." Cell **136**(3): 461-472.
- Smith, H. (2000). "Phytochromes and light signal perception by plants--an emerging synthesis." Nature **407**(6804): 585-591.
- Solanke, A. U. and A. K. Sharma (2008). "Signal transduction during cold stress in plants." Physiology and Molecular Biology of Plants **14**(1-2): 69-79.
- Song, G., R. Zhang, S. Zhang, Y. Li, J. Gao, X. Han, M. Chen, J. Wang, W. Li and G. Li (2017). "Response of microRNAs to cold treatment in the young spikes of common wheat." BMC Genomics **18**(1): 212.
- Song, J., S. Gao, Y. Wang, B. Li, Y. Zhang and Z. Yang (2016). "miR394 and its target gene LCR are involved in cold stress response in *Arabidopsis*." Plant Gene **5**: 56-64.
- Song, J. B., S. Gao, D. Sun, H. Li, X. X. Shu and Z. M. Yang (2013). "miR394 and LCR are involved in *Arabidopsis* salt and drought stress responses in an abscisic acid-dependent manner." BMC Plant Biology **13**: 210.
- Song, J. B., S. Q. Huang, T. Dalmay and Z. M. Yang (2012). "Regulation of leaf morphology by microRNA394 and its target LEAF CURLING RESPONSIVENESS." Plant Cell Physiology **53**(7): 1283-1294.
- Soon, F. F., L. M. Ng, X. E. Zhou, G. M. West, A. Kovach, M. H. Tan, K. M. Suino-Powell, Y. He, Y. Xu, M. J. Chalmers, J. S. Brunzelle, H. Zhang, H. Yang, H. Jiang, J. Li, E. L. Yong, S. Cutler, J. K. Zhu, P. R. Griffin, K. Melcher and H. E. Xu (2012). "Molecular mimicry regulates ABA signaling by SnRK2 kinases and PP2C phosphatases." Science **335**(6064): 85-88.

- Stapleton, A. E. (1992). "Ultraviolet Radiation and Plants: Burning Questions." Plant Cell **4**(11): 1353-1358.
- Steponkus, P. L. (1984). "Role of the Plasma Membrane in Freezing Injury and Cold Acclimation." Annual Review of Plant Physiology **35**(1): 543-584.
- Stockinger, E., S. Gilmour and M. Thomashow (1997). "*Arabidopsis thaliana* CBF1 encodes an AP2 domain-containing transcriptional activator that binds to the C-repeat/DRE, a cis-acting DNA regulatory element that stimulates transcription in response to low temperature and water deficit." Proc Natl Acad Sci U S A **94**(3): 1035-1040.
- Strand, A., T. Asami, J. Alonso, J. R. Ecker and J. Chory (2003). "Chloroplast to nucleus communication triggered by accumulation of Mg-protoporphyrinIX." Nature **421**(6918): 79-83.
- Suetsugu, N. and M. Wada (2013). "Evolution of three LOV blue light receptor families in green plants and photosynthetic stramenopiles: phototropin, ZTL/FKF1/LKP2 and aureochrome." Plant Cell Physiology **54**(1): 8-23.
- Sunkar, R. and J. Zhu (2007). "Micro RNAs and Short-interfering RNAs in Plants." Journal of Integrative Plant Biology **49**(6): 817-826.
- Suping Zhang and H. V. Scheller (2004). "Photoinhibition of photosystem I at chilling temperature and subsequent recovery in *Arabidopsis thaliana*." Plant and Cell Physiology **45**(11): 1595-1602.
- Surpin, M. and J. Chory (1997). "The co-ordination of nuclear and organellar genome expression in eukaryotic cells." Essays in Biochemistry **32**: 113-125.
- Surpin, M., R. Larkin and J. Chory (2002). "Signal Transduction between the Chloroplast and the Nucleus." Plant Cell. **14**: s327-s338.
- Susek, R. E., F. M. Ausubel and J. Chory (1993). "Signal transduction mutants of *Arabidopsis* uncouple nuclear CAB and RBCS gene expression from chloroplast development." Cell **74**(5): 787-799.
- Swiezewski, S., F. Liu, A. Magusin and C. Dean (2009). "Cold-induced silencing by long antisense transcripts of an *Arabidopsis* Polycomb target." Nature **462**(7274): 799-802.
- Sztatelman, O., J. Grzyb, H. Gabrys and A. K. Banas (2015). "The effect of UV-B on *Arabidopsis* leaves depends on light conditions after treatment." BMC Plant Biology **15**: 281.
- Szymańska, R., I. Ślesak, A. Orzechowska and J. Kruk (2017). "Physiological and biochemical responses to high light and temperature stress in plants." Environmental and Experimental Botany **139**: 165-177.
- Tadini, L., P. Pesaresi, T. Kleine, F. Rossi, A. Guljamow, F. Sommer, T. Mühlhaus, M. Schroda, S. Masiero, M. Pribil, M. Rothbart, B. Hedtke, B. Grimm and D. Leister (2016). "GUN1 controls accumulation of the plastid ribosomal protein S1 at the protein level and interacts with proteins involved in plastid protein homeostasis." Plant Physiology **170**: 1817-1830.
- Tam, O. H., A. A. Aravin, P. Stein, A. Girard, E. P. Murchison, S. Cheloufi, E. Hodges, M. Anger, R. Sachidanandam, R. M. Schultz and G. J. Hannon (2008). "Pseudogene-derived small interfering RNAs regulate gene expression in mouse oocytes." Nature **453**(7194): 534-538.
- Tattini, M., C. Galardi, P. Pinelli, R. Massai, D. Remorini and G. Agati (2004). "Differential accumulation of flavonoids and hydroxycinnamates in leaves of *Ligustrum vulgare* under excess light and drought stress." New Phytologist **163**: 547-561.

- Thalhammer, A., G. Bryant, R. Sulpice and D. K. Hinch (2014). "Disordered cold regulated15 proteins protect chloroplast membranes during freezing through binding and folding, but do not stabilize chloroplast enzymes in vivo." Plant Physiology **166**: 190–201.
- Thiebaut, F., A. S. Hemerly and P. C. G. Ferreira (2019). "A role for epigenetic regulation in the adaptation and stress responses of non-model plants." Frontiers in Plant Science **10**: 246.
- Thomashow, M. F. (1999). "PLANT COLD ACCLIMATION: Freezing tolerance genes and regulatory mechanisms." Annual Review of Plant Physiology and Plant Molecular Biology **50**: 571-599.
- Thompson, D., C. Lu, P. Green and R. Parker (2008). "tRNA cleavage is a conserved response to oxidative stress in eukaryotes." RNA **14**(10): 2095–2103.
- Tiwari, B., K. Habermann, M. A. Arif, H. L. Weil, A. Garcia-Molina, T. Kleine, T. Muhlhaus and W. Frank (2020). "Identification of small RNAs during cold acclimation in *Arabidopsis thaliana*." BMC Plant Biol **20**(1): 298.
- Townsend, A., M. Ware and A. Ruban (2018). "Dynamic interplay between photodamage and photoprotection in photosystem II." Plant, Cell and Environment **41**(5): 1098-1112.
- Tripathy, B. C. and R. Oelmuller (2012). "Reactive oxygen species generation and signaling in plants." Plant Signaling and Behavior **7**(12): 1621-1633.
- Turrens, J. F. (2003). "Mitochondrial formation of reactive oxygen species." The Journal of Physiology **552**(Pt 2): 335-344.
- Uemura, M., S. J. Gilmour, M. F. Thomashow and P. L. Steponkus (1996). "Effects of COR6.6 and COR15am polypeptides encoded by COR (cold-regulated) genes of *Arabidopsis thaliana* on the freeze-induced fusion and leakage of liposomes." Plant Physiology **111**(1): 313-327.
- Vazquez, F., T. Blevins, J. Ailhas, T. Boller and F. Meins, Jr. (2008). "Evolution of *Arabidopsis* MIR genes generates novel microRNA classes." Nucleic Acids Research **36**(20): 6429-6438.
- Vazquez, F., H. Vaucheret, R. Rajagopalan, C. Lepers, V. Gascioli, A. C. Mallory, J. L. Hilbert, D. P. Bartel and P. Crete (2004). "Endogenous trans-acting siRNAs regulate the accumulation of *Arabidopsis* mRNAs." Molecular Cell **16**(1): 69-79.
- Verhoeven, A. S., B. Demmig-Adams and I. W. Adams (1997). "Enhanced employment of the xanthophyll cycle and thermal energy dissipation in spinach exposed to high light and N stress." Plant Physiology **113**(3): 817-824.
- Vlad, F., S. Rubio, A. Rodrigues, C. Sirichandra, C. Belin, N. Robert, J. Leung, P. L. Rodriguez, C. Lauriere and S. Merlot (2009). "Protein phosphatases 2C regulate the activation of the Snf1-related kinase OST1 by abscisic acid in *Arabidopsis*." Plant Cell **21**(10): 3170-3184.
- Wang, D., Z. Qu, L. Yang, Q. Zhang, Z. H. Liu, T. Do, D. L. Adelson, Z. Y. Wang, I. Searle and J. K. Zhu (2017). "Transposable elements (TEs) contribute to stress-related long intergenic noncoding RNAs in plants." The Plant Journal **90**(1): 133-146.
- Wang, D. Z., Y. N. Jin, X. H. Ding, W. J. Wang, S. S. Zhai, L. P. Bai and Z. F. Guo (2017). "Gene regulation and signal transduction in the ICE-CBF-COR signaling pathway during cold stress in plants." Biochemistry **82**(10): 1103-1117.

- Wang, H., J. P. Chung, J. Liu, I. Jang, J. M. Kean, J. Xu and C. H. N. (2014). "Genome-wide identification of long noncoding natural antisense transcripts and their responses to light in *Arabidopsis*." Genome Research **24**(3): 444–453.
- Wang, K. C. and H. Y. Chang (2011). "Molecular mechanisms of long noncoding RNAs." Molecular Cell **43**(6): 904-914.
- Wang, L., X. Yu, H. Wang, Y. Z. Lu, M. de Ruiter, M. Prins and Y. K. He (2011). "A novel class of heat-responsive small RNAs derived from the chloroplast genome of Chinese cabbage (*Brassica rapa*)." BMC Genomics **12**: 289.
- Wang, Q., T. Li, K. Xu, W. Zhang, X. Wang, J. Quan, W. Jin, M. Zhang, G. Fan, M. Wang and W. Shan (2016). "The tRNA-Derived small RNAs regulate gene expression through triggering sequence-specific degradation of target transcripts in the oomycete pathogen *Phytophthora sojae*." Frontiers in Plant Sciences **7**: 1938.
- Wang, X. J., T. Gaasterland and N. H. Chua (2005). "Genome-wide prediction and identification of cis-natural antisense transcripts in *Arabidopsis thaliana*." Genome Biology **6**(4): R30.
- Wang, X. Q., J. L. Crutchley and J. Dostie (2011). "Shaping the genome with non-coding RNAs." Current Genomics **12**(5): 307-321.
- Wang, Y., X. Fan, F. Lin, G. He, W. Terzaghi, D. Zhu and X. W. Deng (2014). "*Arabidopsis* noncoding RNA mediates control of photomorphogenesis by red light." Proc Natl Acad Sci U S A **111**(28): 10359-10364.
- Waszczak, C., M. Carmody and J. Kangasjarvi (2018). "Reactive oxygen species in plant signaling." Annual Review of Plant Biology **69**: 209-236.
- Werner, A. and A. Berdal (2005). "Natural antisense transcripts: sound or silence?" Physiological Genomics **23**(2): 125-131.
- Wight, M. and A. Werner (2013). "The functions of natural antisense transcripts." Essays in Biochemistry **54**: 91-101.
- Wightman, B., I. Ha and G. Ruvkun (1993). "Posttranscriptional regulation of the heterochronic gene *lin-14* by *W-4* mediates temporal pattern formation in *C. elegans*." Cell **75**(5): 855-862.
- Wingler, A., P. Lea, W. Quick and R. Leegood (2000). "Photorespiration: metabolic pathways and their role in stress protection." Philos Trans R Soc Lond B Biol Sci. **355**(1402): 1517–1529.
- Woodson, J. D., J. M. Perez-Ruiz and J. Chory (2011). "Heme synthesis by plastid ferrochelatase I regulates nuclear gene expression in plants." Current Biology **21**(10): 897-903.
- Wrona, M., M. Rozanowska and T. Sarna (2004). "Zeaxanthin in combination with ascorbic acid or alpha-tocopherol protects ARPE-19 cells against photosensitized peroxidation of lipids." Free Radical Biology and Medicine **36**(9): 1094-1101.
- Wu, H., Z. Wang, M. Wang and X. Wang (2013). "Widespread long noncoding RNAs as endogenous target mimics for microRNAs in plants." Plant Physiology **161**: 1875–1884.
- Xiao, Y., T. Savchenko, E. E. Baidoo, W. E. Chehab, D. M. Hayden, V. Tolstikov, J. A. Corwin, D. J. Kliebenstein, J. D. Keasling and K. Dehesh (2012). "Retrograde signaling by the plastidial metabolite MEcPP regulates expression of nuclear stress-response genes." Cell **149**(7): 1525-1535.

- Xie, M. and B. Yu (2015). "siRNA-directed DNA Methylation in Plants." Current Genomics **16**(1): 23-31.
- Xu, D. (2019). "COP1 and BBXs-HY5-mediated light signal transduction in plants." New Phytologist: 10.1111/nph.16296.
- Yadav, V. K. a. S. K. (2009). "Proline and betaine provide protection to antioxidant and methylglyoxal detoxification systems during cold stress in *Camellia sinensis* (L.) O. Kuntze." Acta Physiologiae Plantarum **31**: 261-269.
- Yamaguchi-Shinozaki, K. and K. Shinozaki (1993). "Characterization of the expression of a desiccation-responsive rd29 gene of *Arabidopsis thaliana* and analysis of its promoter in transgenic plants." Molecular and General Genetics **236**(2-3): 331-340.
- Yamaguchi-Shinozaki, K. and K. Shinozaki (1994). "A novel cis-acting element in an Arabidopsis gene is involved in responsiveness to drought, low-temperature, or high-salt stress." Plant Cell **6**(2): 251-264.
- Yamori, W., J. R. Evans and S. Von Caemmerer (2010). "Effects of growth and measurement light intensities on temperature dependence of CO₂ assimilation rate in tobacco leaves." Plant, Cell and Environment **33**(3): 332-343.
- Yang, F., J. Cai, Y. Yang and Z. H. Liu (2013). "Overexpression of microRNA828 reduces anthocyanin accumulation in Arabidopsis." Plant Cell, Tissue and Organ Culture **115**: 159–167.
- Yuan, C., J. Wang, A. P. Harrison, X. Meng, D. Chen and M. Chen (2015). "Genome-wide view of natural antisense transcripts in *Arabidopsis thaliana*." DNA Research **22**(3): 233-243.
- Zhang, H., H. He, X. Wang, X. Wang, X. Yang, L. Li and X. W. Deng (2011). "Genome-wide mapping of the HY5-mediated gene networks in *Arabidopsis* that involve both transcriptional and post-transcriptional regulation." The Plant Journal **65**(3): 346-358.
- Zhang, X., Y. Lii, Z. Wu, A. Polishko, H. Zhang, V. Chinnusamy, S. Lonardi, J. K. Zhu, R. Liu and H. Jin (2013). "Mechanisms of small RNA generation from *cis*-NATs in response to environmental and developmental cues." Molecular Plant **6**(3): 704-715.
- Zhang, Y., X. Zhu, X. Chen, C. Song, Z. Zou, Y. Wang, M. Wang, W. Fang and X. Li (2014). "Identification and characterization of cold-responsive microRNAs in tea plant (*Camellia sinensis*) and their targets using high-throughput sequencing and degradome analysis." BMC Plant Biology **14**: 271.
- Zhang, Z., Z. Wu, L. Feng, L. Dong, A. Song, M. Yuan, Y. Chen, J. Zeng, G. Chen and S. Yuan (2016). "Mg-Protoporphyrin IX signals enhance plant's tolerance to cold stress." Frontiers in Plant Science **7**: 1575.
- Zhang, Z. W., S. Yuan, F. Xu, H. Yang, Y. E. Chen, M. Yuan, M. Y. Xu, L. W. Xue, X. C. Xu and H. H. Lin (2011). "Mg-protoporphyrin, haem and sugar signals double cellular total RNA against herbicide and high-light-derived oxidative stress." Plant, Cell and Environment **34**(6): 1031-1042.
- Zhou, B., P. Fan, Y. Li, H. Yan and Q. Xu (2016). "Exploring miRNAs involved in blue/UV-A light response in Brassica rapa reveals special regulatory mode during seedling development." BMC Plant Biol **16**(1): 111.

Zhou, G., F. Wei, X. Qiu, X. Xu, J. Zhang and X. Guo (2018). "Influence of enhanced ultraviolet-B radiation during rice plant growth on rice straw decomposition with nitrogen deposition." Scientific Reports **8**(1): 14512.

Zhou, X., G. Wang and W. Zhang (2007). "UV-B responsive microRNA genes in *Arabidopsis thaliana*." Mol Syst Biol **3**: 103.

Zhu, L., J. Li, Y. Gong, Q. Wu, S. Tan, D. Sun, X. Xu, Y. Zuo, Y. Zhao, Y. Q. Wei, X. W. Wei and Y. Peng (2019). "Exosomal tRNA-derived small RNA as a promising biomarker for cancer diagnosis." Molecular Cancer **18**(1): 74.

Zhu, L., D. W. Ow and Z. Dong (2018). "Transfer RNA-derived small RNAs in plants." Science China Life Sciences **61**(2): 155-161.

Zouari, M., C. Ben Ahmed, N. Elloumi, K. Bellassoued, D. Delmail, P. Labrousse, F. Ben Abdallah and B. Ben Rouina (2016). "Impact of proline application on cadmium accumulation, mineral nutrition and enzymatic antioxidant defense system of *Olea europaea* L. cv Chemlali exposed to cadmium stress." Ecotoxicology and Environmental Safety **128**: 195-205.

5 Acknowledgements

Foremost, I praise and thank god for showering blessings throughout the course of my PhD. My doctoral studies would not be possible without the encouragement, motivation and personal support from many people. I would like to express my deep and sincere gratitude to my colleagues, family and friends.

In particular, I would like to thank:

My mentors, colleagues and collaboration partners:

My supervisor Prof. Wolfgang Frank for giving me the opportunity to pursue a PhD in his lab, for always being available to answer my queries, for never sparing an effort in order to help me with the scientific guidance, documentation or any kind of support. Without his implicit support throughout, especially with the preparation of published papers and thesis, I would not have succeeded.

Dr. M. Asif Arif for getting me started in the lab and introducing me to the protocols of the lab, for his timely scientific guidance and his patience throughout the course of my PhD, and for giving a clear direction in order to troubleshoot the experiments.

Dr. Oguz Top for supporting me and giving great feedback to help me improve my publications and thesis. I am grateful for the time he spent reading my documents over and over again in order to have a better version. Furthermore, it was always great to have interesting conversations with him during break time.

Kristin Habermann for the amazing times working throughout our PhD and sharing our office, for being patient and helpful whenever I needed her help, and for entertaining conversations related to all sorts of topics.

Stefan Kirchner for always being amicable, for helping me with the lab work and for sharing his fun life stories which I found very interesting.

Katie Wong and Mohamed Bennacer, two students who were trained by me, for engaging with me in performing experiments and helping me learn more through their queries.

Dr. Jörg Meurer for his readiness to join my thesis advisory committee and for joining my PhD reviewer commission as a second examiner. I am grateful for his timely guidance during the yearly retreat group meetings.

Prof. Michael Schroda for being a member of my thesis advisory committee and for providing suggestions related to the progress of my doctoral studies.

Mrs. Ute Thomas for being friendly and always helping me with documentation or office related work. She has been very helpful when I wanted her help with speaking german on calls.

Dr. Tatjana Kleine, Dr. Timo Mühlhaus, Dr. Antoni G. Molina and Heinrich Lukas Weil for collaborating and cooperating with us.

My Family and friends:

My father Mr. Sunil Tiwari and my mother Mrs. Binita Tiwari for being loving and supportive of my plans and ideas, even if it meant that I would have to move to a different continent to pursue my PhD studies. I am grateful for their unconditional love, prayers and their sacrifices for educating me and preparing me for the future. I thank them, for being with me through my good or bad times and for celebrating every small victory of my life.

My sister Kanika Tiwari Asthana, brother-in-law Saurabh Asthana and their daughter Ahaana Asthana for making my life colorful and keeping in touch through video calls and not letting me feel that I am so far away from home.

My master's thesis supervisor Prof. Padmanabh Dwivedi and my bachelor's teacher Dr. Monika Koul for their persistent encouragement and readiness to refer me whenever needed.

My dear friends: Kavita Shukla, Sakshi S. Mehta, Payal Agarwal, Parul Arora, Lubna Patel and Ritika Kapoor for their never-ending love and support.

Lastly my beloved, Suraj Giri, for understanding me, never ceasing to encourage me and for being there when I needed him the most.

6

Curriculum Vitae



Bhavika Tiwari

PhD in Molecular Biology



bhavika.tiwari91@gmail.com



+4915901335610



Munich, Germany

TECHNICAL SKILLS

molecular biology

DNA and RNA analysis

qPCR

cDNA

MS Office

Next generation Sequencing

non-coding RNAs

CLC Genomics

Corel Draw

sequencing library

R programming

SOFT SKILLS

Organization

Communication

Lab Management

Teamwork

Presentation

RESEARCH EXPERIENCE

Doctoral Researcher

Ludwig Maximilian University

09/2016 – 03/2021,

Munich, Germany

The research focuses on characterization of small RNAs (sRNAs) in plants responsive to abiotic stresses (cold and high light) and retrograde signaling.

Achievements/Tasks

- Prepared sRNA sequencing libraries to identify differentially expressed sRNAs, mRNAs and lncRNA responsive to abiotic stress treatments.
- Analyzed the Next generation sequencing data using Galaxy and CLC Genomics platforms.
- Designed primers to perform RT-PCR and PCR.
- Performed RT-PCR to validate themiRNA targets and Northern blots to confirm differential expression of sRNAs.
- Collaborated with bioinformatics team from TU Kaiserslautern to establish a miRNA-Transcription factor network of *Arabidopsis thaliana*.
- Independently performed DNA and RNA isolation, PCR, RT-PCR, stem loop PCR, gradient PCR, cDNA synthesis, Dot blot, Native-PAGE, Restriction enzyme digestion.
- Experience using tools and machines such as BLAST, psRNATarget, DAVID bioinformatics, Gel doc, Thermal cycler, Light Microscope, Quantity one for blot visualization, Imaging Win for PAM measurements and Corel Draw.
- Mentored Bachelor/Master students on molecular biology techniques and supervised them with their thesis.

Contact: Prof. Dr. Wolfgang Frank - wolfgang.frank@lmu.de

Master's Thesis

Banaras Hindu University

01/2014 - 06/2014,

Varanasi, India

Nitric Oxide (NO) mediated hypersensitivity response and associated biochemical responses under Tobacco-bacterial pathogen interaction.

Achievements/Tasks

- Performed infiltration of Tobacco leaves with biotic agents (*Xanthomonas oryzae*)
- Conducted biochemical tests to qualitatively and quantitatively estimate the production of Reactive Oxygen Species and enzymes (H₂O₂, APX, PAL, MDA) necessary for ROS removal from the plant.
- Validated increased levels of ROS produced in the infected plant tissues as a result of increased Nitric oxide in the system.

Contact: Prof. Dr. Padmanabh Dwivedi - pdwivedi25@rediffmail.com

Summer Trainee

University of Delhi

06/2013 - 09/2013,

Delhi, India

Worked on studying the interactions of CBL-CIPK proteins with Dr. G.K. Pandey at Dept. of Plant Molecular Biology

Achievements/Tasks

- Performed yeast two Hybrid assay to study interaction between *O. sativa* and *A. thaliana* proteins.
- Assisted in TOPO Cloning of a CIPK gene into the Entry Vector (pENTR/D-TOPO) to generate a construct that was further cloned into the Expression Vector pSITE2CA for localization studies.
- Assisted with mutation of CIPK gene using Site Directed Mutagenesis where Threonine residue was replaced by Aspartate amino acid.

LANGUAGES

English



German



Hindi



EDUCATION

PhD in Molecular Biology

Ludwig Maximilian's University

09/2016 - Present,

Munich, Germany

MSc. Plant Biotechnology

Banaras Hindu University

07/2012 - 07/2014,

Varanasi, India

Bachelor of Education (B. Ed)

Guru Gobind Singh Indraprastha University

06/2011 - 06/2012,

Delhi, India

BSc. (Hons) Botany

Hansraj College, University of Delhi

07/2009 - 07/2011,

Delhi, India

PUBLICATIONS

Tiwari, B. et al. Identification of small RNAs during cold acclimation in *Arabidopsis thaliana*. BMC Plant Biology 20, 298 (2020). <https://doi.org/10.1186/s12870-020-02511-3>

Habermann, K., Tiwari, B. et al. Identification of small non-coding RNAs responsive to GUN1 and GUN5 related retrograde signals in *Arabidopsis thaliana*. The Plant Journal (2020). <https://doi.org/10.1111/tpj.14912>

Identification of small RNAs during high light acclimation in *Arabidopsis thaliana*. (Under review)

ACHIEVEMENTS AND AWARDS

Awarded DST – INSPIRE April '15 Fellowship (Provisional Offer Letter) for pursuing PhD research in India.

Qualified Graduate Aptitude Test in Engineering 2015. This test allows the candidate to pursue PhD in any Indian Institute of Technology (IIT) and Indian Institute of Science Education and Research (IISER) of choice.

Awarded Gold Medal for securing first position in M.Sc. Plant Biotechnology at Banaras Hindu University (2012 – 2014).